



## Durham E-Theses

---

### *Luminescence in crystals of zinc sulpho -selenide*

Mitchell, R. C.

#### How to cite:

---

Mitchell, R. C. (1977) *Luminescence in crystals of zinc sulpho -selenide*, Durham theses, Durham University. Available at Durham E-Theses Online: <http://etheses.dur.ac.uk/8247/>

#### Use policy

---

The full-text may be used and/or reproduced, and given to third parties in any format or medium, without prior permission or charge, for personal research or study, educational, or not-for-profit purposes provided that:

- a full bibliographic reference is made to the original source
- a [link](#) is made to the metadata record in Durham E-Theses
- the full-text is not changed in any way

The full-text must not be sold in any format or medium without the formal permission of the copyright holders.

Please consult the [full Durham E-Theses policy](#) for further details.

The copyright of this thesis rests with the author.  
No quotation from it should be published without  
his prior written consent and information derived  
from it should be acknowledged.

LUMINESCENCE IN CRYSTALS OF

ZINC SULPHO - SELENIDE

by

R.C. MITCHELL

Presented in Candidature for the degree of

Doctor of Philosophy

in the

University of Durham

December 1977

*To my parents*

### ACKNOWLEDGEMENTS

I would like to express my gratitude to my supervisor Dr. J. Woods for his guidance and assistance during the course of this research project. I would also like to thank Professor D.A. Wright for allowing me to use the laboratory facilities of the department and the Science Research Council for the award of a grant for my studies. The help and encouragement given by my many colleagues, especially Dr. M.E. Özsan, Dr. G.J. Russell and Dr. J.R. Cutter, is gratefully acknowledged and also the technical assistance given by Mr. F. Spence and his workshop staff. Particular thanks are due to Mr. N. Thompson for growing the crystals studied in this work.

Finally I would like to express my gratitude to my parents for their many sacrifices and constant encouragement over the years.

## ABSTRACT

Zinc selenide and zinc sulphide are wide band-gap II-VI compound semiconductors which are capable of emitting visible luminescence. These two compounds form a series of solid solutions throughout the whole range of composition, with band-gaps ranging from 2.7 eV in ZnSe to 3.6 eV in ZnS at 300 K. The main purpose of the research reported in this thesis was to study the luminescence of Zn(S,Se) crystals grown in the department, with the eventual aim of producing light-emitting diodes capable of covering a colour range from the red to the blue.

The undoped mixed crystals show two emission bands, whereas ZnSe and ZnS emit single self-activated bands. These emission bands are interpreted as being due to the presence of two distinct self-activated centres in the mixed crystals. It is concluded that the self-activated centre in ZnSe is not directly comparable to the centre in ZnS.

Several samples were doped with copper during the growth. These crystals showed two separate emission bands throughout the range of composition which shift from the red (6450 Å) and the green (5350 Å) in ZnSe through to the green (5320 Å) and the blue (4400 Å) in ZnS. There is a continuous shift in the position of the peaks with varying composition; this contrasts with other reports for the copper emission.

Samples were doped with manganese since this produces an efficient luminescence centre in ZnSe and ZnS. The  $\text{Mn}^{2+}$  emission occurs near 5860 Å with a half-width of 0.15 eV at 85 K throughout the range of composition of the mixed alloys. This has been established by using 5300 Å radiation in the lowest energy excitation band to stimulate the luminescence. The  $\text{Mn}^{2+}$  emission is quenched in ZnSe following treatment in zinc/copper and the red copper emission predominates. The copper emission in such a sample is excited by characteristic manganese excitation radiation, and it is suggested that the  $\text{Mn}^{2+}$  emission may be quenched by a de-excitation to a copper centre.

## CONTENTS

CHAPTER 1	INTRODUCTION	1
CHAPTER 2	LUMINESCENT PROPERTIES OF THE II-VI COMPOUNDS	
2.1	Introduction	7
2.2	Band Structure	7
2.3	Edge Emission	10
2.3.1	Exciton Emission	11
2.3.2	Donor-Acceptor Pair Emission	13
2.4	Deep Centre Emission	14
2.5	Self-Activated Emission	17
2.6	Copper-Activated Emission	19
2.7	Configurational Co-ordinate Model	22
2.8	Manganese Emission	24
2.9	Polarisation of luminescence	26
2.9.1	Self-activated luminescence	26
2.9.2	Copper-blue and green emissions	28
2.10	Electron Spin Resonance	29
2.11	Thermal Quenching	31
2.12	Auger Effect	32
2.13	Photoconductivity	34
CHAPTER 3	CRYSTAL GROWTH AND PREPARATION	
3.1	Crystal Structure and Bonding	36
3.2	Crystal Growth	37
3.2.1	Preliminary Preparation	38
3.2.2	Vapour Phase Growth	39
3.2.3	Chemical Transport	40
3.3	Sample Preparation	41
3.3.1	Etching	41
3.3.2	Ohmic Contacts	42
3.4	Heat Treatment	42
3.5	X-ray Powder Analysis	43

CHAPTER 4	EXPERIMENTAL PROCEDURE	
4.1	Introduction	45
4.2	The Cryostat	45
4.3	Optica Spectrophotometer	47
4.4	Photoluminescence Spectra	48
4.5	Excitation Spectra	49
4.6	Cathodoluminescence	49
4.7	Thermal Quenching	50
4.8	Photoconductivity	51
4.9	Correction Factors	52
CHAPTER 5	UNDOPED CRYSTALS	
5.1	Introduction	53
5.2	Photoluminescence	53
5.2.1	Iodine Transport Crystals	53
5.2.2	Iodine Transport Crystals annealed in zinc	57
5.2.3	Vertical Furnace Crystals	60
5.3	Cathodoluminescence	61
5.3.1	Iodine Transport Crystals	62
5.3.2	Iodine Transport Crystals treated in zinc	63
5.4	Excitation Spectra	65
5.4.1	Iodine Transport Crystals	65
5.4.2	Iodine Transport Crystals treated in zinc	67
5.4.3	Vertical Furnace Crystals	68
5.5	Photoconductivity	69
5.5.1	Iodine Transport Crystals	70
5.5.2	Crystals grown in the Vertical Furnace	72
5.6	Thermal Quenching	72
5.6.1	Iodine Transport Crystals	73
5.7	Discussion	75

CHAPTER 6	COPPER DOPED CRYSTALS	
6.1	Introduction	81
6.2	Unannealed Copper-Activated Samples	82
6.2.1	Photoluminescence	82
6.2.2	Excitation Spectra	85
6.2.3	Thermal Quenching	88
6.3	Annealed Copper-Activated Samples	90
6.3.1	Photoluminescence	90
6.3.2	Excitation Spectra	92
6.3.3	Thermal Quenching	95
6.4	Discussion	96
CHAPTER 7	MANGANESE DOPED CRYSTALS	
7.1	Introduction	104
7.2	Manganese doped Zn(S,Se)	104
7.2.1	Photoluminescence of crystals of Zn(S,Se):I,Mn	104
7.2.2	Excitation spectra for Zn(S,Se):I,Mn	107
7.2.3	Photoconductivity of Zn(S,Se):I,Mn	109
7.3	Copper doped Zn(S,Se):Mn	112
7.3.1	Photoluminescence of Zn(S,Se)I,Mn,Cu,Zn	112
7.3.2	Excitation Spectra	114
7.4	Crystals without iodine	115
7.5	ZnSe:Mn annealed in zinc and selenium	116
7.6	Discussion	118
CHAPTER 8	CONCLUSION	
8.1	Summary of results	122
8.2	Suggestions for further work	126
REFERENCES		128

CHAPTER 1

INTRODUCTION

The luminescence properties of the II-VI compounds have been and still are the subject of much intensive investigation. These wide band-gap materials have long been known and used as efficient photo- and cathodo-luminescent phosphors. No other class of materials displays such a range of luminescence centres capable of producing radiation ranging from the ultra-violet through to the infra-red. Most II-VI compounds are also good conductors of electricity and possess carrier mobilities that are relatively high among compounds of comparable band-gaps. For these reasons, the zinc and cadmium chalcogenides have long been regarded as important materials for realising the efficient conversion of electrical energy into light.

Although great progress has been made in the understanding and technology of the III-V compound light-emitting diodes, particularly GaP and GaAs<sub>x</sub>P<sub>1-x</sub>, the spectral range from the green to the blue is not easily accessible at the present time. The wide band-gap II-VI semiconductors offer the possibility of complementing or replacing existing devices, and of covering the spectral range from the red through to the blue or near ultra-violet.

The work described here is principally concerned with a study of the luminescence of a particular set of II-VI compound alloys. The term luminescence is used to describe the emission of electromagnetic radiation

in excess of thermal radiation. This emission occurs when an electron has been excited to a higher energy state in a solid and relaxes to its original state by releasing some of the excess energy in the form of radiation. Luminescence phenomena have been further classified in terms of the particular type of exciting mechanism and the duration of the emission following the removal of excitation. If a beam of high energy electrons is used to achieve the electronic excitation, the process is known as cathodoluminescence. Photoluminescence occurs when the excitation is provided by means of incident photons ranging in energy from the infra-red to X-rays. Electroluminescence is the result of the application of both D.C. or a.c. electric fields; here, the electrical energy from the applied field is used to excite the electrons to higher energetic states. Triboluminescence occurs when mechanical energy is used to produce the excitation, and chemiluminescence results from the utilisation of the energy of a chemical reaction. Thermoluminescence refers to the thermal stimulation of emission from a material which has previously been excited by another source of energy. Luminescence can be divided into two processes according to the speed of the response of the emission when the source of excitation is removed. These processes are phosphorescence and fluorescence. When the excitation is removed, the luminescence decays initially with a characteristic time shorter than  $10^{-8}$  sec; this is often termed fluorescence. Frequently there is an additional component of the afterglow which decays more slowly with a time constant up to the order of seconds; this process is termed phosphorescence. For intermediate times, however, the distinction between the two processes is not so clear.

Zinc sulphide phosphors have found extensive application in cathode ray tubes and in radiographic screens. Currently one of the main interests

in the luminescence properties of II-VI compounds derives from their potential application in electroluminescent devices. The phenomenon of electroluminescence was first reported by Round (1907) in SiC crystals. Destriau (1936) observed a.c. electroluminescence in powder panels of ZnS phosphor, however his panels had a low brightness and decayed during operational life. It was not until the rapid development of semiconductor technology in the 1950's that much progress was made in the understanding of the principles involved in electroluminescence. The principle of carrier-injection across a p-n junction leading to the emission of light was first advanced by Lehovec et al (1951, 1953). Considerable progress has been made since that time, especially in the investigation of the group III-V single crystal semiconductors, for example GaAs and GaP. The II-VI materials have also received much attention and the electroluminescence properties of these compounds have been reviewed by Aven (1967).

Zinc sulphide has been recognised as an efficient phosphor for photo- and cathodo-luminescence since the 1900's, and has been the subject of much examination, see for example the review by Shionoya (1966). It has been known for some time that the addition of certain metallic impurities, such as Cu, Ag or Au, can provide specific luminescence bands ranging in wavelength from the blue to the red. Comparatively little work has been done on the related compound of zinc selenide, although it has been suggested that there are self-activated and copper emissions similar to those which are observed in zinc sulphide (Halsted et al, 1965). Zinc selenide and zinc sulphide possess wide band-gaps of 2.67 and 3.60 eV respectively at room temperature, which makes both of them important materials for the development of electroluminescent devices. These two compounds form a continuous series of solid solutions, and

Larach et al (1957) have shown that there is a linear shift of band-gap from 2.7 to 3.6 eV, with varying composition of the alloy. Work within this department has already shown that electroluminescence can be achieved in single crystals of zinc selenide, Özsan and Woods (1974, 1975). Solid solutions of zinc sulpho-selenide offer the possibility of extending the colour range to shorter wavelengths.

Previous studies of the luminescence properties of Zn(S,Se) have concentrated mainly on powdered phosphor alloys, Leverenz (1950), Klasens (1953) and Morehead (1963). In the present work effort has been concentrated on single crystal samples grown throughout the range of composition, varying the sulphur content in small intervals. Previous workers have reported various anomalies in the emission distribution with changing composition. Lehmann (1965, 1966), for example, observed a rapid shift in the position of the copper emission bands to lower energies when as little as 1 mole% of ZnSe was incorporated in ZnS:Cu. He also observed two self-activated emission bands in Zn(S,Se) mixed alloys, but noted a single band only in both ZnS and ZnSe. In comparison, Ozawa and Hersh (1973) reported finding one self-activated emission band throughout the range of composition and noted that the blue band in ZnS jumped to the green spectral region, dropping in energy by 0.4 eV when 5 mole% of ZnSe was added. Zinc sulphide doped with manganese has received much attention since divalent manganese is well known as a luminescence activator. The  $Mn^{2+}$  emission band is centred at 5860 Å, almost completely independent of temperature. In contrast to zinc sulphide, the position of the  $Mn^{2+}$  emission band in zinc selenide has been reported at wavelengths between 6350 Å at 291 and 90 K (Apperson et al 1967), and 5900 Å at 290 K (Jones and Woods 1973). Asano et al (1968) examined the luminescence in Zn(S,Se):Mn and observed a complex behaviour of the emission bands with composition; in ZnSe:Mn the emission occurred at 6450 Å at 300 K and

shifted to 6200 Å at 85 K. These bands shifted to 6000 Å for an alloy with composition of 50 mole% ZnS, and thereafter showed little variation with either proportion of ZnS or temperature.

It can be seen from these reports that the emission bands observed in doped and undoped solid solutions of Zn(S,Se) do not behave in a simple manner. The object of the work reported here, therefore, was to study the photoluminescence and photoconductive properties of single crystals of zinc sulpho-selenide in order to resolve the nature of the observed centres.

Following this brief introduction, detailing the background to the present work, some of the luminescence properties of the semiconductors of particular interest are discussed briefly in Chapter 2.

All the single crystal samples of zinc sulpho-selenide, which were examined during this work, were grown in this laboratory. The techniques used in the purification of the starting material, crystal growth, heat treatment of the specimens and doping the sample with impurities have been described in Chapter 3.

The experimental techniques used in the examination of the luminescence properties of the mixed crystals have been described in Chapter 4. This section includes details of the methods employed in measuring the emission spectra, excitation spectra and photoconductivity.

In Chapter 5, a detailed account is given of the self-activated emission observed in undoped crystals of zinc sulpho-selenide grown by both the vapour-transport and chemical-transport methods.

The luminescence observed in crystals of Zn(S,Se) intentionally doped with copper is reported in Chapter 6. In this examination, certain of these copper-doped crystals were annealed in liquid zinc and the results obtained from these treated samples are also included.

In Chapter 7, the luminescence properties of Zn(S,Se) crystals doped with manganese are described. Some samples were annealed in zinc and zinc/copper, and the properties of the manganese-doped crystals after these treatments are reported.

Finally, the present work is summarised in Chapter 8 and some suggestions for future work are put forward.

## CHAPTER 2

### LUMINESCENT PROPERTIES OF THE II-VI COMPOUNDS

#### 2.1 Introduction

The II-VI compounds possess electroluminescent properties which make them useful for possible application in light-emitting devices. The term luminescence is confined to radiation within the visible region of the spectrum and is used to describe the emission of all radiation which is not purely thermal in origin. This work is particularly concerned with photoluminescence; in this process excitation is achieved by the interaction of electrons with incident photons which vary in wavelength from X-ray to infra-red radiation. Electrons returning from a higher energy excited state to the ground state release the excess energy in the form of a characteristic emission. The nature of the observed radiation may be dependent on the band structure of the host lattice, and on the intrinsic crystal defect or extrinsic impurity centres which are present.

In the following sections a brief description will be given of the energy-band structures, impurity centres, and luminescent processes of the II-VI compounds; particular reference will be made to the properties of zinc selenide and zinc sulphide.

#### 2.2 Band Structure

A knowledge of the electronic band-structures of the II-VI

compounds is important in understanding the nature of the electrical and optical effects observed in these materials. The II-VI compounds exist in two main crystal forms, the cubic zinc blende structure and the hexagonal wurtzite structure. This is a result of the covalent contribution to the bonding which produces a tetrahedral coordination in most of the II-VI compounds. Each of the crystal structures possesses its own Brillouin zone structure; the shape of the Brillouin zone for the cubic zinc blende structure is a truncated octahedron, which is shown in Figure 2.1, depicting the lines and points of special symmetry with their conventional labels; the Brillouin zone for the hexagonal wurtzite structure is also hexagonal in form. The high symmetry points and lines of the Brillouin zone for the zinc blende structure are the zone centre ( $\Gamma$ ), and the intersections with the zone faces (L, X, K) on the  $[111]$ ,  $[100]$  and  $[110]$  symmetry axes, respectively.

Various mathematical treatments have been employed to make calculations of the energy band structure within the Brillouin zone. In general the methods use the principle of the superposition of the electron wave functions of the isolated atom when the electrons are brought into the periodic potential of the crystal lattice. These methods may be summarised as follows: the OPW method, in which the crystal wave function is assumed to be plane-wave-like in the inter-space between the atoms constituting the crystal and a mixture of plane-wave and core states within the electron shells of the ions; the APW method, where the crystalline wave functions are taken to be plane-wave-like in the space between ions and similar to atomic functions in the vicinity of the nuclei; the pseudo potential method, which is a semi-empirical use of the OPW formalism incorporating experimental data; and the Linear Combination of Atomic Orbitals

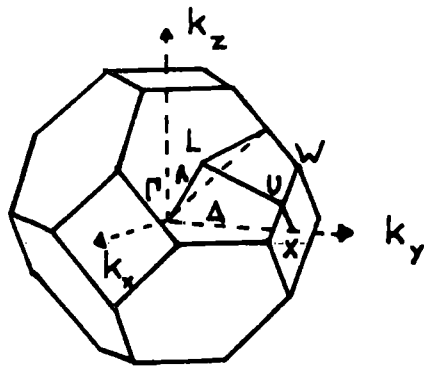
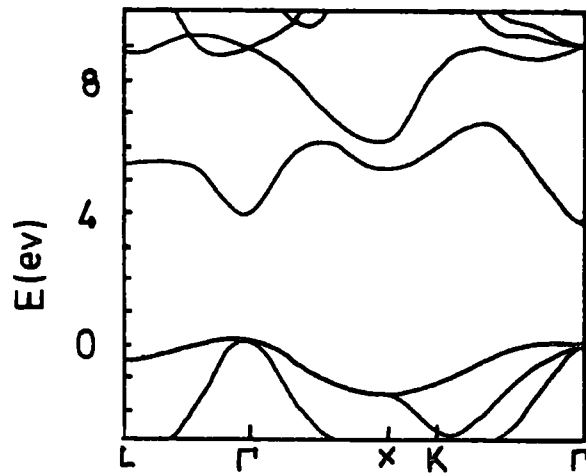
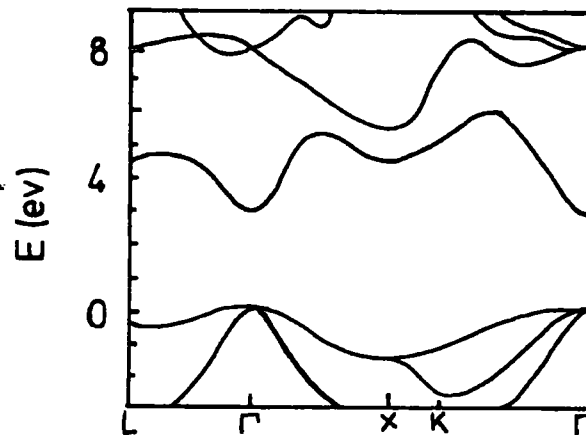


FIG 2.1 brillouin zone for a crystal with f.c.c. structure



ZnS



ZnSe

FIG 2.2 energy band structure of Zn S and Zn Se

scheme, which is the most frequently employed method.

The first electronic band structure calculations on ZnSe, and on thirteen other semiconductors including ZnS, were made by Cohen and Bergstresser (1966), and Bergstresser and Cohen (1967). These authors used the empirical pseudopotential method to fit the band structure to the experimental data on photoemission and reflectivity obtained by Cardona (1961) and Aven et al (1961). The band structures obtained for ZnSe and ZnS are shown in Figure 2.2. It can be seen that both these materials possess a direct minimum energy gap centred on the  $\Gamma$ -point: the energy gap for ZnSe is 2.8 eV and for cubic ZnS is 3.7 eV, both measured at 77 K. Herman and Skillman (1961) have made a calculation of the energy band structure for hexagonal ZnS by the OPW method; this also suggests that there is a direct gap at  $\underline{k} = 0$  with a slightly higher energy gap of 3.8 eV. From experimental data, Larach, Schrader and Stocker (1957) suggested that the range of cubic mixed alloys formed by ZnS and ZnSe all possess a direct gap, and that there is a linear progression of band-gap energy with composition.

The inclusion of the spin-orbit interaction has an influence on the calculated band structure; principally, the effect is to split the degeneracy of the valence band (see for example Parmenter 1955). The most important splitting is that of the six-fold degenerate  $\underline{k} = 0$  state at  $\Gamma_{15v}$  into a four-fold  $\Gamma_8$  state and a lower two-fold  $\Gamma_7$ , (see Figure 2.2a). The  $\Gamma_8$  state is split by an energy, denoted by  $\Delta_{SO}$ , from the lower  $\Gamma_7$  state (the 'split-off' valence band). The  $\Gamma_8$  state is itself split into two parabolic bands  $V_1$  and  $V_2$ , with different curvatures; these represent the heavy-hole and light-hole valence bands respectively. Spin-orbit splitting also occurs at other

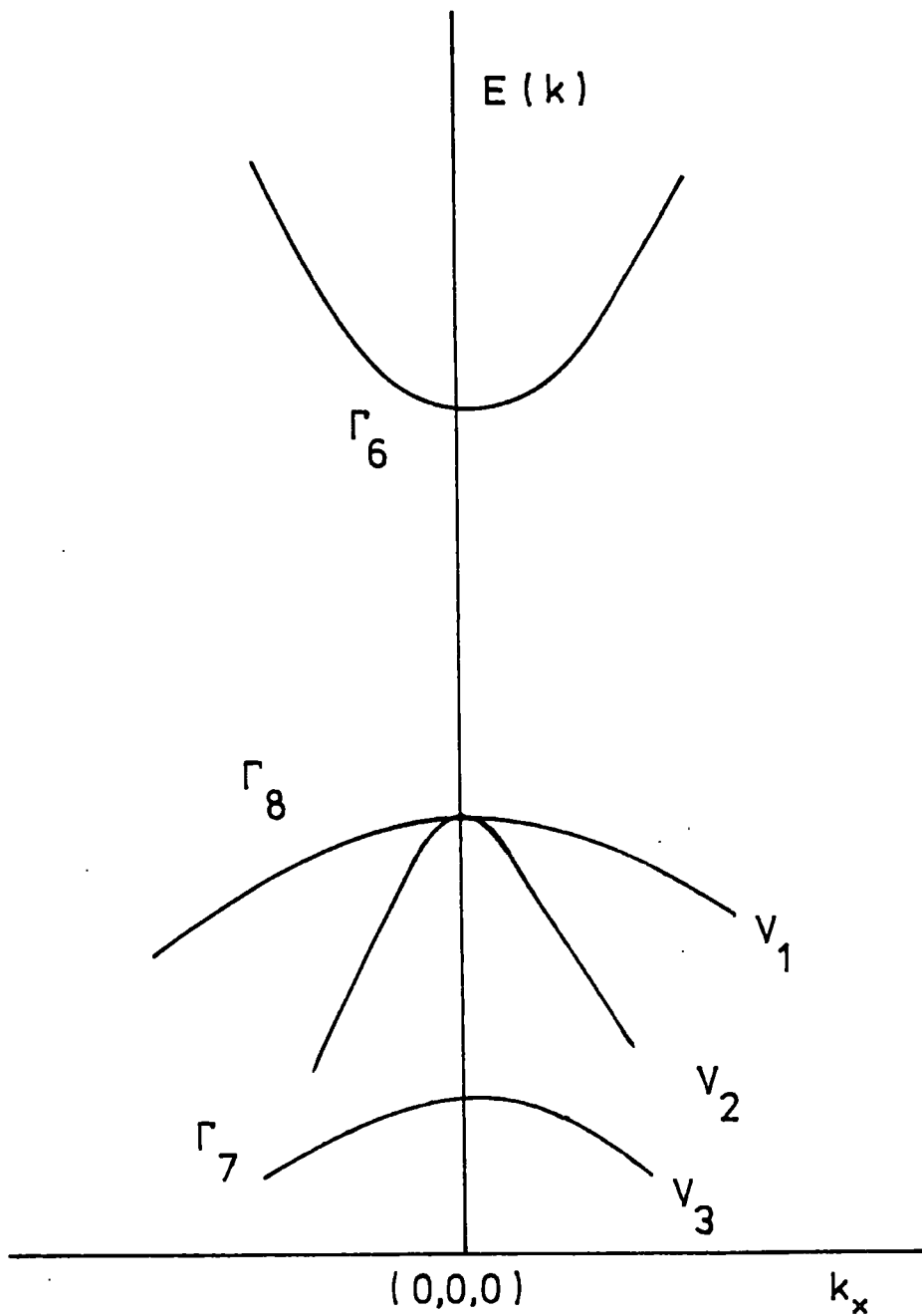


FIG 2.2a CONDUCTION AND SPIN-ORBIT SPLIT VALENCE BANDS OF A ZINC BLENDE CRYSTAL

symmetry states, namely  $L_3$  and  $X_5$  shown in the energy band diagrams.

A consideration of the results of studies on the band structure suggests certain conclusions: the band-gaps tend to widen in the sequence groups IV, III-V, II-VI and I-VII across the periodic table; the lowest conduction band states at symmetry points tend to be the s-levels for the compounds. In addition, there is a tendency for the II-VI compounds to possess a direct minimum energy gap at the  $\Gamma$ -point in the Brillouin zone; this characteristic is confirmed by experiments on the optical absorption properties. In the II-VI compounds the band-gaps generally tend to decrease with increasing atomic number. This decrease is in a large part due to the fact that the s-levels tend to be of lower energy, relative to the p- and other levels in the heavier atoms, as a result of a strong attraction to the nucleus. The band-gap energy in the II-VI compounds, from the uppermost valence band to the conduction band at the  $\Gamma$ -point ( $k = 0$ ), covers the wide range from 3.83 eV in ZnS (in the near U.V.) to 1.59 eV in CdTe (in the red region of the visible spectrum), see Figure 2.3.

### 2.3 Edge Emission

The luminescent emission from semiconductors may be divided into two categories, edge emission and deep centre emission. Edge emission is the term used to cover the radiation which occurs with a photon energy close to that of the band-gap of the material. This emission, which often occurs with the simultaneous emission of phonons, was first reported by Ewles (1938) and Kröger (1940). The radiation can usually be observed at 77 K, but is more readily observable at liquid helium temperatures using high intensity excitation. Three different recombination processes are termed as edge emission, namely: free exciton,

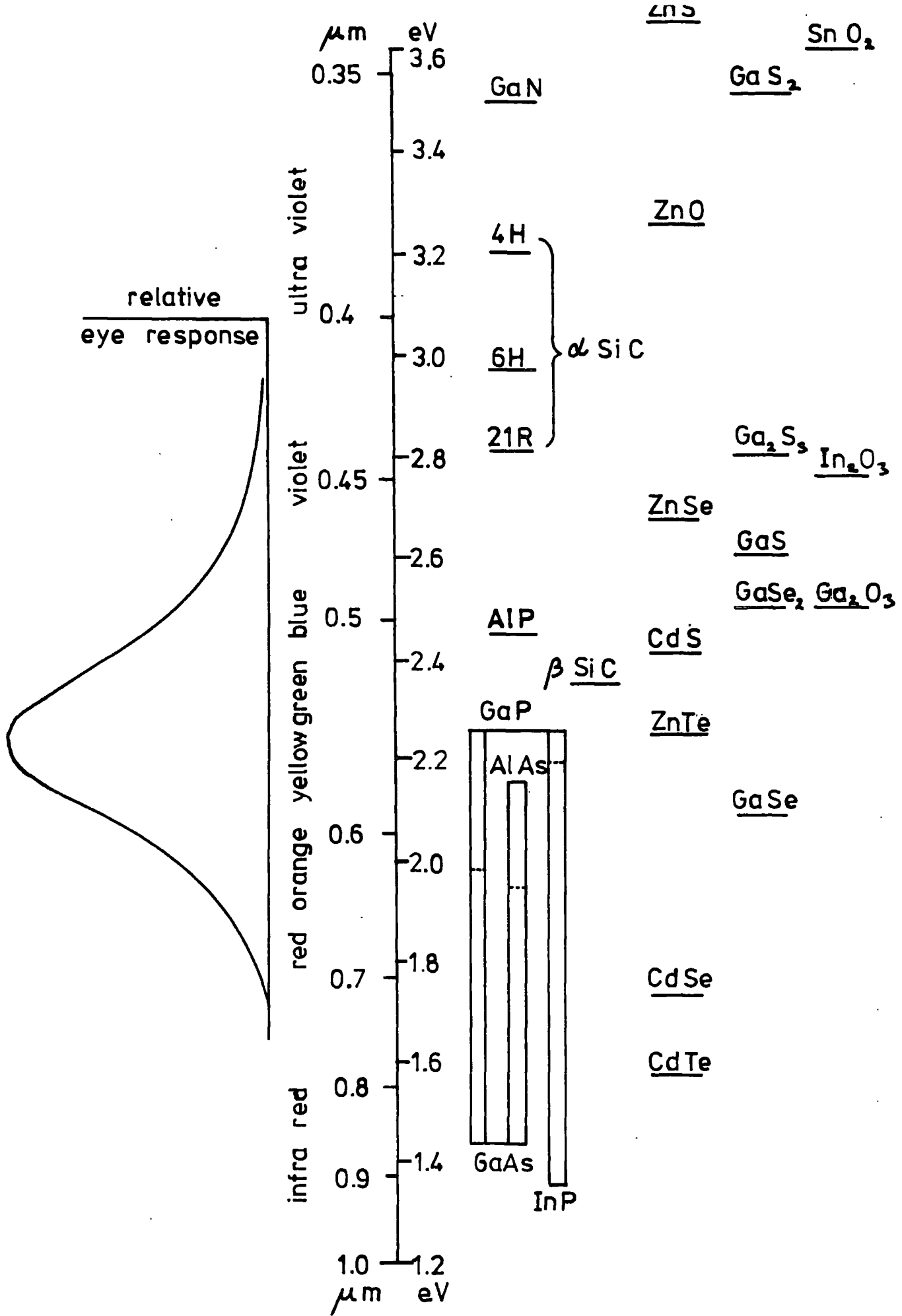


FIG 2.3 RELATIVE BANDGAPS OF VARIOUS SEMICONDUCTORS

bound exciton and distant pair recombination. Normally this emission is quenched in materials to which activator type impurities have been added; these impurities produce levels close to the valence band and lead to deep centre emission.

The most extensive studies of edge emission have been made on cadmium sulphide (Klick 1953, Thomas and Hopfield 1962). The high energy, green edge-emission consists of a series of very narrow lines with half-width approximately 0.005 eV; this emission has been attributed to the recombination of free and bound excitons. Pedrotti and Reynolds (1960) suggested that the most intense peak in the CdS emission at 4.2 K was due to pair emission, which they associated with the recombination between an electron bound to a shallow donor and a hole bound to an acceptor level above the valence band. The associated pair emission diminishes in intensity at temperatures above 4.2 K, since the donor levels are emptied, and the dominant emission results from recombination between free electrons and bound holes.

### 2.3.1 Exciton emission

The absorption by a crystal of energy in excess of the band-gap causes the generation of electron-hole pairs; electrons are excited from states in the valence band to states in the conduction band. The electron-hole pair may become bound due to the coulombic interaction between them. This attraction results in the formation of an exciton possessing an energy slightly below that of the band gap. Excitons can be regarded as the excited states of the host crystal lattice but, unlike the excited states of an isolated atom, they are not localised and possess well defined wave-vectors. Excitons are electrically neutral and have short life-times ( $10^{-8}$  sec in CdS) after which they

make a radiative recombination producing exciton emission in the vicinity of the band-edge.

An exciton can exist either as a free entity, which may move through the lattice and interact with phonons, or as a state bound to a native defect or impurity level. Bound excitons emit radiation lower in energy than free excitons upon recombination, the difference being the energy binding the exciton to the defect. The emission bands associated with the free exciton possess a half-width of approximately 1.0 meV, ten times wider than for bound exciton emission. The bound excitons become thermally freed as the temperature is raised above liquid helium temperatures, and free exciton recombination tends to dominate the emission.

The energy of the photon emitted when a free exciton recombines is equal to the band-gap energy less the binding energy of the exciton. The binding energy of the exciton may be calculated using a simple hydrogen model, taking the electron and hole to orbit about each other at distances large compared with atomic dimensions. The allowed energies of free excitons can be represented by a set of levels with a series limit which coincides with the bottom of the conduction band. The emission energies are given by

$$h \nu_n = h \nu_\infty - \frac{R}{K^2} \cdot \frac{\mu}{m} \cdot \frac{1}{n^2}, \quad n = 1, 2, \dots \quad (2.1)$$

where  $\mu$  is the reduced mass of an exciton,  $K$  is the dielectric constant of the material,  $R$  is the Rydberg constant,  $m$  is the free electron mass and  $h \nu_\infty \equiv E_g$  is the energy-gap of the material, see Figure 2.4.

The ground and excited states of an exciton can be found experimentally from absorption, reflection and emission measurements. Aven et al (1961) measured the reflectivity and absorption of cubic zinc

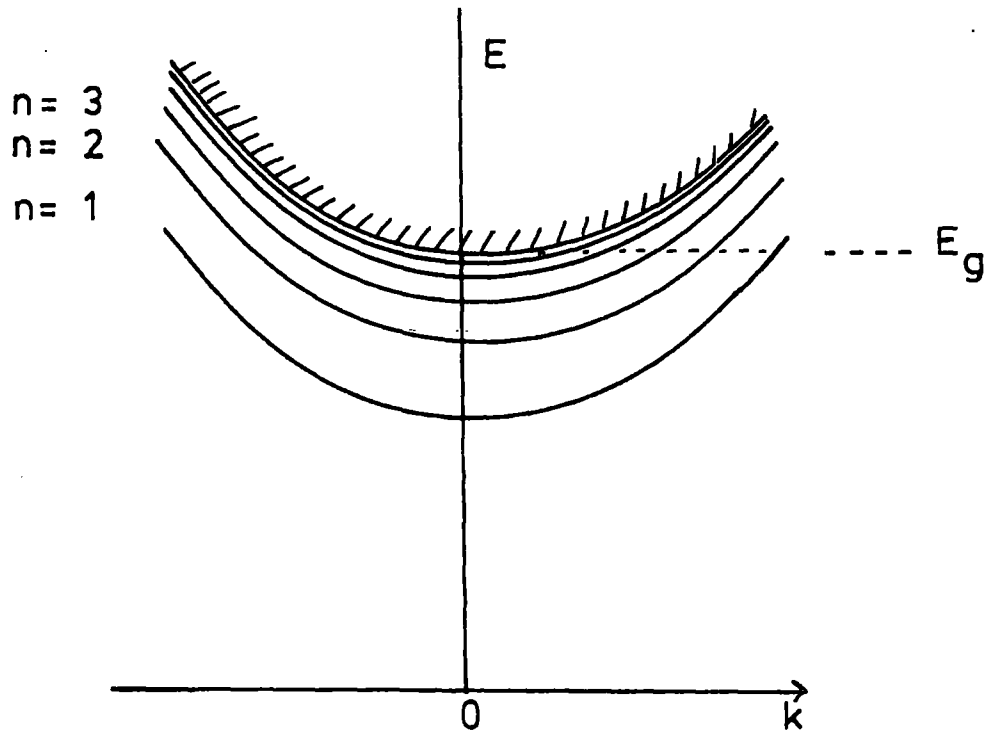


FIG 2.4 ENERGY OF EXCITON BANDS AS A FUNCTION OF EXCITON MOMENTUM  $k$

I	II	III	IV	V	VI	VII
		B	C	N	O	F
		Al	Si	P	S	Cl
Cu	Zn	Ga	Ge	As	Se	Br
Ag	Cd	In	Sn	Sb	Te	I
Au	Hg					

FIG 2.5 PORTION OF PERIODIC TABLE SHOWING ACTIVATOR COACTIVATOR, AND HOST LATTICE ATOMS

selenide, and observed the ground ( $n=1$ ) state of the exciton 2.81 eV above the valence band. Lempicki et al (1961) measured the reflectance of cubic zinc sulphide crystals at 14 K; they observed the characteristic direct exciton lines and attributed the lowest energy line (3.799 eV) to be the ground state.

Bound excitons are usually observed in the presence of ionised and neutral crystal defects. The bound excitons observed in CdS have been extensively examined, and Thomas and Hopfield (1962) have postulated four excitonic complexes giving rise to emission lines referred to as  $I_1$ ,  $I_2$ ,  $I_3$  and  $I_4$ . These correspond to excitons bound to neutral acceptors and donors, and ionized donors and acceptors, respectively. The ionisation energy  $E_i$  for the bound exciton is given by  $E_i = E_{ex} + E_b$ , where  $E_{ex}$  is the free exciton binding energy and  $E_b$  is the additional energy binding the free exciton to the centre.

### 2.3.2 Donor-Acceptor Pair emission

The model of donor-acceptor pair emission was first suggested by Prener and Williams (1956) in order to explain the broad green and red luminescence bands observed in ZnS. In this model, recombination takes place between an electron on a donor and a hole on an acceptor. The energy separating the pair of states is modified by a coulombic interaction and is given by

$$E(r) = E_g - (E_a + E_d) + \frac{e^2}{K r} \quad (2.2)$$

where  $E_g$  is the band gap energy,  $E_a$  and  $E_d$  are the ionisation energies of the isolated acceptors and donors respectively,  $r$  is the donor-acceptor spacing,  $K$  is the dielectric constant and  $e$  is the electronic

charge. The values of  $r$  are discretely distributed, since the possible sites for the donor and acceptor are restricted by the crystal structure, and an emission spectrum consisting of discrete lines results. Evidence for this model was obtained by Hopfield et al (1963) and Thomas et al (1964) who observed the characteristic line structure resulting from many different discrete pairs in gallium phosphide.

Transitions between the close pairs are more probable than transitions between distant pairs. At large separations ( $> 40 \text{ \AA}$ ) the emission lines overlap to form a broad spectral band. The life-time of the pairs varies with separation, and hence time-resolved-spectroscopy is an effective method for investigating the pair emission process. The spectral distribution of a decaying pair band after flash excitation will shift to lower energies. This is a consequence of the more rapid decay of the pairs with smaller separations which contribute the higher energy photons. The pairs with large  $r$  with the longer decay times are saturated with increasing excitation intensity. This results in a shift of the pair emission band to higher energies with increasing excitation intensity.

#### 2.4 Deep Centre Emission

In many of the wider band-gap II-VI compounds it has long been the practice to enhance the luminescent properties by the inclusion of certain impurities. Metallic impurities, such as copper, silver and gold, were found to produce activator levels above the valence band (Aven and Potter 1958) and other impurities, such as the halogens, aluminium, indium and gallium, produce coactivator levels below the conduction band. A possible explanation of the role of activators and coactivators, in terms of a charge compensation mechanism, was first proposed by Kröger

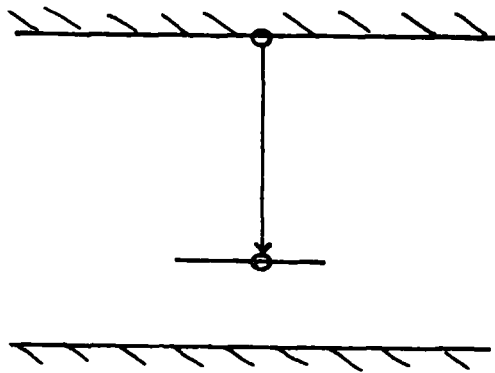
and Hellingman (1949): The relationship of the activator and coactivator impurities to acceptors and donors was pointed out by Klasens (1953), Bowers and Melamed (1955) and Prener and Williams (1956). This relationship is demonstrated in Figure 2.5: the activator impurities Cu, Ag and Au when substituted for Zn, Cd or Hg, or P, As and Sb when substituted for S, Se or Te, would be expected to act as acceptors. Analogously the coactivators Cl, Br or I at anion sites or Al, Ga at cation sites, would be expected to have donor properties. These donor and acceptor defects could then give rise to localised levels near the conduction or valence bands, respectively.

It was initially believed that the recombination of the photo-generated electrons or holes with the opposite carrier trapped at activator or coactivator levels gave rise to the observed luminescence bands. Now, however, the luminescence centres are considered to be more complex than compensated, isolated, randomly distributed donor or acceptor impurities at substitutional sites. In addition to defects created by deliberately added impurities, there exist natural defects such as zinc and sulphur or selenium vacancies which produce self-activation and coactivation in the II-VI compounds. The zinc and sulphur (selenium) vacancies behave as double acceptor and double donor impurities, respectively. Incorporation of either activator or coactivator impurities can lead to self-compensation by lattice defects which themselves may give rise to localised levels. Association at near neighbour sites of the activator or coactivator impurities with sulphur or zinc vacancies, respectively, is thought to be responsible for two of the observed luminescence bands in II-VI compounds. Where specific activator and coactivator impurities are introduced together in II-VI compounds, the observed luminescence bands have been shown to depend on the absolute and relative concentration

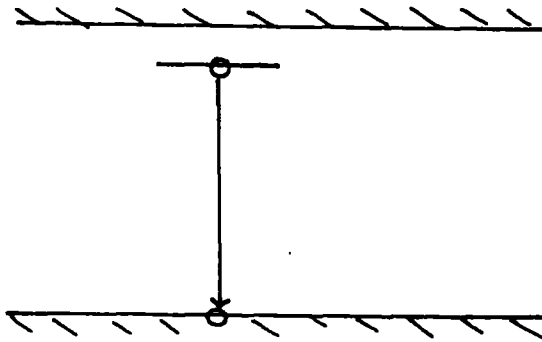
of the two impurities. Van Gool (1961) has carried out much work on ZnS in relation to the doping with copper, and this will be discussed further in a later section.

There are three basic models for interpreting the non-localised luminescent transitions, that is the emission resulting from the radiative recombination of free carriers with electrons and holes at defect levels located in the forbidden energy gap; these defect levels are positioned at a greater depth than the hydrogenic levels already described in these compounds. The mechanisms of the three emission processes are illustrated in Figure 2.6. According to the Schön-Klasens model (Schön 1942, 1948; Klasens 1946, 1953) the luminescence results from the radiative recombination of a photo-generated electron in the conduction band with a hole trapped at a localised acceptor-like level above the valence band. The Lambe-Klick model (Lambe and Klick 1955) describes the luminescence transition due to the recombination of a hole in the valence band with an electron trapped at a level below the conduction band. The third model proposed by Prener and Williams (1956), describes the luminescence as being due to a localised electron transition within the associated pair formed by the association between compensated donor- and acceptor-type impurities at various interatomic distances.

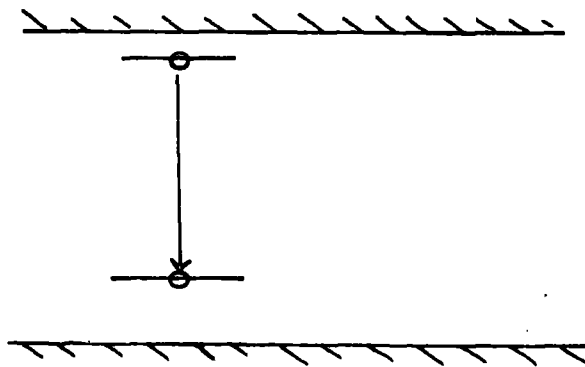
The luminescence emission from ZnS has received wide attention, and the results obtained have been shown to apply generally to most of the II-VI compounds. Shionoya et al (1964) have reported the temperature dependence of the peak energies and half-widths of various luminescences observed in ZnS, see Figure 2.7. These authors pointed out that the luminescence emissions may be divided into two groups; one including the copper-green and copper-blue emission, and the other including the self-activated and copper-red emissions. In the first group, the



a) Schön - Klasens model



b) Lambe - Klick model



c) Prener - Williams model

FIG 2.6 schematic representation of models for radiative transition processes

emission peak generally shifts to lower energies with increasing temperature, in the direction of the variation of the band-gap energy, and the half-widths have values of 0.2 to 0.3 eV which increase slightly with temperature. In the second group, the emission peak shifts towards higher energies with increasing temperature, and the half-widths have values of 0.3 to 0.5 eV at low temperature and increase markedly with temperature as  $T^{\frac{1}{2}}$ ; this behaviour of half-width and peak position with temperature may be explained by applying the configurational coordinate model. This model is used to describe optical transitions within localised centres, such as transition metal ions, and will be described later.

#### 2.5 Self-Activated Emission

As has been mentioned, crystal defects in the II-VI compounds produce self-activated and coactivated levels near the valence and conduction bands respectively, due to the creation of anion and cation compensating vacancies and interstitials. The exact position of the self-activated luminescence band has been shown to be dependent on the nature of the added coactivator impurity, for example Cl, Br, I, Al or Ga. Van Gool (1961) has shown that in ZnS the peak wavelength varies with coactivator impurity type from 4560 to 4710 Å at 80 K. A similar behaviour has been reported in ZnSe (Holton et al 1965) and in CdS, ZnTe and CdTe (Halsted et al 1965).

The mechanism of the self-activated luminescence in II-VI compounds has not been generally resolved. However, much work has been done on ZnS and a consistent interpretation of the self-activated luminescence has been achieved on the basis of a single model. The fact that a variety of different coactivator impurities produced similar

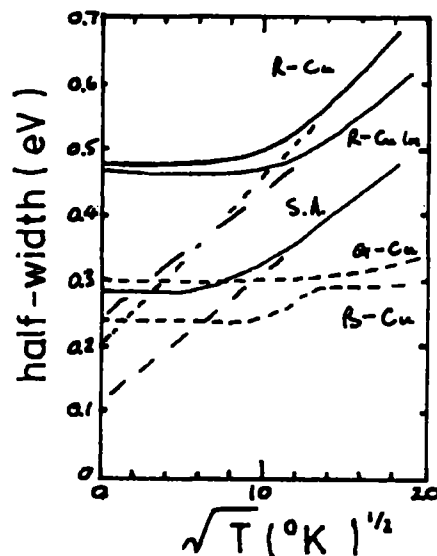
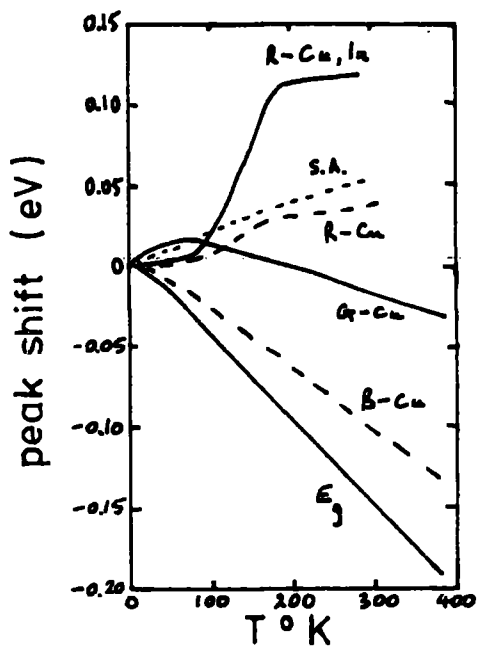


FIG 2.7 dependence of peak position and halfwidth of ZnS emissions on temperature

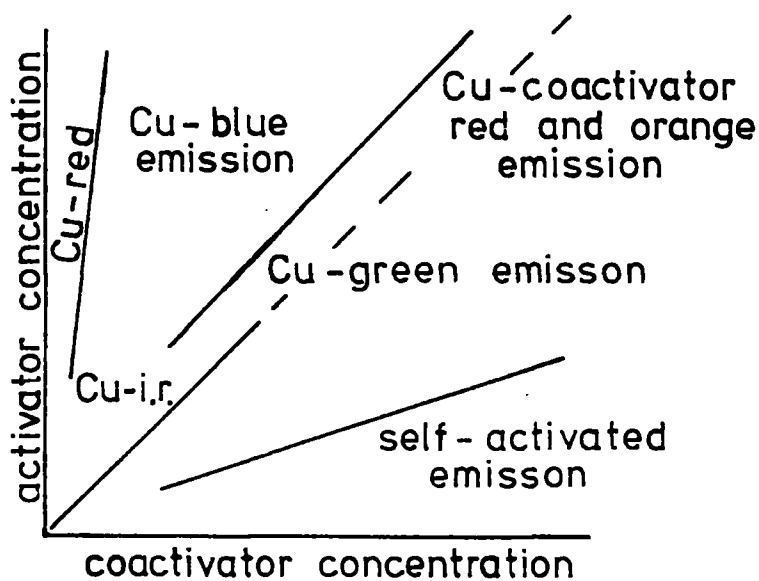


FIG 2.8 dependence of luminescence of ZnS on Cu and coactivator concentration

emission bands caused Kröger and Vink (1954) to suggest that the luminescence centre was a zinc vacancy with a hole trapped in its vicinity ( $V_{Zn}^-$ ). This defect was formed in order to compensate the effective single positive charge of the coactivator. Magnetic susceptibility measurements caused this model to be modified, and Prener and Williams (1956) suggested that the luminescence centre consisted of an association at nearest neighbour sites of the doubly-ionised zinc acceptor vacancy defect ( $V_{Zn}^{2-}$ ) and the ionised impurity donor. This association resulted in a complex such as  $(V_{Zn} \cdot Cl)^-$ , with an effective single negative charge; the complex was considered to behave as a compensated singly-ionisable acceptor introducing a localised level above the valence band. The excitation and luminescence were explained in terms of the Schön-Klasens model as a transition between the conduction band and this localised level. A similar analysis has also been applied by Holton et al (1965) to the self-activated emission in ZnSe. Koda and Shionoya (1964, 1965) investigated the polarisation of the self-activated luminescence in cubic zinc sulphide crystals doped with chlorine. They found that the luminescence showed particular polarisation properties specific to  $C_{3v}$  symmetry which tended to confirm a localised centre of the form  $(Cl_S - V_{Zn})$ . Physically the luminescence transition was pictured as a localised transition between a donor-like upper level, due to the chlorine at a sulphur site, and the ground acceptor-like level due to the zinc vacancy. Shionoya et al (1965) measured the decay characteristics of the self-activated emission and found a monomolecular decay, characteristic of a localised transition.

Self-activated emission in ZnSe has been reported at wavelengths in the orange spectral region between 6020 and 6450 Å. There is some uncertainty about the position of this band and the nature of the centre

responsible has not been resolved. By comparison, the self-activated emission in ZnS occurs in the blue region in the range from 4560 to 4710 Å. Lehmann (1967) has reported that in mixed phosphors of ZnS-ZnSe:Br the blue emission band is gradually replaced by a second band in the green-orange region as the Se content is increased, and that the green band appears with the addition of as little as 1% Se. Ozawa and Hersh (1973) observed that the S.A. band in crystals of Zn(S,Se):I jumped from the blue spectral region in ZnS to the green region when small amounts of ZnSe were added. These authors concluded that there were different self-activated centres involved in ZnS and in Zn(S,Se) alloys. The emission processes in the Zn(S,Se) mixed alloys have not been resolved.

## 2.6 Copper-Activated Emission

Copper activation is probably the most widely used form of sensitisation in producing efficient practical phosphors, and copper is also often unintentionally present as an impurity. The luminescent properties of copper as an activator have been most widely studied in ZnS. Van Gool (1961) has investigated in great detail the fluorescent emission of copper-activated ZnS with both halide and aluminium co-activation. He observed that the emission bands are dependent on the ratio of activator to co-activator concentrations, see Figure 2.8. Copper in ZnS produces four main emission bands in the blue, green, red and infra-red spectral regions. The copper-green and blue emissions are sensitive to small changes in copper concentration, the presence of excess copper relative to the added co-activator concentration enhances the dominance of the blue band. At 85 K, this blue band has a maximum between 4300 and 4440 Å and the green band between 5160 and 5250 Å;

the actual values depend on whether a group III or group VII co-activator is present, and in addition may be due to the fact that the emission consists of a number of unresolvable sub-bands. The distinct difference between the copper-blue and self-activated blue emissions was demonstrated by Shrader and Larach (1956) who reported that the maxima of the two emission bands moved in opposite directions with changing temperature; the copper-blue, and the copper-green, moving to higher energy with decreasing temperature.

The mechanism associated with the copper-blue and green emissions has not been resolved. Curie (1964) has suggested that the green emission results from a Prener-Williams transition between a co-activator level and an associated copper activator level. Time resolved spectroscopy on the green emission (Shionoya et al, 1966) has shown that the decay of luminescence shifts to lower energies with time delay. This tends to confirm an association model, in which the pairs separated by greater distances take longer to decay and have smaller transition energies. The copper-blue emission has been considered to result from a Schön-Klasens transition to the same centre associated with the copper-green emission (G. and D. Curie 1960). An alternative model was proposed (Broser and Schulz 1961) in which the two bands of emission were considered to result from Schön-Klasens transitions to different ionisation states of the copper centre.

In ZnSe the wavelengths of the emission bands associated with copper have been established as 5300 Å in the green, and 6360 Å, in the red at 85 K (Halsted et al 1965). These bands have been considered to be equivalent to the copper-blue and copper-green emission, respectively, in ZnS. Morehead (1963) investigated the luminescence of Zn(S,Se):Cu,Cl phosphors and concluded that the emissions could be

explained with a modified Schön-Klasens model with recombination to two of the three possible states of a single, doubly-ionisable centre. Lehmann (1966) observed that in Zn(S,Se):Cu,Cl the blue and green emissions at 4440 Å and 5280 Å in ZnS were replaced by bands at 4770 Å and 5530 Å, respectively, when less than 1% of ZnSe was incorporated; further increase in the proportion of ZnSe caused only a slow shift towards the positions observed in ZnSe:Cu,Cl. From this it may be seen that the copper emission in the mixed crystals is not well understood.

Zinc sulphide containing a high ratio of copper to co-activator concentration also shows a red band of emission at 6970 Å (85 K), which shifts to shorter wavelengths on increasing the temperature; this is in contrast to the behaviour of the blue and green emissions. The centre responsible for this emission is believed to be a copper atom associated with sulphur vacancy ( $\text{Cu}_{\text{Zn}} - \text{V}_{\text{S}}$ ). Dielemann et al (1964) made E.S.R. studies of the copper-red emission and concluded that the associated centre behaves as a singly-ionisable donor defect. The emission is considered to result from a Lambe-Klick transition from the associated donor level to the valence band.

In addition to the visible luminescence, ZnS exhibits infra-red emission in bands at 1.46 μm, 1.65 μm and 1.80 μm. This emission is enhanced when the phosphor is prepared under an excess pressure of sulphur. The treatment is thought to reduce the concentration of sulphur vacancies leaving the copper in an uncompensated state. The nature of the infra-red emission has not been resolved but it is believed to involve a transition from the copper acceptor level. Suggestions have included a Lambe-Klick transition involving the ground and excited states of a hole bound to the copper impurity, and transitions between a single copper level and the spin-orbit split valence bands.

## 2.7 Configurational Co-ordinate Model

Another form of luminescence observed in the II-VI compounds is that due to localised transitions, especially those associated with ions of the transition metal elements such as manganese or the rare earths. The absorption and emission processes in this transition take place within the electronic configuration of the ion; the excited state is an electronic state of the ion, and there is no interaction with free electrons or holes. The electronic absorption and emission processes are best described by the configurational co-ordinate model which was first suggested by Seitz (1939) and was improved by Williams (1953). In this model the impurity ion is thought of as being surrounded by the neighbouring lattice ions which vibrate about it. The energy of the system is determined by the interaction of the electronic states of the impurity ion with the vibrational states of the neighbouring lattice, and can be described as a function of the configurational co-ordinate distance  $r$ , see Figure 2.9. Plotted vertically is the potential energy of the system near the impurity ion for the electron in the ground and excited states of the centre, taking into account both electronic and vibrational energy. This energy is plotted against  $r$ , which is a parameter specifying the configuration of the ions around the centre. The configurational co-ordinate curve is assumed to be parabolic, following a classical harmonic oscillation, the frequency of the simple harmonic motion being the same as the phonon frequency,  $\nu$ .

In the configuration shown in Figure 2.9, the ground and excited states of the system are represented by two parabolic curves, and the exact energy of the system is defined by the co-ordinate  $r$ . The minimum energy of the excited state is usually displaced to a

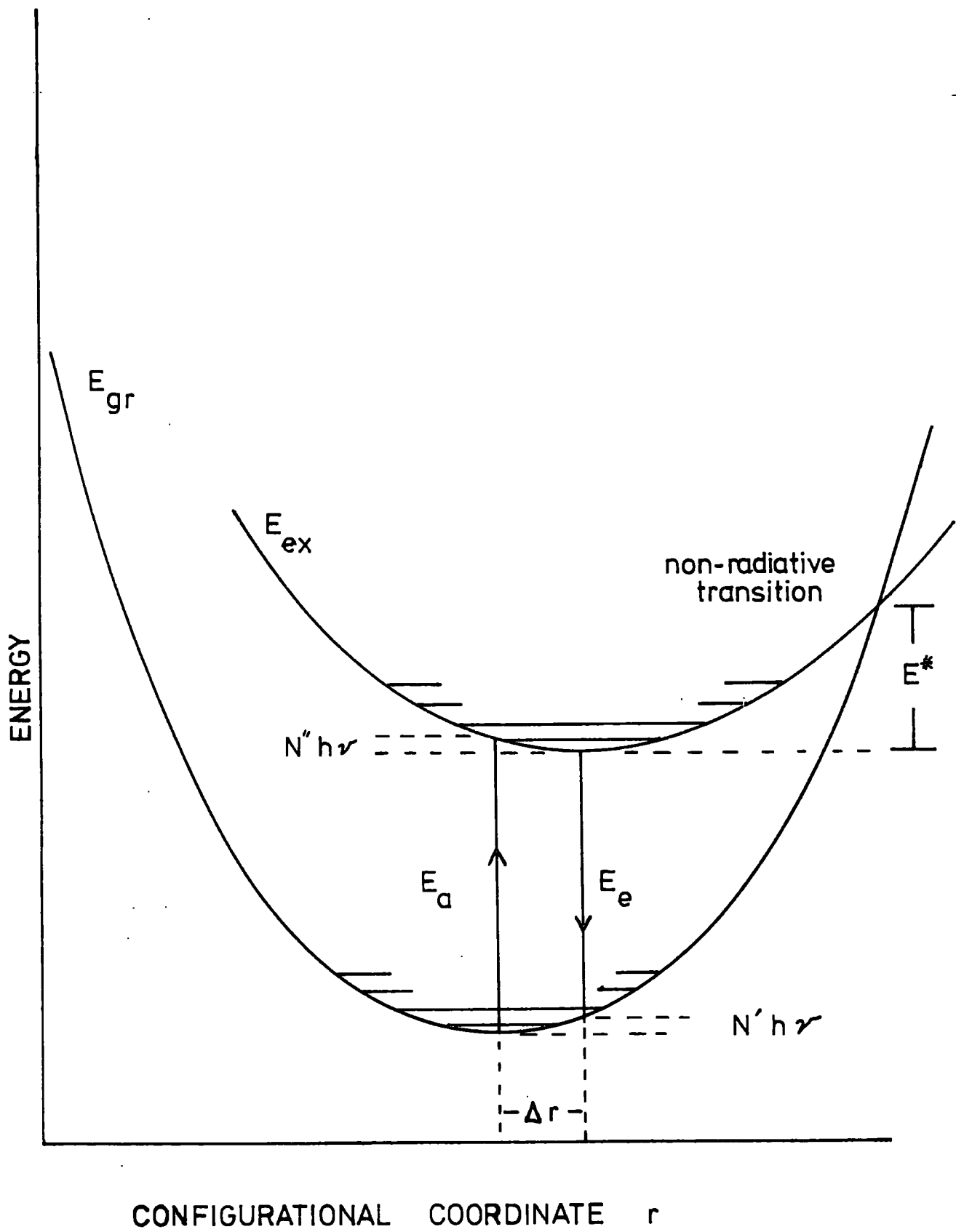


FIG 2.9 CONFIGURATIONAL COORDINATE MODEL

different value of  $r$  compared with the minimum of the ground state. According to the Frank-Condon principle, optical transitions take place in a time much shorter than the lattice takes to relax to such a change and hence absorption and emission of photons occur without configurational change. Subsequently the system can relax to the minimum energy condition by emitting phonons. As a result, the emitted photon energy is less than the absorbed photon energy, represented in the diagram by  $E_e$  and  $E_a$ . This is the well known Stokes law of fluorescence.

Since the energy of the system is quantised, the observed emission and absorption bands are in fact the envelopes of numerous lines each of which is due to a transition between one vibrational level of the excited state and one vibrational level of the ground electronic state. As the temperature is raised, more phonons can couple with the electron giving rise to a wider range of energies. The energy distribution of the electron within the vibrational states is determined by Maxwell-Boltzmann statistics, and a consequence of this distribution is that the emission band takes a Gaussian form.

One of the results of the configurational co-ordinate model is the predicted form of the temperature dependence of half-widths  $\omega(T)$  of the emission and absorption bands.

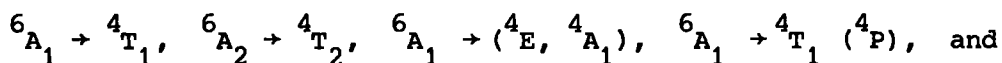
$$\omega(T) = \omega(0) \left[ \coth (h\nu / 2 kT) \right]^{\frac{1}{2}} \quad (2.3)$$

where  $\omega(T)$  is the half-width at T K, and  $h\nu$  is the phonon energy associated with the vibrational mode of the excited state. At high temperature ( $2 kT \gg h\nu$ )  $\omega(T)$  varies as  $T^{\frac{1}{2}}$ , and at low temperatures  $\omega(T)$  is independent of temperature and reduces to  $\omega(T) = \omega(0)$ . Hence measuring the variation of half-width with temperature can indicate

the nature of the type of luminescent transition and give a value for the phonon energy.

## 2.8 Manganese Emission

Manganese as an impurity in ZnS has received a great deal of attention. It is generally agreed that the manganese  $Mn^{2+}$  ion occupies substitutional zinc sites in the lattice, and gives rise to a band of orange emission centred at  $5860 \text{ \AA}$ . The radiative transition responsible for the observed emission occurs within the outermost 3d shell which is split by an interaction with the lattice. The ground state of the  $Mn^{2+}$  ion ( $3d^5$  configuration) has a spherically symmetrical  $^6S$  configuration in which all five 3d electrons have parallel spin. In the excited states, one of the electron spins is reversed giving rise to four levels  $^4G$ ,  $^4P$ ,  $^4D$  and  $^4F$ . These free ion states are split by interaction with the crystal field of the cubic lattice as shown in Figure 2.10 (Orgel 1955): the ground state is  $^6A_2(^6S)$  and the next higher states are  $^4T_1$ ,  $^4T_2$  and  $(^4E, ^4A_1)$  derived from the  $^4G$  free ion state. The observed excitation and absorption spectra (McClure 1963, Langer and Ibuki 1965) consists of five separate bands at  $5350 \text{ \AA}$ ,  $4980 \text{ \AA}$ ,  $4650 \text{ \AA}$ ,  $4300 \text{ \AA}$  and  $3900 \text{ \AA}$ , which have been attributed to transitions between the ground state and the higher states:



The radiative transition is ascribed to an electron returning from the first excited state to the ground state  $^4T_1 (^4G) \rightarrow ^6A_1 (^6S)$ .

The splitting of the electron levels of the  $Mn^{2+}$  ion is determined by the crystal-field splitting energy and this would be expected

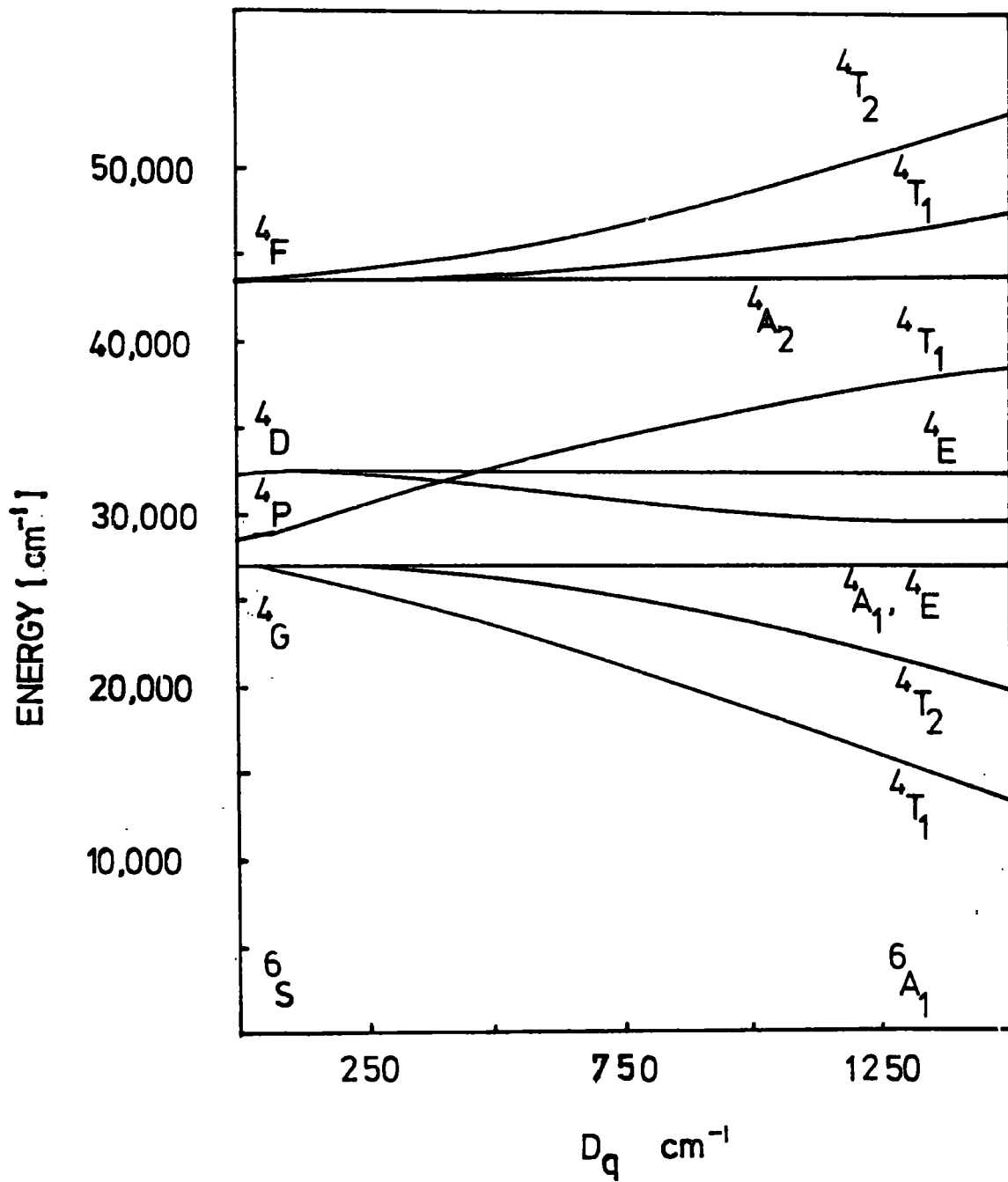


FIG2.10 ENERGY LEVEL DIAGRAM OF  $Mn^{2+}$  ION IN A CUBIC FIELD

to be similar in ZnSe to ZnS, assuming that the ion occupies an equivalent lattice site. The activation of ZnSe with manganese has received relatively little attention and there are conflicting reports of the position of the emission band between 5900 and 6400 Å (Asano et al 1968, Apperson et al 1967, Jones and Woods 1973); this variation may be due to the presence of overlapping self-activated and copper emission bands. Jones and Woods showed that a band is observed at 5860 Å when ZnSe:Mn is selectively excited in a characteristic  $Mn^{2+}$  excitation band, and that self-activated emission dominates the luminescence when u.v. excitation is used. Langer and Richter (1966) examined the absorption of ZnSe:Mn and observed two bands at 5300 Å and 4995 Å which they associated with the transitions  ${}^6A_1 \rightarrow {}^4T_1$  ( ${}^4G$ ) and  ${}^6A_1 \rightarrow {}^4T_2$  ( ${}^4G$ ). Asano et al also studied phosphors of Zn(S,Se) doped with manganese and reported that the emission shifted non-linearly from 6500 Å in ZnSe:Mn to 5900 Å in ZnS:Mn. They associated this behaviour with a varying arrangement of sulphur and selenium ions around the  $Mn^{2+}$  ion which altered with composition. From this it can be seen that there is uncertainty concerning the position of the manganese emission in ZnSe and Zn(S,Se).

Whilst excitation and absorption measurements give consistent values for the separation of the electron levels within the  $Mn^{2+}$  ion, there is no agreement on the position of the  ${}^6A_1$  ground state relative to the band edges of the host lattice. Gumlich et al (1963), using an energy cycle method, placed the ground state 10 eV below the valence band edge in ZnS, while Allen (1964) using crystal field theory concluded that the ground state of  $Mn^{2+}$  lies some tenths of an eV above the valence band. Braun et al (1972) using photocapacitance measurements placed the ground state of  $Mn^{2+}$  in ZnSe some

0.6 eV above the balance band. Hence it can be seen that the position of the ground state has not been resolved.

## 2.9 Polarisation of luminescence

Measurement of the polarisation of luminescence can give useful information concerning the nature and symmetry of luminescence centres. For example, Lempicki (1959,1960) observed that the copper-blue emission from hexagonal ZnS:Cu crystals is polarised preferentially perpendicular to the c-axis independently of whether the excitation is polarised. Koda and Shionoya (1963,1964) examined the polarisation of the self-activated luminescence in cubic ZnS:Cl crystals and observed a particular polarisation of the luminescence if polarised characteristic excitation was used. There was no polarisation of the luminescence if the excitation was unpolarised.

The polarisation properties may be categorised into two types: one which is independent of the state of polarisation of the exciting light, and the other which is dependent on it. An examination of different emissions has shown that the copper-blue and copper-green bands in ZnS are of the first type and that the self-activated emission and copper red bands in ZnS are of the second.

### 2.9.1 Self-activated Luminescence

Koda and Shionoya (1963,1964) examined the azimuthal dependence of the degree of polarisation of the luminescence in crystals of ZnS:Cl under different conditions, varying the wavelength and polarisation of the excitation. The experimental results indicated that there were two characteristic excitation bands for the polarisation spectra at 3.42 eV and 3.76 eV, and that the second band produced

negative values for the polarisation  $P(\theta)$ , where

$$P(\theta) = \left[ (I_{\parallel} - I_{\perp}) / (I_{\parallel} + I_{\perp}) \right]_{\theta} \quad (2.4)$$

and  $I_{\parallel}$  and  $I_{\perp}$  are the emission intensities measured with the analyser parallel and perpendicular to the polariser, respectively, and  $\theta$  is the angle between the optical axis of the polariser and a particular crystal axis. The existence of the second excitation band was interpreted as indicating that the transition involved a dipole oriented perpendicular to the dipole emitting the luminescence. From the azimuthal dependence of the polarisation  $P(\theta)$ , it was concluded that the polarisation of the self-activated centre is caused by the local symmetry possessed by the centre. This local symmetry is of a lower order than that of the host lattice. Koda and Shionoya considered that the luminescence centre could be described in terms of  $\pi$  and  $\sigma$  electric dipole oscillators oriented along the  $\langle 111 \rangle$  axis in the ZnS cubic lattice, see Figure 2.11. By  $\pi$  or  $\sigma$  oscillator is meant a dipole in which charge is oscillating linearly along the dipole axis or circulating around it, respectively. This suggestion is in agreement with the model for the self-activated centre proposed by Prener and Williams (1956) that the centre is a zinc vacancy with its two holes ionised, and with one of its two charge compensating halogen ions occupying one of the nearest neighbour sites. According to this model the centre should have the axial symmetry of  $C_{3v}$ , and each energy state of the centre should belong to one of the irreducible representations,  $A_1$ ,  $A_2$  or E of the  $C_{3v}$  group. A Group theoretical treatment indicates that optical dipole transitions are allowed in  $A_1 \leftrightarrow A_1$  for linearly polarised light along the symmetry axis, and  $A_1 \leftrightarrow E$  for circularly polarised light around the axis. These two

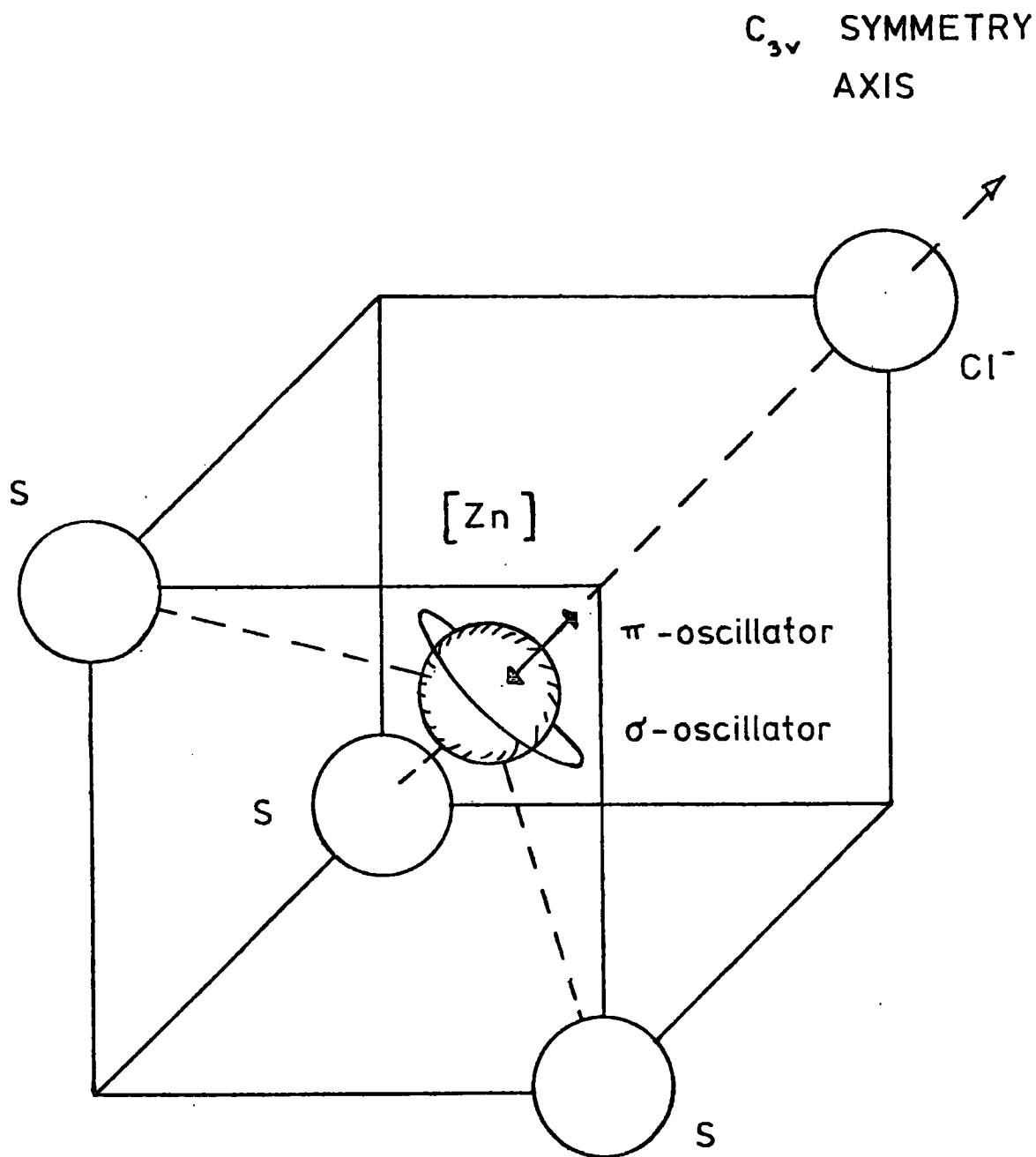


FIG 2.11 ASSOCIATION MODEL FOR SELF-ACTIVATED  
LUMINESCENCE CENTRE IN CUBIC  $ZnS:Cl$

kinds of transition are equivalent to the classic  $\pi$  and  $\sigma$  electric dipoles, see Figure 2.11.

### 2.9.2 Copper-blue and green emissions

In hexagonal ZnS:Cu crystals both the copper-blue (see Lempicki 1959,1960) and copper-green (Shionoya et al 1965) emissions are polarised preferentially perpendicular to the c-axis regardless of whether the excitation is polarised; the polarisation of the luminescence is also independent of whether characteristic or host excitation radiation is used. The ratio of the intensity of the emission with  $\underline{E} \perp c$  to that with  $\underline{E} // c$  for both luminescence bands has been shown to be in the range 1.2 to 1.4 approximately, and the ratio increases slightly with decreasing temperature. Lempicki concluded from a theoretical analysis that his results for the copper-blue luminescence cannot be interpreted on the assumption that the luminescence is caused by an electric oscillator which is fixed in the centre and has some anisotropic orientation. Birman (1959,1960) pointed out that this polarisation may be interpreted by attributing it to the symmetry nature of the energy bands of the hexagonal host lattice and the selection rules associated with it. He presented several models for the transitions in terms of the Schön-Klasens and Lambe-Klick models predicting polarisation perpendicular to the c-axis. In the Lambe-Klick model it was assumed that transitions occurred between the luminescence centre and the  $\Gamma_9$ ,  $\Gamma_7$  levels of the split valence band; in the Schön-Klasens model it was assumed that the luminescence centre possesses a structure which is a duplicate of the split valence band, and that transitions occurred between the conduction band and the split levels of the centre. An examination of the polarisation properties in terms of the two models

indicates (Shionoya 1965) that a simple Lambe-Klick model cannot be applied to both the copper-blue and copper-green centres, and Shionoya has suggested that both emissions may be described in terms of the Schön-Klasens model.

## 2.10 Electron Spin Resonance

Electron Spin Resonance (E.S.R.) is a technique which is proving to be a useful method for investigating the atomic environment of an impurity or defect in the II-VI compounds. E.S.R. measurements can confirm the various models for the luminescence centres which are inferred from optical and electrical measurements. The bonding in the II-VI compounds is partly ionic and partly covalent, but the spins of the bonding electrons are paired and as a result there is no net spin for the electrons. Hence, the perfect lattice, free of impurities and defects, is diamagnetic. The inclusion of defects and impurities causes a perturbation in the surroundings of the defect. This irregularity may upset the pairing of the spins of the bonding electrons and introduce a paramagnetic character which can be detected by E.S.R. Transition metal ions possess a natural paramagnetic character due to the unpaired d and f electrons in the core of the atom; E.S.R. measurements can be made, therefore, in the study of these defects.

The bonding electrons in many defects may become paired because of the tendency for defects in II-VI compounds to be compensated. This leads to no paramagnetic moment being present. The effect can be overcome by optically exciting the defect to create an electron-hole pair and leave an unpaired electron or hole on the defect. It is a necessary condition when optical excitation is used, that the lifetime of the trapped electron or hole should be long. There are two reasons for

this; (1) the number of unpaired defects must be greater than the minimum number detectable by the apparatus. The number of such sites is determined by the intensity of the optical excitation and the lifetime of the electron or hole on the defect. (2) The lifetime must be longer than the spin lattice relaxation time, which is a measure of the time it takes for an electron to relax to its ground magnetic state when excited by resonance to an excited magnetic state. It is possible to obtain information about the defect by monitoring the intensity of the E.S.R. spectrum as a function of the optical excitation wavelength, and comparing the result with the luminescence excitation spectra.

For a paramagnetic centre in a solid, there is an interaction between the ion and the crystalline electric field produced by the charges on the diamagnetic neighbours in the lattice. Because of this interaction the energy levels of the ion in the solid are different from those in the free ion and are dependent on the local symmetry of the paramagnetic ion. As a result the E.S.R. spectra can give information about the local environment of the paramagnetic ion. Hyperfine interactions may occur between the spin on the ion and the nuclear spins on neighbouring lattice sites. This can give information about the nature of the ions in the vicinity of the paramagnetic centre.

E.S.R. studies have been made of the self-activated defect in ZnS, and Kasai and Otomo (1961,1962) have reported an E.S.R. absorption in ZnS:Cl and ZnS:Br when excited with ultra-violet light. The paramagnetic state of the self-activated centre is produced when holes are trapped on the centre and electrons are trapped at a compensating defect or impurity. The observed E.S.R. spectra showed symmetry about the  $\langle 111 \rangle$  axis and were interpreted in terms of the model proposed by Prener and Williams (1956), see Figure 2.11. Holton et al (1965) and

Schneider et al (1965) have observed hyperfine structure in the E.S.R. spectra which were attributed to the presence of Ga, Br and I in the vicinity of the paramagnetic defect.

In ZnS five resonances have been identified as involving a copper impurity (Holton et al 1964), two of which are photosensitive and occur in crystals showing characteristic copper-luminescence. Dielemann et al (1964) have observed a resonance due to an association of a sulphur vacancy and a copper impurity in ZnS. An interpretation of the E.S.R. spectra observed due to the presence of copper may lead to more information concerning the nature of the complexes formed.

#### 2.11 Thermal Quenching

In general, the intensity of emission from a phosphor is found to be temperature dependent, and decreases with increasing temperature. This process is mainly caused by an increase in non-radiative transitions and is referred to as thermal quenching. In terms of a non-localised transition of the Schön-Klasens type, the quenching process may be envisaged as an electron being thermally excited from the valence band to fill an empty activator state. This prevents an electron in the conduction band making a radiative transition to the activator centre. Similarly, in a Lambe-Klick transition, an electron at a co-activator centre may be thermally excited to the conduction band before it has sufficient time to recombine with a free hole. In the case of a localised transition, the quenching may be explained in terms of the configurational co-ordinate model, see Figure 2.9.: the ground and excited states are represented as crossing at some point at an energy  $E^*$  above the minimum of the excited state. When the temperature is raised the electron can reach this cross-over energy and

return to the ground state non-radiatively.

When the temperature of a phosphor is raised beyond a certain point, the luminescence efficiency is observed to decay exponentially. The variation of the luminescence efficiency with temperature (T) is given by

$$\eta = \left[ 1 + C \exp \left( \frac{-E}{kT} \right) \right]^{-1} \quad 2.5$$

where C is a constant and E is the activation energy. For the non-localised transitions of the Schön-Klasens or Lambe-Klick types, the activation energy represents the separation of the activator state from the valence band and of the co-activator state from the conduction band, respectively. For the localised transition, the activation energy is represented by E\* on the configurational co-ordinate diagram. By making measurements of the thermal quenching of luminescence it is possible to obtain values for the activation energy.

The quenching transition may also be excited by optical means. Infra-red radiation can excite electrons to luminescence centres causing a reduction in the emission efficiency. In practice, the measured optical and thermal activation energies are not equivalent. This difference can be explained in terms of the Frank-Condon principle which states that there is insufficient time during an optical transition for the lattice to adjust to a change of energy, whereas the lattice may relax during a thermal transition requiring less energy for excitation. As a result, the measured optical quenching energies are higher than the equivalent thermal quenching energies.

#### 2.12 Auger Effect

In many semi-conductors the non-radiative transition is the

dominant recombination process. It has been calculated that in germanium the non-radiative recombination process is at least a thousand times more probable than the radiative transition. The term non-radiative recombination describes the process in which an excited state returns to the ground state releasing the difference in energy by a means which does not involve the emission of a photon. In the Auger effect, the energy released by a recombining electron is immediately absorbed by another electron which then dissipates this energy by emitting phonons. This process involves the interaction of two electrons and a hole and the three-body collision results in no net photon emission. In an n-type material where electrons are the majority carriers, the second electron transforms the energy which it absorbs from the recombination transition into kinetic energy, by being excited high into the conduction band; in a p-type material, the second electron is excited from deep in the valence band, this can also be considered to be a hole being excited deep into the valence band. Since the Auger effect is dependent on a carrier-carrier interaction, the effect should become more intense as the carrier concentration increases. It would be expected, therefore, that the Auger effect would increase as a function of temperature and concentration of donors or acceptors.

The Auger effect has been used in a model to explain the quenching of manganese luminescence in zinc treated zinc selenide. Jones and Woods (1973) and Allen et al (1973) have reported that the characteristic  $Mn^{2+}$  emission at  $5860 \text{ \AA}$  in ZnSe was not observed following annealing in zinc, although the manganese was shown to be still present. The effect of heating in liquid zinc is to increase the conductivity of the material by many orders of magnitude by decreasing the concentration of acceptors associated with zinc vacancies. Brin et al (1972)

reported that the  ${}^4T_1$  first excited state of the  $Mn^{2+}$  ion lies  $\sim 0.1$  eV close to the conduction band in ZnSe. Allen et al proposed that the manganese emission cannot be excited in the presence of a large concentration of free electrons because the radiative energy excites Auger electrons high into the conduction band where the energy is released as phonons. However, more work is required in this area in order to establish the mechanism conclusively.

### 2.13 Photoconductivity

Photoconductivity may be described as the increase in electrical conductivity of an insulating crystal following the absorption of incident radiation. The absorption of radiation of a suitable frequency can lead to the creation of free electron-hole pairs. Radiation in excess of the band-gap energy creates free carriers in the valence and conduction bands and, if there are levels lying within the forbidden gap, radiation of longer wavelengths may also generate charge carriers. In the II-VI compounds holes are generally much less mobile than electrons and consequently are captured more readily by defect centres.

When the photoconductivity is measured as a function of wavelength, a maximum response is usually found at that wavelength for which the absorption constant is approximately equal to the reciprocal of the crystal thickness. At higher energies the absorption constant is much greater resulting in only the surface regions being excited. In the surface regions the carrier lifetime is less than in the bulk and as a result the photosensitivity decreases. Radiation with energy less than the band gap is only partially absorbed which again leads to a resultant decrease in photosensitivity. Hence the peak in the variation

of photoconductivity with wavelength can give a measure of the band gap in the material. If imperfections are present in the crystal, the spectral response of the photoconductivity may be extended to longer wavelengths by the direct excitation of centres lying within the forbidden gap. This may reveal information about the impurities involved in radiative transitions.

In a process similar to that of the quenching of luminescence, the photoconductivity may be quenched by optical or thermal means. The free electrons or holes created by optical excitation may become trapped at levels within the band-gap leading to an increase in the lifetime of the photocarriers and an increase in the photosensitivity of the material. Stimulating the crystal by thermal means or by a secondary optical source emitting in the infra-red can lead to an emptying of the traps and a reduction in photosensitivity. Measurement of the thermal or optical quenching of photoconductivity can give activation energies for the levels within the material which may be compared with values for the quenching of luminescence.

Bube and Lind (1958) and Bube (1960) have made studies of the photoconductivity in cubic ZnSe crystals, and have reported a maximum in the response at  $4620 \text{ \AA}$  (2.68 eV) corresponding to the absorption edge. With the introduction of acceptor impurities the peak sensitivity was shifted to longer wavelengths, and in heavily copper-doped samples a broad peak was observed at  $5100 \text{ \AA}$  (2.42 eV). Stringfellow and Bube (1967) have observed the excitation of p-type photoconductivity in ZnSe:Cu crystals and noted that the energy required for excitation was similar to that for quenching n-type photoconductivity. These authors associated the behaviour with a copper centre located 0.72 eV above the valence band. Clearly measuring photoconductivity is a useful method of obtaining information concerning the position of centres within the band-gap.

### CHAPTER 3

#### CRYSTAL GROWTH AND PREPARATION

##### 3.1 Crystal Structure and Bonding

The many possible applications of the wide band-gap II-VI semiconductors in opto-electronics has meant that their crystal growth has received wide attention. The compounds formed from the elements in groups II and VI have properties which are partially ionic and partially covalent in nature, and are generally more ionic than the corresponding group IV element. The ionic influence produces the large band-gaps, low mobilities and high melting points compared with those of the III-V compounds and group IV elements. The covalent nature is reflected in the tetrahedral bonding resulting from the directional  $sp^3$  hybridised orbitals. This tetrahedral orbital configuration produces two main crystal types in II-VI compounds: the hexagonal (or wurtzite) structure and the cubic (or zinc blende) structure.

Both zinc sulphide and zinc selenide can exist with the cubic and hexagonal structures depending on the conditions during growth. However, the zinc blende structure is the more stable phase of zinc selenide at room temperature; this structure is very similar to that of diamond which has two interpenetrating face-centred cubic lattices. In zinc selenide different ions occupy the points of the two sub-lattices. The cubic lattice parameter has a value of  $5.67 \text{ \AA}$  for zinc selenide and  $5.41 \text{ \AA}$  for zinc sulphide.

Unlike the group IV elements, where vacancies have relatively little effect on the electrical and optical properties of the material,

non-stoichiometry in the II-VI compounds results in self-doping and compensation effects. It has been found that, with the exception of CdTe, the II-VI compounds when conducting are in either n-type or p-type form, but not both. There are fifteen possible alloy combinations of II-VI compounds, and eight have been shown to be miscible over the entire range of composition, while others form solid solutions over large parts of the range.

The Zn(S,Se) solid solution has been shown to be miscible throughout the whole range of composition. Larach, Schrader and Stocker (1957) have examined the optical diffuse reflectance spectra in this alloy and have shown that the band-gap varies linearly with the proportion of sulphur.

### 3.2 Crystal Growth

The two basic methods for crystal preparation are growth from a liquid phase and growth from a vapour phase. Crystal growth from stoichiometric and non-stoichiometric melts has not met much success in the II-VI compounds because of the high melting point, and the high dissociation pressures which lead to mass transport. Also, the unavailability of suitable high temperature materials for containment makes growth from the melt difficult. Those furnace materials which are used often cause the contamination of the crystals or are permeable to impurities at the temperatures involved. (For example, growth of ZnSe from the melt requires a temperature of 1500°C and this prevents the use of silica. In spite of this, Fischer (1959) and Tsujimoto (1966) have successfully grown ZnSe from the melt.) Growth from the vapour phase is much more practicable in the II-VI compounds since the process

can be carried out at significantly lower temperatures, and since both elemental components have sufficiently high vapour pressures that transport action through the vapour phase is possible.

The crystals used during the course of this work were grown within the department by two techniques: vapour phase transport and chemical transport. Details of these two techniques will now be described since the method of growth has an influence on the properties of the samples.

### 3.2.1 Preliminary Preparation

High purity starting materials of zinc sulphide and zinc selenide were necessary for the preparation of mixed crystal samples. B.D.H. Optran grade zinc sulphide and zinc selenide powder was used to produce most of the crystals examined. In addition, some starting material was prepared by the direct combination of the elements, which were obtained in 6 N purity from Metal Research Ltd. A furnace with three temperature zones, see Figure 3.1, was used for preparing the starting material from the elements: selenium or sulphur was placed in the first zone and zinc in the second zone. A stream of high purity argon was passed through the system, and crystals grew in the third zone where the metallic and non-metallic vapours reacted and condensed. In a similar way, the compound starting materials were purified by sublimation in a stream of argon as shown in Figure 3.2. The powder was placed in a silica tube and heated to  $600^{\circ}\text{C}$  for twelve hours in high purity argon in order to remove all volatile impurities. The temperature was then raised to  $1160^{\circ}\text{C}$  for about a week; in this time the powder sublimed along the tube to a cooler region leaving any non-volatile impurities behind.

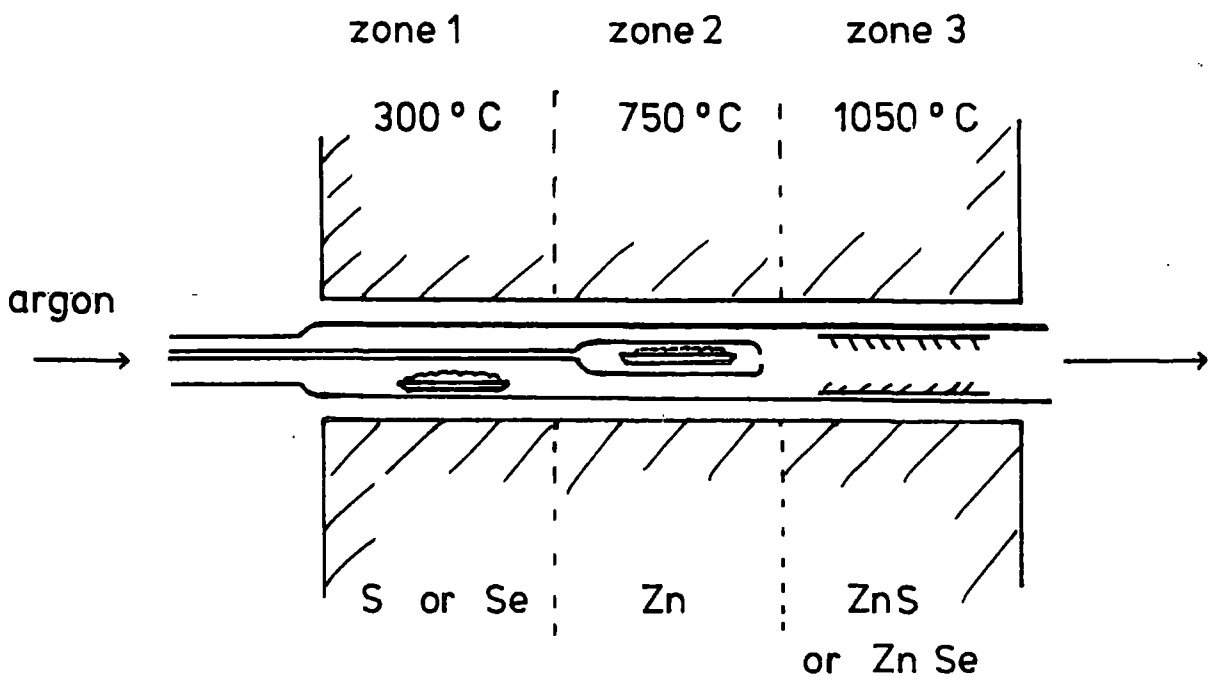


FIG 3.1 SYSTEM FOR DIRECT COMBINATION OF ELEMENTS

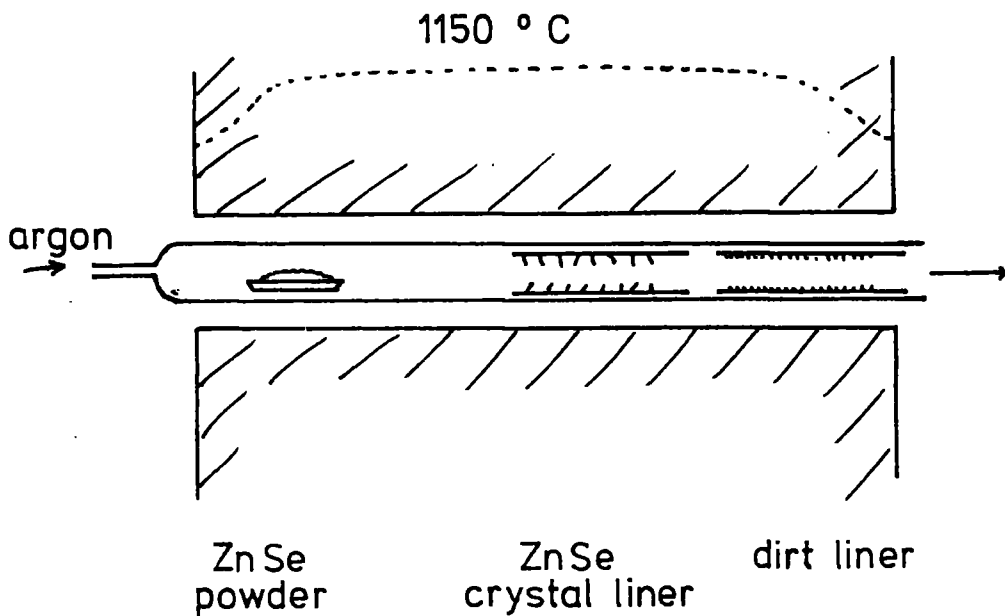


FIG 3.2 ARGON FLOW CRYSTAL GROWTH SYSTEM

The zinc selenide and zinc sulphide crystallised out in the form of small platelets several mm. square which were used as the charges for the following crystal growth procedures.

### 3.2.2 Vapour Phase Growth

Large crystals of zinc selenide were grown by a method developed by Burr and Woods (1971) from the original method of Clark and Woods (1968) used for preparing CdS. This method, which is a modification of the technique of Piper and Polich (1961), involves sublimation down a temperature gradient in an ambient pressure of one of the constituent elements. A typical arrangement for the growth system is shown in Figure 3.3. Approximately 20 gm of flow-run platelets were included in the growth capsule and about 0.2 gm of zinc was held in the tail. The growth tube was evacuated, baked and flushed with argon in order to remove volatile impurities. It was then evacuated to  $10^{-6}$  torr, sealed and mounted vertically in the furnace arrangement. The charge was held in a temperature region at  $1160^{\circ}\text{C}$  while the zinc tail was held at  $550^{\circ}\text{C}$ . The tail reservoir was necessary to control the pressure of one of the components and achieve a near stoichiometric composition of the vapour in the growth region of the capsule. The charge sublimates and condensation occurs at the growth tip which was held at  $1100^{\circ}\text{C}$ . The quartz tube was raised at about 3 cm. a day for a week, and 1 cm. diameter crystals between 3 and 4 cm. long were produced.

Single crystals of the solid solution  $\text{Zn}(\text{S},\text{Se})$  could be grown by this method, and in this case a mixture of zinc selenide and zinc sulphide flow-run powder in the desired proportion was used as the charge. The temperatures of the zinc reservoir, (required to control

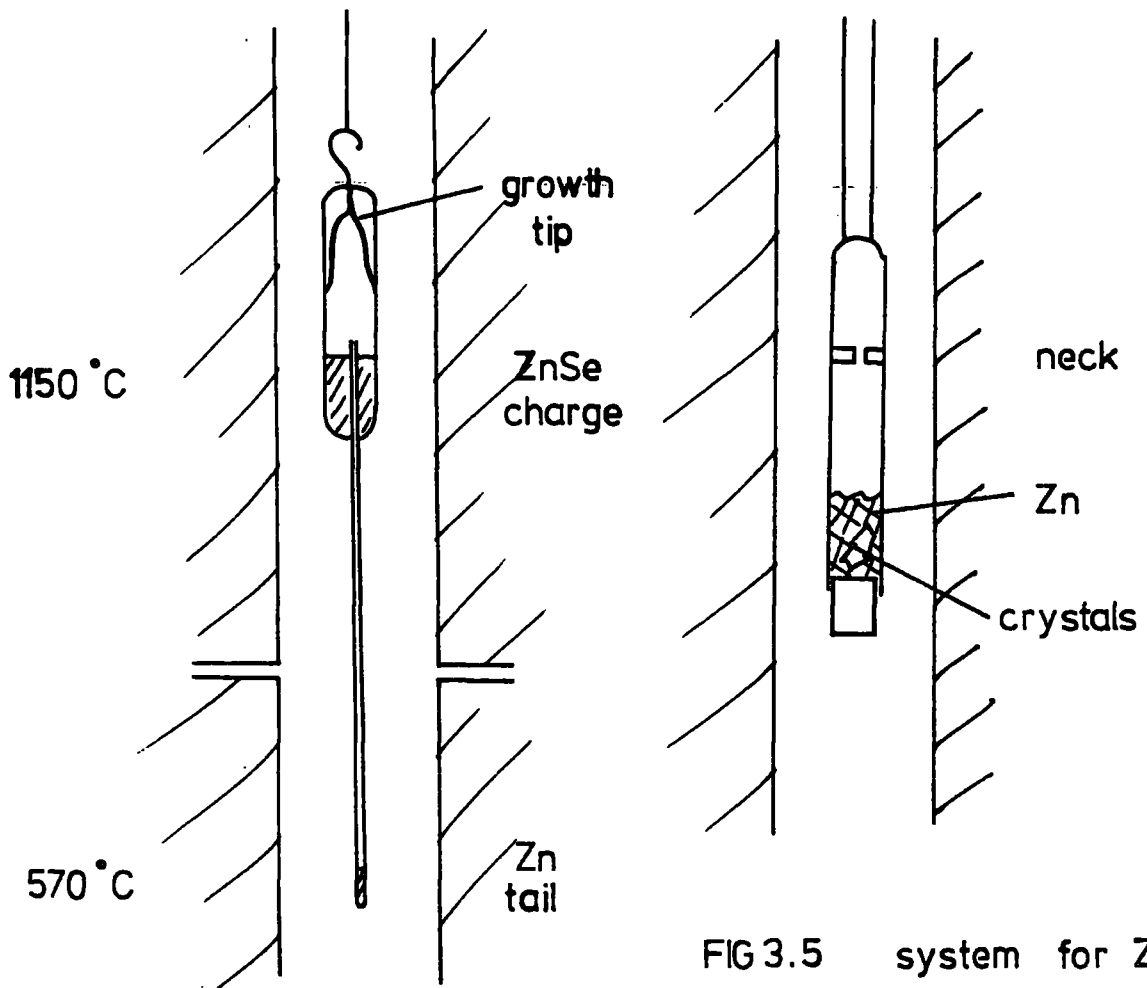


FIG 3.5 system for Zn treatment

FIG3.3 growth system for vapour phase transport

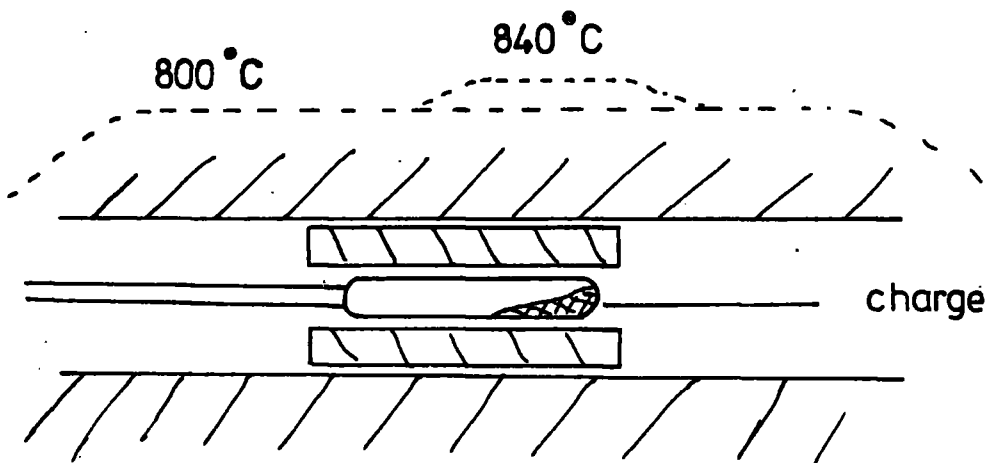


FIG 3.4 chemical transport growth system

the ambient pressure), and of the growth tip depend upon the composition of the crystal being grown and have been examined by Cutter et al (1976). This method of crystal growth has only been successful for compositions of up to 60 molar% sulphur. Higher concentrations of sulphur led to multiple nucleation and non-uniform boules.

It was possible to dope the crystals grown by this method by the addition of impurities to the charge. Chlorine could be introduced as zinc chloride, while copper could be added as the metal or the selenide. Manganese was incorporated as the metal, the selenide, or the chloride, and doping levels of up to 2000 ppm could be achieved.

### 3.2.3 Chemical Transport

Most of the crystals studied in the present work were grown by the chemical transport method using iodine as the transporting agent. The underlying principle of this method is that a chemical reaction occurs in one temperature zone and is reversed in an adjacent zone at a different temperature. This technique was based on the method described by Nitsche (1960), and the system used is shown in Figure 3.4. The system consisted of two furnaces, one maintaining a temperature of 800°C and the second producing a temperature gradient down the growth tube. The charge, consisting of approximately 4 gm. of flow-run material and 4 mgm of iodine, was placed in a silica tube which was then flushed with high purity argon, evacuated to  $10^{-4}$  torr and sealed. The silica tube was mounted horizontally in the furnace such that the charge was held at a temperature of 840°C and the growth tip at 800°C. The capsule was held in this temperature gradient for approximately 14 days. At the end of this period single crystals of about 5 - 6 mm.

diameter and 1 cm. in length had grown. Using this method it was possible to produce good single crystals of Zn(S,Se) throughout the range of composition.

Crystals grown by this method were doped with copper or manganese by including the impurity as the metal in the charge. With this arrangement up to 1% by weight of manganese could be incorporated in the crystals compared with a limit of 2000 ppm in samples grown by the vapour phase technique. It was found that the manganese displaced some of the zinc in the crystal and inhibited the growth. As a result it was necessary to extract the growth tube from the furnace after 14 days and remove the excess zinc. The residue was then re-encapsulated and the growth procedure continued for a further 14 days.

### 3.3 Sample Preparation

#### 3.3.1 Etching

Experimental samples for examination were prepared by cutting a section from the crystal boule with a diamond wheel. The sample dimensions were of the order of 5 mm long by 2 x 2 mm in cross-section. Surface damage created by the cutting was removed by polishing with 5  $\mu$  diamond paste followed by chemical etching. The etchant used was that recommended by Sagar et al (1968a); the procedure for treating a sample was to immerse the crystal in a 0.4% solution of bromine in methanol for one to two minutes. The crystal was quickly washed in methanol and then immersed in carbon disulphide for about 5 minutes to remove the compounds of bromine and selenium which tend to form as a red deposit on the surface. Finally the sample was washed in chloroform to remove the carbon disulphide and to prevent drying stains.

### 3.3.2 Ohmic Contacts

Ohmic contacts were required on those samples to be used for photoconductivity measurements. The crystals to be prepared were cut and etched as described above. The opposite end faces of the rectangular specimen were cleaved to present two uncontaminated surfaces on to which pellets cut from pure indium wire were pressed. In order to form a good ohmic contact it was necessary to heat the samples at a temperature of 250 - 350°C for five minutes in an atmosphere of argon. A slow cycling process was used, taking 15 minutes to reach temperature and to cool down. It is believed that the indium may form a thin layer of alloy on the surface of the crystal. Blount et al (1966) have described the process of ohmic contact formation on zinc selenide using indium in terms of the penetration of a chemical impurity layer followed by the indiffusion of the indium. However, Kaufman and Dowber (1974) have described the formation of contacts on Zn(S,Se) using indium as a liquid epitaxial process. As the percentage of sulphur in the mixed crystals was increased, the annealing temperature had to be progressively raised from 250°C in zinc selenide to about 350°C in order to form satisfactory contacts. It proved possible to form good ohmic contacts on zinc sulpho-selenide alloys containing up to 80% of sulphur. With more sulphur it was difficult to form ohmic contacts, especially if the samples were to be used at 85 K. The crystals were mounted on a thin silica glass slide and electrical contact was made to the indium electrodes using an air-drying silver paste.

### 3.4 Heat treatment

Aven and Woodbury (1962) reported that trace impurities of copper

and silver could be removed from zinc selenide and zinc sulphide by heating the crystals in molten zinc. The impurities were more soluble in the zinc and segregated between the crystal and the molten solution. This technique may be used in reverse by incorporating an impurity with the zinc in order to dope the crystals. This process of zinc treatment not only had the effect of purifying the samples, but lowered the resistivity from  $10^{12} - 10^{14}$  ohm cm in as-grown crystals to the range 1 - 100 ohm cm by reducing the concentration of compensating zinc vacancy centres.

The apparatus used for treating the samples in molten zinc is shown in Figure 3.5. The crystals were placed at one end of a silica tube, and pellets of 6 N zinc metal were placed at the other end above a neck in the tube to prevent passage of the crystals. The system was evacuated and flushed with high purity argon, and sealed at a pressure of  $4 \times 10^{-6}$  torr. The silica tube was suspended vertically in a furnace at a temperature of  $850^{\circ}\text{C}$  for a period of a week. After this time the tube was removed from the furnace and inverted, causing the molten zinc to drain away from the crystals to the bottom of the capsule. The crystals were then extracted and etched in bromine/methanol.

### 3.5 X-ray Powder Analysis

X-ray powder photographs were taken of the range of mixed alloy zinc sulpho-selenide crystals which were grown, in order to determine the structure and lattice parameter of the samples. An examination of the powder photographs indicated that all the crystals grown by both vapour transport and chemical transport techniques were cubic in structure. However, Cutter et al (1976), using a transmission electron

microscope, observed that there were small amounts of the hexagonal component of almost the same composition as the cubic main phase in mixed crystals grown by the vapour transport technique. The measured lattice parameters for the range of samples examined is listed in Table 3.1. It was assumed that the lattice parameter varied linearly with composition from  $5.67 \text{ \AA}$  in ZnSe to  $5.41 \text{ \AA}$  in ZnS, and an estimate of the composition was made from the measured lattice parameter. A 'theoretical' value of the composition was calculated from the weight percent of ZnSe and ZnS starting material incorporated in the growth tube to produce a particular mixed crystal. In making this calculation it was assumed that the constituents combined in strict proportion. The interpolated and 'theoretical' values of the composition listed in Table 3.1 show a good agreement; this confirms that the assumption that composition varies linearly with lattice parameter is correct.

Table 3.1: Composition of Mixed Alloy Crystals

Crystal (Nominal Composition)	Lattice Parameter Å	Calculated <sup>(1)</sup> Composition % S	Theoretical <sup>(2)</sup> Composition % S
ZnSe	5.669	0	0
940 ZnS <sub>0.1</sub> Se <sub>0.9</sub>	5.626	16	14
945 ZnS <sub>0.2</sub> Se <sub>0.8</sub>	5.600	26	27
947 ZnS <sub>0.3</sub> Se <sub>0.7</sub>	5.559	42	39
953 ZnS <sub>0.4</sub> Se <sub>0.6</sub>	5.528	54	50
954 ZnS <sub>0.5</sub> Se <sub>0.5</sub>	5.510	61	60
956 ZnS <sub>0.6</sub> Se <sub>0.4</sub>	5.476	74	70
958 ZnS <sub>0.7</sub> Se <sub>0.3</sub>	5.460	80	78
960 ZnS <sub>0.8</sub> Se <sub>0.2</sub>	5.437	89	86
961 ZnS <sub>0.9</sub> Se <sub>0.1</sub>	5.428	92	93
962 ZnS <sub>0.9</sub> Se <sub>0.1</sub>	5.411	99	99
ZnS	5.409	100	100
975 ZnS <sub>0.25</sub> Se <sub>0.75</sub> :Mn	5.574	37	33
971 ZnS <sub>0.5</sub> Se <sub>0.5</sub> :Mn	5.509	62	60
978 ZnS <sub>0.75</sub> Se <sub>0.25</sub> :Mn	5.452	83	82
984 ZnS <sub>0.1</sub> Se <sub>0.9</sub> :Cu	5.642	10	14
981 ZnS <sub>0.25</sub> Se <sub>0.75</sub> :Cu	5.574	37	33
977 ZnS <sub>0.5</sub> Se <sub>0.5</sub> :Cu	5.518	58	60
982 ZnS <sub>0.75</sub> Se <sub>0.5</sub> :Cu	5.444	86	82
987 ZnS <sub>0.9</sub> Se <sub>0.1</sub> :Cu	5.412	99	93

(1) Calculated from measured lattice parameter.

(2) Calculated from molar volumes incorporated in growth tube

## CHAPTER 4

### EXPERIMENTAL PROCEDURE

#### 4.1 Introduction

The purpose of this work was to obtain more detailed information about the optical properties of zinc sulpho-selenide crystals throughout the range of composition. An examination was made of the luminescence spectra, excitation spectra, photoconductivity and thermal quenching of luminescence over the range of temperatures between 295 K and 15 K. The present chapter describes the techniques and apparatus used.

#### 4.2 The Cryostat

A brass cryostat constructed within the department was used to house the specimen sample for all low temperature experimental work down to liquid helium temperature. The design of the cryostat, illustrated schematically in Figure 4.1, consisted of a liquid nitrogen jacket with a two litre capacity, a liquid helium pot with a 1.3 litre capacity and a demountable copper sample holder with a demountable radiation shield. Electrical and thermocouple leads could be attached to the sample and taken via a lead-through to connections outside the cryostat. In the central liquid helium pot, two carbon resistors mounted on a thin stainless steel tube were used to measure the depth of helium during transfer and give an indication of the temperature of the sample. The vacuum within the cryostat was maintained at a pressure

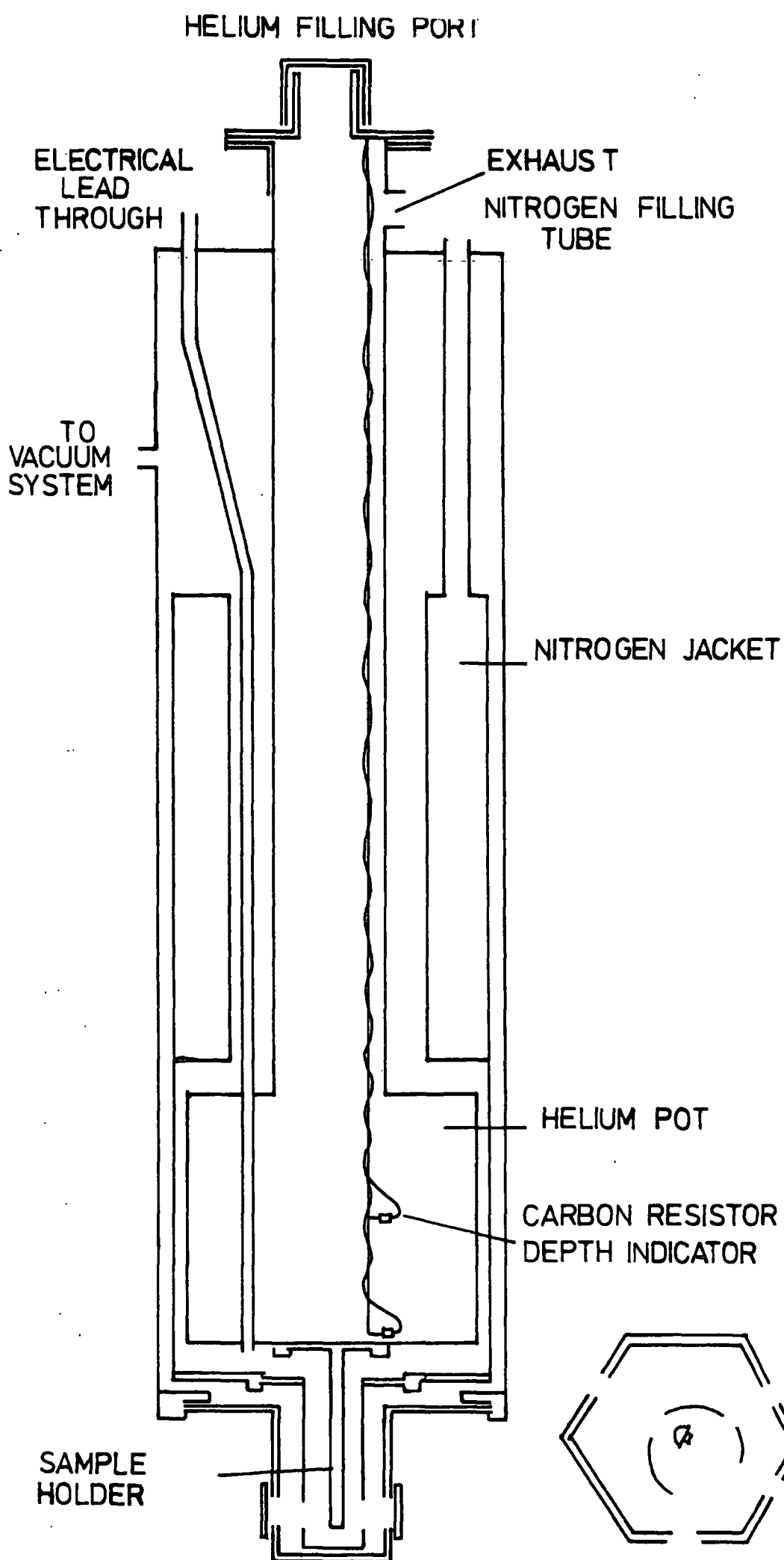


FIG 4.1 HELIUM CRYOSTAT

of less than  $10^{-3}$  torr by using conventional rotary and oil diffusion pumps to evacuate the system. The central liquid helium pot could be pumped-on via the exhaust port in order to lower the pressure above the coolant and thus further reduce the temperature of the sample.

Samples were attached to the demountable copper cold finger using indium metal. This ensured that good thermal and electrical contact was made to the cryostat. A pellet of indium was melted on the sample holder, a crystal was immersed in the molten metal, and the whole assembly was quickly quenched to produce solidification. It was assumed that the heating to  $\sim 100^{\circ}\text{C}$  in air for a limited period of time would have negligible effect on the crystals.

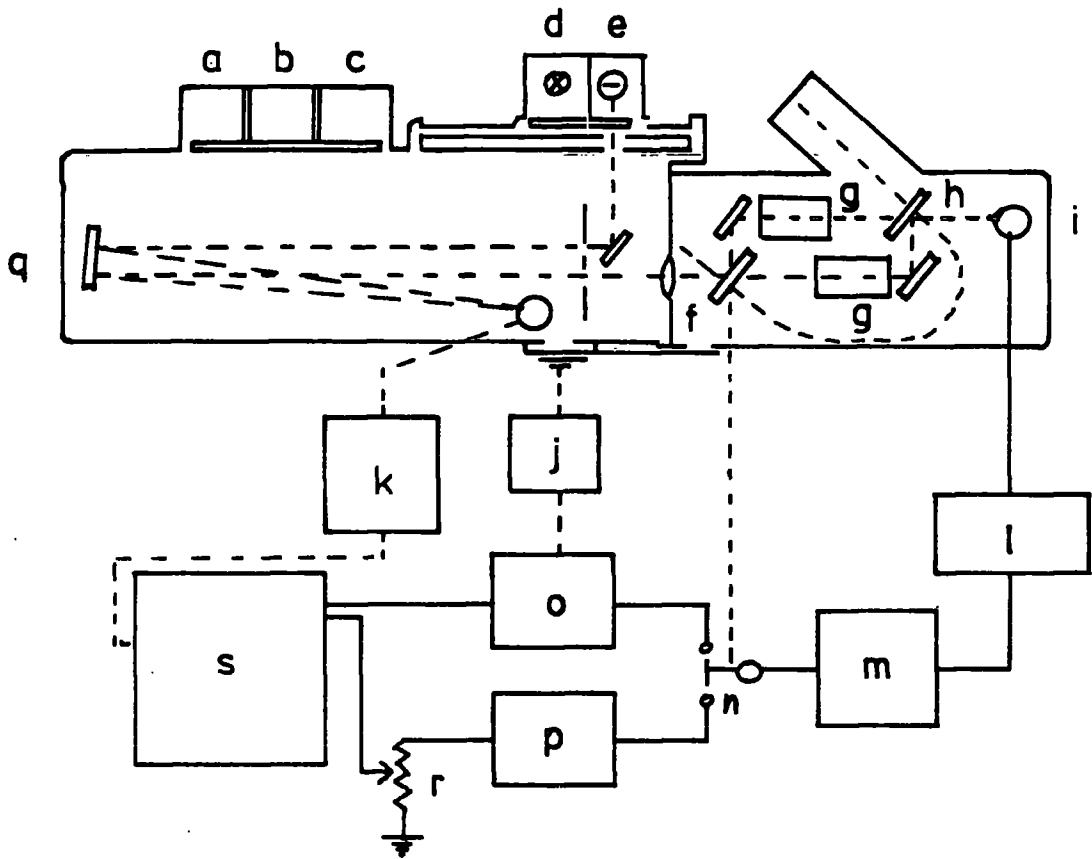
Temperature measurements were made using gold/iron-chromel and copper-constantan thermocouples attached close to the sample on the coldfinger. In making temperature measurements, a small difference may have existed between the actual sample temperature and that recorded by the thermocouple. When the sample was cooled, it was allowed to reach equilibrium before temperature measurements were taken. Using liquid helium in the central pot of the cryostat the temperatures recorded were between 10 and 15 K when the ultra-violet radiation was incident on the sample holder; the temperature rose to  $\sim 25$  K if the sample holder was irradiated with light from the quartz-iodine lamp. The equivalent temperatures recorded with liquid nitrogen in the central pot were 82 K and 85 K, respectively. Pumping on liquid nitrogen could produce temperatures between 65 and 68 K. The procedure for cooling the sample to liquid helium temperatures was first to cool the central pot with liquid nitrogen; the liquid nitrogen was then removed using a siphon by applying an over-pressure of dry nitrogen gas. After this pre-cooling, the liquid helium was transferred. The pre-cooling of

the cryostat reduced the volume of coolant required for a run; the sample could be maintained at a temperature of approximately 10 K for up to three hours by transferring one litre of liquid helium.

#### 4.3 Optica Spectrophotometer

An Optica 4 NI grating spectrophotometer was used in a modified form to perform all the spectroscopic analysis in this experimental work. The instrument, see Figure 4.2, is principally designed for making absorption and transmission measurements and has a spectral range from 0.185 to 3.1  $\mu\text{m}$ . The monochromator section of the instrument is of the Littrow type with two interchangeable plane gratings as the dispersive elements. The standard monochromator dispersion was approximately 16  $\text{\AA}/\text{mm}$  with a ruled grating of 600 lines/mm for the ultra-violet and visible regions (0.185 to 1.0  $\mu\text{m}$ ), and was 32  $\text{\AA}/\text{mm}$  for the near infra-red region (0.9 to 3.1  $\mu\text{m}$ ) when a 300 lines/mm grating was used. The slit width of the monochromator had a maximum value of 3.6 mm and was variable in divisions of 0.02 mm. In the arrangement for making absorption measurements, the light beam emerged from the monochromator section and was condensed on to a system of rotating mirrors which splits the beam into reference and sample beams. A differential signal was obtained by recombining these beams using a series of mirrors rotating in phase with the first system. This signal was proportional to the absorption of a specimen placed in the sample beam.

In order to examine the emission and excitation spectra, the Optica was split into the monochromator and detector/mirror sections, and only the monochromator was employed. An EMI photomultiplier type 9558 with a tri-alkali S.20 photocathode was used as the detector for



- a hydrogen power supply
- b photomultiplier power supply
- c tungsten power supply
- d hydrogen lamp
- e tungsten lamp
- f rotating mirror
- g reference / sample cell
- h rotating mirror
- i detector
- j slit servo
- k wavelength drive
- l preamplifier
- m amplifier
- n commutator
- o reference demodulator
- p sample demodulator
- q grating
- r 100 % adjustment
- s pen recorder

FIG 4.2 OPTICAL SPECTROPHOTOMETER

both emission and excitation analysis. This detector was coupled to the output slit of the monochromator. The calibrated spectral response for the particular photomultiplier is shown in Figure 4.3. The photomultiplier was run at voltages up to 1200 V obtained from a Brandenburg stabilised power supply, model 475R. The output from the collector was earthed via a 10 k $\Omega$  low noise resistor and the voltage signal developed across the load was taken to a Philips valve voltmeter type PM 2440, and to a Brookdeal 9401 lock-in amplifier. A Brookdeal variable frequency multi-bladed chopper was included in the optical path of the system; this provided the reference signal for the lock-in amplifier. The output signal from the amplifier was recorded on a Honeywell chart recorder. In general, the reference frequency of the chopper was set at 200 Hz during the course of these measurements.

#### 4.4. Photoluminescence Spectra

The experimental arrangement used for measuring the emission spectra of the crystals is shown in Figure 4.4. The photoluminescence of the crystals was excited by ultra-violet radiation from a 250 watt high pressure mercury lamp. Two Chance glass OX1A filters were used in order to isolate the 3650  $\text{\AA}$  mercury line. The mercury lamp was run at 82 V and 4 A from a stabilised d.c. supply and provided a total radiative flux of approximately 100 watts. After filtering, approximately 8 watts remained in the 3650  $\text{\AA}$  radiation to be focussed on to the sample. This exciting radiation could be further reduced in intensity by the incorporation of neutral density filters, manufactured by Barr and Stroud, between the source and the sample. A cell containing a saturated solution of copper sulphate was placed between the sample and the mercury lamp in order to remove red and infra-red

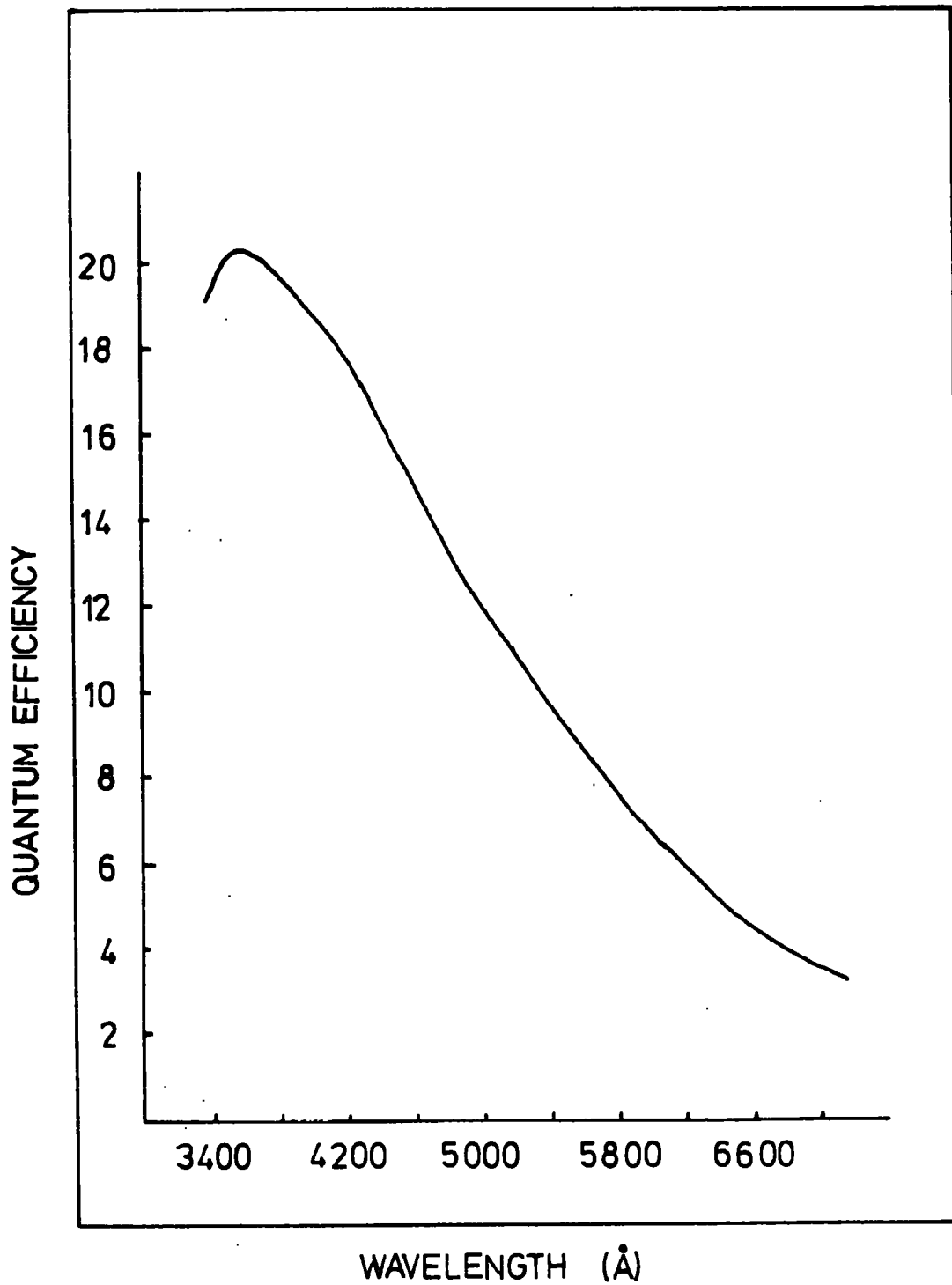


FIG 4.3 RESPONSE OF PHOTOMULTIPLIER 9558 AM

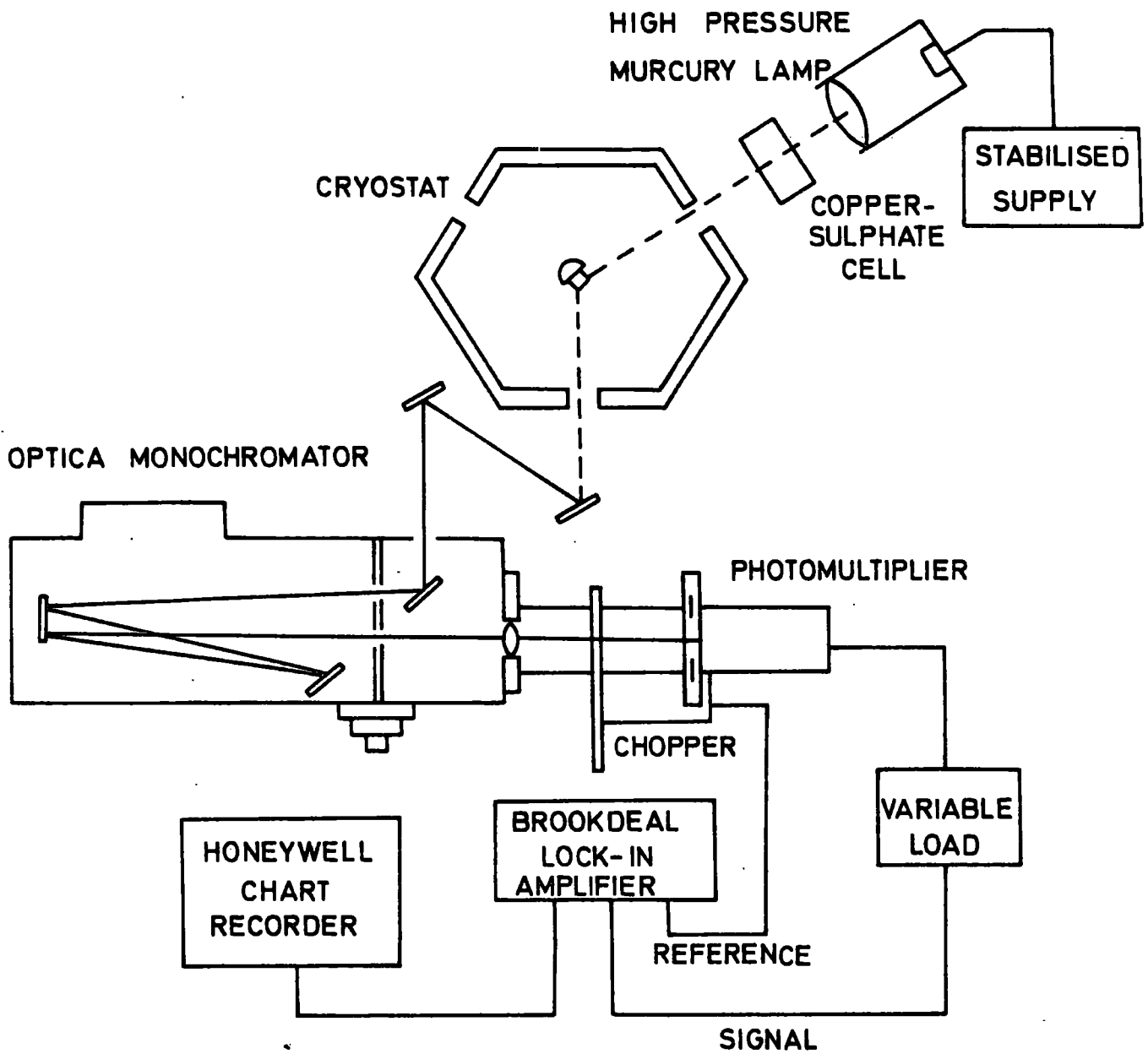


FIG. 4.4 EXPERIMENTAL ARRANGEMENT FOR MEASURING PHOTOLUMINESCENT EMISSION SPECTRA.

components from the radiation passed by the OX1A filters. The luminescence excited by the ultra-violet radiation was focussed and collimated on the entry slit of the monochromator using a system of mirrors. The monochromator was automatically scanned through the luminescence band of interest and the radiation was monitored using the photomultiplier tube.

#### 4.5 Excitation Spectra

The experimental arrangement used for measuring the excitation spectra of the crystals is shown in Figure 4.5. Radiation from a quartz-halogen lamp was focussed on to the entrance slit of the Optica and the spectrometer was used to produce a monochromatic beam of light which was focussed on the crystal sample. An Oriel variable interference filter, in conjunction with a selection of Chance glass wide-band filters, was used to isolate the luminescence band of interest from the exciting radiation. This combination of filters was arranged to have a bandwidth of approximately 300 Å at 6000 Å. The variable filter was adjusted to give optimum transmission of a particular band of luminescence when the crystal was excited. The light chopper was incorporated between the crystal and the photomultiplier detector since it had previously been found that chopping the exciting radiation before it was incident on the crystal produced spurious effects; this was considered to be due to relaxation processes occurring in the sample.

#### 4.6 Cathodoluminescence

The experimental arrangement for analysing cathodoluminescence spectra was similar to that shown in Figure 4.4 for measuring the

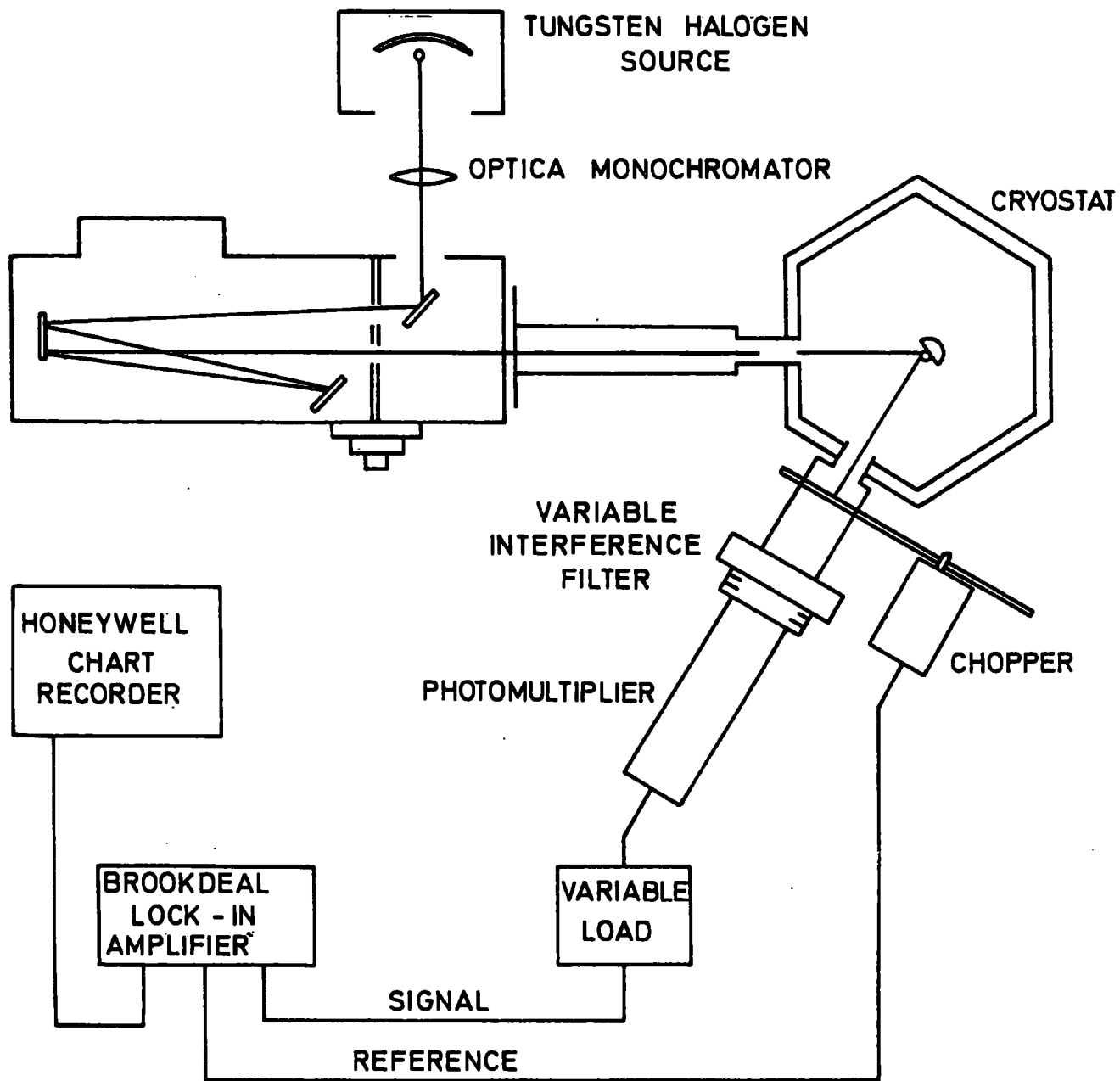


FIG. 4.5 EXPERIMENTAL ARRANGEMENT FOR MEASURING PHOTOLUMINESCENT EXCITATION SPECTRA.

photoluminescence of the crystals. In this case, the excitation source was replaced by an electron gun system which was produced within the department. The electron gun, manufactured by 20th Century Electronics model ED221, was a demountable triode type with a tungsten emitter. This electron gun produced a divergent electron beam which could be magnetically focussed to a spot approximately 2 mm in diameter on the sample. The tungsten emitter enabled the gun to be exposed repeatedly to the atmosphere when changing samples without significant degradation of the cathode surface. Typical operating conditions for the electron gun were: an anode voltage of 20 kV, a filament current of 5.0 A and a maximum beam current of 1 mA. The electron gun assembly was attached to a modified demountable bottom-plate for the liquid helium cryostat; this whole system was mounted on a hydraulic ram such that samples could be mounted on the cold-finger and the cryostat closed in situ. A cold trap and diffusion pump were coupled to the cryostat bottom-plate. These were in close proximity to the electron gun assembly in order to ensure a good vacuum within the system.

#### 4.7 Thermal Quenching

A smaller all-metal cryostat was employed for making measurements of the thermal quenching of luminescence. Using this cryostat, the rate of warming could be controlled externally by a heater attached to the sample block. The crystal was mounted on a large mass copper sample-holder with a high thermal capacity which minimised fluctuations in the sample temperature. The crystal was illuminated with radiation from either a high pressure mercury lamp, or a quartz-halogen lamp using suitable interference filters to isolate a particular band of excitation. In both cases, a cell containing a saturated solution of

copper sulphate was positioned between the excitation source and the sample to remove any infra-red components of the radiation which might have quenched the luminescence. The excitation sources were run from a stabilised supply to prevent random fluctuations occurring in the intensity of the luminescence.

The experimental arrangement used for examining the thermal quenching of luminescence was similar to that for recording the luminescence spectra. The monochromator was set at the wavelength of interest and the slit width was adjusted to encompass the band of radiation being examined. The measurement of the sample temperature was made using a copper-constantan thermocouple attached in the immediate vicinity of the crystal. A heater indirectly in contact with the sample holder was used to control the rate of warming. This allowed a range of temperatures to be examined up to  $\sim 400$  K. The crystal sample was cooled in the dark using liquid nitrogen, and the excitation was applied when the temperature had reached equilibrium at 85 K.

#### 4.8 Photoconductivity

Crystals were prepared for photoconductivity measurement by cutting them into rectangular bars and alloying indium metal pellets on to the end faces to form electrical contacts. The samples were mounted on thin silica glass plates using silicone grease to ensure a good thermal contact; electrical connections were made by applying air-drying silver paste to the indium contacts and inserting short copper wires. At this stage the contacts were examined to establish that they were ohmic. The silica glass plate was mounted on the copper cold-finger using silicone grease in order to ensure a good thermal contact between the sample and the cryostat, and electrical connections were made from the sample to leads within the vessel.

To make the electrical measurement, a potential of 90 volts d.c. was applied across the crystal using a battery; this provided a stable noise-free source. The current passed by the sample was monitored using a Keithley Electrometer model 610C in the current-measurement mode; this instrument possessed a sensitivity down to  $10^{-14}$  A. The output from the instrument was displayed directly on a Honeywell chart recorder. The crystals were excited using a quartz-halogen lamp in conjunction with the spectrometer to produce a monochromatic beam of radiation; this radiation was focussed on the sample in an arrangement similar to that for examining the excitation spectra.

#### 4.9 Correction Factors

In order to display the results it was necessary to make corrections to the experimental data. The photoluminescence spectra were corrected for the spectral sensitivity of the photomultiplier as calibrated by the manufacturers at E.M.I. The excitation and photoconductivity spectra were corrected for the energy distribution of the quartz-halogen exciting source.

## CHAPTER 5

### UNDOPED CRYSTALS

#### 5.1 Introduction

In this chapter the results of the measurement of the emission and excitation spectra and the photoconductivity of undoped Zn(S,Se) mixed crystals are presented. The luminescence spectra of powdered phosphors in this ternary system have been described previously by Leverenz (1950), Klasens (1953) and Morehead (1963). There are reports of various discontinuities in the variation in position of the band maxima with changing composition. Samples examined in this work were all crystalline in nature and either contained iodine or were nominally pure depending on the mode of preparation. Certain crystals were annealed in molten zinc in an attempt to remove the impurities and increase the conductivity. The experimental curves in the figures illustrating the emission spectra, the excitation spectra and the photoconductivity have been corrected for the response of the photomultiplier and excitation source and have been normalised. No attempt has been made to give a quantitative measure of the relative intensities.

#### 5.2 Photoluminescence

##### 5.2.1 Iodine Transport Crystals

The photoluminescence spectra of Zn(S,Se):I crystals grown by

the iodine transport technique were examined first because of their availability which was a direct result of the relative convenience of their preparation. The body colour of the crystals varied from a deep orange for ZnSe to a pale white for ZnS. An analysis of the trace impurities contained in these crystals has shown the presence of copper, oxygen and silicon in concentrations of up to a few p.p.m. The photoluminescence emission spectra resulting from ultra-violet excitation ( $\lambda = 3650 \text{ \AA}$ ) are shown in Figs. 5.1 and 5.2. At room temperature there is a gradual shift of the peak position towards higher quantum energy with increasing sulphur content, accompanied by a broadening of the emission band. A high energy shoulder becomes apparent for values of  $x$  in excess of 0.5 (where  $x$  is the mole fraction of sulphur) and two distinct bands may be resolved for  $x > 0.9$ . However, with ZnS:I and ZnSe:I single bands only are resolved with peak maxima at  $4740 \text{ \AA}$  (2.62 eV) and  $6250 \text{ \AA}$  (1.98 eV) and with half-widths of 0.47 eV and 0.49 eV respectively. Jones and Woods (1974) have shown that a copper-red band exists in ZnSe at  $6400 \text{ \AA}$  and this may account for the broadening of the emission observed in the sample of zinc selenide. The luminescence from the crystal of ZnS appears to be similar to that reported by Shionoya (1964) for self-activated emission with chlorine as a coactivator, where the band was located at  $4750 \text{ \AA}$  with a half-width of 0.44 eV. Cooling the samples to 85 K led to a marked improvement in the resolution of the emission bands. A high energy shoulder could be resolved in samples with  $x > 0.2$ , and in the crystals containing a high proportion of sulphur the high energy band dominated the luminescence. In ZnS and ZnSe, single bands were again observed at  $4720 \text{ \AA}$  (2.63 eV) and  $6200 \text{ \AA}$  (2.00 eV) with half-widths of 0.44 eV and 0.29 eV respectively. The half-width observed in the sample of ZnS was not greatly reduced on cooling, contrary to expectation for

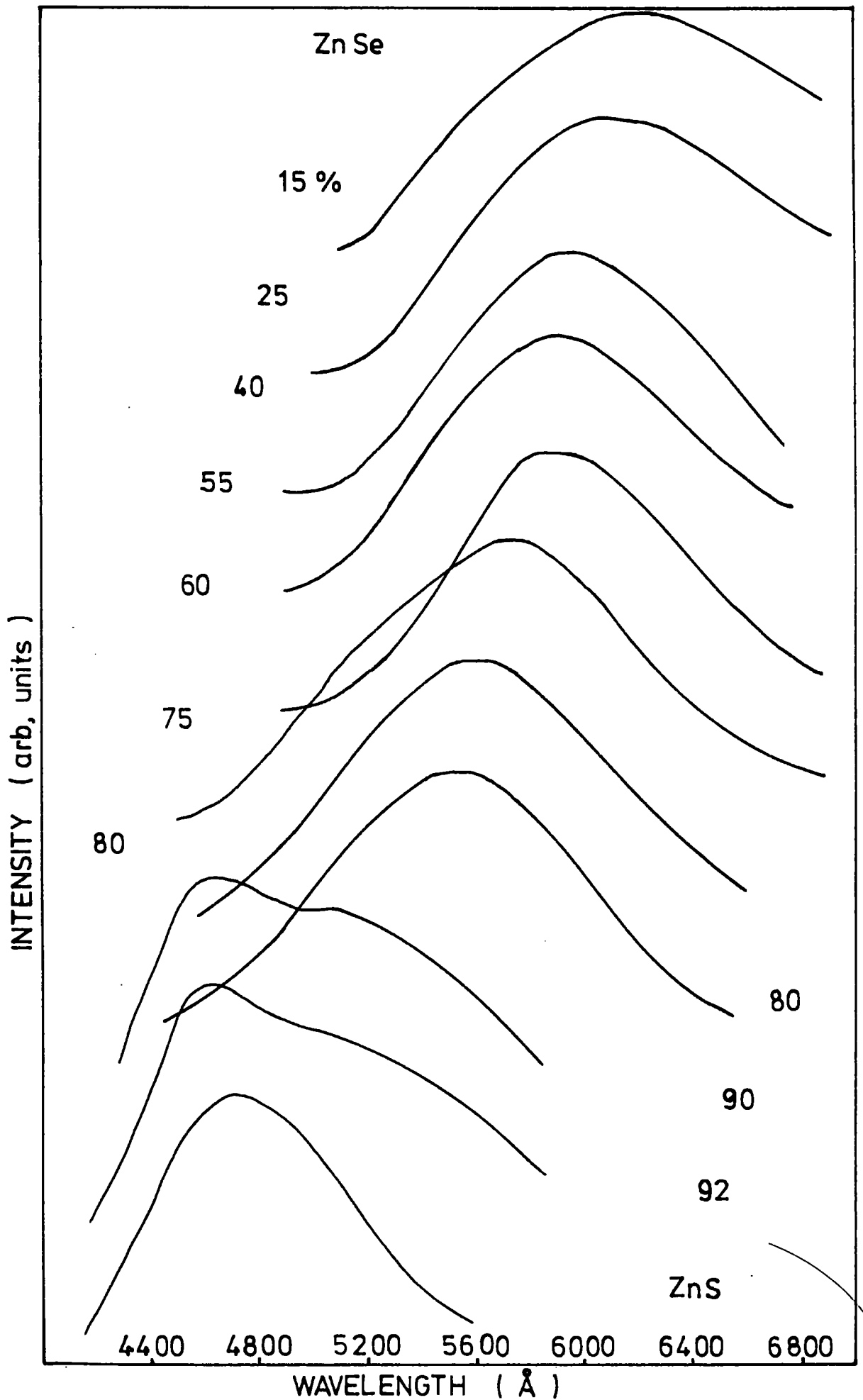


FIG 5.1 PHOTOLUMINESCENCE OF Zn(S,Se) AT 300°K

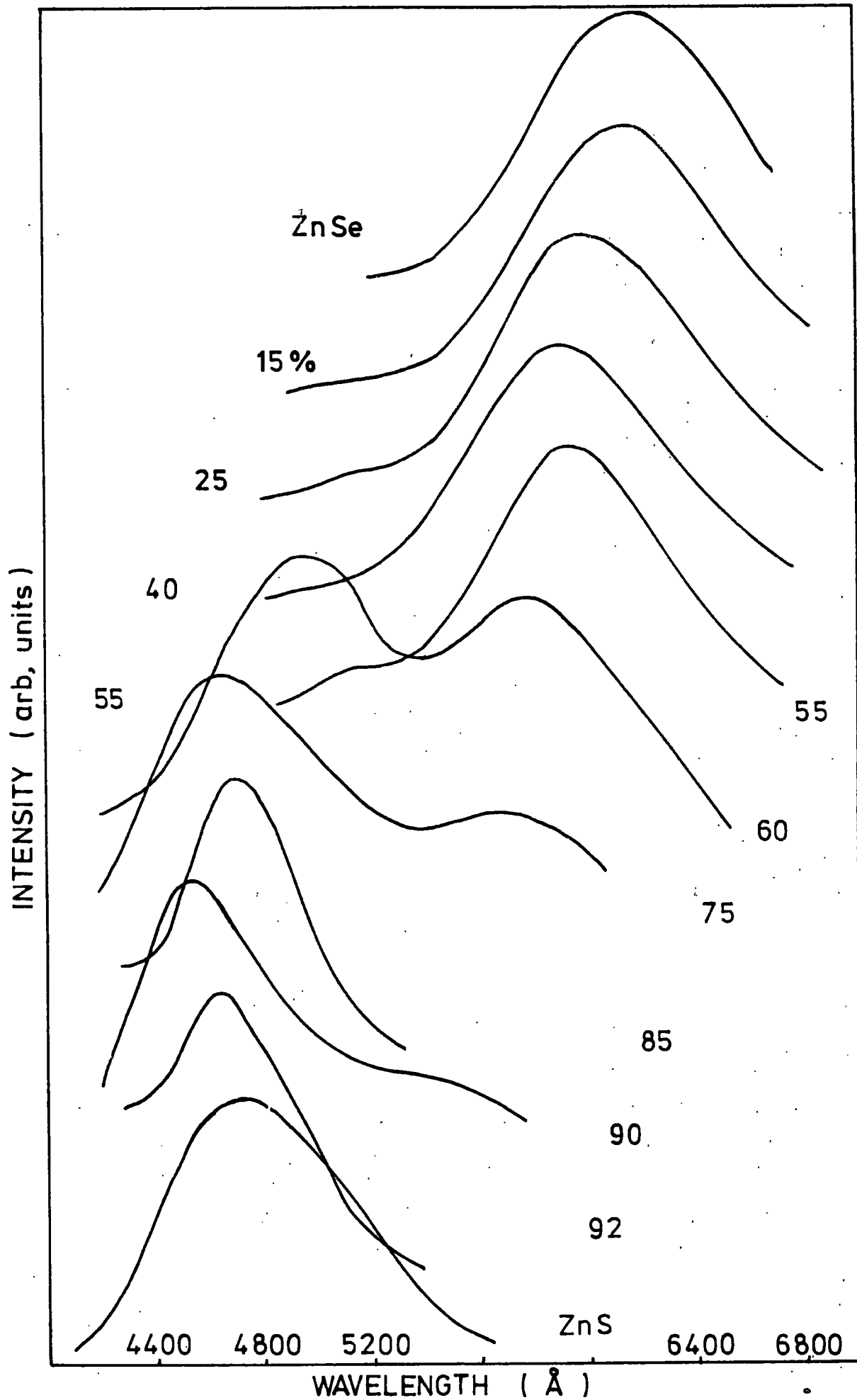


FIG 5.2 PHOTOLUMINESCENCE OF Zn(S,Se):I AT 85° K

a self-activated transition. However, Lehmann (1967) also found a half-width of 0.40 eV in ZnS phosphor material coactivated with bromine. In general, however, the half-widths of the luminescence bands were much reduced when the temperature was decreased, and there was a slight shift of the peak position to lower energies for compositions with  $x < 0.6$ . For compositions with  $x > 0.6$  the positions of the emission maxima remained almost constant.

It was also noted that the high and low energy emission bands in the sulphur rich alloys ( $x > 0.8$ ) were sensitive at room temperature to the intensity of the ultra-violet excitation. The photoluminescence spectra for sample 961 ( $x = 0.92$ ) and sample 962 ( $x = 0.99$ ) are shown in Figs. 5.3 and 5.4. Neutral density filters were included between the U.V. source and the sample in order to reduce the intensity of excitation, and at the same time the monochromator entrance slit width was increased to obtain a measurable signal: no relative scale of intensity is implied between the various curves. The results indicate that there was a marked dependence of the ratio between the intensities of the high and low energy bands, with the lower energy band becoming increasingly dominant as the excitation intensity was reduced. This behaviour can be explained in terms of multiple recombination processes with different capture cross-sections. An important feature to emphasise is the appearance of a green low energy band in crystal 962 which contained as little as one atomic percentage of selenium in zinc sulphide. Fonger (1965) interpreted the emission bands which he observed in Zn(S,Se) phosphors in terms of the overlap of a number of transitions involving activator ions surrounded by various combinations of sulphur and selenium atoms. This model, in which each activator may be coordinated with  $j$  sulphur atoms and  $(4 - j)$

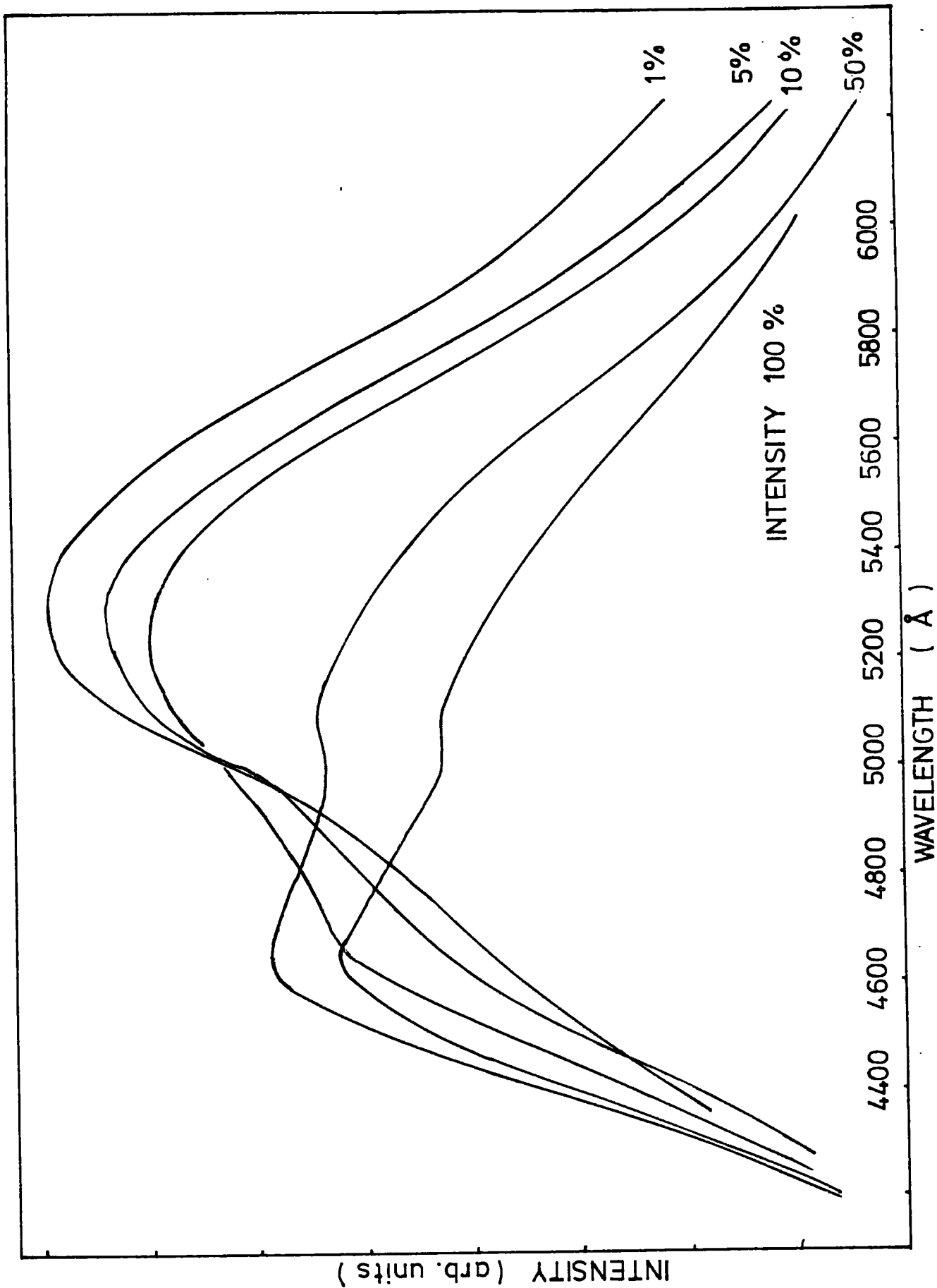


FIG 5.3 PHOTOLUMINESCENCE OF  $ZnS_{0.9}Se_{0.1}$  AT  $300^{\circ}K$   
 VARIATION WITH EXCITATION INTENSITY

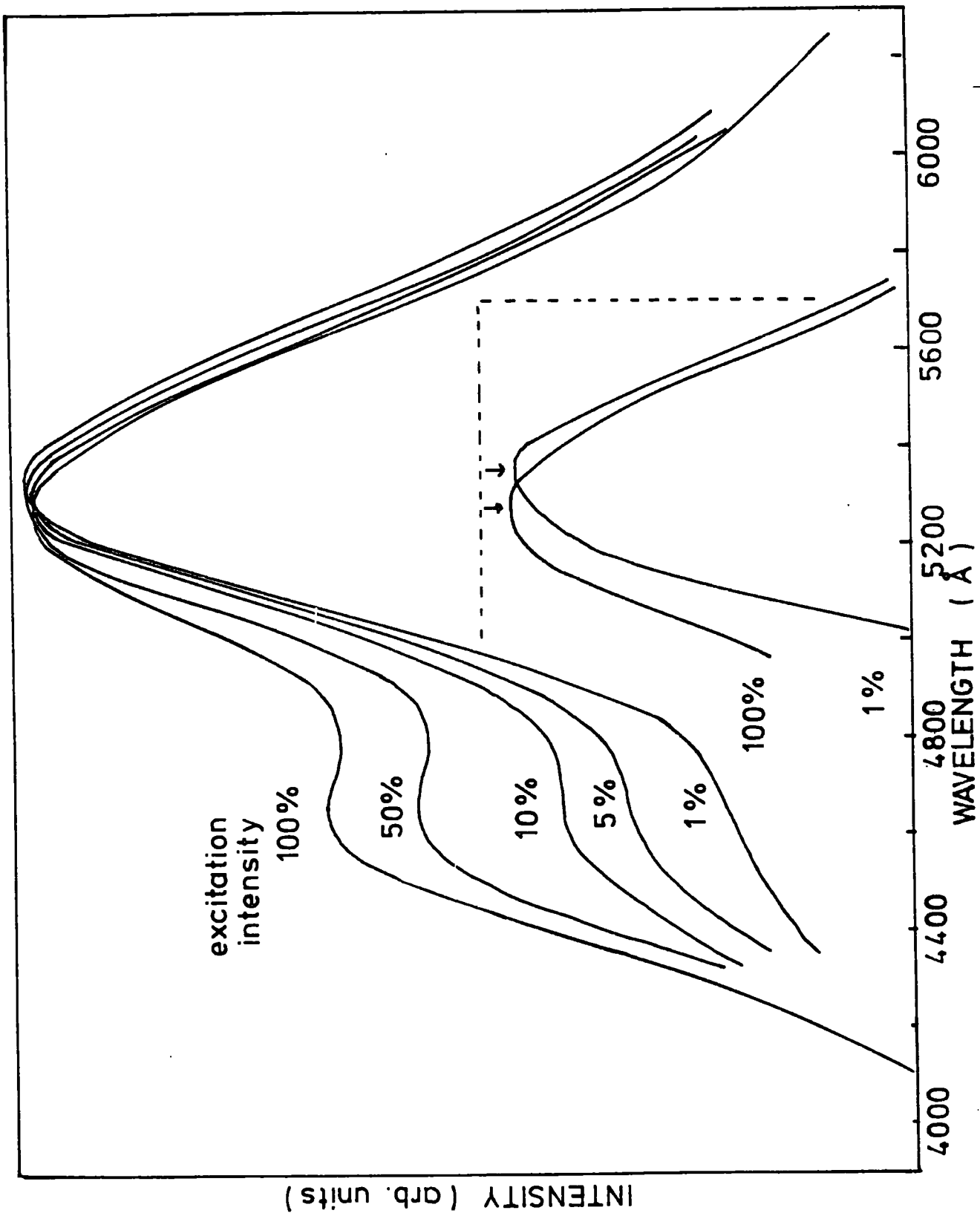


FIG 5.4 PHOTOLUMINESCENCE OF ZnS<sub>0.99</sub>Se<sub>0.01</sub> AT 300°K

selenium atoms (where  $j = 0, 1, 2, 3, 4$ ) would also explain the existence of the single luminescence bands observed in ZnSe and ZnS at the ends of the series. One complication for this model of overlapping bands is that the low energy green band results from the incorporation of very small percentages of selenium in ZnS, as shown in Fig. 5.4 for crystal 962 containing 1% Se. No such similar observation is made when Se atoms in ZnSe are replaced by small percentages of sulphur. The maximum of the low energy green emission in Fig. 5.4 can also be seen to have shifted to lower energies when the excitation intensity was reduced: the luminescence maxima occurred at  $5280 \text{ \AA}$  (2.35 eV) with 100% excitation and at  $5345 \text{ \AA}$  (2.32 eV) with 1% excitation. This shift to lower energies would be expected if the suggestion made by Shionoya (1964) and Prener and Williams (1956) is correct, that is that the self-activated emission results from transitions between two localised levels within the forbidden gap.

The variation of the photon energies of the emission maxima with the composition of the alloy, calculated from x-ray powder photograph measurements, is shown in Fig. 5.5 at room temperature and 85 K. In the diagram photon energies were plotted against lattice parameters. Larach, Stocker and Shrader (1957) have examined the diffuse reflectance spectra in the mixed alloy crystalline powders and have concluded that there is a linear variation of the band-gap with composition in the Zn(S,Se) system. These authors give the room temperature band-gap in cubic ZnS as 3.60 eV and in cubic ZnSe as 2.66 eV. For purposes of comparison the variation of the energy gap, which is assumed to be linear, is plotted on the same graph. It can be seen that there are distinct differences between the variation in energy of the high and low energy band emissions. The low energy band series exhibited a linear variation of peak position

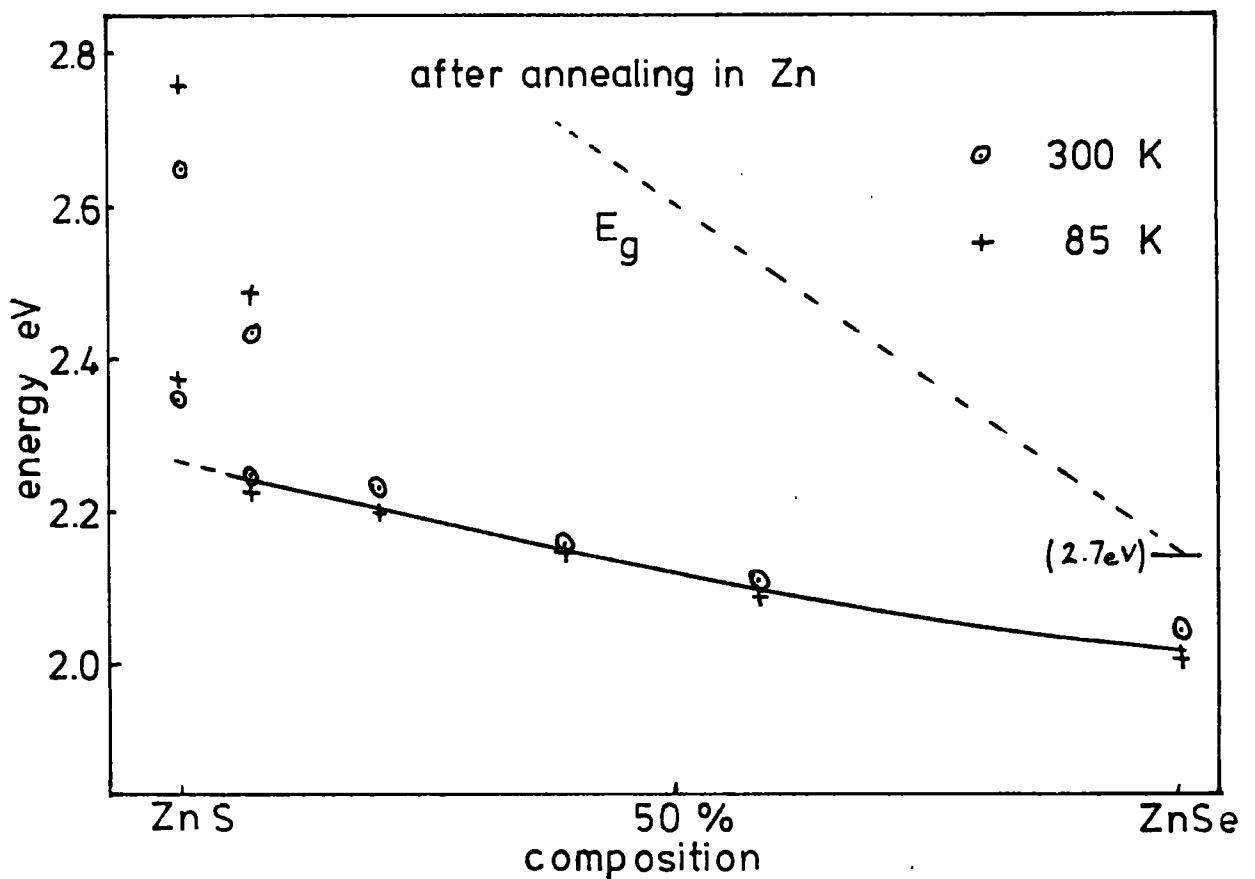
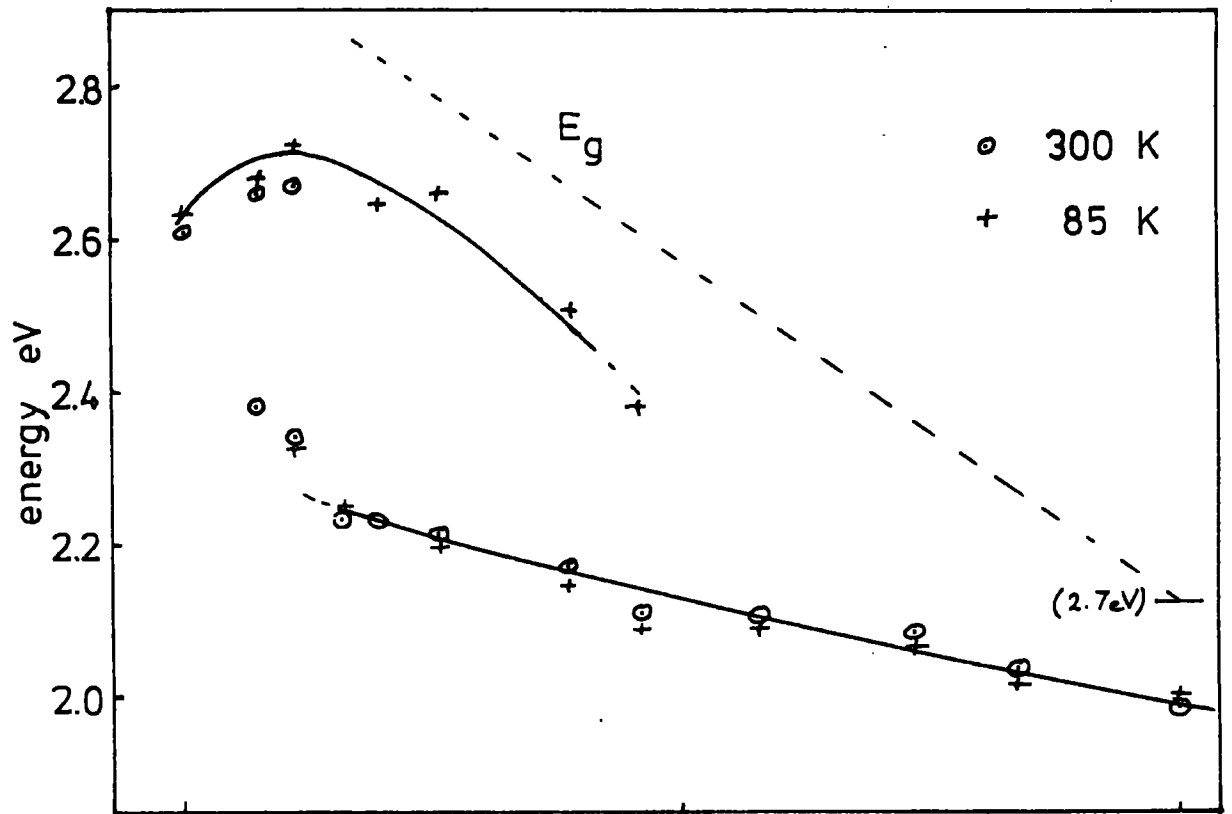


FIG 5.5 variation of photoluminescence peak position with composition before and after annealing in Zn

with sulphur content up to  $x \sim 0.9$ , and there was a shift to lower energy by approximately 20 meV when the temperature was reduced from 300 to 85 K. Between  $x \sim 0.9$  and  $x = 1.0$  there was a rapid shift in the peak position to higher photon energies by  $\sim 400$  meV. Ozawa and Hersh (1973) have reported that the blue luminescence band of ZnS at  $4600 \text{ \AA}$  (2.70 eV) "jumped" to the green spectral region on first introducing ZnSe and thereafter monotonically shifted to longer wavelengths with further increase in the proportion of ZnSe in  $\text{Zn(S,Se):I}$ . The results presented here indicate that there is a large initial change in the position of the luminescence bands with the addition of small percentages of ZnSe. The high energy band becomes resolvable at 85 K and, with  $x > 0.5$ , emerges as a discrete peak which shifts in energy in a manner following the variation in the band-gap for values of  $x$  up to 0.8. For  $x > 0.8$  there is a departure from linearity and the emission peak reaches a maximum photon energy before dropping by  $\sim 100$  meV to the position of the single luminescence band observed in zinc sulphide at 2.62 eV.

### 5.2.2 Iodine Transport crystals annealed in zinc

As stated previously the alloys of  $\text{Zn(S,Se)}$  may contain trace impurities, especially copper, with concentrations of the order of a few p.p.m. Aven and Woodbury (1962) have shown that copper may be extracted from zinc chalcogenides by heating samples in molten zinc at temperatures near  $850^\circ\text{C}$ . The as-prepared mixed crystal samples were annealed in liquid zinc for five days at  $1000^\circ\text{C}$  in an attempt to minimise the effect of impurities on the luminescence properties. Contaminants such as copper segregate out and dissolve in the molten solution. Zinc has been shown to diffuse into the crystals and reduce the sample resistivity.

The zinc extraction process, as it is called, is used within the department for the preparation of low resistivity material for electroluminescent devices. Qualitatively it was observed that the effect of annealing in zinc was to enhance the intensity of the photoluminescence emission. It is concluded that the zinc diffuses through the crystal lattice and may occupy sites responsible for the quenching of radiative transitions.

The photoluminescence emission spectra excited by 3650 Å radiation at room temperature and 85 K are shown in Figs. 5.6 and 5.7 respectively. At room temperature, with the exception of sample 965 which will be discussed later, a single band of luminescence only remained after annealing in zinc. This emission band shifted towards higher quantum energy with increasing sulphur content. On cooling to liquid nitrogen temperature, a second band became apparent as a high energy shoulder on the peak observed at room temperature. The relative intensity of the high energy band to that of the low energy band increased with sulphur mole fraction until, as with sample 961, the higher energy band dominated the emission. The variation of the position of the photoluminescence peaks with composition is shown in Fig. 5.5. The low energy band varied linearly with composition and the behaviour of this emission band is similar to that shown in the crystals before annealing in zinc. Cooling the samples to 85 K led to a shift of the low energy band to slightly lower energies by approximately 25 meV. The half-widths of the luminescence bands are recorded in Table 5.1; in calculating the half-widths the assumption has been made that the overlapping bands of radiation should be approximately Gaussian in form. The reduction in the half-widths with decreasing temperature from 300 to 85 K was approximately 140 meV throughout the whole range of compositions. This value is in good agreement

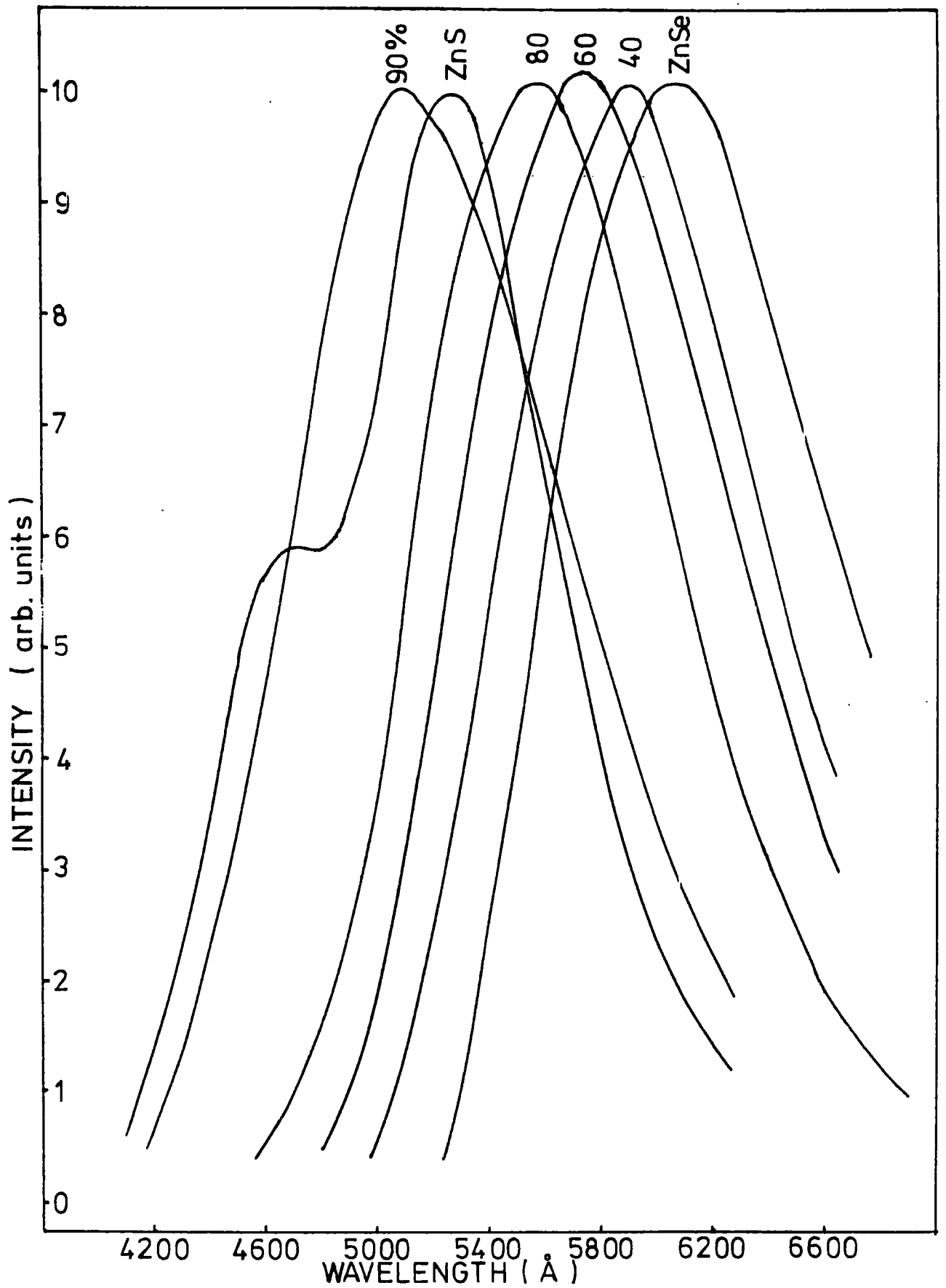


FIG 5.6 PHOTOLUMINESCENCE OF Zn(S, Se) : I, Zn  
AT 300 ° K

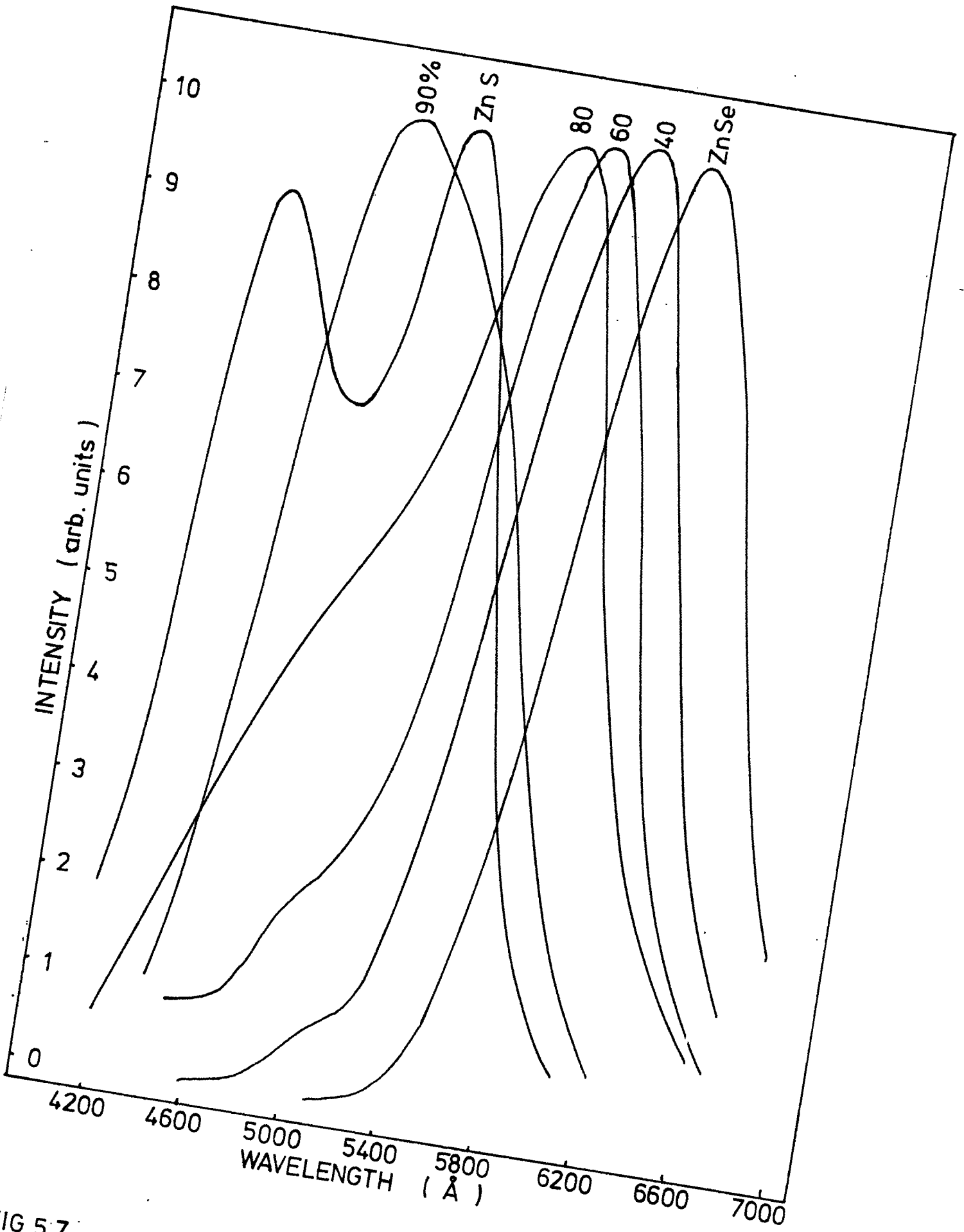


FIG 5.7  
 PHOTOLUMINESCENCE OF Zn(S,Se):I,Zn  
 AT 85 ° K

TABLE 5.1

HALF-WIDTHS OF EMISSION BANDS AFTER TREATMENT  
IN ZINC

Sample	Peak $\lambda$ ( $\text{\AA}$ )	Half-Width at 300 K (eV)	Half-Width at 85 K (eV)
ZnSe	6050	0.40	0.26
ZnS <sub>0.4</sub> Se <sub>0.6</sub>	5950	0.41	0.28
ZnS <sub>0.6</sub> Se <sub>0.4</sub>	5780	0.44	0.30
ZnS <sub>0.8</sub> Se <sub>0.2</sub>	5650	0.43	0.33
ZnS <sub>0.9</sub> Se <sub>0.1</sub>	4950	0.49	0.39
ZnS	4750	0.39	0.28

with that reported for the self-activated luminescence in ZnS and ZnSe; the magnitude and direction of the shift in energy of the emission maxima also suggests that this low energy band is due to a self-activated emission.

The sample of ZnS which was annealed in zinc, crystal 965, was not the same crystal as was examined in the previous section. An examination of the luminescence results tends to suggest that this particular crystal was heavily contaminated with copper. The sample exhibited two narrow emission bands at room temperature with peaks at  $4720 \text{ \AA}$  (2.63 eV) and  $5280 \text{ \AA}$  (2.35 eV) shifting to  $4490 \text{ \AA}$  (2.76 eV) and  $5220 \text{ \AA}$  (2.37 eV) at 85 K. The positions of these bands and their shift to higher energies on cooling agree with the observations of Shionoya (1964) on the copper-blue and copper-green bands in zinc sulphide. Uncontaminated samples of ZnS containing iodine as a co-activator have shown a single band at  $4760 \text{ \AA}$  (2.60 eV) at 85 K.

The second, higher-energy band appears in all crystals of mixed composition containing both Se and S; this band can be observed as a shoulder on the lower energy band, but cannot be resolved as a distinct peak following the annealing in zinc. The effect of zinc diffusing through the crystal lattice may be to affect the centres responsible for the low-energy and high-energy band emissions and alter the relative recombination rates at these centres. It is also worth noting that the relative intensity of the high-energy band to the low-energy band varies with varying sulphur content; the relative intensity of the high-energy band increases with the mole fraction of sulphur, either as a direct result of the number of sulphur atoms present in or around the luminescence centre, or as an indirect result with the lattice parameter and thus the band-gap changing.

### 5.2.3 Vertical Furnace Crystals

Mixed crystal samples, grown in a vertical furnace by the technique developed by Burr and Woods (1971), were examined next in order to compare their properties with those of crystals grown with iodine as a coactivator. Qualitatively the intensity of the luminescence from these samples was lower than that of the Iodine Transport crystals, and in general the emission could be monitored only at liquid nitrogen temperature. It was difficult to produce crystals by this growth method and as a result only four samples throughout the range of composition were produced and examined.

The photoluminescence spectra measured at room temperature and 85 K respectively are shown in Figs. 5.8 and 5.9. It was not possible to measure the photoluminescence at room temperature of either the sample of ZnSe or  $\text{ZnS}_{0.6}\text{Se}_{0.4}$  because of the low levels of emission. At room temperature the other two crystals of ZnS and  $\text{ZnS}_{0.9}\text{Se}_{0.1}$  showed two emission bands centred at approximately 4600 Å (2.70 eV) and 5180 Å (2.39 eV). At 85 K the two bands of emission from the sample of ZnS became more pronounced at 4650 Å (2.67 eV) and 5150 Å (2.41 eV); the sample of  $\text{ZnS}_{0.9}\text{Se}_{0.1}$  showed a shift of the main band to higher energy at 4470 Å (2.77 eV) while still showing a tail on the lower energy side. The samples of  $\text{ZnS}_{0.5}\text{Se}_{0.5}$  and ZnSe show broad bands of emission centred at 4960 Å (2.50 eV) and 5900 Å (2.10 eV) respectively. A comparison of the results obtained here with those observed by Shionoya (1966) for ZnS seems to indicate that both the sulphur rich crystals were contaminated with copper and show the 'copper-green' emission at ~5100 Å and the 'copper-blue' emission at ~4450 Å when the samples are cooled to 85 K. The band at 4650 Å in the sample of ZnS agrees well with the position reported for the self-activated emission.

The crystals grown in the vertical furnace were annealed in zinc using a treatment similar to that applied to the iodine-transport crystals.

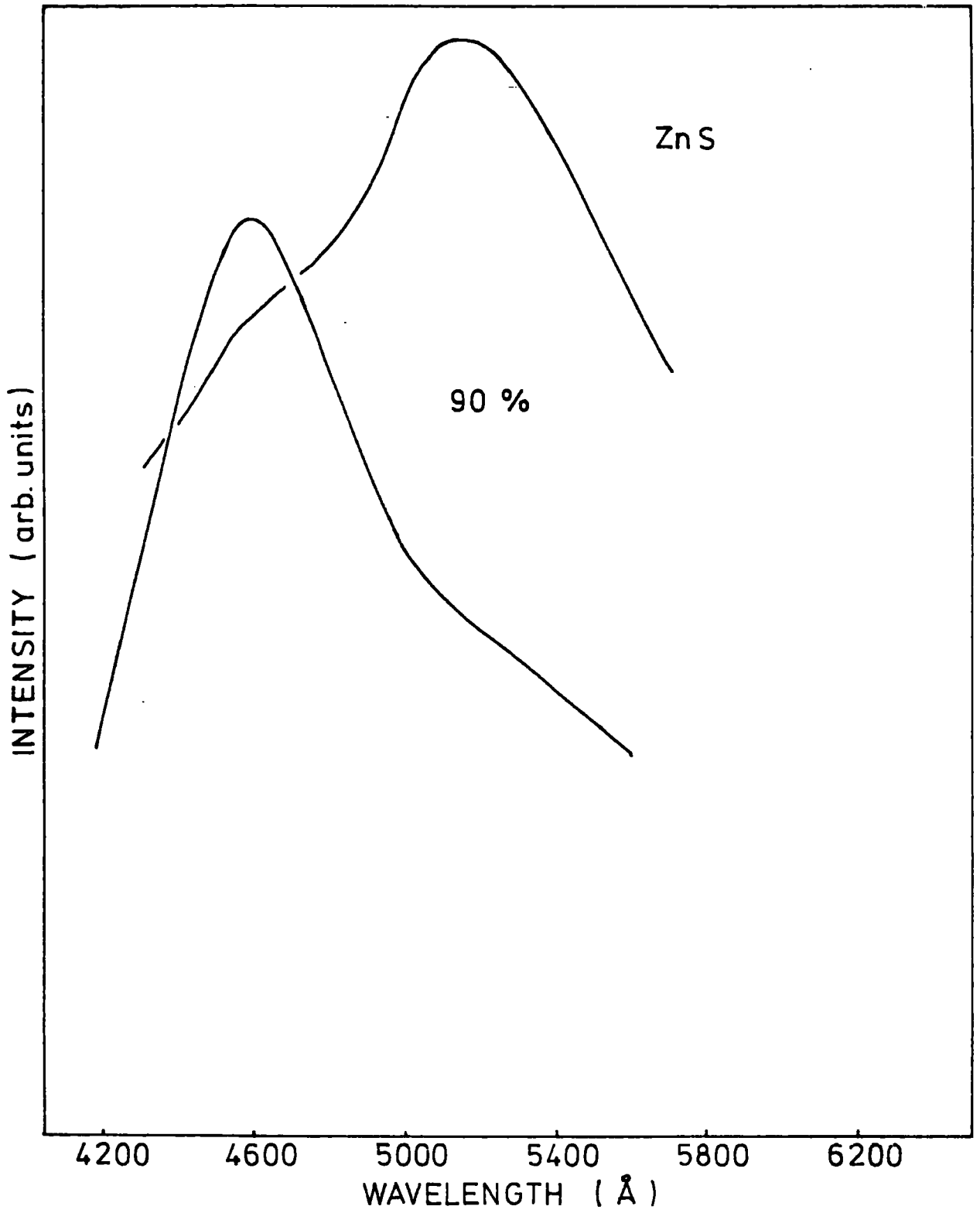


FIG 5.8 PHOTOLUMINESCENCE AT 300 K OF VERTICAL FURNACE CRYSTALS

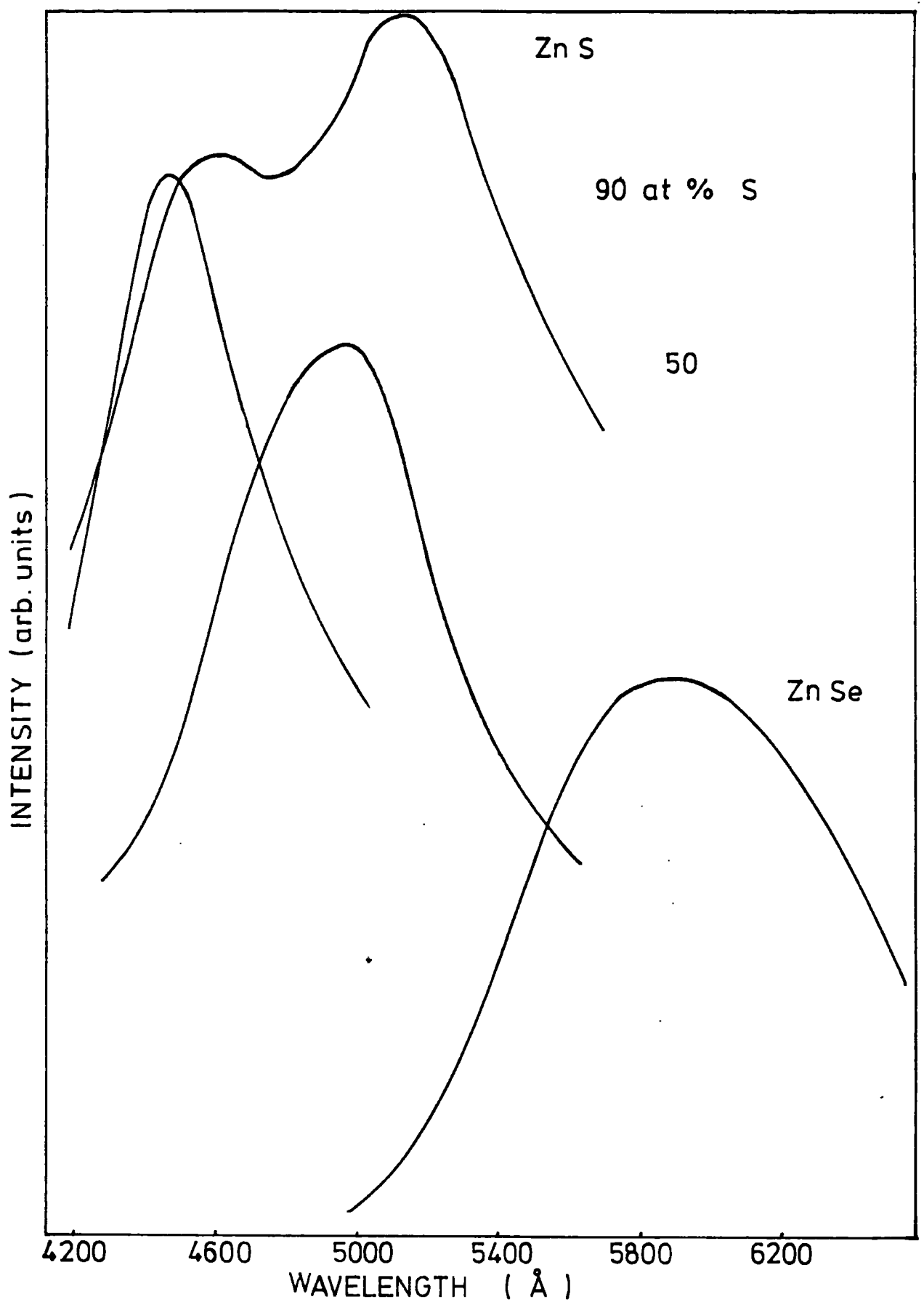


FIG 5.9 PHOTOLUMINESCENCE AT 85 K OF VERTICAL FURNACE CRYSTALS

The samples were then re-examined and the resultant photoluminescence is shown in Figs. 5.10 and 5.11 at room temperature and 85 K respectively. The emission spectra at 85 K were markedly changed after annealing in zinc: the sample of ZnS exhibited a shift of the shorter wavelength band to a higher energy at 4440 Å (2.79 eV) while the second band remained unchanged at 5140 Å (2.41 eV). These bands correspond to the positions reported for the Cu-Blue and Cu-Green emissions in ZnS. The sample of  $\text{ZnS}_{0.5}\text{Se}_{0.5}$ , crystal 346, which previously had exhibited a band at 4960 Å (2.50 eV) with a low energy tail, showed two emission bands at 4980 Å (2.49 eV) and 5990 Å (2.07 eV). The sample of ZnSe, which originally had a broad band centred at 5900 Å (2.10 eV), showed two bands at 5330 Å (2.24 eV) and 6350 Å (1.95 eV) after annealing in zinc; these positions are in good agreement with the bands associated with copper emission in zinc selenide. The evidence from the photoluminescence spectra tends to suggest that the crystals had become contaminated with copper during the annealing treatment in zinc.

### 5.3 Cathodoluminescence

The luminescence emitted by the mixed crystals under electron bombardment was also examined in order to make a comparison with the results obtained under ultra-violet excitation. As already stated, the relative intensities and positions of the emission bands were affected by a change in the intensity of photo-excitation, and it was hoped that the high intensity electron beam might provide further information. The ultra-violet source emitted radiation at 3650 Å (3.4 eV), i.e. photons with less energy than the band-gap for the high sulphur content crystals and it was felt that this might have affected the observed emission as the composition was varied.

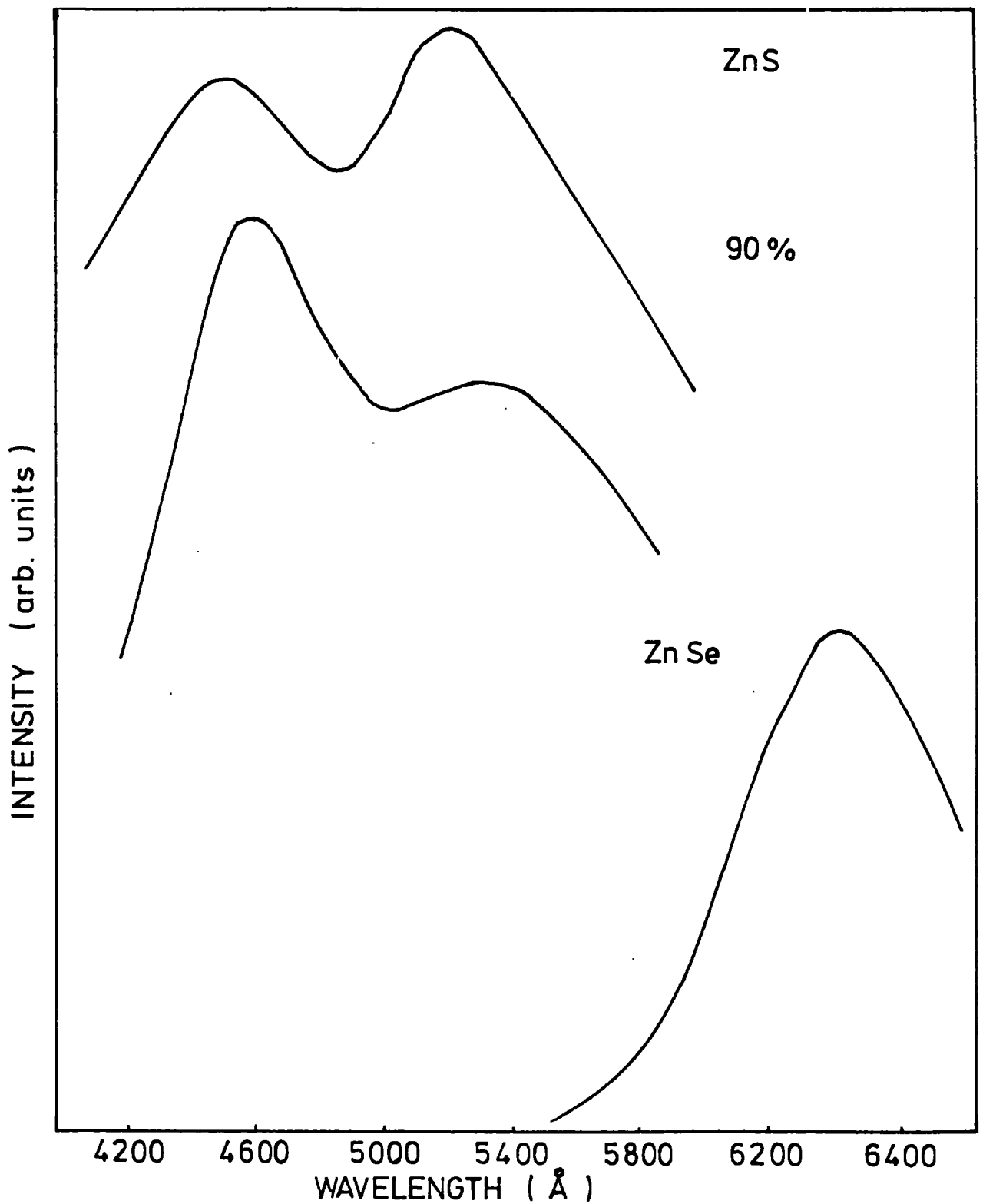


FIG 5.10 PHOTOLUMINESCENCE AT 300°K OF VERTICAL FURNACE CRYSTALS ANNEALED IN Zn

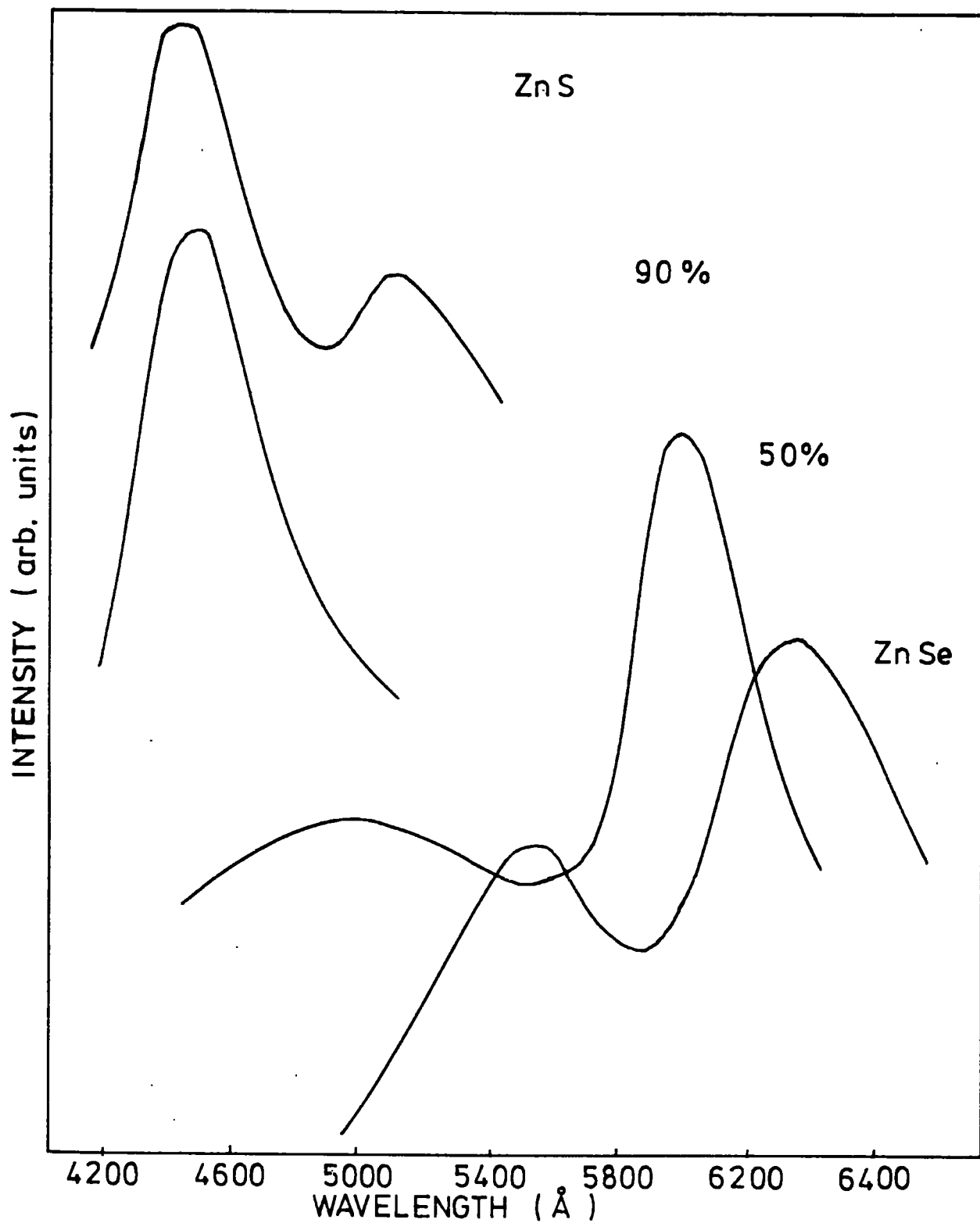


FIG 5.11 PHOTOLUMINESCENCE AT 85°K OF VERTICAL FURNACE CRYSTALS ANNEALED IN Zn

### 5.3.1 Iodine Transport Crystals

The cathodoluminescence spectra of the series of mixed crystals grown by iodine transport are shown in Figs. 5.12 and 5.13 at room temperature and 85 K respectively. At room temperature the peak positions and band shapes were in good agreement with those obtained from the photoluminescence spectra of the same samples. There was a general shift of the low-energy band to shorter wavelengths as the sulphur content was increased. For high values of  $x$  the high-energy band appeared first as a broadening of the emission as in sample 958, and then as a separate band which dominated the emission as in sample 961. With crystal 961, where  $x \sim 0.9$ , the high-energy band appeared at  $4590 \text{ \AA}$  (2.70 eV) at a shorter wavelength than the corresponding band in the sample of ZnS at  $4720 \text{ \AA}$  (2.63 eV). On cooling the crystals to 85 K, all the mixed crystals showed distinctly the presence of both the high- and low-energy bands either as two separate bands or with the shorter wavelength band as a shoulder on the longer wavelength band. The samples of ZnSe and ZnS had shoulders in the emission at  $\sim 6500 \text{ \AA}$  and at  $\sim 4400 \text{ \AA}$  respectively indicating the presence of copper as a contamination.

The samples containing a large percentage of sulphur,  $x > 0.6$  emitted a narrow high energy band which was close to the band-gap energy for the particular composition. For example, sample 961 with composition  $\text{ZnS}_{0.9}\text{Se}_{0.1}$  would possess a band-gap of 3.63 eV at 85 K, assuming the linear variation of energy gap with composition predicted by Larach, Stocker and Shrader (1957); the observed edge-emission in this crystal occurred at  $3675 \text{ \AA}$  (3.37 eV) with a half-width of  $\sim 0.25 \text{ eV}$ . An inspection of the shape of the edge-emission from sample 961 showed that the luminescence band was asymmetric and possessed a tail on the low energy side. However, it was not possible to resolve any fine structure. The

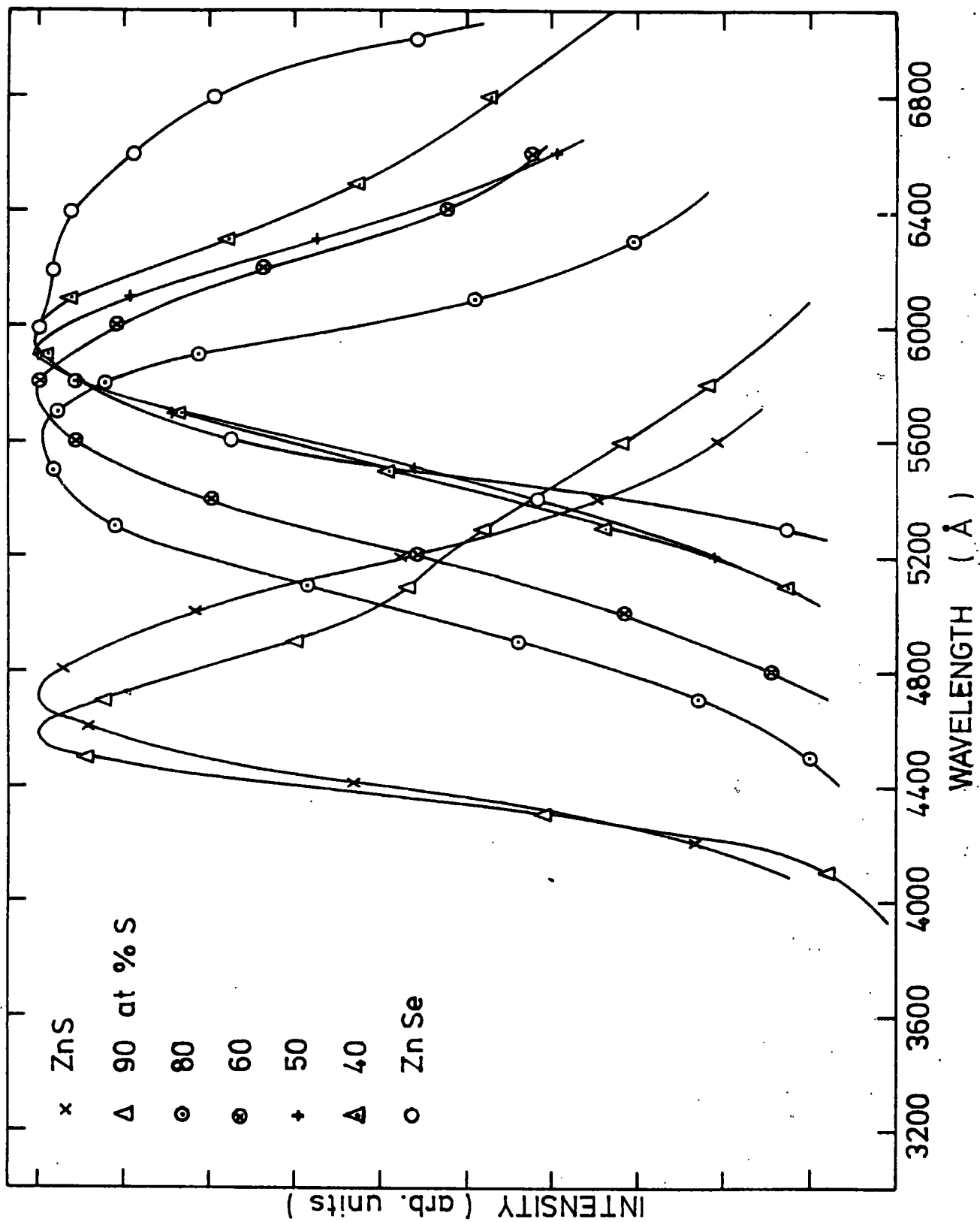


FIG 5.12 CATHODOLUMINESCENCE OF Zn(S,Se):I AT 300° K

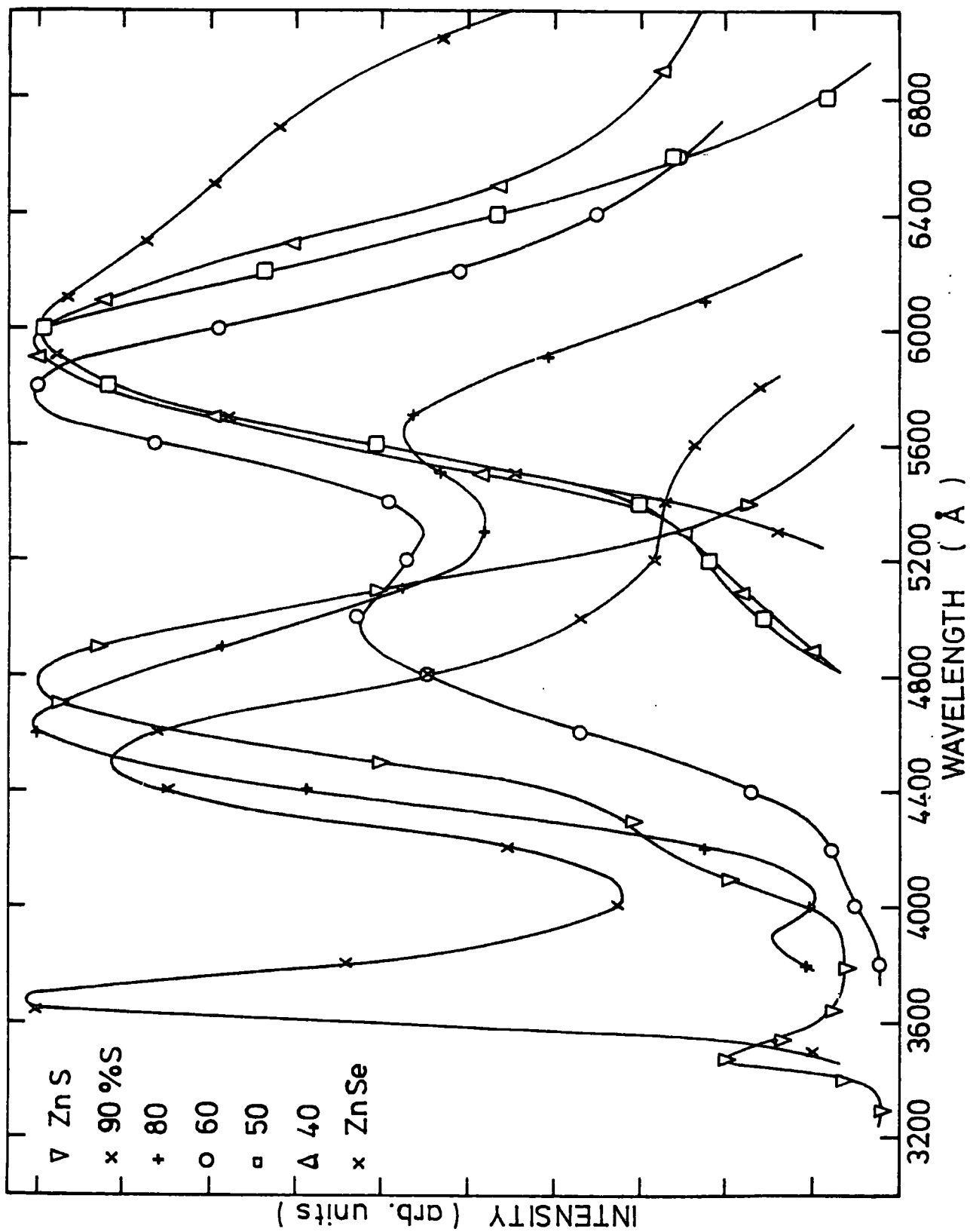


FIG 5.13 CATHODOLUMINESCENCE OF Zn(S,Se):I AT 85 ° K

relative intensity of the edge-emission increased markedly with the sulphur content of the crystals, and it can be seen that the edge-emission dominated the luminescence in sample 961.

The positions of the peaks of the luminescence bands as a function of composition are shown in Fig. 5.14 at both room temperature and 85 K. A second sample of ZnS:I, crystal 965, was examined and the emission bands shown in Fig. 5.18 are also included in Fig. 5.14 for comparison. There appear to be four distinct series of emission bands: (1) the edge-emission which can be observed only at low temperatures and which is rapidly quenched on warming; (2) the high-energy band which exhibits a shift in position to higher energies on reducing the temperature; (3) the low-energy band which moves to lower energies; (4) an emission which appears at an intermediate energy between the high-energy and low-energy bands in certain crystals and which shifts to lower energies on cooling. It has not been possible to make any quantitative measurement of the effect of temperature on the half-widths of the emissions since most bands tend to overlap.

### 5.3.2 Iodine Transport crystals treated in zinc

The annealed crystals previously examined under ultraviolet excitation were also studied under cathodo-excitation. The cathodo-luminescence spectra measured at room temperature and at 85 K are shown in Figs. 5.15 and 5.16. The effect of the treatment in zinc on the room temperature spectra is to reduce the half-width of the luminescence bands, and the bands appear to be more nearly Gaussian in shape. For example, crystal 961  $\text{ZnS}_{0.9}\text{Se}_{0.1}$ , which previously exhibited a peak at  $4590 \text{ \AA}$  (2.70 eV) with a shoulder at approximately  $5100 \text{ \AA}$  (2.43 eV), now had a single broad band centred at  $4920 \text{ \AA}$  (2.52 eV) at 300 K. On reducing the

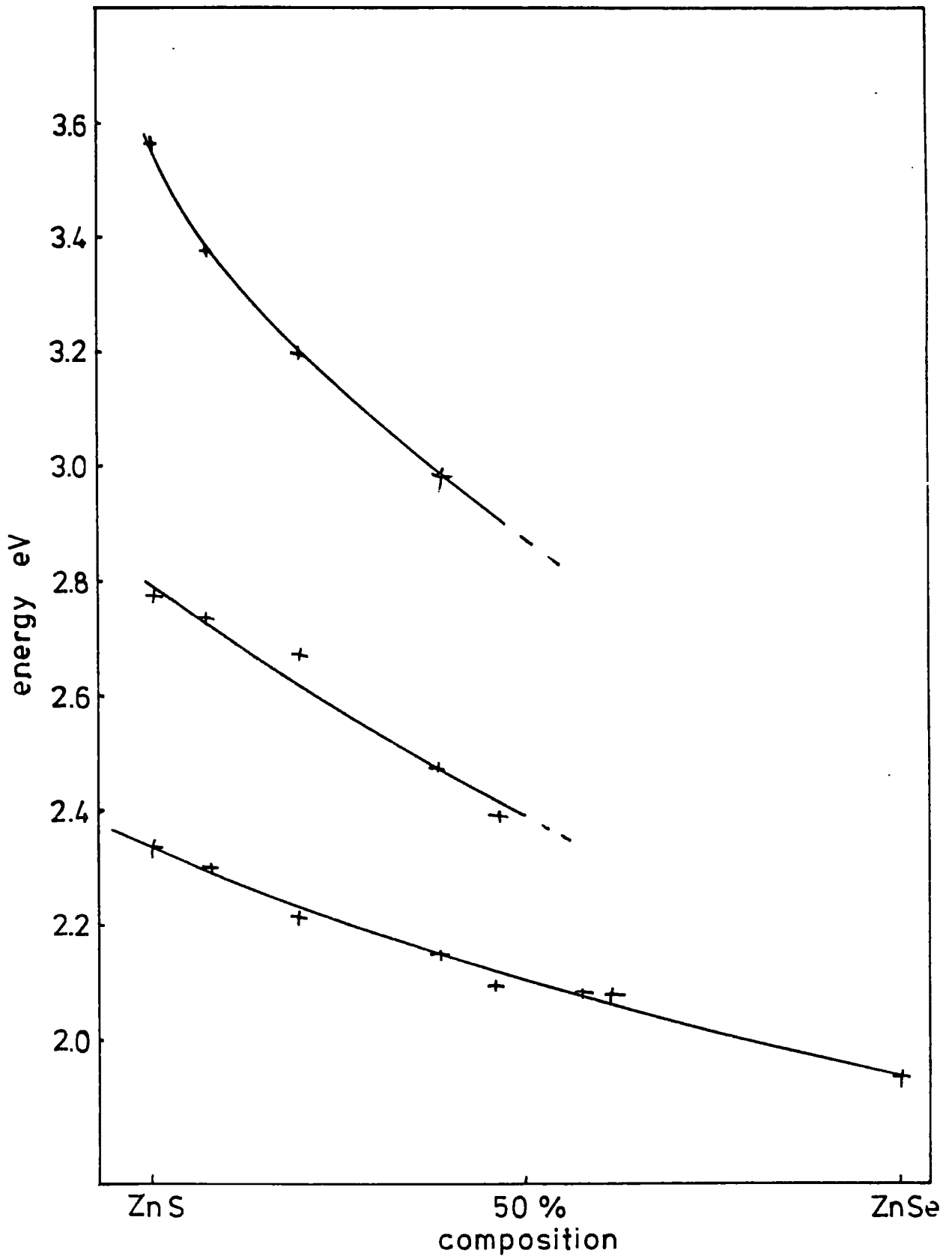


FIG 5.14 VARIATION OF CATHODOLUMINESCENCE PEAK POSITION WITH COMPOSITION IN  $\text{Zn}(\text{S},\text{Se}):\text{I}$

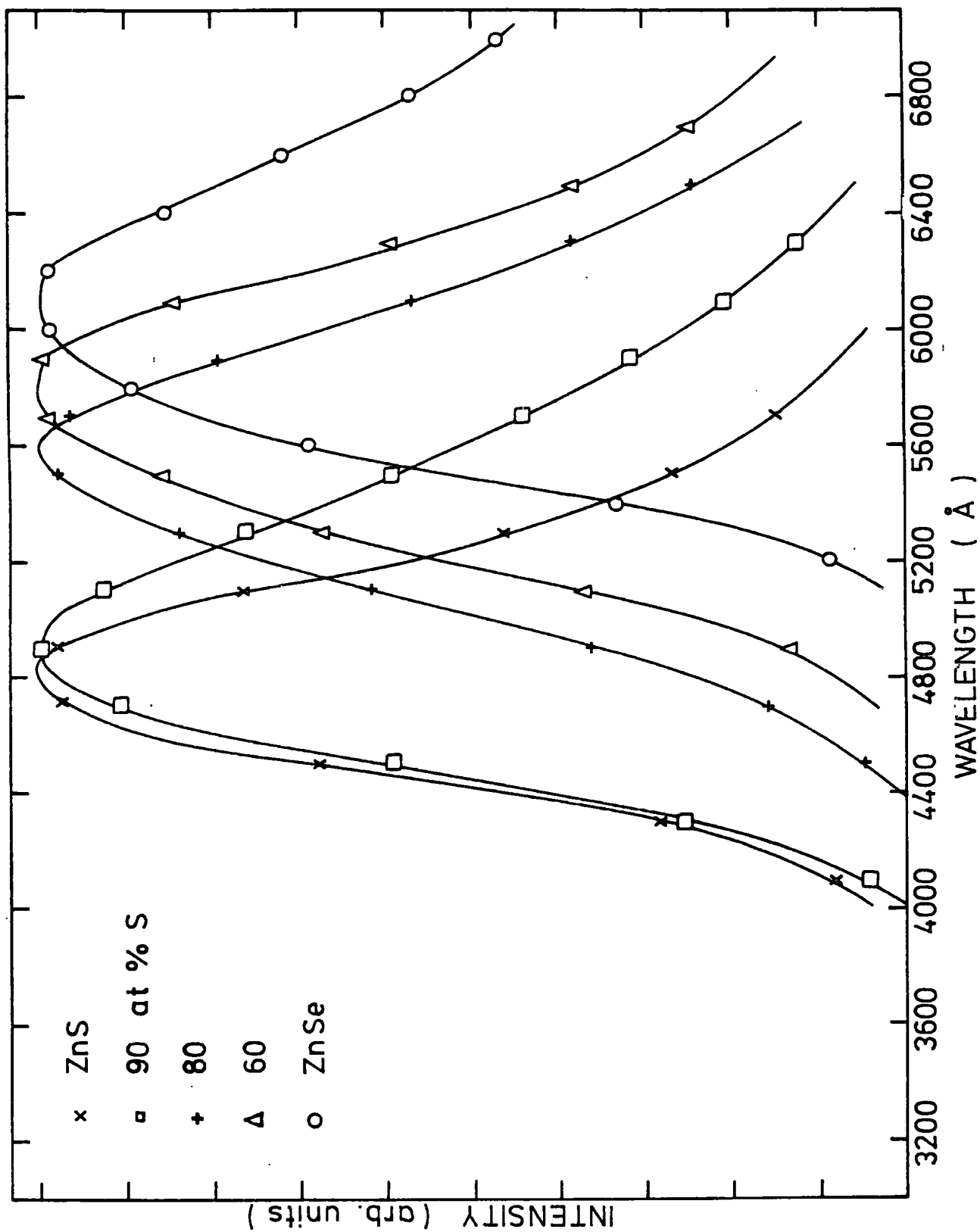


FIG 5.15 CATHODOLUMINESCENCE OF  $Zn(S,Se):I,Zn$  AT  $300^{\circ}K$

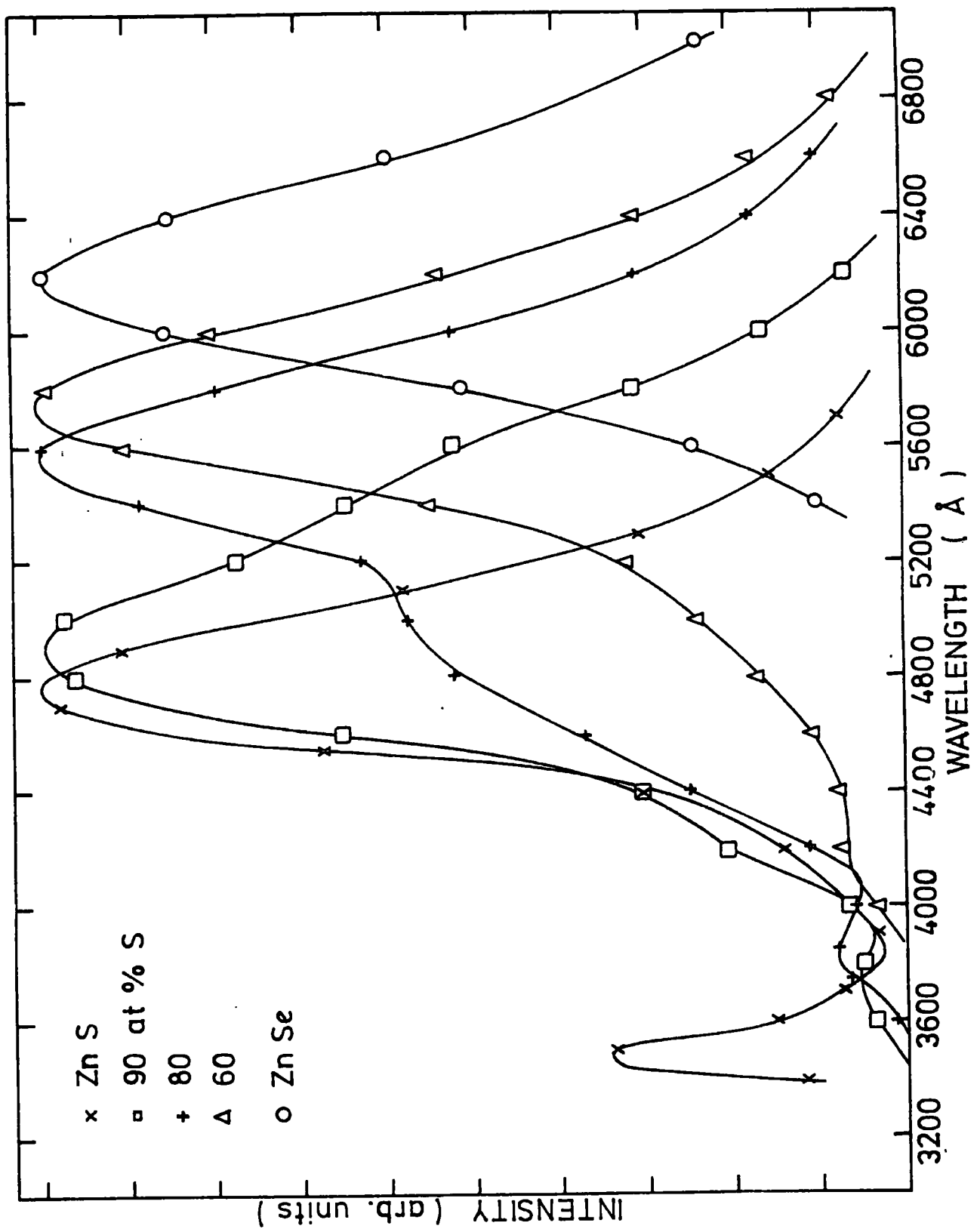


FIG 5.16 CATHODOLUMINESCENCE OF Zn(S,Se):I,Zn AT 85°K

temperature to 85 K, the low-energy band was little changed in position, however the relative intensity of the edge emission was much reduced by comparison with that observed prior to the annealing in zinc and the high-energy band was shifted to lower energies by approximately 150 meV.

The variation of the peak position with composition is shown in Fig. 5.17 after the treatment in zinc. A comparison with the results before annealing indicates that there was no measurable difference in the energy of the edge-emission or of the low-energy band. The high-energy band was either much reduced in intensity or was not present, and a new band appeared in an intermediate energy position. To illustrate these features, the spectra for two samples of ZnS:I with and without zinc treatment are shown in Fig. 5.18. The untreated sample 965 exhibited two deep centre emission bands at 4480 Å and 5280 Å, whereas after annealing the sample showed a single band at 4780 Å with a slight shoulder in the region of 4300 Å. A comparison with the results reported by Shionoya (1964) would indicate that the bands in the green and blue are associated with copper contamination, and that annealing in zinc results in the removal of these trace impurities leaving the self-activated luminescence band in an intermediate energy position. The cathodoluminescence spectra for two sulphur-rich crystals, sample 961  $\text{ZnS}_{0.9}\text{Se}_{0.1}$  and sample 958  $\text{ZnS}_{0.8}\text{Se}_{0.2}$ , are shown in Figs. 5.19 and 5.20 after annealing in zinc. The luminescence spectra of these crystals consisted of up to four overlapping bands of emission. It has been widely reported, see for example Shionoya (1966), that the individual luminescence bands observed in zinc sulphide are approximately Gaussian in shape. The emission spectra of samples 961 and 958 have therefore been analysed assuming a Gaussian distribution, and in this way peak energy positions have been obtained for the overlapping bands.

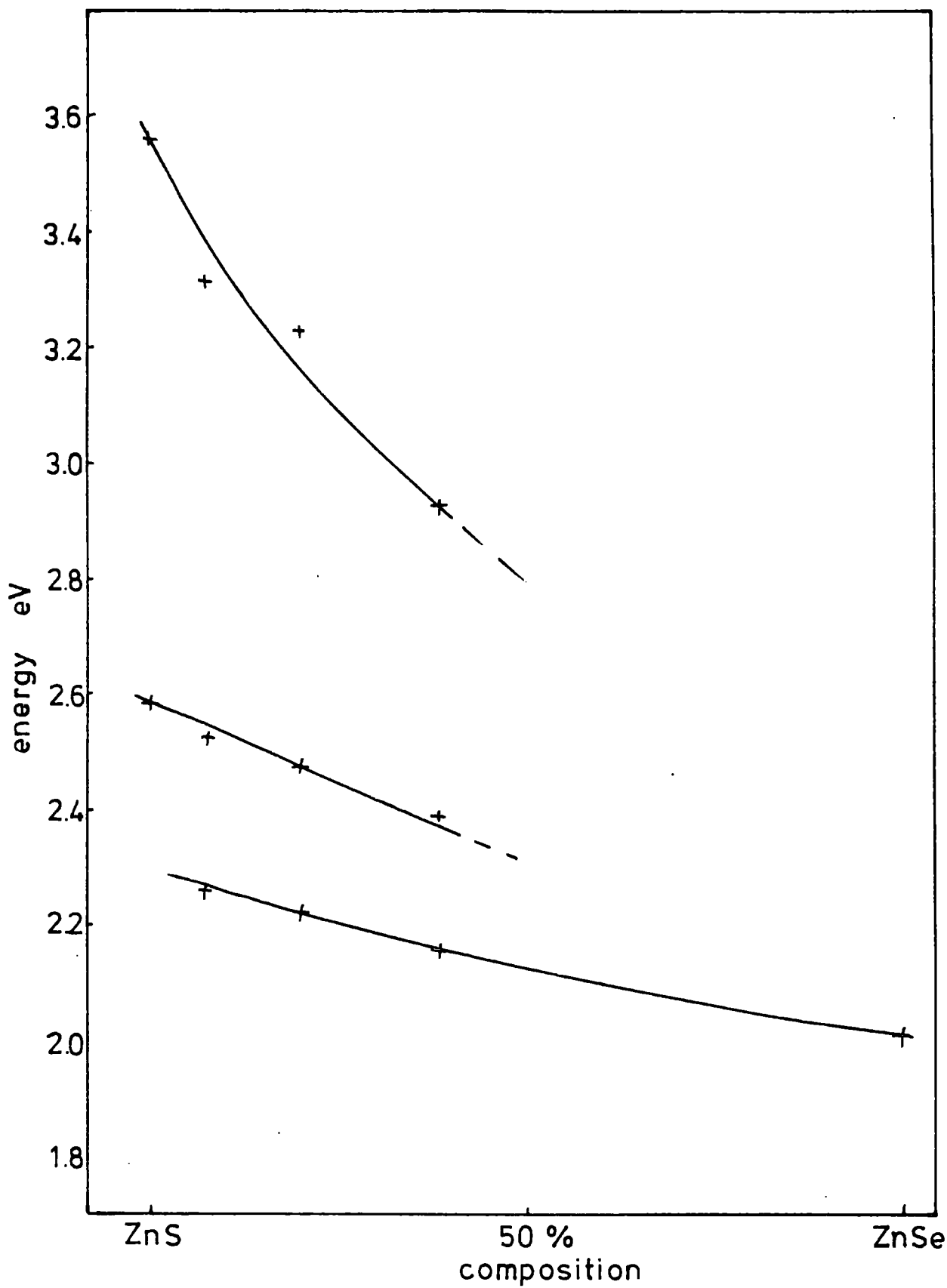


FIG 5.17 VARIATION OF CATHODOLUMINESCENCE PEAK POSITION WITH COMPOSITION IN  $Zn(S,Se):I,Zn$

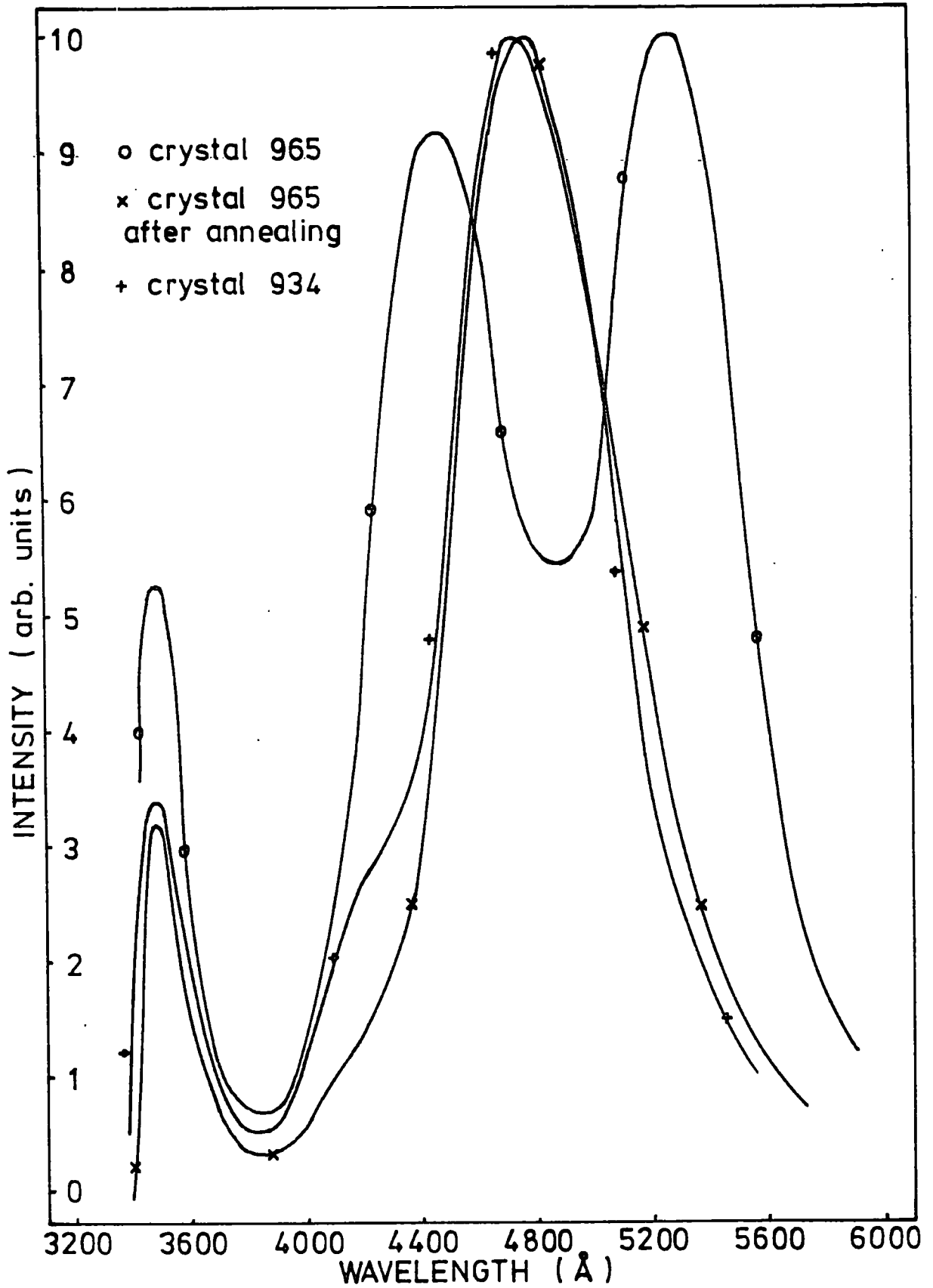


FIG 5.18 CATHODOLUMINESCENCE OF ZnS CRYSTALS  
 AT 85 °K

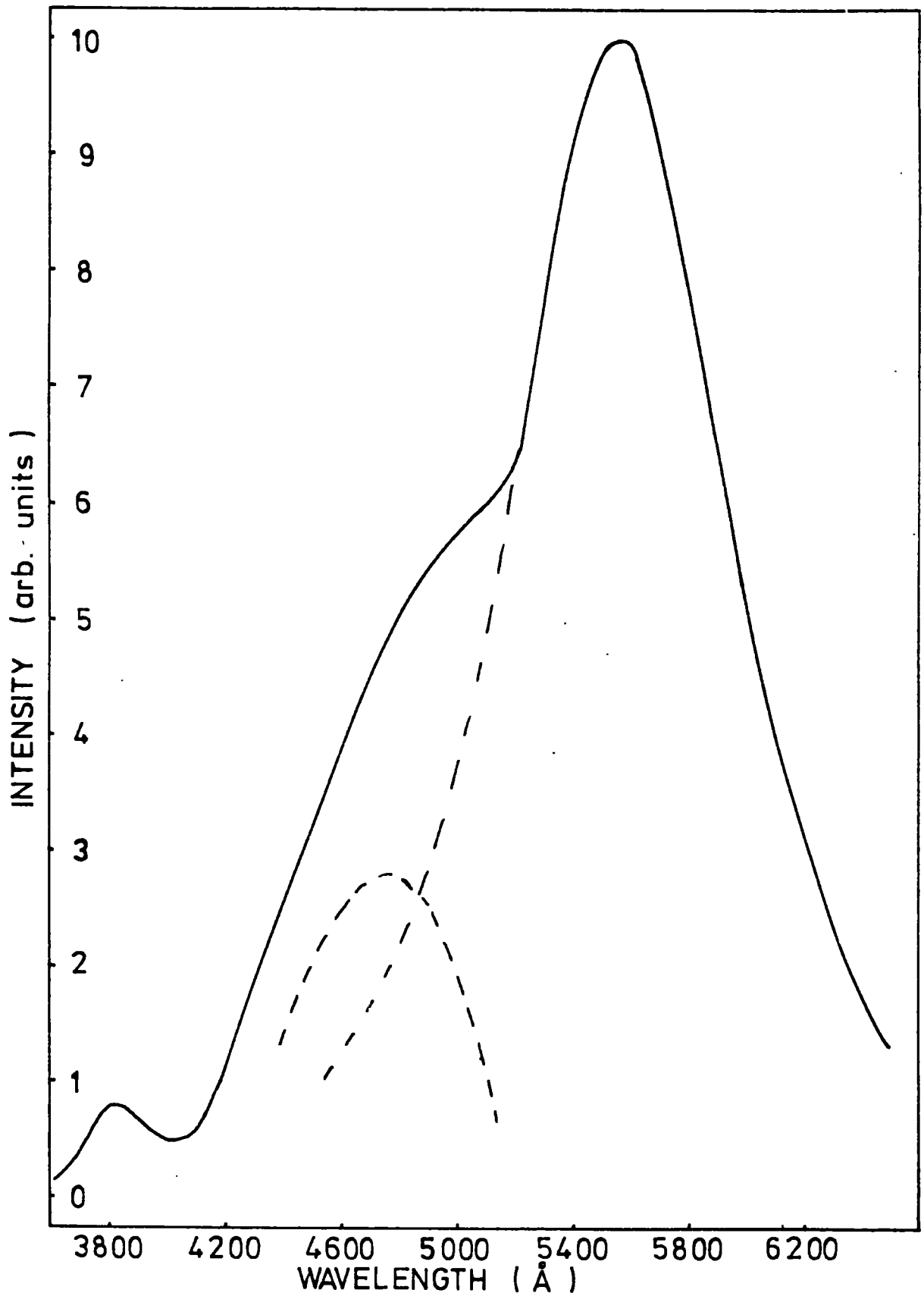


FIG 5.19 CATHODOLUMINESCENCE OF CRYSTAL 958  $ZnS_{0.8}Se_{0.2}$   
AT 85 °K

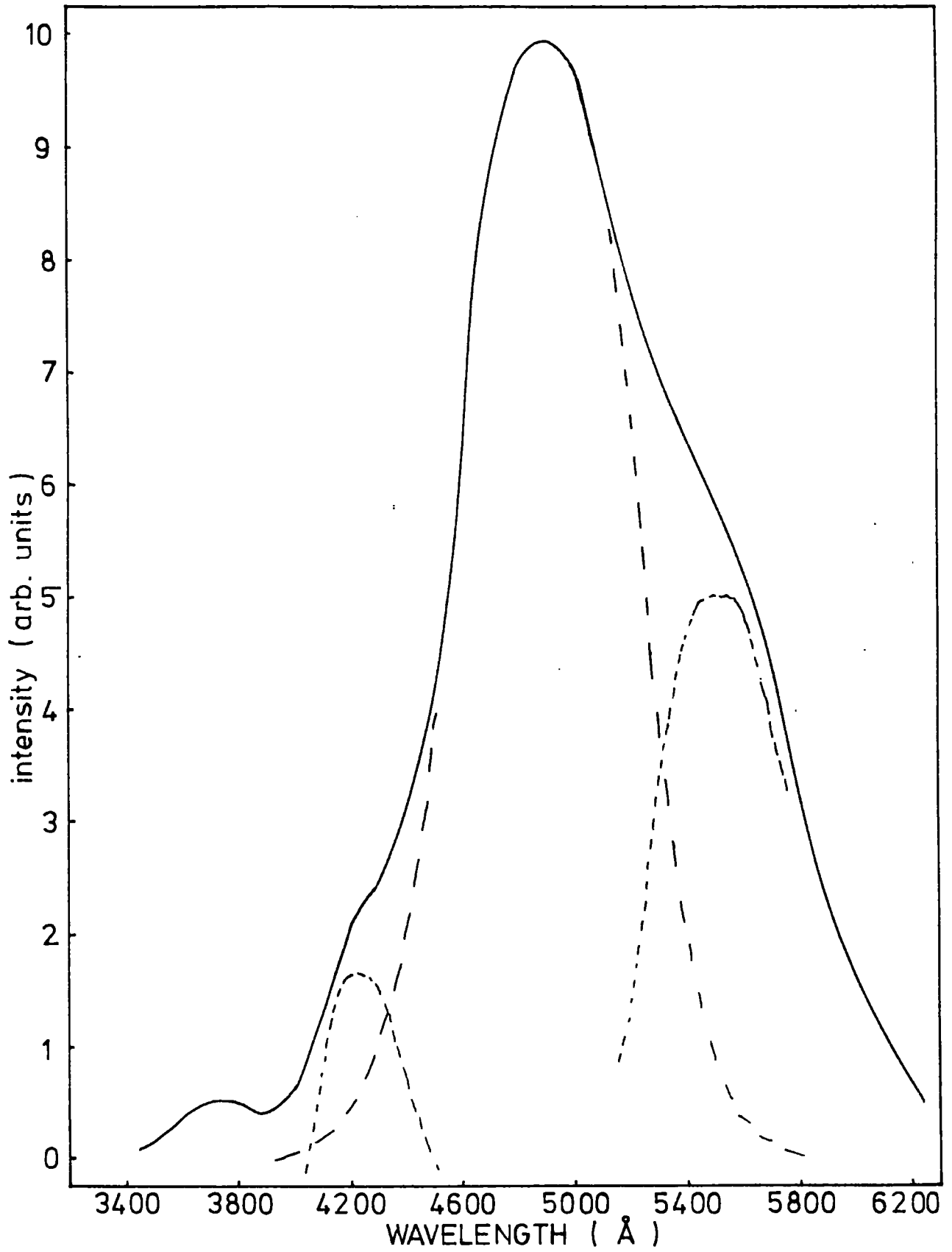


FIG 5.20 CATHODOLUMINESCENCE OF CRYSTAL 961



In Chapter 6 the emission spectra from mixed crystals doped with copper are examined, and the positions of 'copper-blue' and 'copper-green' bands due to two copper centres have been established. It will be suggested that the overlapping emission bands observed in the undoped mixed crystals are the result of the presence of self-activated and copper contamination centres.

#### 5.4 Excitation Spectra

As has been mentioned, as many as four emission bands have been observed in the luminescence of mixed crystals of Zn(S,Se). The excitation spectra for the series of crystals have therefore been studied in an effort to obtain more information about the processes involved and to resolve the nature of the centres responsible for the transitions.

It was difficult in practice, however, to measure the excitation spectra of the undoped crystals grown by iodine-transport because of the very low level of emission intensity from these samples prior to treatment in zinc. It was necessary, therefore, to use wide band passes for both the monochromator and isolating filter during the measurement of the excitation spectra with a consequent reduction in resolution.

##### 5.4.1 Iodine Transport Crystals

The low-energy band excitation spectra measured at 85 K for the untreated series of mixed crystals are shown in Fig. 5.21. The spectra demonstrated the presence of two bands of excitation: a narrow band at an energy close to the band-edge for the particular composition of the crystals, this band could sometimes be resolved only as a shoulder on the second peak; and a deep-lying broad band of excitation which shifted in wavelength from  $\sim 4700 \text{ \AA}$  in ZnSe to  $\sim 4050 \text{ \AA}$  in ZnS. The variation

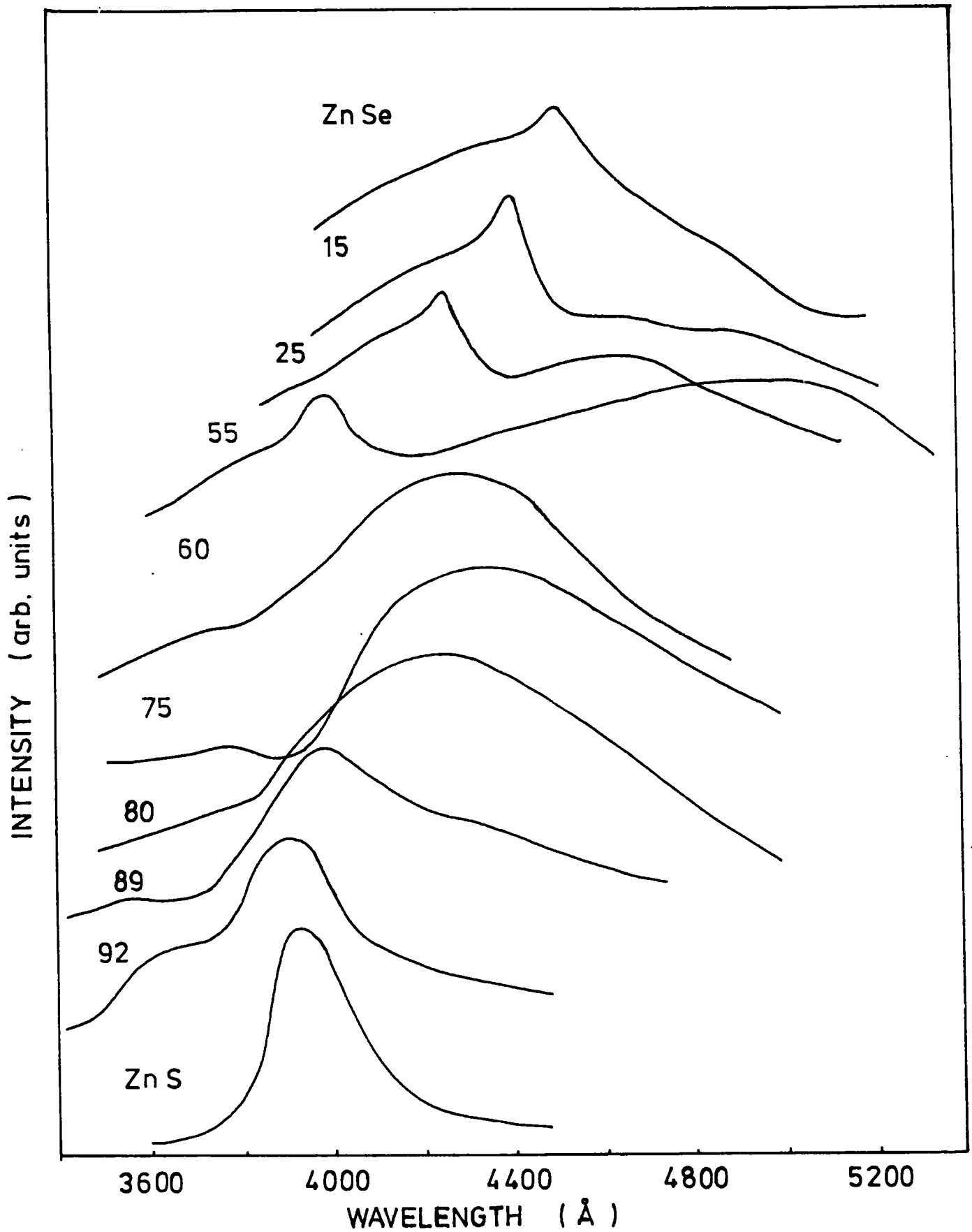


FIG 5.21 EXCITATION SPECTRA AT 85 °K

in the energy of the excitation bands as a function of composition is shown in Fig. 5.22; this diagram includes the excitation band energies for the high-energy emission observed only in sulphur-rich crystals at 85 K. The higher energy excitation peak appears to follow the absorption edge in the series of crystals and shifts from  $\sim 2.75$  eV in ZnSe to  $\sim 3.65$  eV in ZnS examining the long wavelength emission band at 85 K; there is a shift in the excitation peak position to lower energies by about 100 meV on raising the temperature to 300 K. However, the shift of the high energy excitation peak with composition is not linear which is contrary to the suggestion made by Larach, Shrader and Stocker (1957) that the band-edge varies linearly in the Zn(S,Se) alloy system. The position of the lower energy excitation peak appeared to be unaffected by changing the temperature, however a small change in position would not have been detected since this band was approximately  $500 \text{ \AA}$  wide.

By comparison, Jones (1974) has reported finding an excitation band in ZnSe at  $4880 \text{ \AA}$ , together with band-edge excitation, which was associated with self-activated emission with iodine as coactivator; Melamed (1958) has measured the excitation spectra for both self-activated emission and 'copper-green' emission in ZnS:Cu,Cl phosphor and found bands at  $\sim 3500 \text{ \AA}$  and  $\sim 4000 \text{ \AA}$  respectively. Shionoya (1963) has reported a band in the excitation spectra for the self-activated luminescence in cubic ZnS:Cl single crystals at  $\sim 3550 \text{ \AA}$ .

It is suggested here that the excitation spectra observed are the composite of a number of bands which result from the fact that the luminescence emission is of weak intensity and composed of several overlapping bands. It would also appear from the tail of the deep-lying excitation band to long wavelengths that copper contamination as well as the self-activated centres are playing a part in the luminescence processes.

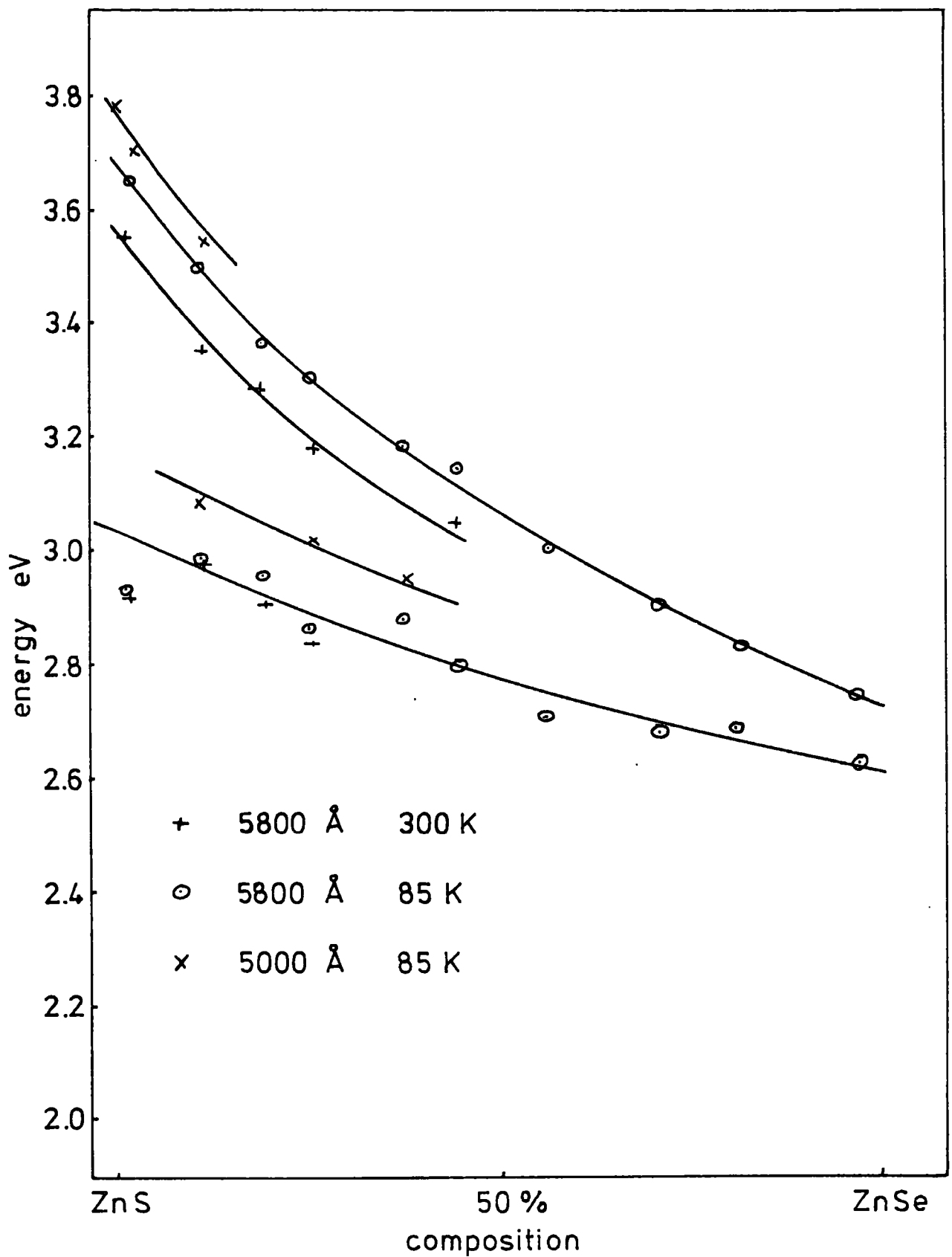


FIG 5.22 VARIATION OF EXCITATION PEAK POSITION WITH COMPOSITION IN Zn ( S, Se )

#### 5.4.2 Iodine Transport crystals treated in zinc

Annealing the samples of Zn(S,Se) in zinc has been shown to reduce the impurity content of the crystals especially by leaching out copper. The excitation spectra of the treated samples were therefore re-examined in an attempt to establish the native centres responsible for the luminescence. Qualitatively the intensity of the emission was observed to be enhanced subsequent to this treatment in zinc, and the luminescence bands became narrower.

The excitation spectra measured while monitoring the high-energy and low-energy band emissions are shown in Figs. 5.23 and 5.24 at room temperature and at 85 K respectively. The variable interference filter was used to isolate the luminescence band of interest. The low-energy emission band was excited in two bands: one was associated with a transition close to the energy of the band-gap, while the second was a broad band due to a deep centre. There was an indication from the shape of the second excitation band that it might be formed from the superposition of transitions from two separate levels, and this was more evident in the excitation bands after annealing in molten zinc. For crystals containing more than 40 atomic % sulphur, it was possible to measure the excitation of the high-energy shoulder which appeared on the low-energy band luminescence. The excitation spectra for this second band were similar to those for the low-energy band emission, but there appeared to be a less pronounced low energy tail. Since the observed emission bands were approximately 800 Å broad and tended to overlap, it was not possible to resolve distinctly the transitions responsible for the different emission bands. However, it would appear that the centres associated with the low-energy luminescence band are situated near the band-edge and deep in the gap, whilst the centres associated with the high energy band are

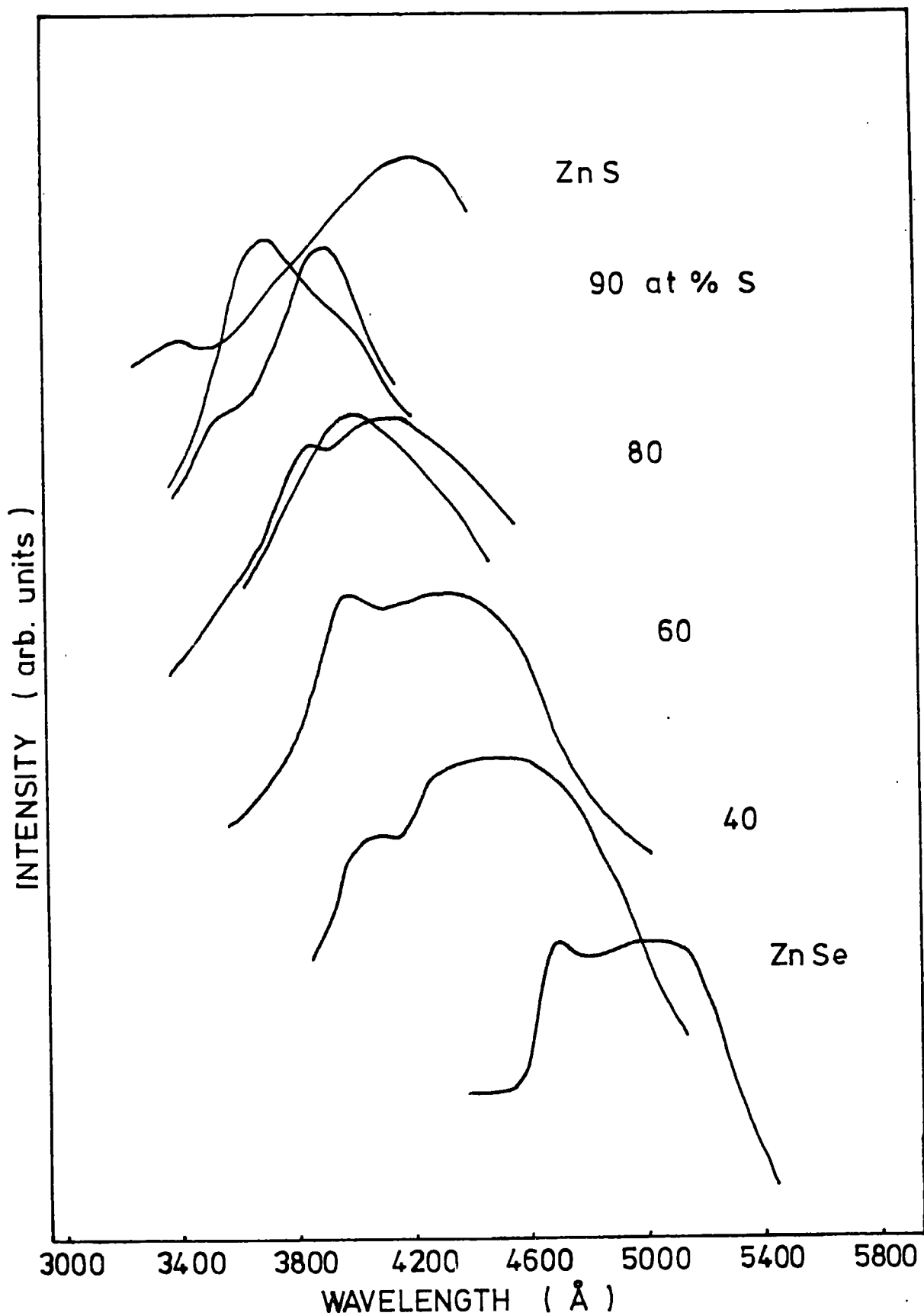


FIG 5.23 EXCITATION SPECTRA OF Zn(S,Se):I AT 300°K  
MONITORING S.A. EMISSION

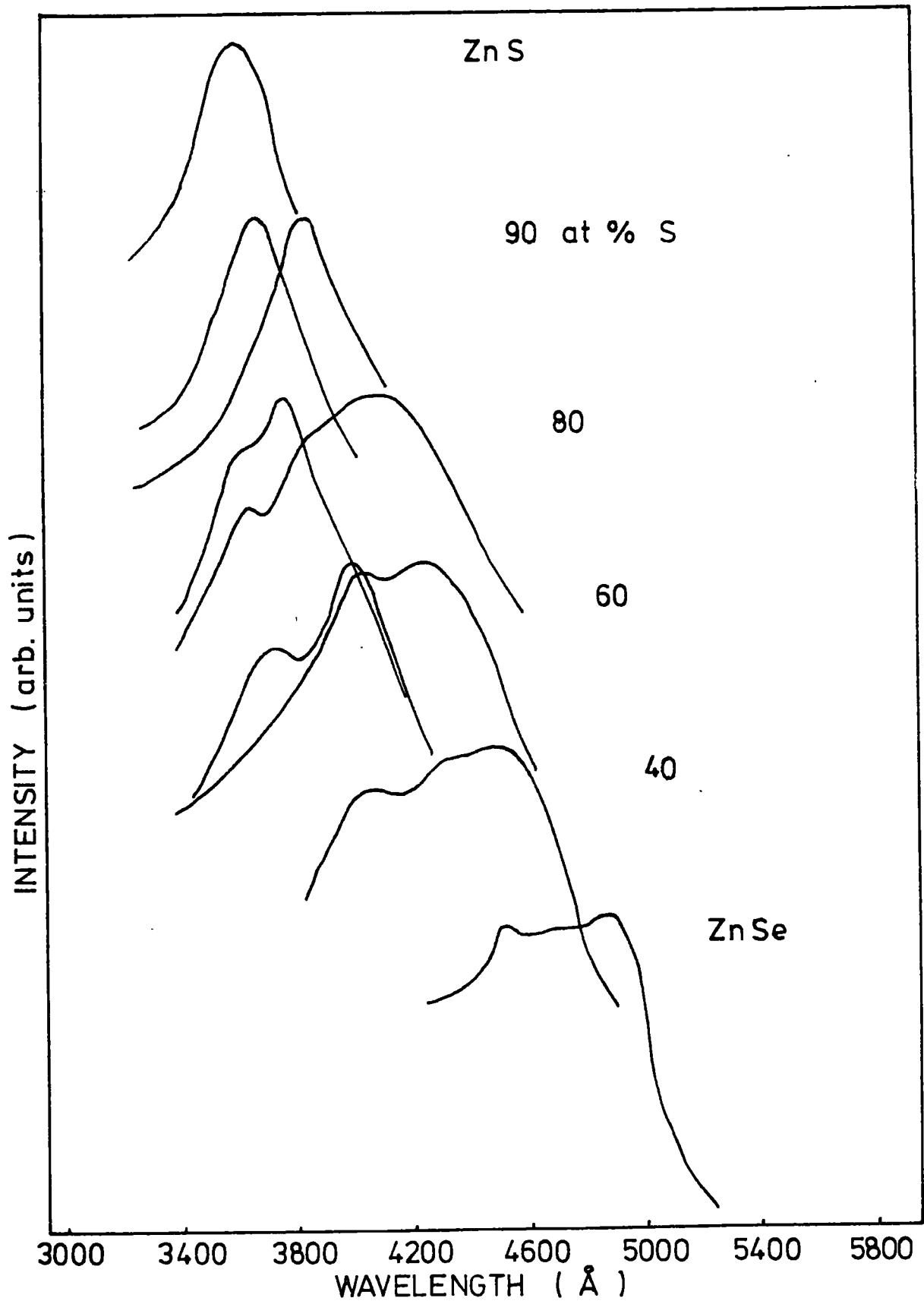


FIG 5.24 EXCITATION SPECTRA OF Zn(S,Se):I AT 85 ° K  
 MONITORING S.A. EMISSION

situated closer to the band-edge. The variation of the energy of the excitation peak with composition is shown in Figs. 5.25 and 5.26 at room temperature and at 85 K respectively. It can be seen that the excitation bands shift in an almost parallel manner to higher energies as the sulphur content increases. In the sulphur-rich samples at room temperature, the deeper-lying band appears to remain fixed at approximately 2.9 eV. However, this may be due to the fact that the excitation band is extremely broad and this makes the peak energy difficult to determine.

#### 5.4.3 Vertical Furnace Crystals

A small number of mixed crystals grown by the vertical furnace technique were available for examination. Nominally crystals prepared by this method should not have contained any halogen coactivator. An examination of the impurity content, during the course of work on the crystal growth, using a mass spectroscopy technique has revealed levels of contamination with copper of several p.p.m. Samples grown by this method showed low levels of luminescence emission, and hence the excitation spectra were measurable only at 85 K using wide pass bands for both the monochromatic excitation and the isolation of the emission. The variable interference filter used to isolate the luminescence was optimised on the emission peak.

The excitation spectra measured are shown in Fig. 5.27. Two bands of excitation were observed in most crystals, one close to the band-edge and a second approximate 200 meV lower in energy. Both excitation peaks shifted to higher energies as the mole fraction of sulphur was increased and for the sulphur-rich crystals the lower energy peak appeared to dominate. The bands observed in ZnSe at 85 K were centres at 4520 Å (2.74 eV) and 4920 Å (2.52 eV) and these are in good agreement with the

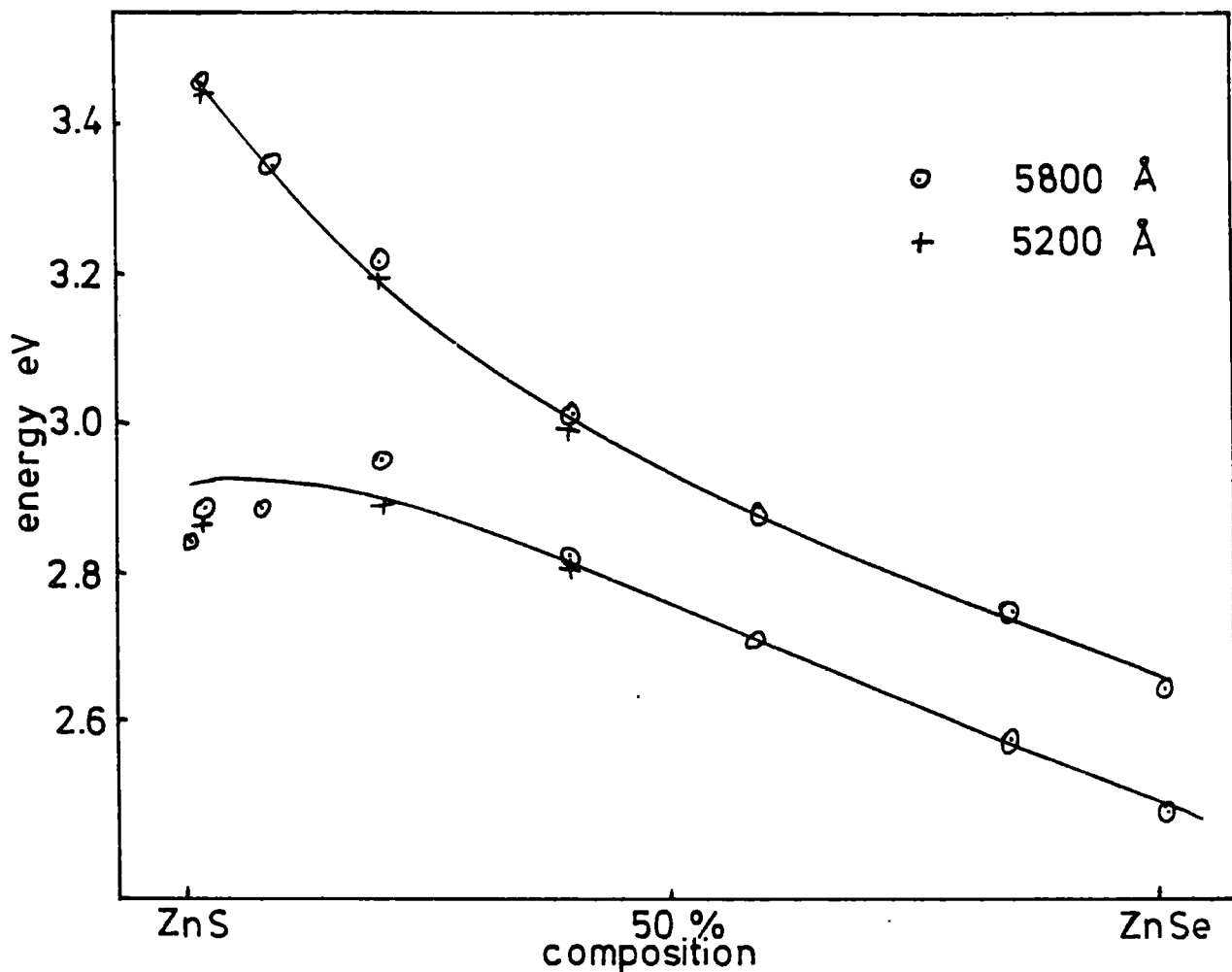


FIG 5.25 variation of excitation peak with composition 300 K

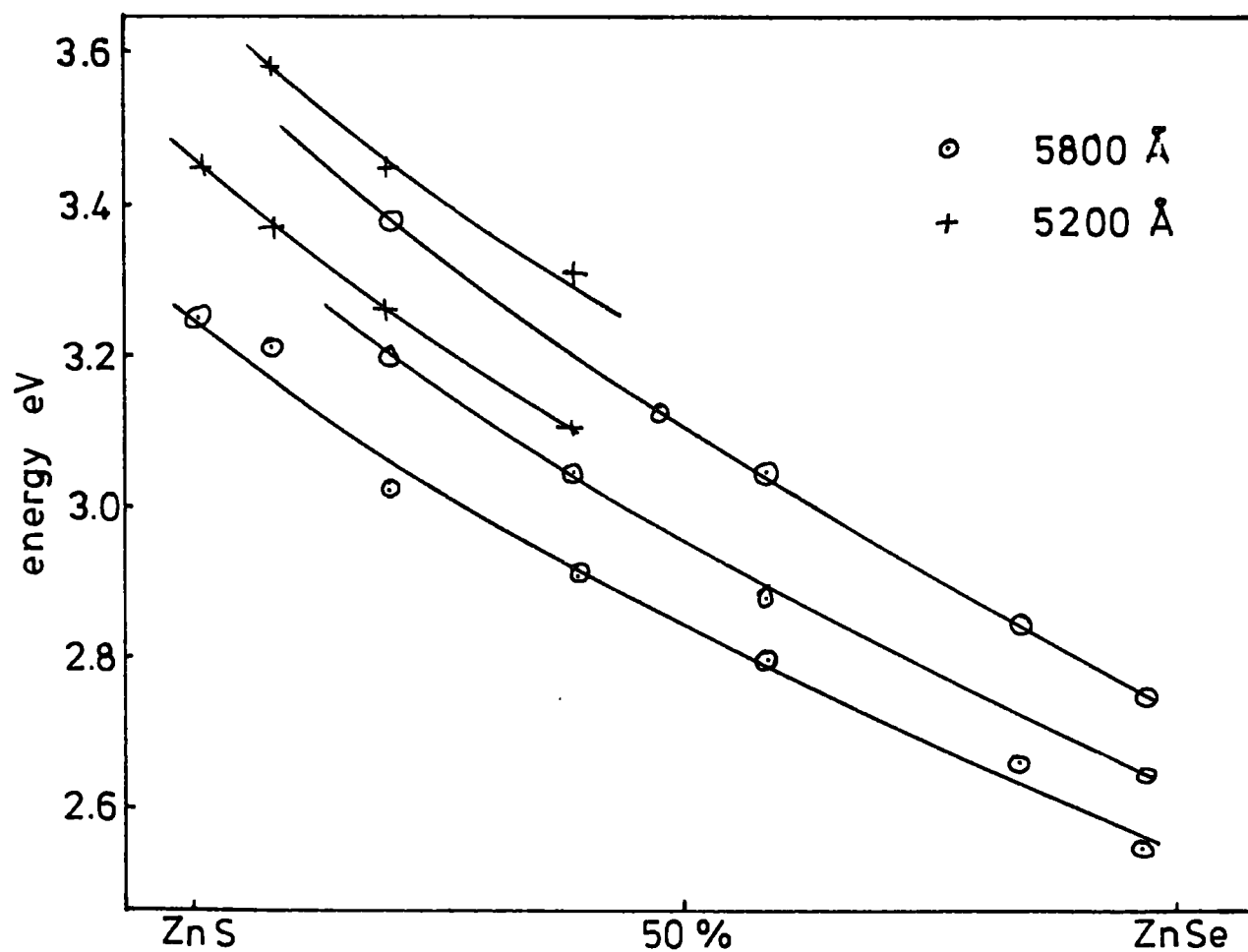


FIG 5.26 variation of excitation peak with composition 85 K

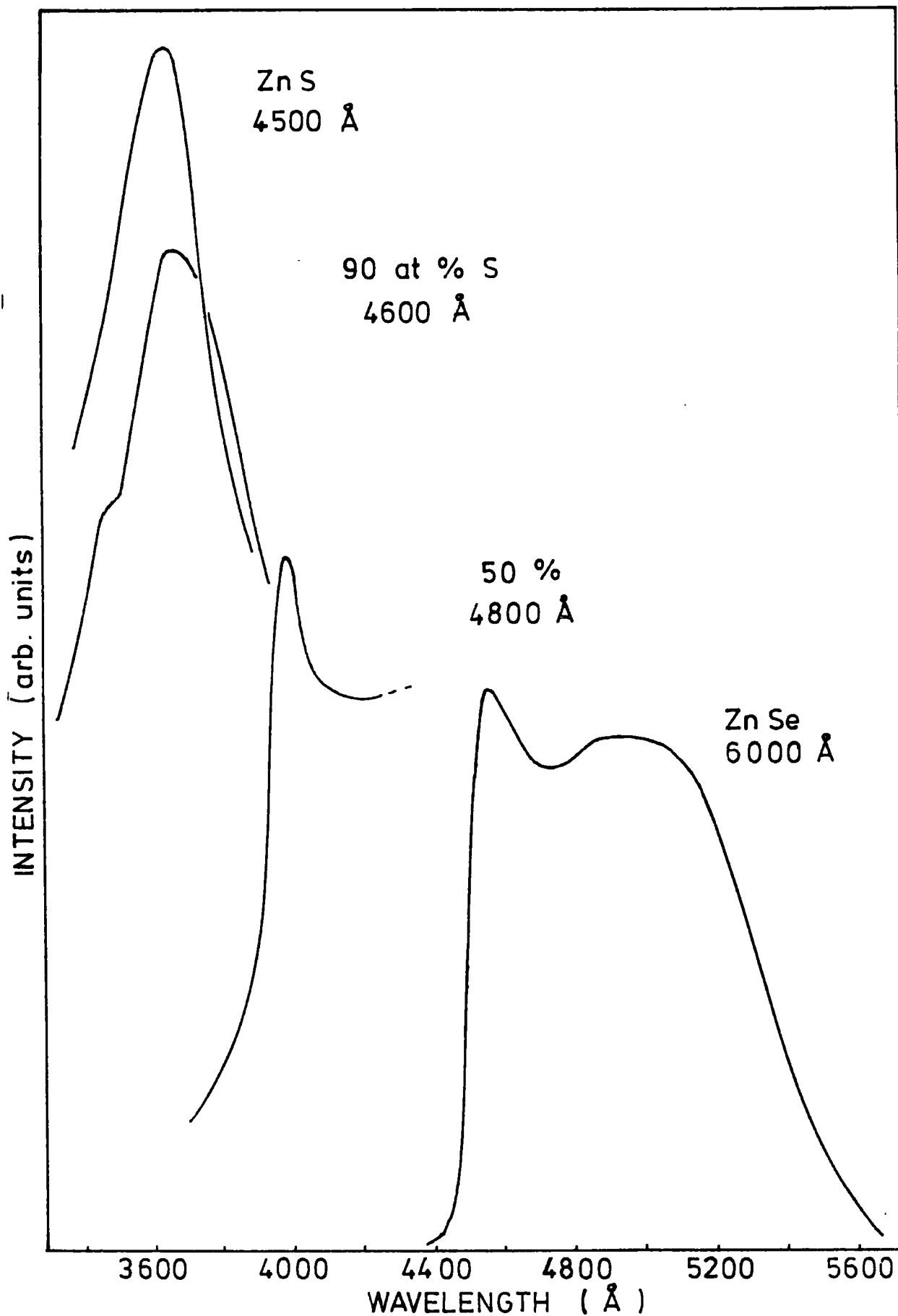


FIG 5.27 EXCITATION SPECTRA OF VERTICAL FURNACE  
Zn ( S , Se ) AT 85 K

results reported by Jones and Woods (1974) for the excitation of the self-activated emission centre. In the sample of ZnS only the lower peak was observed at  $3630 \text{ \AA}$  (3.41 eV) which agrees with the results of Melamed (1958) and Shionoya (1964) for the excitation of the self-activated centre.

### 5.5 Photoconductivity

When the photoconductivity of a crystal is measured as a function of the wavelength of excitation, a maximum response is usually found at that wavelength for which the absorption constant is approximately equal to the reciprocal of the crystal thickness. There is a fall-off on either side of the maximum because at shorter wavelengths light is absorbed near the surface where the density of trapping states is higher, and at longer wavelengths the light is only partially absorbed. Hence the short wavelength photoconductivity peak can give a measure of the position of the band-edge. Imperfections present in the crystal lead to absorption of photons of lower energies and lead to a tail on the longer wavelength side of the photoconductivity peak. Measurements were made, therefore, of the photoconductivity of the iodine-transport crystals in order to compare the results with those for the luminescence excitation spectra. It was noted that after treating these crystals in zinc, the dark conductivity was increased by up to two orders of magnitude and it was not possible to measure any photocurrent.

Contacts were applied to the crystals by alloying indium into the cleaved sample faces. It was found to be increasingly difficult to prepare good ohmic contacts on the samples as the proportion of sulphur was increased. This created problems in the measurements of the photoconductivity, especially when the crystals were examined at 85 K.

### 5.5.1 Iodine Transport Crystals

The photocurrent measured as a function of wavelength is shown in Figs. 5.28 and 5.29 at room temperature and 85 K respectively. A more detailed plot of the results obtained for three crystals with low sulphur content is shown in Fig. 5.30. Two maxima were usually observed in the photocurrent: a sharp peak close to the band-gap and a deep-centre band lying approximately 300 meV lower in energy. With some crystals possessing a higher sulphur content, the longer wavelength band was  $\sim 500 \text{ \AA}$  broad and might have been due to the overlap of more than one band. Sample 953,  $\text{ZnS}_{0.5}\text{Se}_{0.5}$ , showed distinctly the presence of three separate bands at 3950, 4400 and 4880  $\text{ \AA}$ . This particular crystal also showed the presence of three bands in the excitation spectra.

The variation of the energies of the photoconductivity bands with composition are shown in Fig. 5.31 at 300 K and 85 K. There was a linear shift to higher energies with increasing sulphur content up to approximately 80 atomic % sulphur. For crystals with a higher sulphur content, the high-energy photocurrent band shifted more rapidly with composition. The lower-energy photocurrent band moves nearly parallel with the high-energy band for different compositions: lying  $\sim 270$  meV lower in energy in ZnSe;  $\sim 400$  meV lower in  $\text{ZnS}_{0.8}\text{Se}_{0.2}$ ; and  $\sim 550$  meV lower in ZnS. Both photocurrent bands shifted by approximately 100 meV to higher energies on cooling to 85 K.

In nominally pure ZnSe, Birchak, Serdyuk and Chemeresyuk (1976) found photocurrent peaks at 4750  $\text{ \AA}$  (2.61 eV) and 5250  $\text{ \AA}$  (2.36 eV) at room temperature, while Terada (1976) found peaks at 4500  $\text{ \AA}$  (2.72 eV) and 5100  $\text{ \AA}$  (2.40 eV) at 100 K. Iida (1969) has examined the photoconductivity of ZnSe containing copper impurity, detected by flame-photometric analysis, and reported bands in the excitation spectra of the photoconductivity at

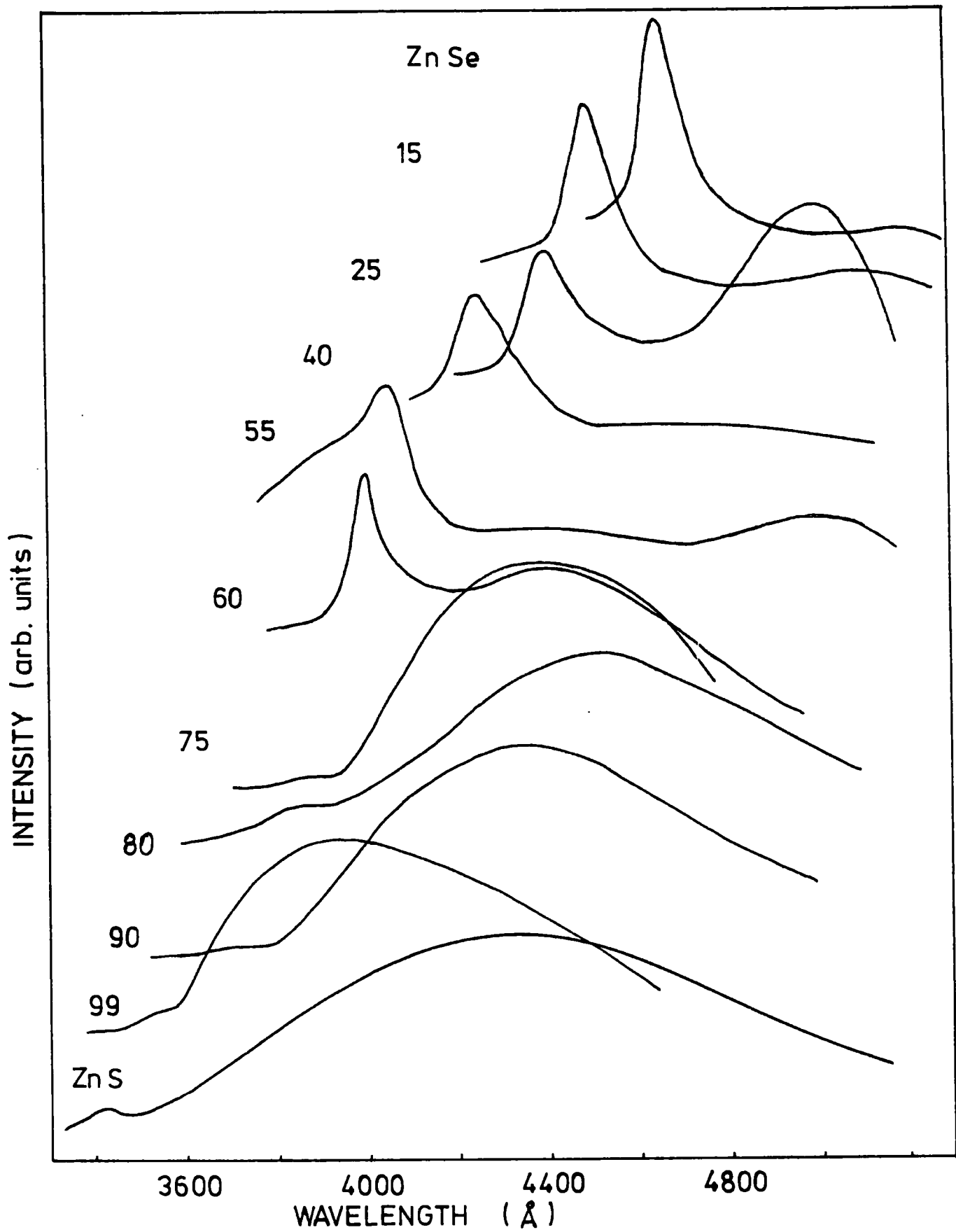


FIG 5.28 PHOTOCONDUCTIVITY AT 300 °K

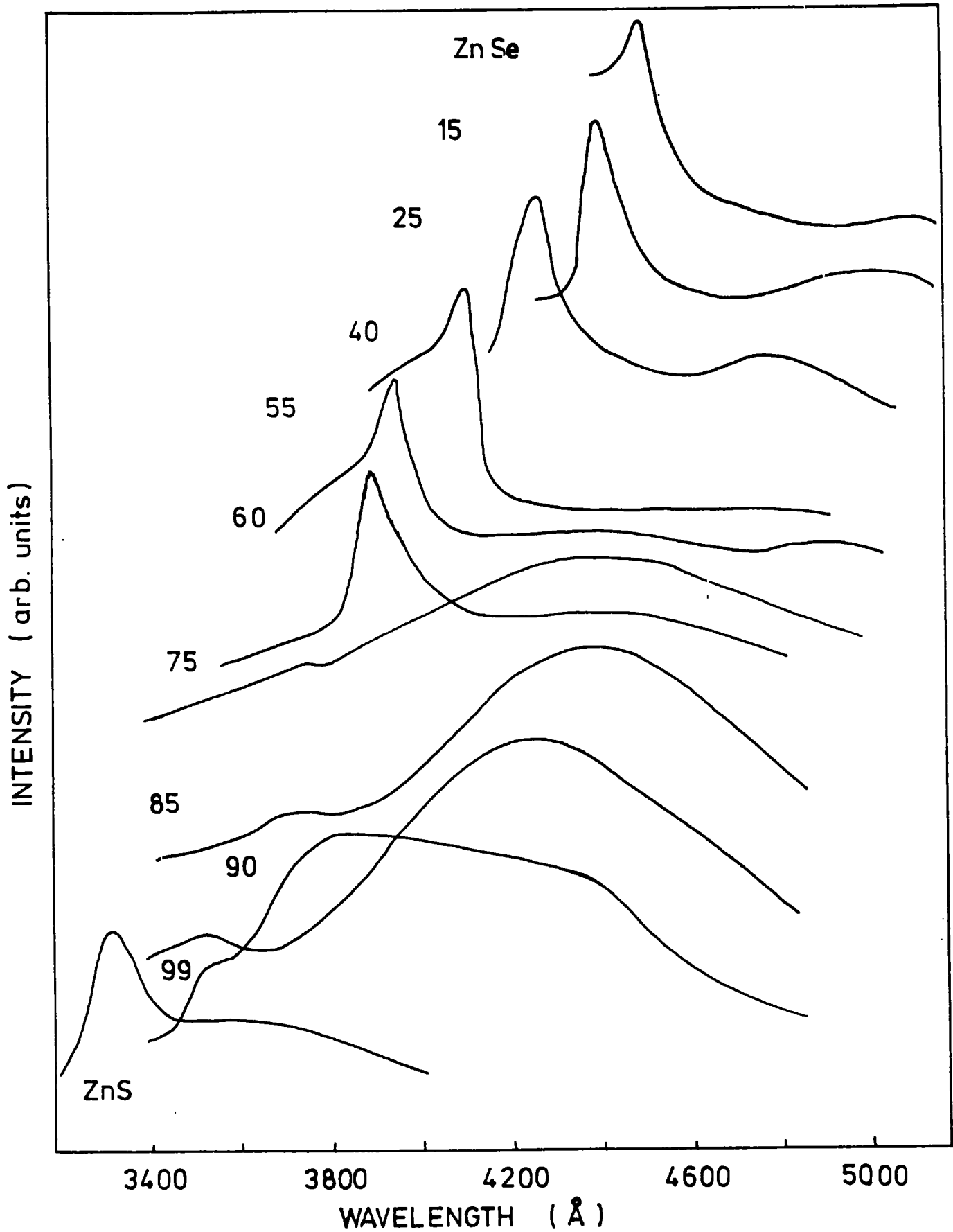


FIG 5.29 PHOTOCONDUCTIVITY AT 85 °K

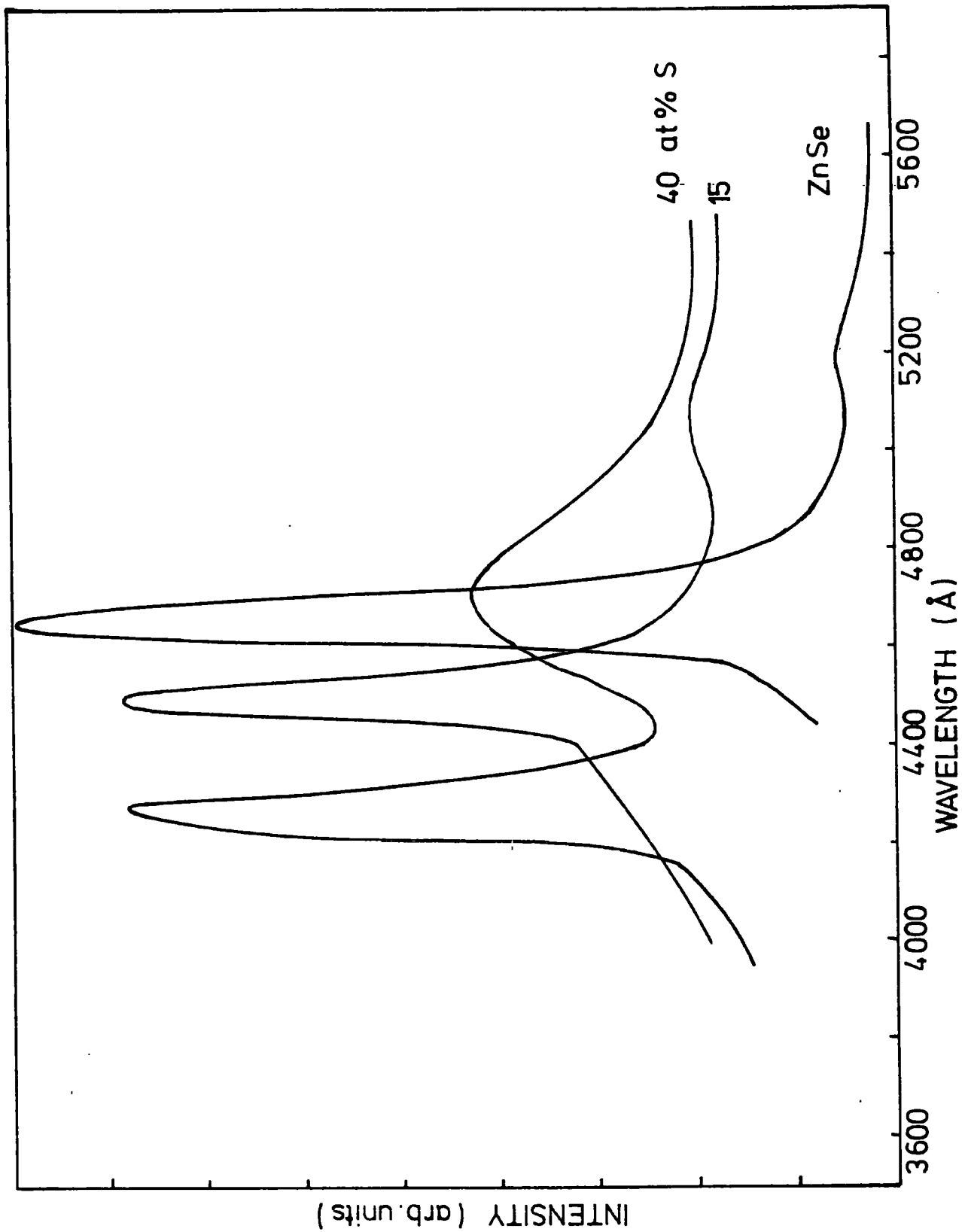


FIG 5.30 PHOTOCONDUCTIVITY MEASURED AT 300°K



4620 Å (2.68 eV) and 5200 Å (2.38 eV) at room temperature. All this data is in reasonable agreement with the positions of the photocurrent peaks reported here at 4660 Å (2.66 eV), 5160 Å (2.40 eV) and 4500 Å (2.75 eV), 5000 Å (2.48 eV) at 300 K and 85 K respectively. Ghosh and Addiss (1973) examined the photocurrent in cubic ZnS grown epitaxially on GaAs. They found a single peak at 3300 Å (3.76 eV) at 77 K which they associated with the same centre which can be excited to produce the self-activated luminescence. Narita and Sugiyama (1965) examined crystals of ZnS grown by a vapour phase reaction method using bromine. These authors found a peak in the photocurrent at  $\sim 3400$  Å (3.65 eV) at 293 K which they associated with excitation close to the absorption edge. At longer wavelengths, a side-band extended as far as  $\sim 3900$  Å in nominally pure crystals and as far as  $\sim 4600$  Å with samples doped with low levels of copper ( $\sim 3 \times 10^{-5}$  g.atom/mol). The photocurrent peaks were attributed to self-activated and 'copper-green' centres lying  $\sim 0.4$  eV and  $\sim 0.95$  eV above the valence band respectively. The spectral response of the photoconductivity of ZnS in Figs. 5.28 and 5.29, at room temperature and 85 K, showed a long wavelength tail with a peak at  $\sim 4350$  Å (2.85 eV) corresponding to the 'copper-green' excitation and a peak at 3600 Å (3.44 eV) corresponding to self-activated excitation. The variation of the peaks with temperature agreed with the results of Narita and Sugiyama who found that the 'copper-green' photoconductivity diminished as the temperature was lowered.

An examination of the location of the photocurrent peaks for the range of Zn(S,Se):I crystals would indicate that the excitation occurs in a band close to the absorption edge and also at longer wavelengths, where the broad band is probably due to the overlap of the excitation of self-activated and copper-green centres. In the crystals with a low

sulphur content, the longer wavelength copper-green excitation dominated over the self-activated excitation. This might be due to the fact that the self-activated centre lies close to the valence-band in ZnSe and holes produced at this centre may become free more easily than in ZnS.

### 5.5.2 Crystals grown in the Vertical Furnace

For comparison with the results obtained from Iodine Transport crystals, the photoconductivity of a sample of nominally pure ZnSe grown by the Vertical Furnace method was examined. The photocurrent spectra for this sample are shown in Fig. 5.32 and compared with the spectra for an Iodine Transport crystal. The spectra at both 300 and 85 K consisted of two bands, a narrow peak close to the absorption edge with a broad shoulder at longer wavelengths  $\sim 5100 \text{ \AA}$ . This latter band would appear to imply the presence of impurity centres deep in the gap. The short wavelength peak was positioned at  $\sim 4800 \text{ \AA}$  (2.58 eV) at 300 K and at  $4575 \text{ \AA}$  (2.71 eV) at 85 K. This band was at a slightly lower energy than the corresponding band in ZnSe:I.

### 5.6 Thermal Quenching

As has been explained, measurements of the thermal quenching of the photoluminescence emission can give information concerning the position of luminescence centres relative to the band edges. An emission band was therefore isolated using filters, and its intensity was monitored as a function of the crystal temperature. It was necessary to ensure that the maximum of the emission band was always monitored since it shifted with temperature. In practice the small shifts of position were minimised by the large band passes of the spectrometer which were employed.

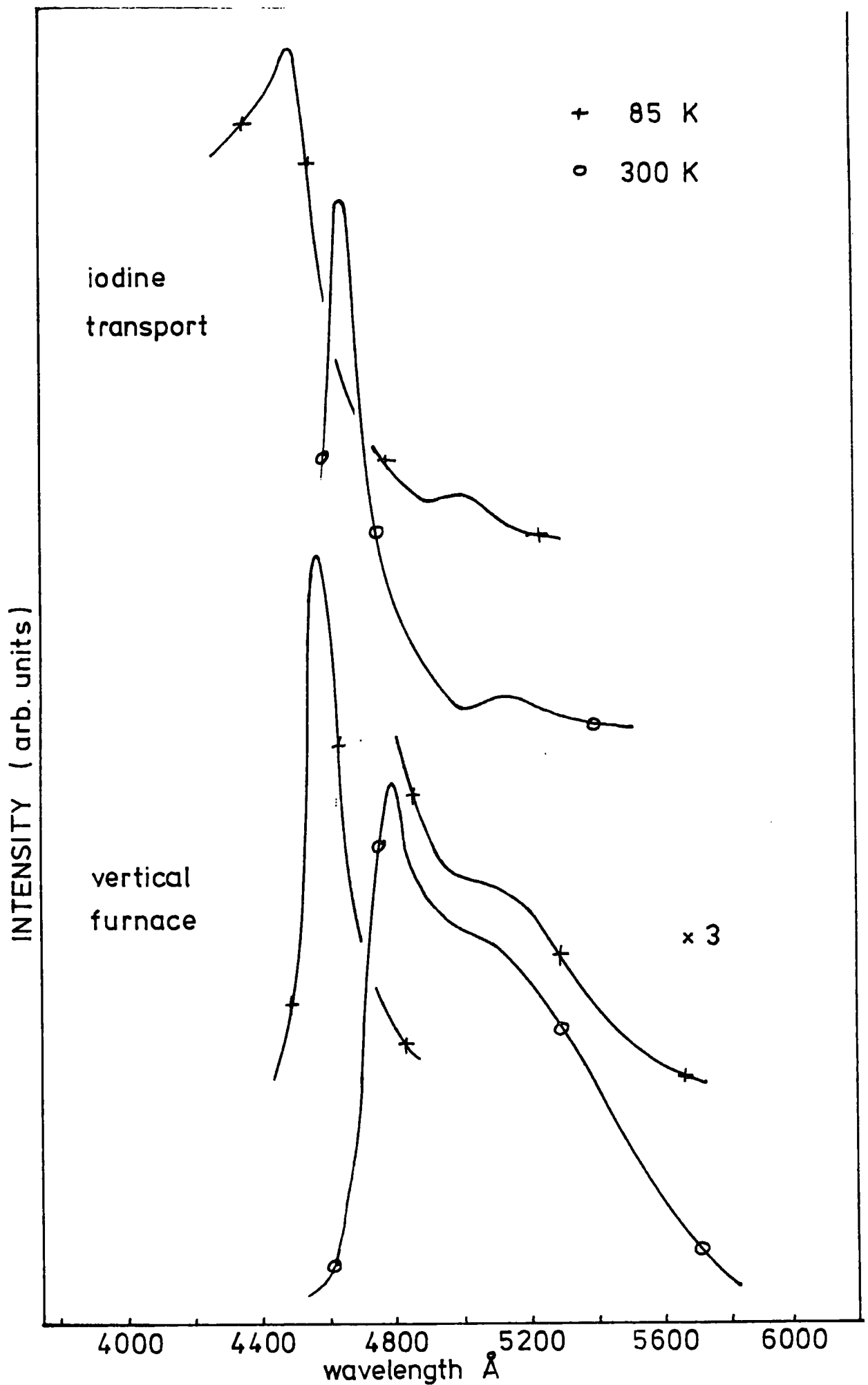


FIG 5.32 photoconductivity of vertical furnace and iodine transport samples of ZnSe

It was also necessary to ensure that the emission was stimulated in the appropriate excitation band and that this did not change in intensity or position during the experiment. The luminescence was stimulated by either a 3650 Å ultra-violet source or a tungsten-halogen lamp with suitable filters; both of these excitation sources were run from stabilised power supplies.

#### 5.6.1 Iodine Transport Crystals

The thermal quenching of a number of Zn(S,Se):I crystals was examined throughout the range of composition. It was shown in Section 5.2.1 that the photoluminescence of these samples consisted of a number of broad overlapping bands which might be associated with self-activated and impurity luminescence. In samples exhibiting two emission bands, both bands were monitored in order to compare the various transitions occurring.

The thermal quenching curves obtained for two typical crystals, sample 958  $\text{ZnS}_{0.8}\text{Se}_{0.2}:\text{I}$  and 954  $\text{ZnS}_{0.6}\text{Se}_{0.4}:\text{I}$ , are shown in Fig. 5.33 monitoring both emission bands for each crystal. The results obtained for a crystal of ZnSe:I and a low sulphur crystal 947  $\text{ZnS}_{0.4}\text{Se}_{0.6}:\text{I}$  are shown in Fig. 5.34. Both of these crystals showed only a single broad band of luminescence, which may have been formed by the overlap of more than one emission band. In all the crystals examined, the intensity of the longer wavelength yellow/orange emission band decreased slowly as the temperature was raised to ~ 200 K and then decreased more rapidly. As the sulphur content increased, the point at which rapid quenching set in shifted to higher temperatures. In contrast, the short wavelength band was rapidly quenched at temperatures below ~ 250 K. It was noted that the longer wavelength emission was sometimes enhanced in this temperature

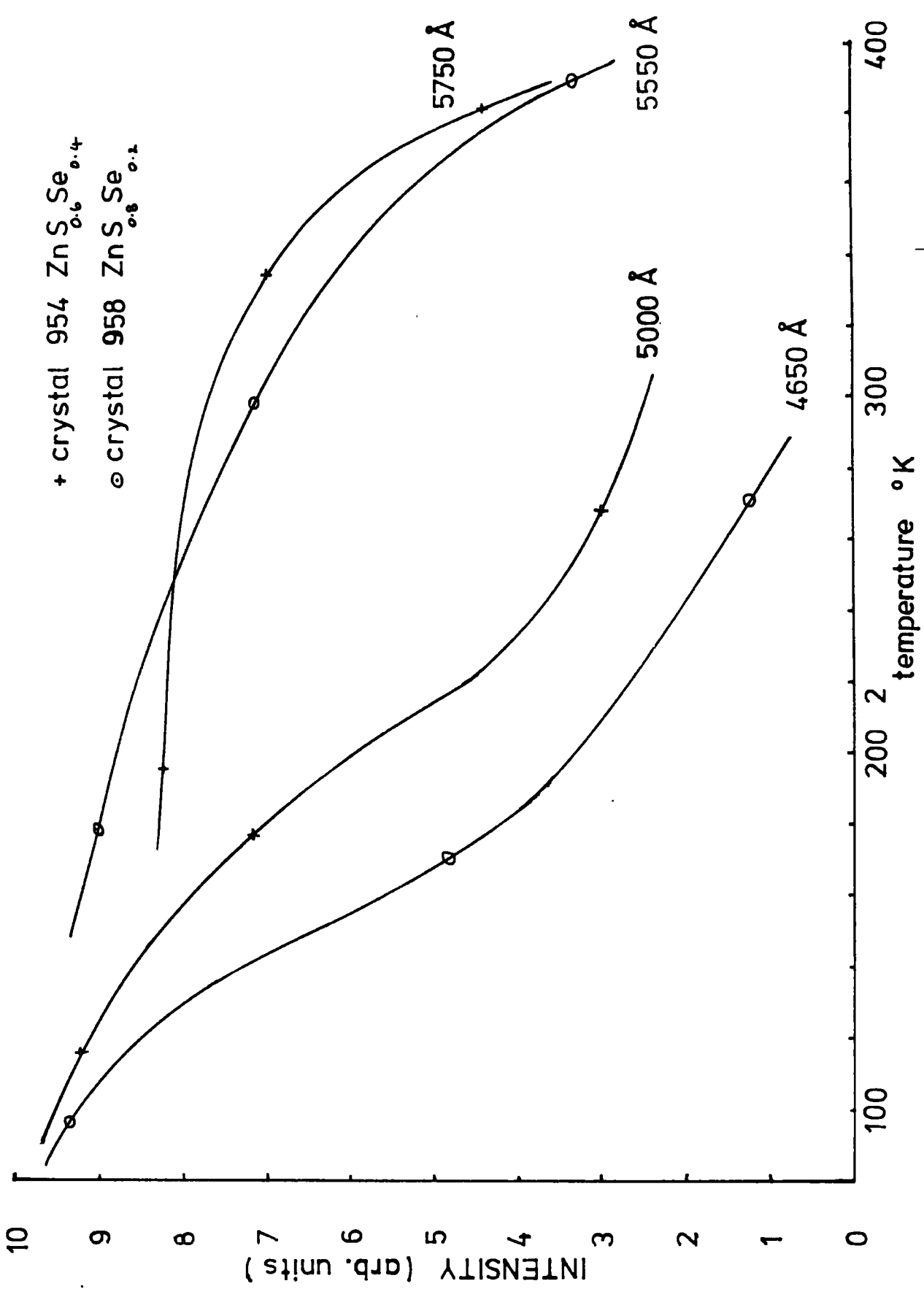


FIG 5.33

VARIATION OF LUMINESCENCE INTENSITY  
WITH TEMPERATURE

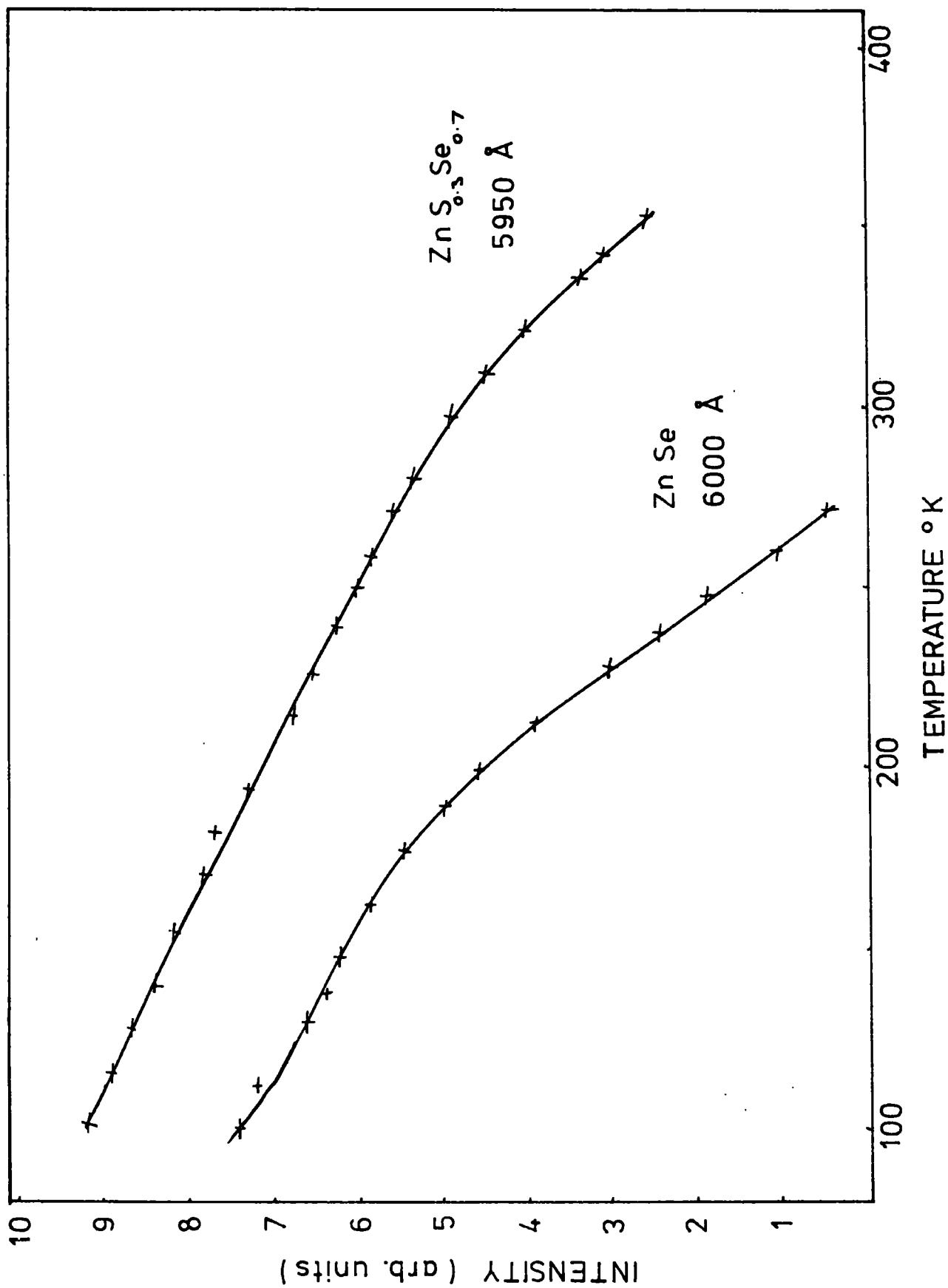


FIG 5.34 THERMAL QUENCHING CURVES FOR  
Zn (S, Se) : I

range up to 250 K, and it is felt that there may be a redistribution in the recombination transitions at the two centres responsible for the emission.

The relationship for the luminescence efficiency  $\eta$  is given by:

$$\eta = \frac{1}{1 + C \exp(-\omega/kT)} .$$

If  $I_0$  is the emission intensity before quenching occurs and  $I$  is the intensity at temperature  $T$ , the efficiency is given by

$$\eta = I/I_0 .$$

Hence

$$I/I_0 = \frac{1}{1 + C \exp(-\omega/kT)}$$

$$\log_e \left( \frac{I_0}{I} - 1 \right) = \log_e C - \omega/kT$$

Therefore plotting  $\log_e \left( \frac{I_0}{I} - 1 \right)$  against  $1/T$  should produce a straight line of slope  $-\omega/k$  from which the activation energy  $\omega$  may be found.

Plots of  $\log_e \left( \frac{I_0}{I} - 1 \right)$  against  $1/T$  for the various emission bands throughout the range of composition are shown in Figs. 5.35 and 5.36. The curves usually consisted of two straight line regions for each emission band. The calculated activation energies are listed in Table 5.2.

With the sample of ZnSe, the activation energy obtained for the low temperature region was 0.028 eV and in the high temperature region 0.17 eV. Jones and Woods (1974) have reported quenching energies of 0.03 and 0.41 eV in ZnSe, and Iida (1968) found a quenching energy of 0.35 eV. The activation energies progressively increased in magnitude

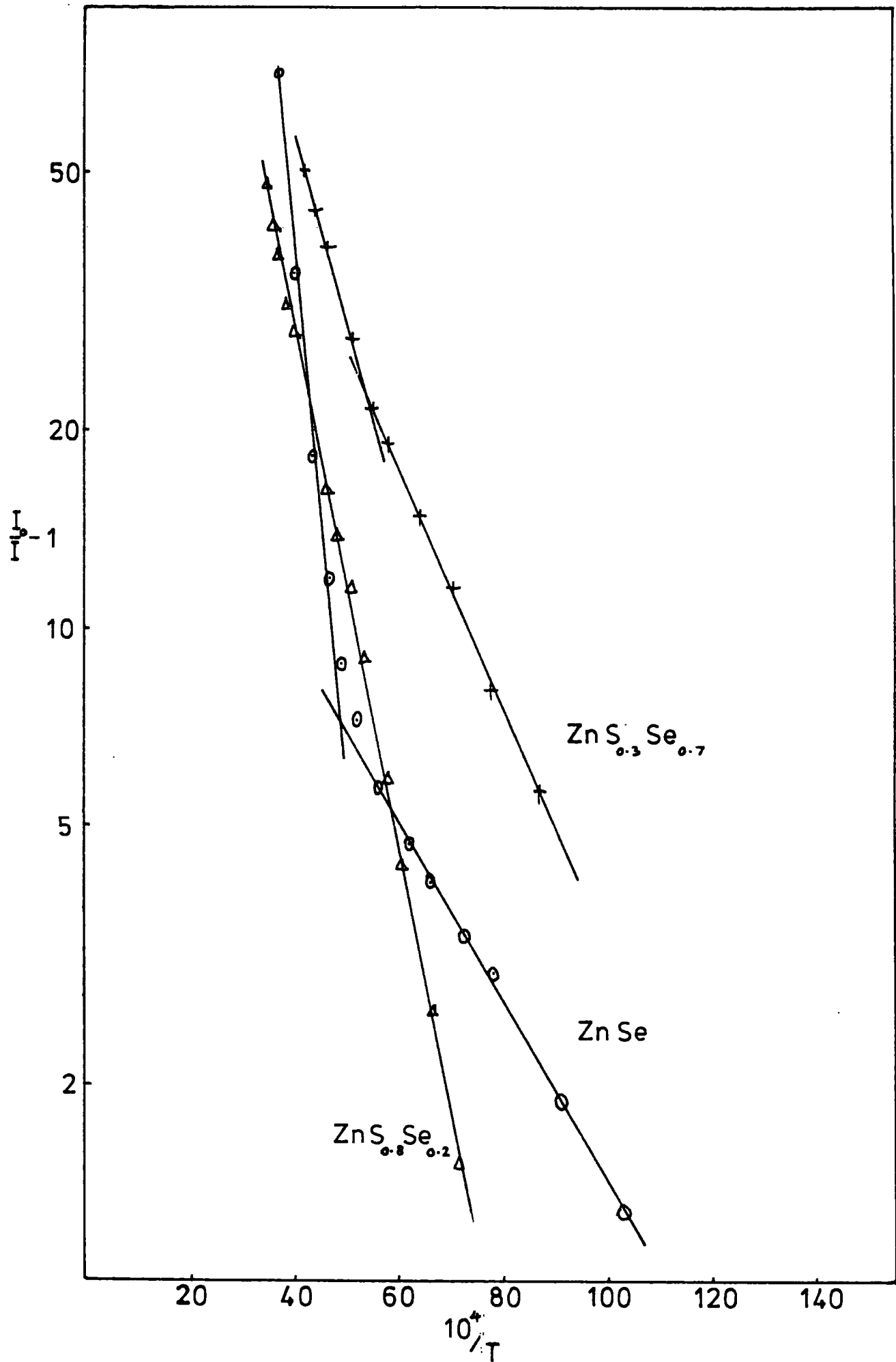


FIG 5.35 THERMAL QUENCHING OF Zn ( S , Se ) : I

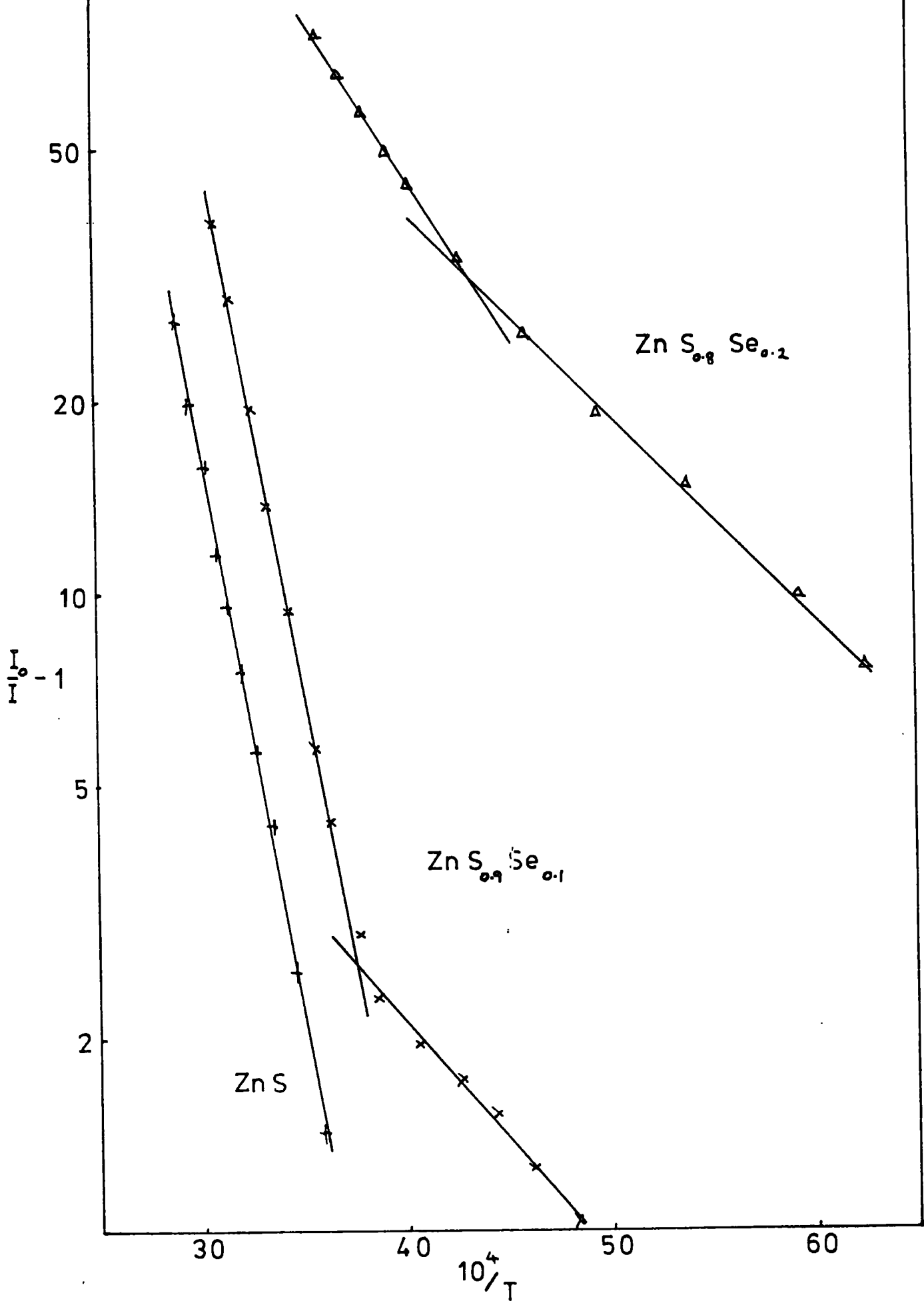


FIG 5.36 THERMAL QUENCHING OF  $\text{Zn}(\text{S}, \text{Se}) : \text{I}$

TABLE 5.2

THERMAL QUENCHING ACTIVATION ENERGIES

Sample	Peak $\lambda$ (Å)	Activation Energy (eV)	
ZnSe	6000	0.028	0.170
ZnS <sub>0.4</sub> Se <sub>0.6</sub>	5950	0.037	0.058
ZnS <sub>0.6</sub> Se <sub>0.4</sub>	5750	0.163	0.294
	5000	0.072	
ZnS <sub>0.8</sub> Se <sub>0.2</sub>	5550	0.155	0.226
	4650	0.075	
ZnS <sub>0.9</sub> Se <sub>0.1</sub>	5350		
	4500	0.077	0.346
ZnS	5200		
	4450		0.354

as more sulphur was included in the mixed crystal composition. A quenching energy of 0.35 eV was found for the blue emission band of sample 965 ZnS:I and this compares with a value of 0.40 eV reported by Narita and Sugiyama (1965) in self-activated ZnS. Ghosh and Addiss (1973) found no strong quenching of the self-activated luminescence in ZnS, and these authors concluded that the relative temperature dependences of the different trapping and recombination processes were responsible for the temperature effects observed. This contrasts markedly with the strong quenching of the self-activated emission reported by Koda and Shionoya (1964). The thermal quenching of the green emission in sample 965 ZnS:I and 961 ZnS<sub>0.9</sub>Se<sub>0.1</sub>:I, at 5200 Å and 5350 Å respectively, was examined; this emission showed a slow decrease in intensity with increasing temperature over a range up to ~450 K. It would appear that this temperature dependence cannot be attributed to a quenching mechanism since no activation energy can be associated with it.

The behaviour of the luminescence bands with varying temperatures is complex. The decrease in intensity of the emission with increasing temperature may be due in part to a thermal quenching mechanism associated with which two activation energies may be observed. The mixed crystals have been shown to exhibit more than one emission band and the temperature dependence of the emission intensity may be influenced by the different recombination rates at the various luminescence centres responsible for the bands. In general, however, the shorter wavelength band has been observed to be strongly thermally quenched at temperatures up to ~250 K and the longer wavelength band shows a limited temperature dependence.

## 5.7 Discussion

The luminescent properties of powdered Zn(S,Se) phosphors have been

Bryant and Manning (1974) have also observed two bands of luminescence

in Zn(S,Se) ternary compounds over certain ranges of composition;

these results are in agreement with those shown in Fig. 5.87.

studied by Leverenz (1950), Klasens (1953) and Morehead (1963); all these authors varied the composition between zinc sulphide and zinc selenide in large steps. There is general agreement that the emission bands shift monotonically to higher energies as the proportion of sulphur is increased. The blue emission band of self-activated ZnS is reported to be gradually replaced by a green band if the sulphur is replaced by selenium, see for example Bundel et al (1961). The 'copper-green' emission observed in ZnS has been reported to shift steadily to a 'copper-red' emission in ZnSe. Halsted et al (1965) have made an examination of the 'copper-blue' emission in ZnS and have reported that this band shifts to the green region in ZnSe. Cubic Zn(S,Se):Cu,Cl phosphors were examined by Lehmann (1966) and these phosphors exhibited two emission bands: blue (4440 Å, 2.79 eV) and green (5280 Å, 2.35 eV) in ZnS, and green (5300 Å, 2.34 eV) and red (6350 Å, 1.95 eV) in ZnSe. Lehmann observed that replacement of less than 1% of the ZnS by ZnSe gave rise to the appearance of two new bands at 5560 Å (2.23 eV) and 4770 Å (2.60 eV), and that subsequent increase of the selenium concentration caused only a comparatively slow shift of both bands towards the red. Lehmann (1967) also studied the self-activated emission in Zn(S,Se) phosphors doped with halogens and noted two emission bands in the mixed alloy compounds which were ascribed to self-activated luminescence centres. In zinc sulphide a single band only was observed in the blue (4750 Å, 2.61 eV), and similarly in zinc selenide a single band in the red (6230 Å, 1.99 eV). It was noted that the replacement of 1% sulphur by selenium resulted in the appearance of a shoulder in the green at 5400 Å (2.30 eV). Ozawa and Hersh (1973) have studied the luminescence of Zn(S,Se):I crystals subsequent to annealing in liquid zinc, varying the composition of the mixed alloys in large steps. These authors observed a single band of

luminescence approximately  $1000 \text{ \AA}$  broad at half-height; the position of this emission band shifted monotonically to shorter wavelengths with an increase in ZnS content, however, the blue band of ZnS jumped to the green spectral region with a small increase in ZnSe content. Ozawa and Hersh concluded that the self-activated centre observed in  $\text{Zn(S,Se):I,Zn}$  differs from that of  $\text{ZnS:Cl}$  which is known to be a pair consisting of a vacancy and a halogen ion occupying the nearest neighbour site, see Kasai and Otomo (1962).

It is clear that there are a number of centres responsible for the various emission bands observed in the  $\text{Zn(S,Se)}$  mixed alloys. The exact behaviour of the photoluminescence bands as a function of composition is complex and no explanation has been put forward for the reported discontinuity in the position of the emission peak on introducing small percentages of selenium. The work reported here has examined the luminescent processes observed in nominally undoped and iodine-doped  $\text{Zn(S,Se)}$  crystals as-grown and after annealing in liquid zinc.

As many as four bands of luminescence have been observed in the  $\text{Zn(S,Se):I}$  crystals. The positions of some of these bands at 85 K are shown in Fig. 5.37; for the sake of clarity certain emission bands have been omitted. In Chapter 6 studies of the photoluminescence of mixed crystals doped with high ( $\sim 100 \text{ ppm}$ ) and low (few ppm) concentrations of copper are described. The emission bands observed in these crystals have been included in Fig. 5.37 for comparison with the results for the undoped self-activated crystals.

A high energy emission has been observed in a position close to the band-edge, approximately 150 meV deep in the sample of ZnS. This emission is rapidly quenched on warming from 85 K and was not observable at room temperature. This band is attributed to edge-emission which has been

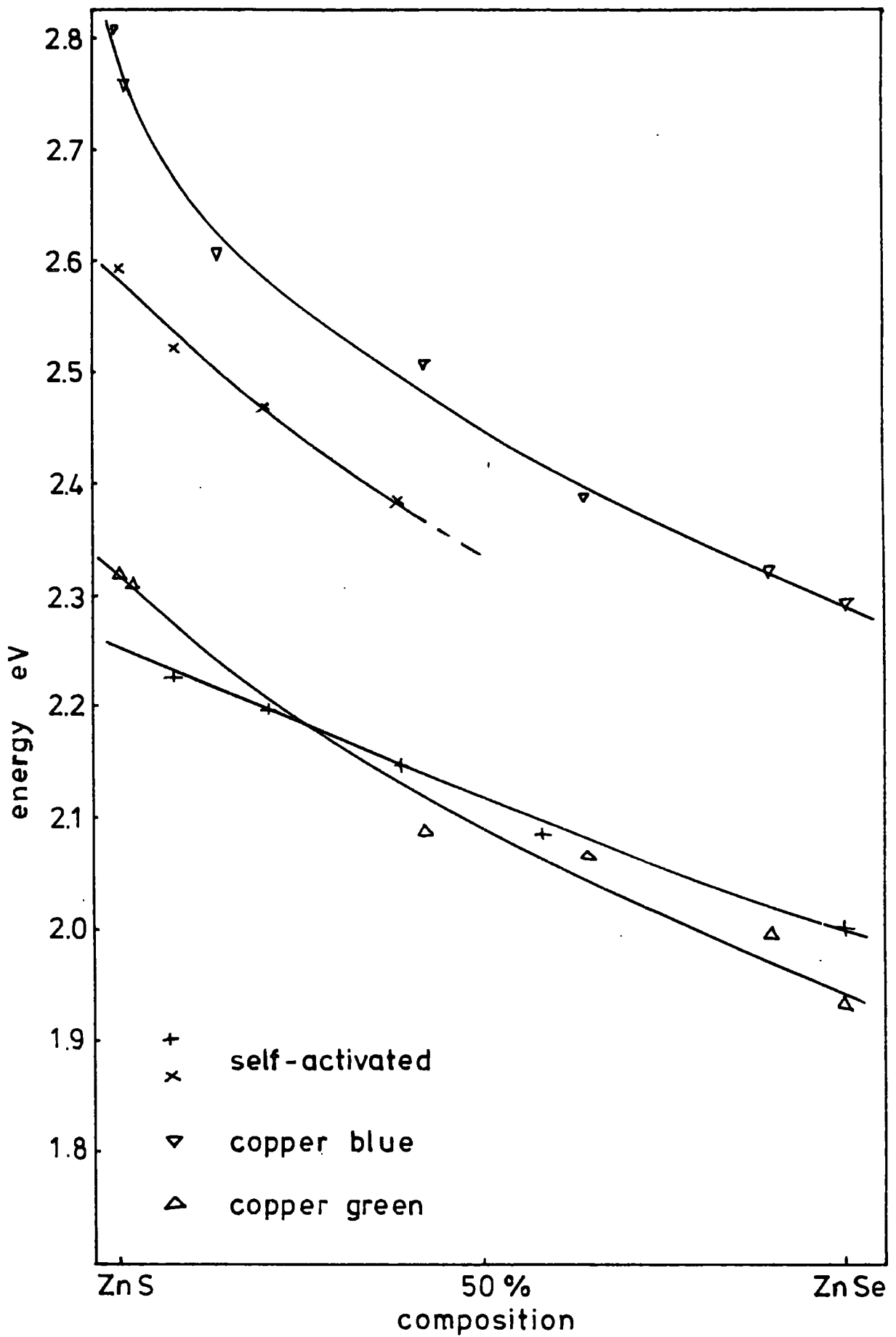


FIG 5.37 SELF-ACTIVATED AND COPPER EMISSION IN Zn ( S , Se )

reported in ZnS by Kröger (1940) and in CdS by Lambe et al (1956). The peak position in the sample of ZnS occurs at  $3480 \text{ \AA}$  (3.57 eV); this is in good agreement with the edge-emission reported by Uchida (1964) which he associated with interstitial sulphur.

In the undoped samples there is a low-energy band which shifts from the position of the self-activated luminescence observed in ZnSe at  $5950 \text{ \AA}$  (2.08 eV) to  $5560 \text{ \AA}$  (2.23 eV) in  $\text{ZnS}_{0.8}\text{Se}_{0.2}$ . There is no evidence of this low-energy band in ZnS; in this sample the characteristic self-activated emission is observed at  $4780 \text{ \AA}$  (2.60 eV). Cooling the mixed crystal samples to 85 K causes a shift in the wavelength of the low-energy band to larger values in a similar manner to that observed for the self-activated emission in both ZnS and ZnSe. By comparison the deeper-lying 'copper-green' emission is present throughout the whole range of composition shifting from  $6400 \text{ \AA}$  (1.93 eV) in ZnSe to  $5340 \text{ \AA}$  (2.32 eV) in ZnS; this band shifts to shorter wavelengths on cooling the samples to 85 K. It is concluded that the low-energy band observed in the mixed crystals of  $\text{Zn(S,Se):I}$  is distinct from the 'copper-green' emission observed in copper-doped samples. The low-energy band is considered to be due to a centre similar to that responsible for the self-activated emission in zinc selenide crystals.

A short wavelength shoulder on the self-activated band observed for ZnSe appears in the mixed crystals; this second emission band tends to dominate the emission as the proportion of sulphur is increased. This band appears as a separate peak at  $4430 \text{ \AA}$  (2.80 eV) in ZnS prior to annealing in zinc. This band corresponds with the position of the 'copper-blue' emission reported in ZnS. An examination of the excitation and photoconductivity spectra indicates that the as-grown crystals may be contaminated with copper; this has been confirmed by an examination of

the impurity content which has indicated the presence of copper at levels up to several p.p.m. Subsequent to annealing the mixed crystals in zinc in order to remove impurity copper, the high-energy band is observed at longer wavelengths while the position of the low-energy self-activated band remains unchanged. The higher energy band, previously observed in the blue-green region at  $4430 \text{ \AA}$  (2.80 eV) in ZnS, is no longer present in the annealed samples and a new band appears ranging from  $5200 \text{ \AA}$  (2.38 eV) in  $\text{ZnS}_{0.6}\text{Se}_{0.4}$  to  $4780 \text{ \AA}$  (2.59 eV) in ZnS. For crystals with a sulphur content below 60 At.%, the band cannot be resolved as a separate peak, but appears as a shoulder on the lower energy self-activated emission. This high-energy band corresponds in energy with that of the self-activated luminescence reported in ZnS at  $4750 \text{ \AA}$  (2.61 eV). An examination of the emission spectra for both ZnS and ZnSe indicates that in these crystals there is only a single self-activated band. However, in the range of zinc sulpho-selenide mixed crystals there are two distinct bands of self-activated emission.

The nature of the blue self-activated emission in ZnS, which occurs when coactivator halogen ions are incorporated in the lattice, has received much attention. The examinations made by Prener and Williams (1956), Kasai and Otomo (1962), Dischler et al (1964), Schneider et al (1965) and Koda and Shionoya (1964) have confirmed that the self-activated luminescence is produced by an electronic transition between localised states of a centre consisting of a zinc vacancy paired with a substitutional halogen ion on an adjacent sulphur site. These conclusions have been drawn by correlating the results of several experiments examining the polarisation of emission, time decay of luminescence, excitation spectra and electron spin resonance. On an atomic level, the self-activated centre is pictured as a zinc ion vacancy surrounded by three

sulphur ions and a halogen ion giving the centre  $C_{3v}$  symmetry. In the ground state of the associated centre, the three band orbitals surrounding the zinc vacancy are all filled with electrons; when excited by light one of these electrons will be transferred to the halogen ion in the centre leaving a positive hole in the band orbitals, and this excited hole will rotate around the symmetry axis of the centre due to resonance among the three band orbitals. Less work has been done on the self-activated luminescence in ZnSe, but Holton, de Wit and Estle (1965) have examined the emission and concluded that the self-activated centre in ZnSe is entirely analogous to that in ZnS.

The work reported here, however, has identified two separate self-activated emission bands in the range of zinc sulpho-selenide mixed crystals; also, contrary to expectation, there is no simple, direct transition between the self-activated emission observed in ZnS and that in ZnSe when the composition of the alloy is varied. A possible explanation for this behaviour might be that the self-activated centres in ZnS, ZnSe and their alloys are more complex than has been postulated and directly involve the group VI host atom in the localised centre, If, when the coactivator halogen ion enters the lattice substitutionally, an interstitial S or Se atom is produced in the immediate locality this would lead to two distinct centres: a zinc vacancy-halogen-sulphur interstitial complex and zinc vacancy-halogen-selenium interstitial complex. This model might then explain the existence of two self-activated bands in the mixed alloys, while only a single band is present in the pure materials at the ends of the range of composition.

## CHAPTER 6

### COPPER DOPED CRYSTALS

#### 6.1 Introduction

Copper is well-known as an efficient activator of photoluminescence in ZnS, see for example the review by Shionoya (1966). It has already been stated that crystals grown in this department by both the iodine-transport and vapour-transport techniques have been unintentionally contaminated with copper at levels up to a few p.p.m. In this work, samples of Zn(S,Se):I have been deliberately doped with copper in order to determine the effect on the photoluminescence. The copper was introduced into the crystals by incorporating a small amount of the metal in the powder charge from which the samples were grown. The body colour of the doped material varied from pale brown in ZnSe:I,Cu through green to dark green/black in ZnS:I,Cu. By comparison, the undoped samples varied from orange in ZnSe:I through yellow to colourless in ZnS:I. The doped crystals were annealed in liquid zinc in order to examine the effect of this treatment on the luminescence. Subsequent to annealing, the body colour varied from red in ZnSe:I,Cu,Zn through orange to yellow/green in ZnS:I,Cu,Zn. Aven and Woodbury (1962) have shown that annealing crystals of ZnSe and ZnS in liquid zinc has the effect of reducing the copper concentration since the copper segregates between the bulk and the solution. From the observation of the colour change in the crystals, it would appear that a redistribution of the

impurities occurs throughout the bulk of the material. In order to study the luminescence processes involved, the emission and excitation spectra and the thermal quenching of photoluminescence were examined throughout the whole range of composition. In the diagrams illustrating the emission and excitation spectra of the various crystals, the intensities are in arbitrary units and have been corrected for the response of the photomultiplier and excitation source.

## 6.2 Unannealed Copper-Activated Samples

These crystals were prepared by the iodine-transport technique as described in Chapter 3. In order to introduce copper into the samples, a small amount of metal was incorporated with the powder charge in the growth tube. The doped samples produced were of poor crystalline quality containing many voids and with small crystallites a few  $\text{mm}^3$  in volume. The introduction of copper into the charge appeared to inhibit growth so that the crystals produced were smaller than comparable undoped samples. The crystals appeared dark in colour which may indicate the presence of precipitates in the bulk.

### 6.2.1 Photoluminescence

The spectral distribution of the luminescence for the range of  $\text{Zn}(\text{S},\text{Se}):\text{I},\text{Cu}$  crystals is shown in Figures 6.1 and 6.2 at 300 K and 85 K respectively. The emission was excited by ultra-violet radiation with  $\lambda = 3650 \text{ \AA}$ . At room temperature a single broad band of luminescence was observed which shifted to shorter wavelengths as the proportion of sulphur was increased. The peak of the emission band occurred at  $6270 \text{ \AA}$  (1.98 eV) in  $\text{ZnSe}:\text{I},\text{Cu}$  and  $5000 \text{ \AA}$  (2.48 eV) in  $\text{ZnS}:\text{I},\text{Cu}$  with half-widths of 0.30 eV and 0.40 eV respectively. At liquid nitrogen

INTENSITY (ARBITRARY UNITS)

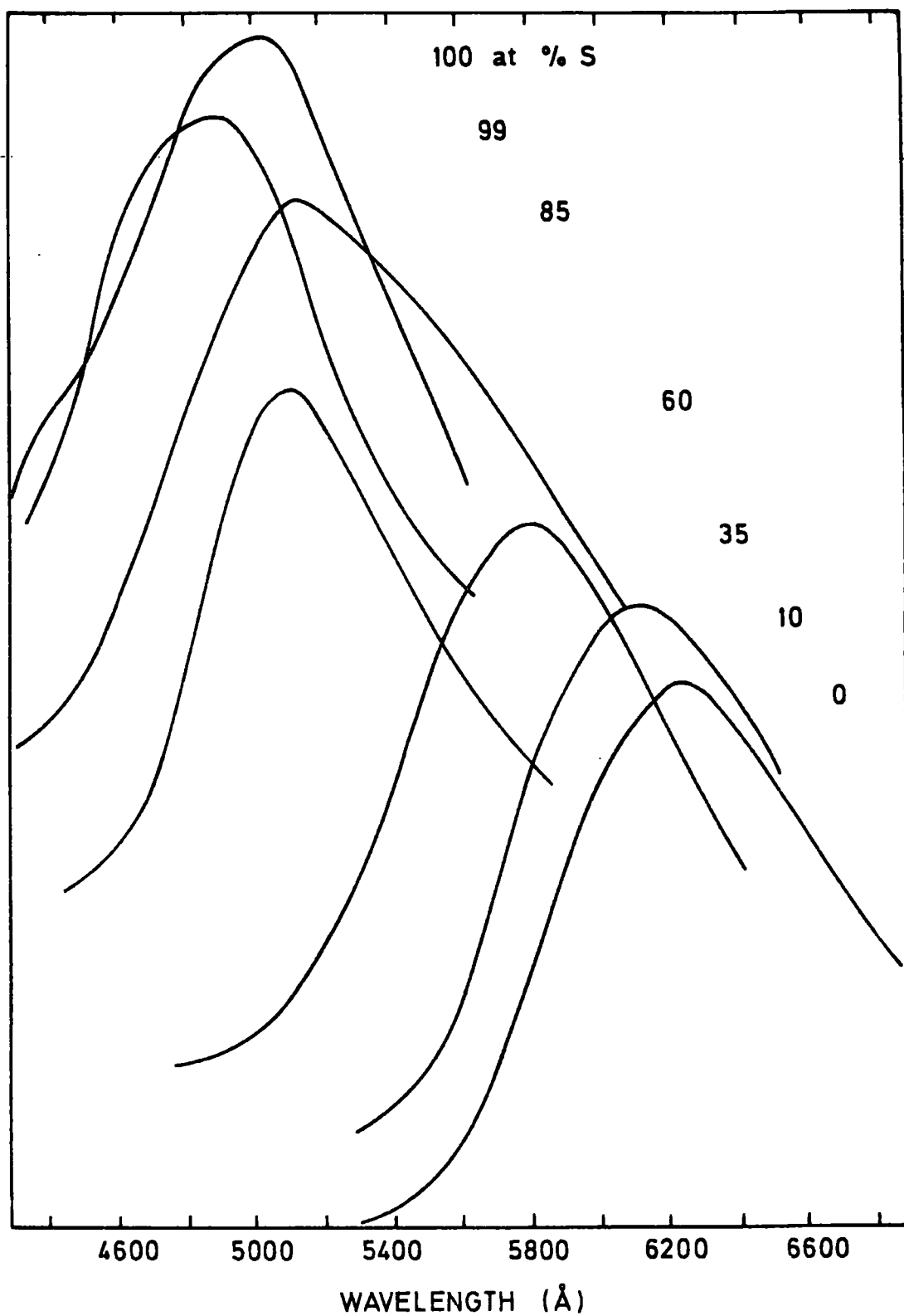


FIG. 6.1 Photoluminescence spectra of Zn(S,Se) :I,Cu crystals at 300°K.

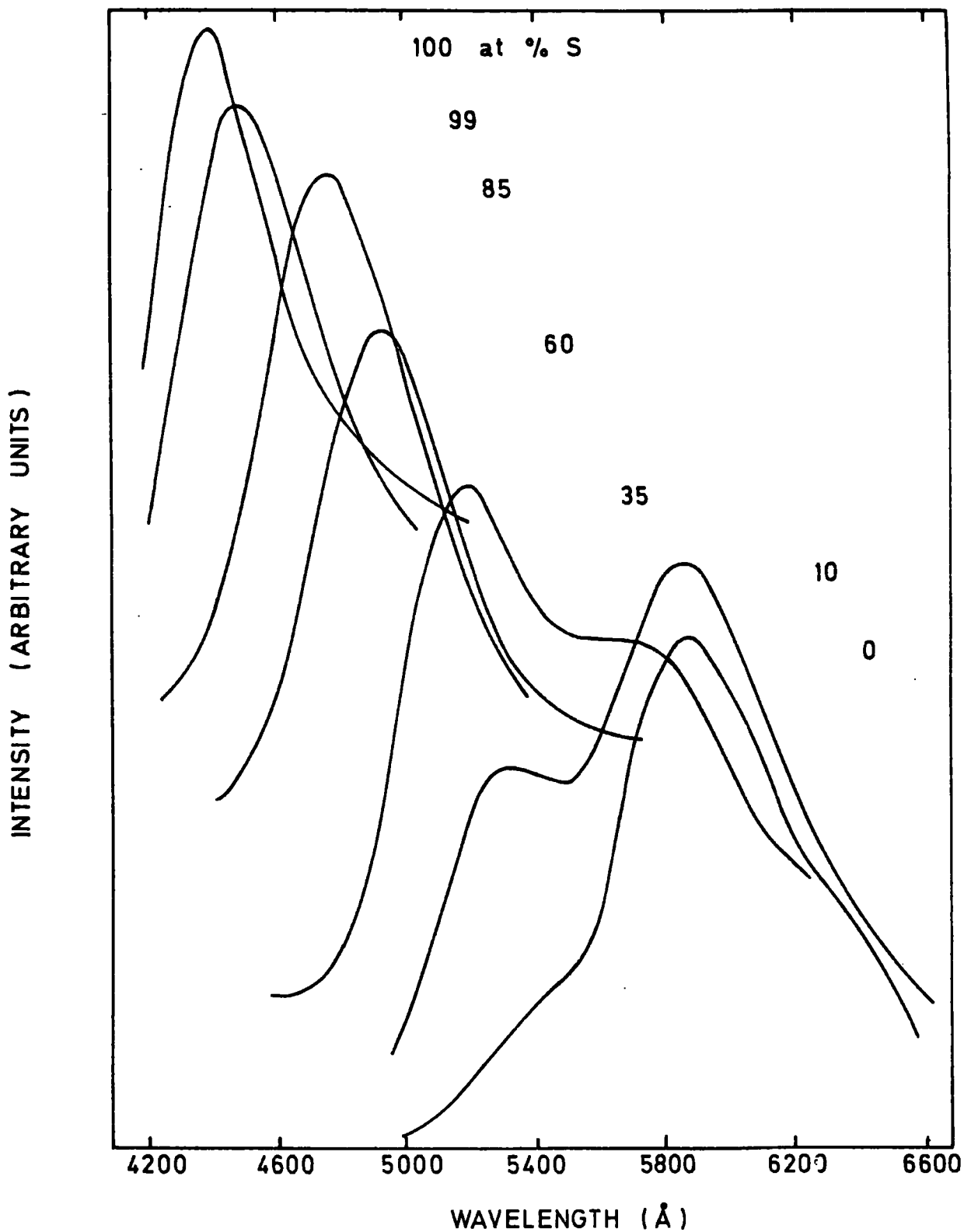


FIG. 6.2 Photoluminescence spectra of  $\text{Zn}(\text{S}, \text{Se}) : \text{I}, \text{Cu}$  crystals at  $85^\circ\text{K}$ .

temperature a large difference was apparent. The sulphur-rich samples showed a single narrow band of emission shifted to higher energies with respect to the room temperature position; but on the longer wavelength side there was a low energy tail extending into the green region of the spectrum. Sample 980, ZnS:I,Cu had an emission band peaking in the blue at  $4400 \text{ \AA}$  (2.82 eV) with a half-width of 0.25 eV. The low energy tail was more apparent in crystals with a low sulphur content and two separate emission bands could be resolved. Sample 984,  $\text{ZnS}_{0.1}\text{Se}_{0.9}$ :I,Cu showed two bands at  $5320 \text{ \AA}$  (2.33 eV) and  $5860 \text{ \AA}$  (2.11 eV) in the green and orange regions respectively. The sample of ZnSe:I,Cu No.979 emitted an orange band centred at  $5900 \text{ \AA}$  (2.10 eV) with a side-band in the green at approximately  $5400 \text{ \AA}$  (2.30 eV) and in the red at approximately  $6300 \text{ \AA}$  (1.97 eV). By comparison, van Gool and Cleiren (1960) have reported finding a blue band in ZnS at  $4350 \text{ \AA}$  (2.85 eV) with a half-width of 0.25 eV in samples containing a high ratio of copper to donor concentration. Jones and Woods (1974) have examined the luminescence of ZnSe doped with copper and have reported observing a red band at  $6400 \text{ \AA}$  with a half-width of 0.28 eV measured at room temperature, and two emission bands at 85 K in the green at  $5450 \text{ \AA}$  and in the red at  $6340 \text{ \AA}$  with half-widths of 0.20 eV. There are various reports, see Jones and Woods (1974), Morehead (1963), Halsted et al (1965), that the red and green emission bands in ZnSe:Cu are analogous to the green and blue emission bands, respectively, in ZnS:Cu; the terms 'copper-green' and 'copper-blue' will be used to describe the respective series of bands in  $\text{Zn}(\text{S},\text{Se})\text{:Cu}$ .

Iida (1969) has reported the presence of three photoluminescent bands in ZnSe doped with copper in the green, yellow and red spectral regions at  $5300 \text{ \AA}$ ,  $5700 \text{ \AA}$  and  $6400 \text{ \AA}$ . The green and yellow emission bands appeared only at temperatures below 300 K, and either red and green

or red and yellow emissions were observed together. In sample 979 ZnSe:I,Cu, however, the luminescence appeared to be uniform across the surface of the sample and was resolved as three separate bands. Iida reported that the yellow emission was monitored from portions of the crystal in which copper was the major detected impurity. He concluded that the green and red emissions in ZnSe:Cu are due to the copper impurity and that the yellow emission can be attributed to a donor-acceptor pair recombination. The orange band observed in this work in the ZnSe:Cu sample 979 may be analogous to a band reported by Bancie-Grillot (1954) at  $5080 \text{ \AA}$  in ZnS:Cu,Cl which has been attributed by Curie (1960) to substitutional copper in association with sulphur vacancies.

The peak positions and half-widths throughout the range of composition are given in Table 6.1 as measured at room temperature and at 85 K. The half-widths at room temperature vary from 0.30 eV in ZnSe to 0.40 eV in ZnS; at 85 K the half-width is approximately 0.25 eV in all samples. The variation of the photon energy of the emission band maximum against lattice parameter is shown in Figs. 6.3 and 6.4. At room temperature the 'copper-green' emission band shifts linearly from 1.97 eV ( $6280 \text{ \AA}$ ) in ZnSe:I,Cu to 2.52 eV ( $4920 \text{ \AA}$ ) in ZnS:I,Cu. The position of this 'copper-green' emission appears to be displaced to higher energies, towards the position of the self-activated luminescence, in comparison with the reports of other workers, i.e. 1.94 eV ( $6400 \text{ \AA}$ ) in ZnSe by Iida (1969) and 2.30 eV ( $5300 \text{ \AA}$ ) in ZnS by Shionoya (1966). At 85 K, the 'copper-blue' emission shifts from 2.29 eV ( $5420 \text{ \AA}$ ) in ZnSe to 2.82 eV ( $4400 \text{ \AA}$ ) in ZnS. The shift appears to be linear initially, however there is a rapid shift from sample 982  $\text{ZnS}_{0.9}\text{Se}_{0.1}$  at 2.62 eV ( $4740 \text{ \AA}$ ) with higher sulphur concentrations. Lehmann (1966) has reported that the blue emission observed in ZnS powder phosphors shifts from 2.82 eV ( $4450 \text{ \AA}$ ) to 2.60 eV ( $4770 \text{ \AA}$ ) with the

TABLE 6.1

PEAK POSITION AND HALF-WIDTHS OF Zn(S,Se):I,Cu

Sample	Temperature 300 K		Temperature 85 K	
	Peak Position (Å)	Half-Width (eV)	Peak Position (Å)	Half-Width (eV)
ZnSe	6260	0.30	5450 5890 6350	- 0.23 -
ZnS <sub>0.1</sub> Se <sub>0.9</sub>	6120	0.32	5340 5870	- 0.23
ZnS <sub>0.4</sub> Se <sub>0.6</sub>	5900	0.33	5190 5700	- 0.25
ZnS <sub>0.6</sub> Se <sub>0.4</sub>	5110	0.34	4940	0.26
ZnS <sub>0.85</sub> Se <sub>0.15</sub>	5120	0.40	4760	0.38
ZnS <sub>0.99</sub> Se <sub>0.1</sub>	4890	0.41	4490	0.30
ZnS	5000	0.40	4400	0.25

TABLE 6.2

THERMAL QUENCHING ACTIVATION ENERGY OF Zn(S,Se):I,Cu

Sample	Emission Peak (Å)	Activation Energy (eV)	
ZnSe	5400 5890	0.048 0.062	- 0.38
ZnS <sub>0.4</sub> Se <sub>0.6</sub>	5190	0.062	0.071
ZnS <sub>0.6</sub> Se <sub>0.4</sub>	4940	0.043	0.17
ZnS <sub>0.85</sub> Se <sub>0.15</sub>	4760	0.087	-
ZnS <sub>0.85</sub> Se <sub>0.15</sub>	4400	0.049	0.078

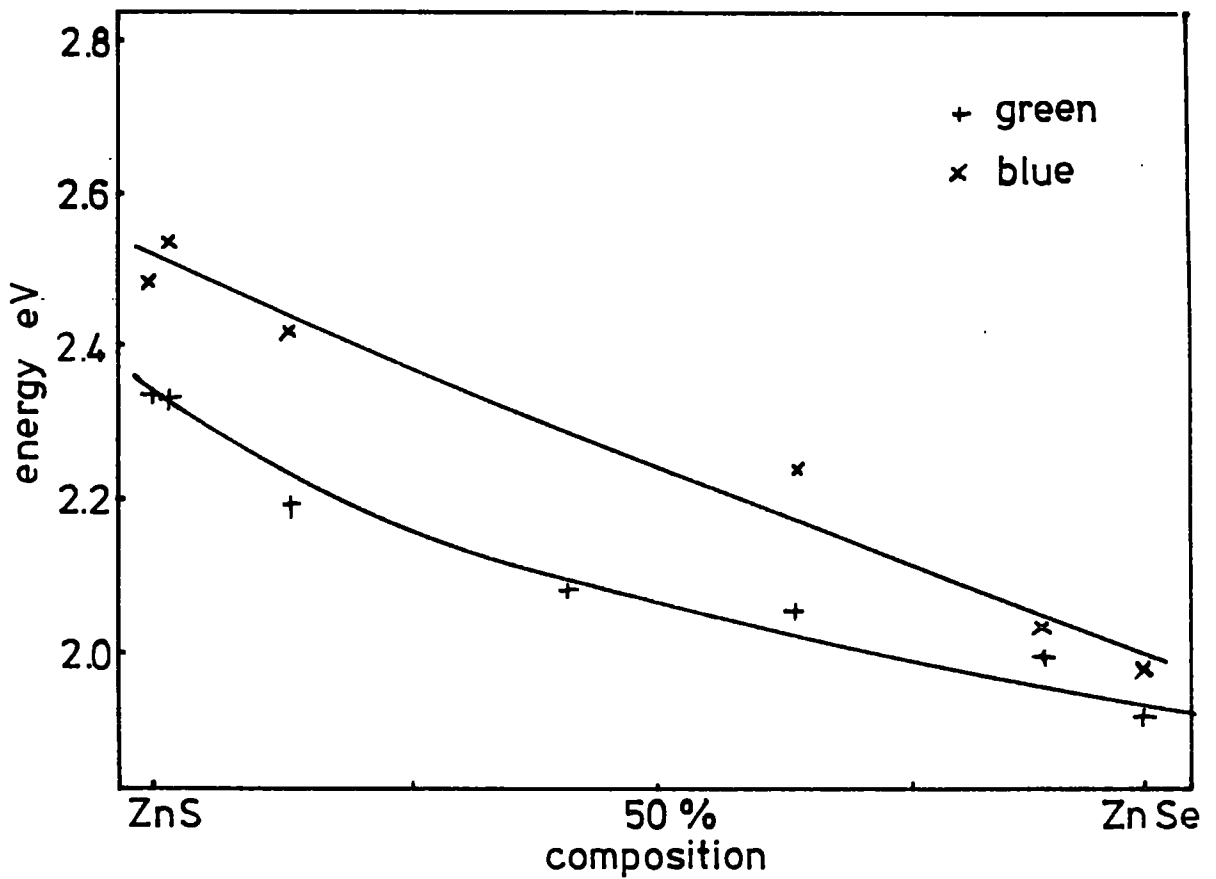


FIG 6.3 emission peak position variation with composition at 300 K

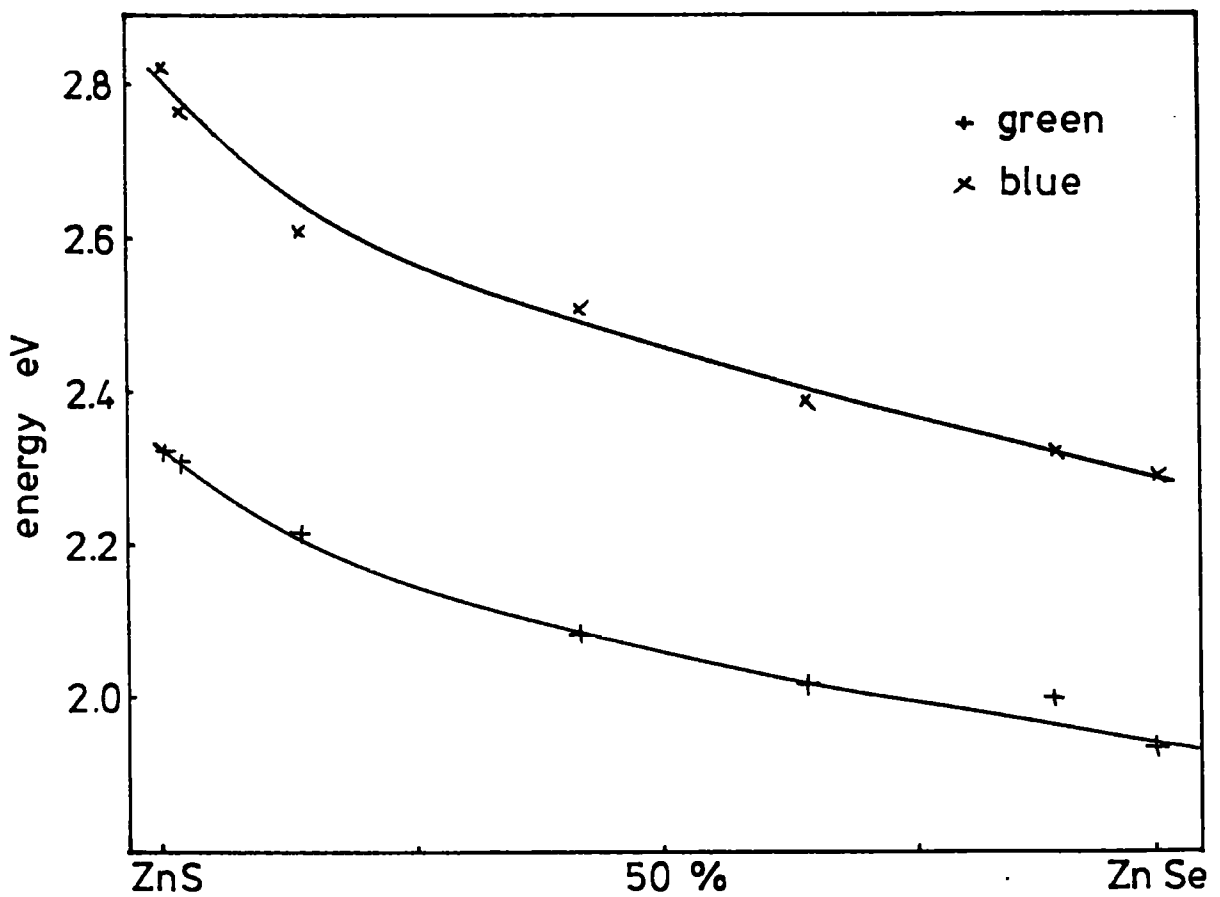


FIG 6.4 emission peak position variation with composition at 85 K

incorporation of as little as 1% of ZnSe. The results presented here indicate that there is no discontinuity in the observed variation of the position of the emission bands: there is a continuous shift from the blue emission in ZnS to the green emission in ZnSe.

In summary the luminescence results obtained from the highly doped Zn(S,Se):I,Cu mixed crystals are as follows: at room temperature a red emission is observed in ZnSe which shifts in position to the green in ZnS; at liquid nitrogen temperature a higher energy emission band appears in the green in ZnSe shifting continuously in energy to the blue in ZnS. The lower energy band, observed at room temperature, also appears as a separate peak in the red region in the low sulphur content samples becoming a shoulder on the main emission band as the percentage of sulphur increases. In the sample of ZnSe:I,Cu a third emission band was observed at  $\sim 5900 \text{ \AA}$  in the yellow.

### 6.2.2 Excitation Spectra

The excitation spectra of the luminescence emission observed in the mixed crystals have been examined throughout the range of composition. Most samples showed a low level of emission intensity at room temperature, and consequently it was only possible to measure the excitation spectra at 85 K. A variable interference filter was used to isolate the emission being examined. The variable filter had a pass band of approximately  $400 \text{ \AA}$  and the filter position was optimised at the wavelength of interest. In the crystals with low sulphur content which showed more than one emission band, all peaks were monitored.

The excitation spectra obtained at 85 K for the range of Zn(S,Se):I,Cu crystals are illustrated in Fig. 6.5. The crystals

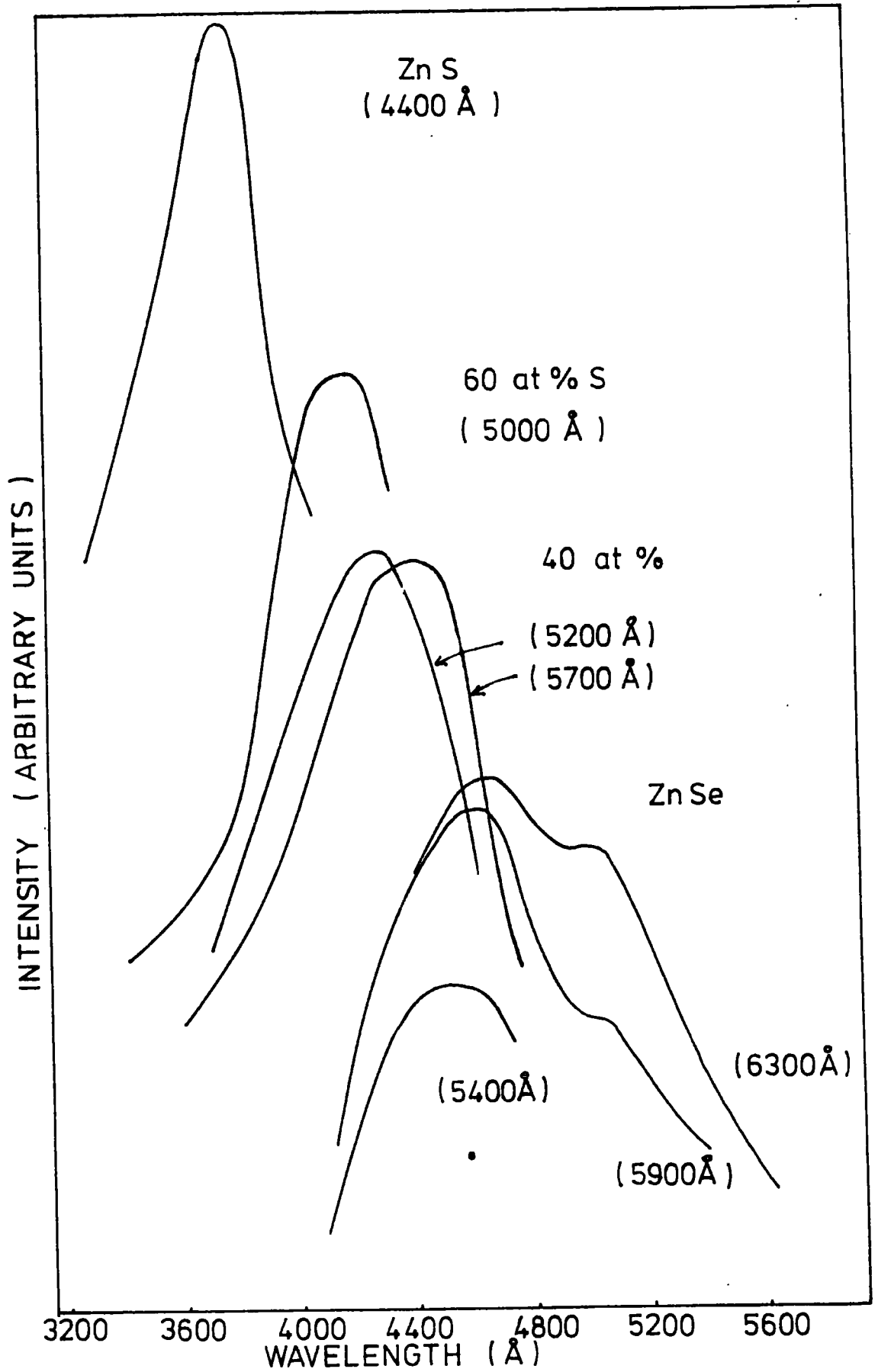


FIG 6.5 EXCITATION SPECTRA OF Zn ( S, Se ) : I, Cu AT 85 K .

containing a large proportion of sulphur all showed the 'copper-blue' band of emission with a slight low energy tail. In the low sulphur content crystals the lower energy emission band was also examined. Monitoring the blue emission in the sample of ZnS:I,Cu through to the green emission in the sample of ZnSe:I,Cu revealed a single excitation band at  $3750 \text{ \AA}$  (3.31 eV) shifting to  $4600 \text{ \AA}$  (2.69 eV). The variation of the peak excitation energy with composition is shown in Fig. 6.6. The excitation peak for the 'copper-blue' emission appears to shift linearly in energy with composition between the positions observed in ZnS and in ZnSe. Narita and Sugiyama (1965) have reported finding an excitation peak in the region  $3600 \text{ \AA} - 3700 \text{ \AA}$  monitoring the blue emission from crystals of ZnS:Br,Cu doped with 500 p.p.m. of copper. Iida (1969) has examined the excitation spectra of ZnSe containing copper as the major impurity at levels of  $\sim 10$  p.p.m., and observed an excitation band at  $4600 \text{ \AA}$  when monitoring the green emission at  $5400 \text{ \AA}$ . In a review of the II-VI materials, Halsted, Aven and Coghill (1965) suggested that the excitation of the blue emission in ZnS should be directly analogous to the excitation of the green emission in ZnSe; the results obtained in this work indicate that this suggestion is correct.

The sample of ZnSe:I,Cu crystal No.979 showed three bands of luminescence when excited by ultra-violet radiation, corresponding to the green, yellow and red regions of the spectrum. The excitation spectra for the red and yellow emissions from this sample were also examined and these are shown in Fig. 6.5. When monitoring either of the two emission bands at  $5900 \text{ \AA}$  or  $6300 \text{ \AA}$ , two bands were observed in the excitation spectra at  $4600 \text{ \AA} \sim 4650 \text{ \AA}$  (2.70  $\sim$  2.67 eV) and  $\sim 5000 \text{ \AA}$  (2.48 eV). The intensity of the  $5000 \text{ \AA}$  excitation band relative to the  $4600 \text{ \AA}$  band was

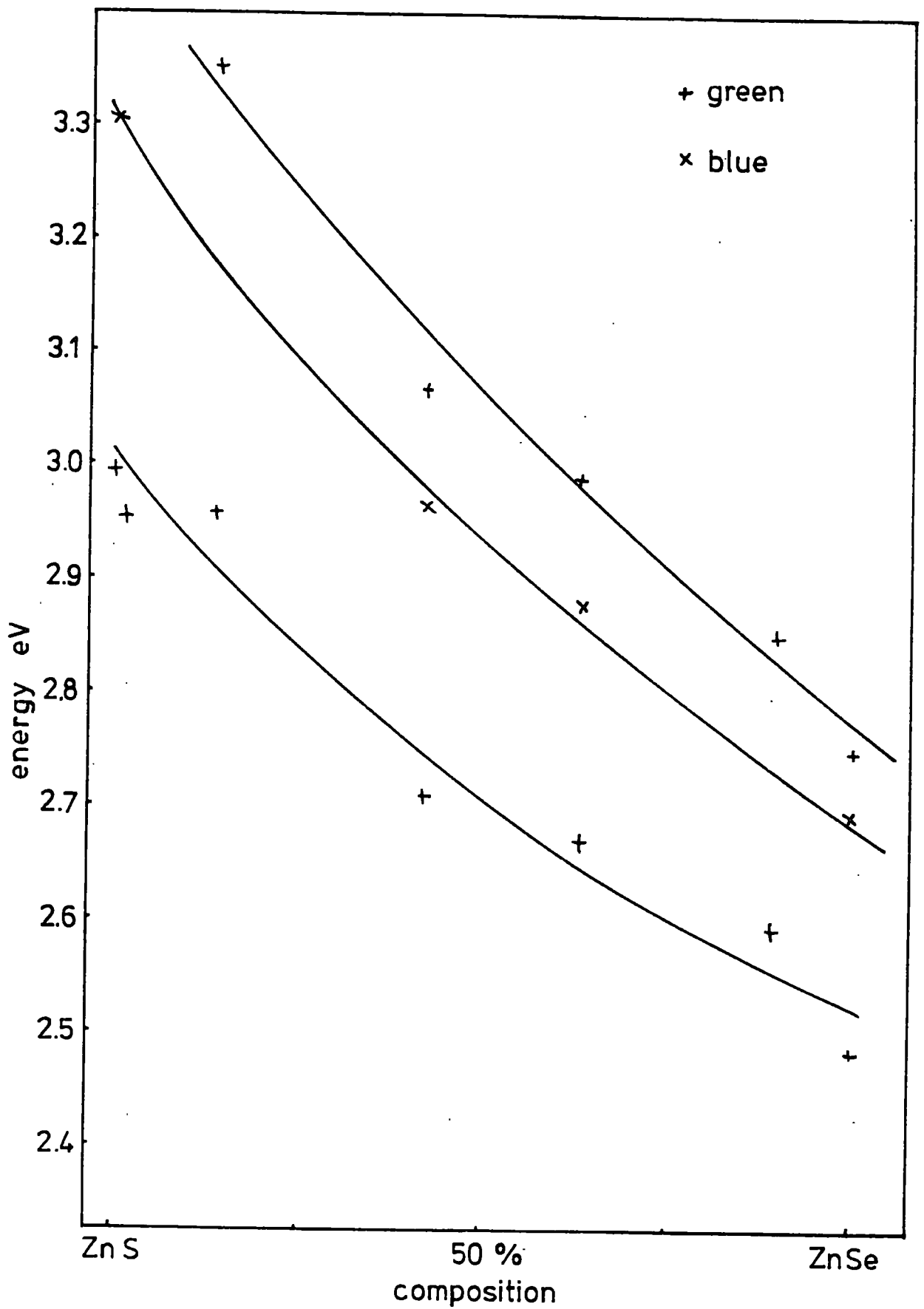


FIG 6.6 variation of excitation peak position with composition at 85 K

reduced when monitoring the yellow emission rather than the red. This may be due to the fact that the 5000 Å excitation band is associated with the red emission, but the excitation spectra are complicated by the fact that the red and yellow emissions overlap each other. In comparison, Jones and Woods (1974) have examined the excitation of the red emission at 6400 Å in ZnSe:Cu and have reported observing a broad excitation band with maxima at 4700 Å and 5100 Å. Iida (1969) and Terada (1976) also observed a yellow emission band in copper doped ZnSe and Iida has reported that this is excited by a narrow band of radiation close to the band edge at 4520 Å, while the red emission is excited by broad overlapping bands with maxima at approximately 4650 Å and 5200 Å. From these results it may be concluded that the green emission in ZnSe:Cu is excited in a narrow band of radiation just below the band edge; the red emission is excited by a broad band with a maximum just below the band edge and with a second maximum approximately 0.2 eV below the energy of the first excitation peak. In samples of ZnSe doped with copper which show yellow luminescence, the emission is excited predominantly by radiation near the band-edge with some evidence of a weak lower energy excitation process which may have been observed because of the overlap of the red and yellow emissions.

Throughout the range of composition of the Zn(S,Se):I,Cu crystals, the "copper-blue" emission is excited by a single band of radiation close to the band edge: the maximum energy of excitation is approximately 0.5 eV less than the band-gap energy in ZnS and 0.1 eV less in ZnSe. The position of the excitation band shifts linearly in energy as the composition is varied.

### 6.2.3 Thermal Quenching

The quenching of the luminescence from a variety of crystals through the range of composition has been measured in the temperature range from 85 to 350 K. The upper temperature limit was imposed by the nature of the cryostat in which the samples were mounted for examination. A 3650 Å ultra-violet radiation source was used to excite the emission in the samples. The maximum of the appropriate emission band was monitored when making measurements, and wide slit-widths were used to encompass the whole band of luminescence and to allow for shifts in the peak position on warming.

The variation of the 'copper-blue' emission intensity with temperature is shown in Fig. 6.7 for a number of mixed crystals. The intensity of the luminescence decreased immediately the temperature was raised above 90 K, and the rate of quenching became more rapid as the temperature increased. Whilst there are marked differences in the form of the emission quenching curves, in general the quenching occurred at lower temperatures as the percentage of sulphur in the mixed crystals increased.

In the sample of ZnSe:I,Cu both the yellow and green emissions were monitored and their thermal quenching is also shown in Fig. 6.7. The green emission band at 5400 Å was rapidly quenched above 80 K and levelled off beyond 180 K. By comparison the yellow emission at 5860 Å decreased slowly in intensity, with the luminescence intensity at 180 K reaching a level approximately 80% of that at 85 K. The yellow emission was then quenched more rapidly at temperatures above ~ 220 K. Since there was more than one band of emission in this sample, a redistribution might have been occurring between the recombination processes as the temperature was varied.

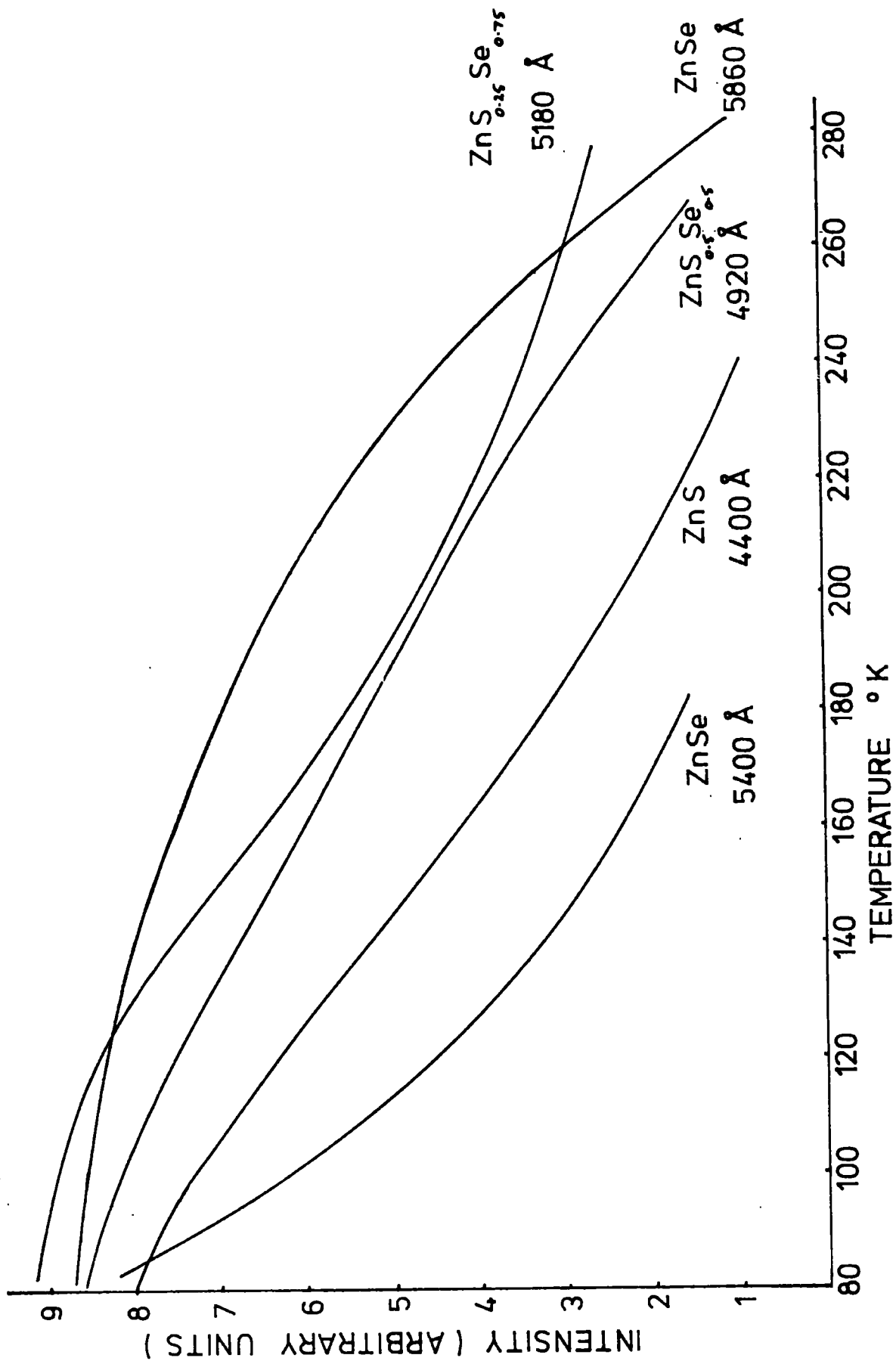


FIG 6.7 THERMAL QUENCHING CURVES FOR  
 $\text{Zn}(\text{S}, \text{Se}) : \text{I}, \text{Cu}$

If it is assumed that the luminescence efficiency,  $\eta$ , can be described by the equation

$$\eta = \left[ 1 + C \exp \left( -\frac{\omega}{kT} \right) \right]^{-1}$$

where  $C$  is a constant and  $\omega$  is the activation energy for thermal quenching, then  $\omega$  may be found by plotting  $\ln(1/\eta - 1)$  against  $1/T$ . When the curves of thermal quenching shown in Fig. 6.7 were plotted in the form  $\ln(1/\eta - 1)$  versus  $1/T$  as in Figs. 6.8 and 6.9, the resultant curves appeared to be composed of one or two straight lines. Since the slope of the line gives  $\omega$ , the suggestion is that there may be two activation energies associated with the quenching of the luminescence. The values calculated for the activation energies are listed in Table 6.2. In the low temperature region the values obtained ranged from 0.043 eV to 0.087 eV, and in the high temperature region from 0.07 eV to 0.17 eV. The quenching of the yellow emission observed in the crystal of ZnSe:I,Cu gave an activation energy of 0.38 eV in the high temperature region. No particular trend emerges from this data and it would be necessary to examine a greater number of samples in order to establish the variation between crystals of the same composition. However, all the samples showed a small activation energy for the low temperature quenching of the luminescence. Jones (1973) has reported observing quenching energies of 0.03 and 0.41 eV in both self-activated and copper doped ZnSe. The lower energy is comparable with the activation energy found in all our crystals, and the higher energy compares with the value found for the quenching of the yellow emission in ZnSe:I,Cu. Since all the samples have a high donor concentration due to the presence of included iodine, it is suggested that this may be having an effect on the low temperature quenching of the luminescence. In the high temperature quenching of the 'copper-blue'

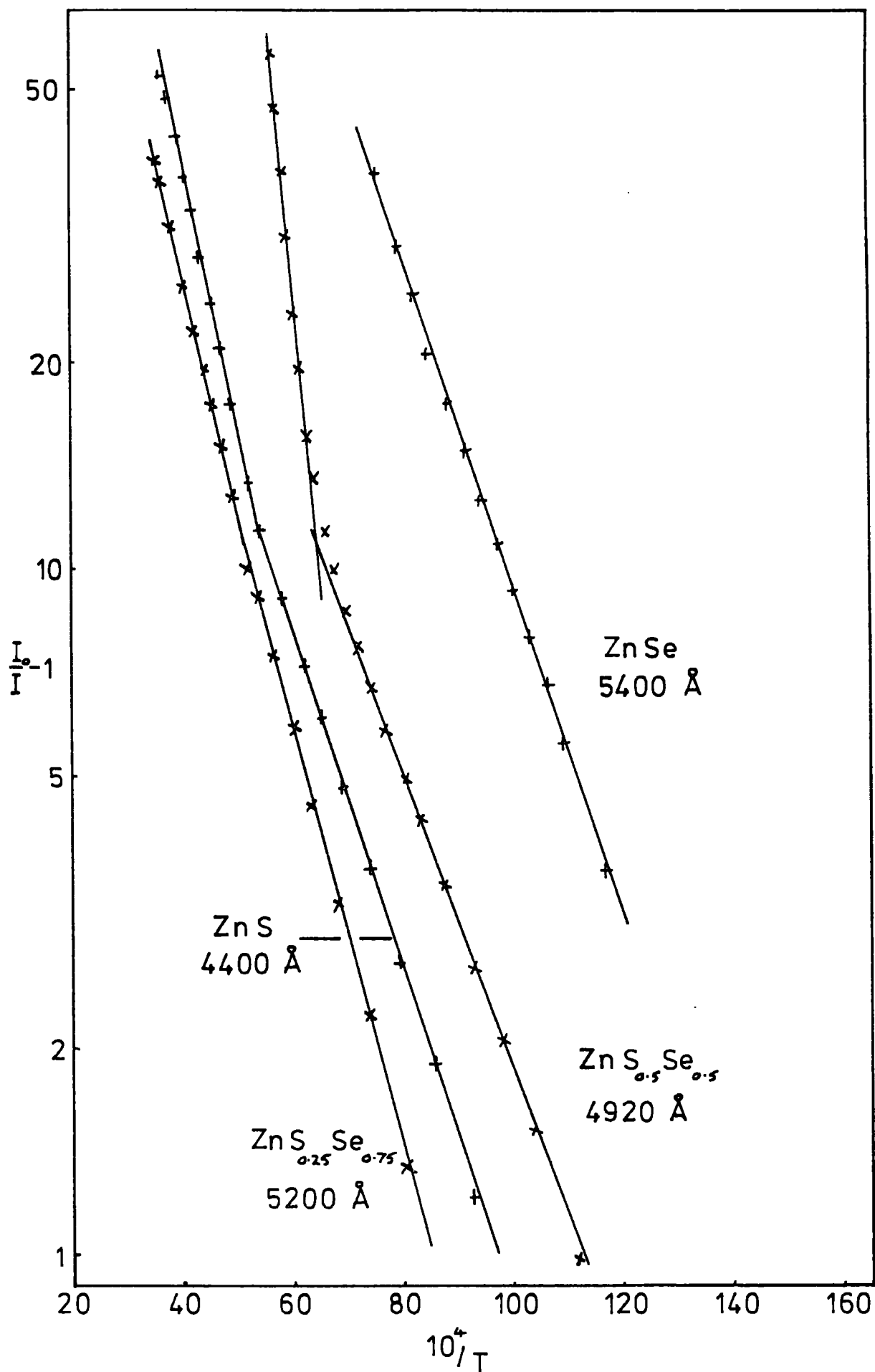


FIG 6.8 THERMAL QUENCHING CURVES FOR  
Zn ( S , Se ) : I , Cu

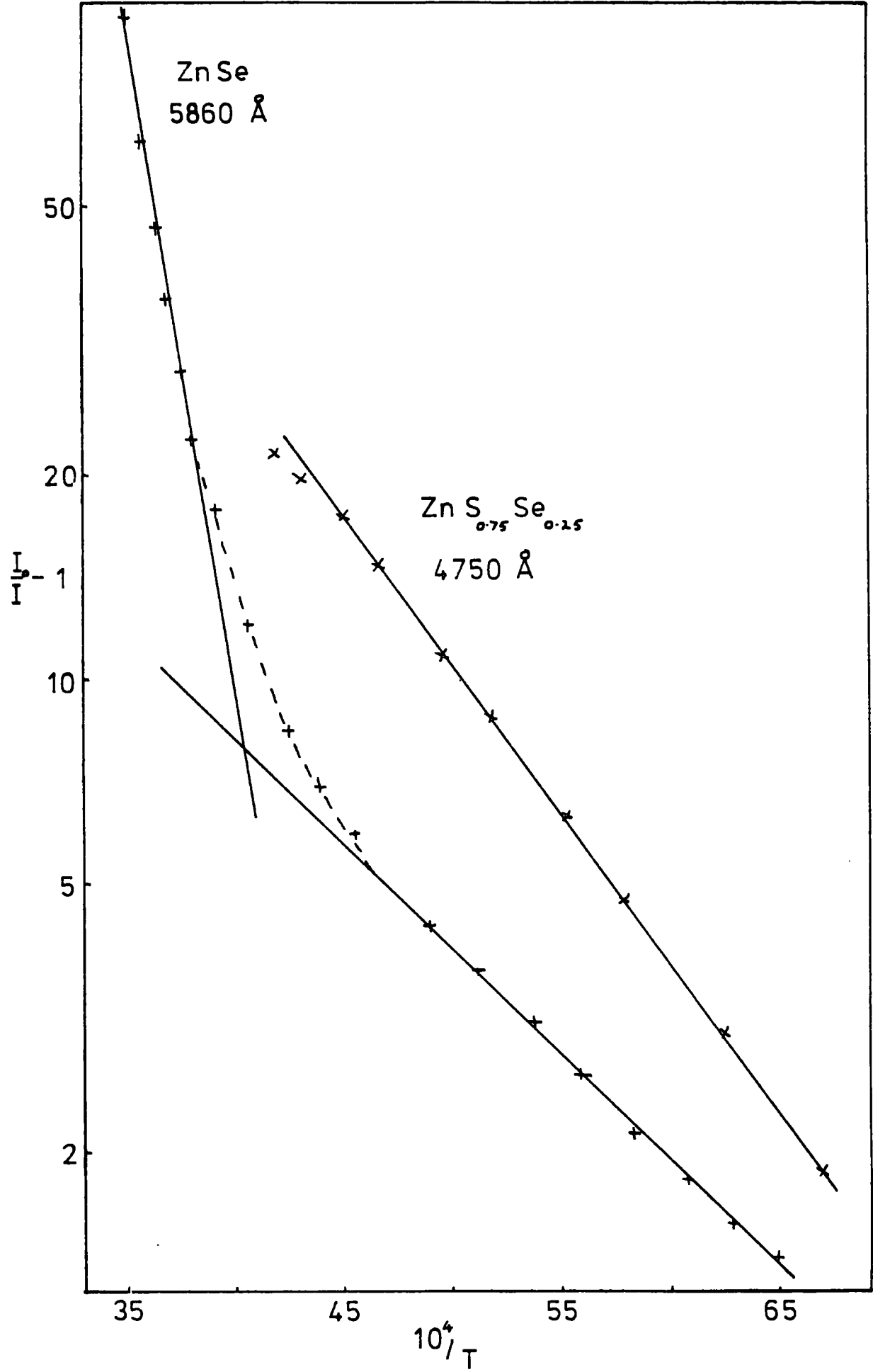


FIG 6.9 THERMAL QUENCHING CURVES FOR  
 Zn ( S , Se ) : I , Cu

emission, no activation energies have been observed comparable with the value of 0.61 eV reported by Narita and Sugiyama (1965) in ZnS:Br,Cu. However, the high energy quenching processes would be expected to occur at elevated temperatures outside the range which could be covered with the present equipment.

### 6.3 Annealed Copper-Activated Samples

The crystals described in the previous section showed the 'copper-blue' type luminescence which has been reported by Van Gool (1961) to occur in ZnS doped with a high ratio of copper to coactivator concentration. The samples were annealed in liquid zinc for a period of 120 hours at 850°C in order to remove a proportion of the copper present and to examine the effect of the treatment on the luminescence properties. Ozawa and Hersh (1973), and Özsan (1976) have reported that annealing mixed crystals in zinc results in the resistivity being reduced by several orders of magnitude. Ozawa and Hersh observed an exponential relationship between the resistivity of annealed mixed crystals and the proportion of sulphur in the solid solution. This annealing technique is used within the department for the preparation of suitable material for electro-luminescent device fabrication. Visually, the intensity of the luminescence was much enhanced after this treatment. The effect of annealing the Zn(S,Se):I crystals in liquid zinc is to purify the samples; the zinc reduces the concentration of many impurities and crystal defects which form the quenching and non-radiative centres.

#### 6.3.1 Photoluminescence

The spectral distribution of the luminescence of the annealed

Zn(S,Se):I,Cu,Zn crystals is shown in Figs. 6.10 and 6.11 at 300 K and 85 K respectively. At room temperature, a single broad band of emission was excited by 3650 Å ultra-violet radiation, and this emission shifted from the red spectral region in ZnSe through to the green in ZnS. The peak of the emission band occurred at 6450 Å (1.92 eV) in ZnSe:I,Cu,Zn and 5300 Å (2.33 eV) in ZnS:I,Cu,Zn with half-widths of 0.30 eV and 0.34 eV respectively. At liquid nitrogen temperature, the emission peak was narrower and had shifted to higher energies compared with the luminescence at room temperature. A high energy shoulder appeared on the shorter wavelength side of the main band: this shoulder could be resolved as a separate peak at 4550 Å (2.72 eV) in the sample of zinc sulphide.

The peak positions and half-widths for the range of mixed crystals are given in Table 6.3. The half-widths vary between 0.30 and 0.44 eV at room temperature and between 0.23 and 0.36 eV at liquid nitrogen temperature. No trend in the variation of the half-width with composition was observed. This may have been due to the fact that there was a high energy shoulder on the main emission peak influencing the shape of the observed luminescence band. The high energy shoulder became more apparent when the samples were cooled to 85 K and as the percentage of sulphur in the crystals was increased. Cooling the sample caused a reduction in the half-width by approximately 0.08 eV.

The variation of the photon energy for maximum emission as a function of composition is shown in Figs. 6.3 and 6.4 at room temperature and at 85 K respectively. At room temperature the emission band shifted linearly from 1.91 eV (6490 Å) in ZnSe to 2.33 eV (5320 Å) in ZnS. The corresponding photon energies in the unannealed crystals were 1.97 eV (6280 Å) and 2.52 eV (4920 Å). Cooling the samples to 85 K led to the emission bands becoming narrower, but the peak positions were little

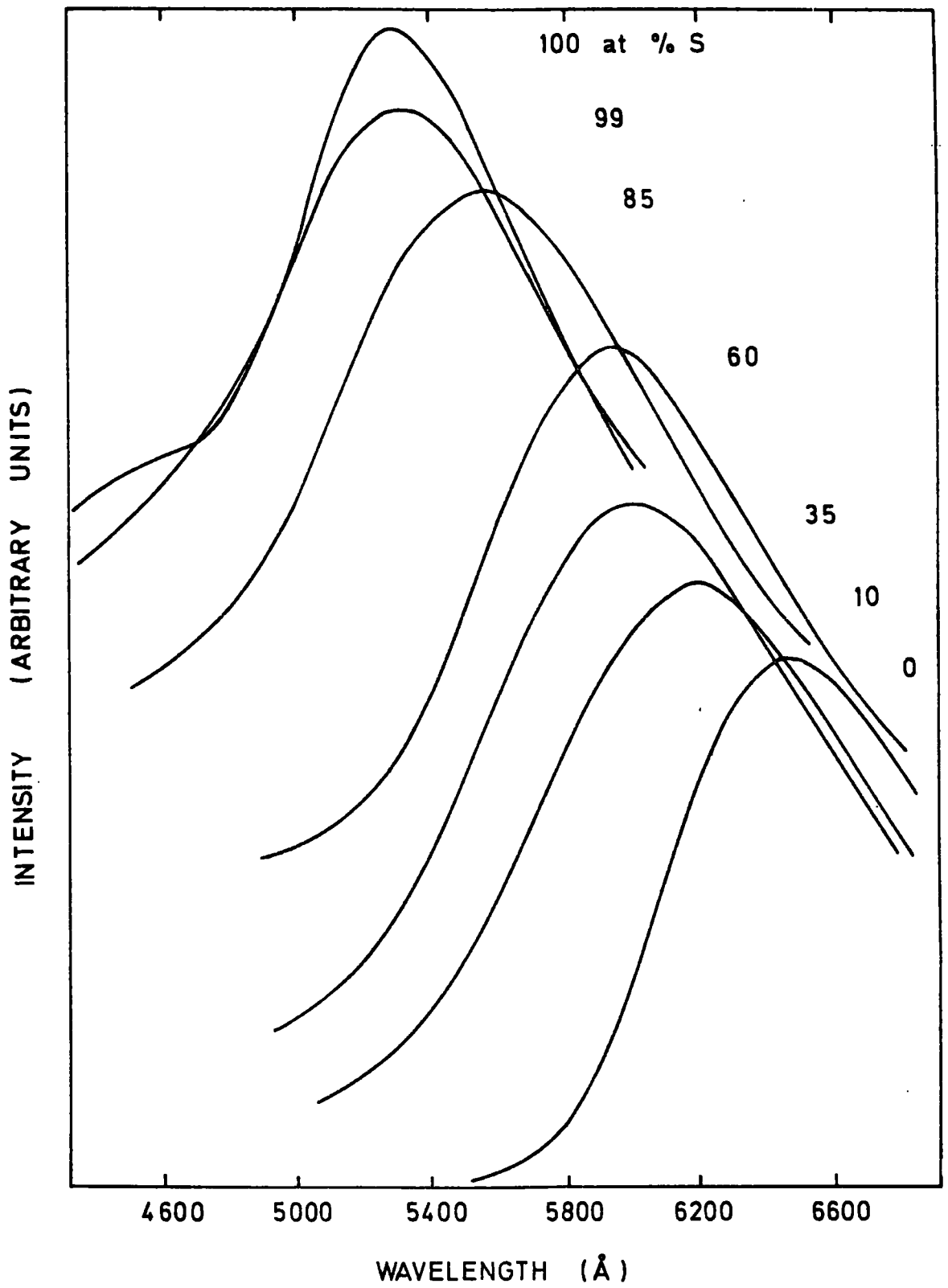


FIG. 6.10 Photoluminescence spectra of  $\text{Zn}(\text{S}, \text{Se}) : \text{I}, \text{Cu}, \text{Zn}$  crystals at  $300^\circ\text{K}$ .

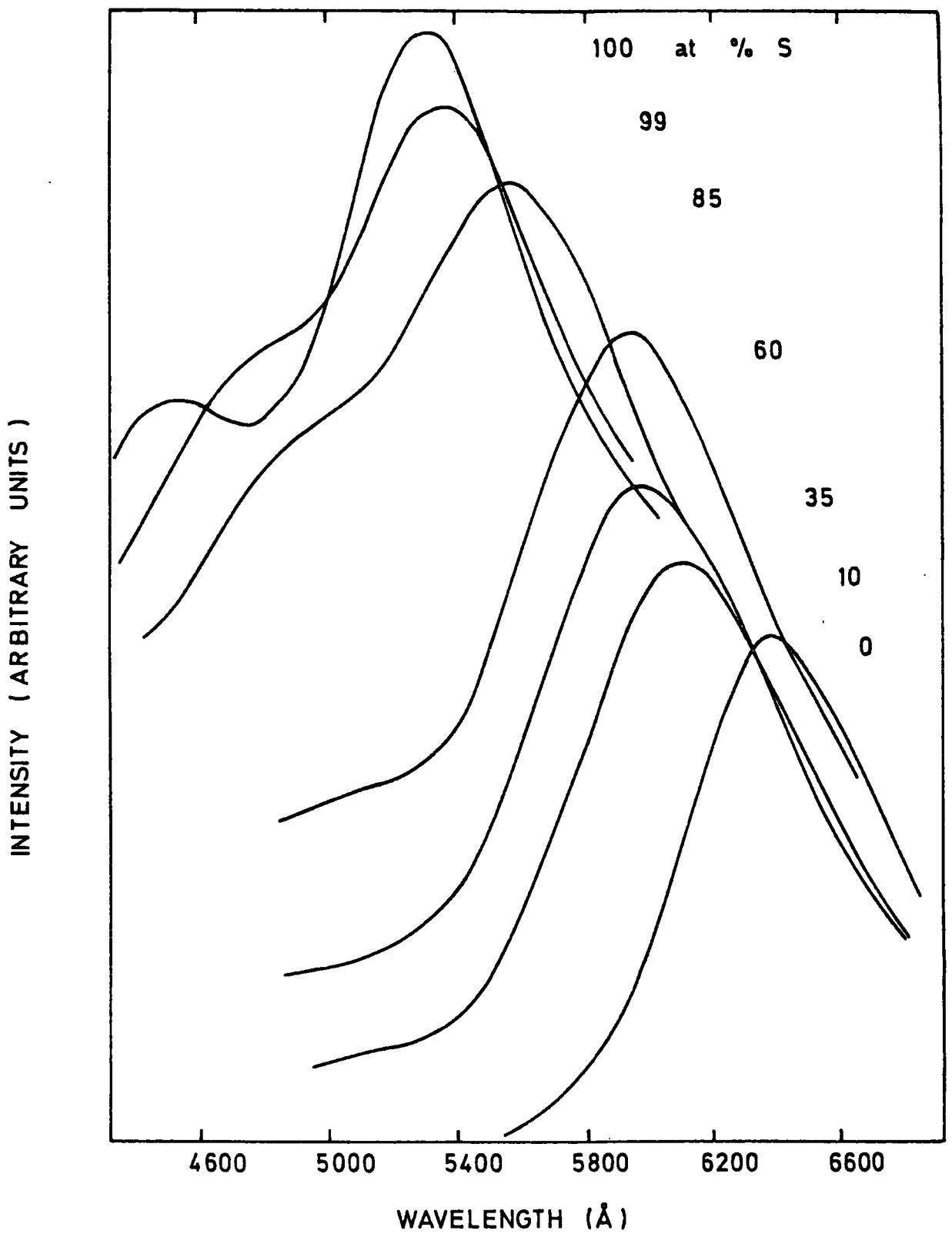


FIG. 6.11 Photoluminescence spectra of  $\text{Zn}(\text{S}, \text{Se}) : \text{I}, \text{Cu}, \text{Zn}$  crystals at  $85^\circ\text{K}$ .

**TABLE 6.3**

PEAK POSITION AND HALF-WIDTHS OF Zn(S,Se):I,Cu,Zn

Sample	Temperature 300 K		Temperature 85 K	
	Peak Position (Å)	Half-Width (eV)	Peak Position (Å)	Half-Width (eV)
ZnSe	6460	0.30	6410	0.23
ZnS <sub>0.1</sub> Se <sub>0.9</sub>	6200	0.37	6110	0.28
ZnS <sub>0.4</sub> Se <sub>0.6</sub>	6020	0.38	5990	0.29
ZnS <sub>0.6</sub> Se <sub>0.4</sub>	5950	0.35	5950	0.27
ZnS <sub>0.85</sub> Se <sub>0.15</sub>	5590	0.42	5600	0.34
ZnS <sub>0.99</sub> Se <sub>0.01</sub>	5320	0.44	5340	0.36
ZnS	5310	0.30	4550 5310	- 0.29

**TABLE 6.4**

THERMAL QUENCHING ACTIVATION ENERGY OF Zn(S,Se):I,Cu,Zn

Sample	Emission Peak (Å)	Activation Energy (eV)
ZnSe	6350	0.041
ZnS <sub>0.1</sub> Se <sub>0.9</sub>	6050	0.046
ZnS <sub>0.4</sub> Se <sub>0.6</sub>	5950	0.039
ZnS <sub>0.6</sub> Se <sub>0.4</sub>	5880	0.033

affected: the emission band varied from 1.93 eV (6420 Å) in ZnSe to 2.32 eV (5340 Å) in ZnS.

Jones and Woods (1974) examined crystals of ZnSe which had been annealed in molten zinc containing copper. They reported observing a red emission band at 6400 Å (1.94 eV) with a half-width of 0.22 eV at 85 K. Iida (1969) reported a red luminescence band at 6320 Å (1.96 eV) at 77 K in crystals of ZnSe containing grown-in copper. Morehead (1963) observed a green emission band at 5180 Å (2.40 eV) at 77 K in powder phosphors of ZnS:Cu,Cl. A comparison of these results with the emission bands reported here shows good agreement for the crystals of ZnSe and of ZnS. However, the reported position of the emission band varies slightly when different coactivators are incorporated in the crystal and with different copper concentrations. Lehmann (1967) examined the copper emission in phosphors of cubic Zn(S,Se) doped with copper and chlorine. He observed a green band at 5200 Å (2.38 eV) in ZnS which was replaced by a new band at 5550 Å (2.23 eV) when less than 1% of ZnSe was incorporated in the phosphor. Further increase of the ZnSe concentration caused a slow shift of the emission band toward the red band at 6350 Å (1.95 eV) in ZnSe:Cu,Cl. The results obtained in the present investigation, as illustrated in Fig. 6.4, indicate that there is a single low-energy copper emission which shifts continuously in position from 2.32 eV in zinc sulphide to 1.93 eV in zinc selenide. A sample with a small selenium content was examined, crystal 987  $\text{ZnS}_{0.99}\text{Se}_{0.01}$ , and this showed an emission band at 2.31 eV only slightly below that observed in ZnS.

### 6.3.2 Excitation Spectra

The excitation spectra for the 'copper-green' type emission observed in the mixed crystals after annealing in zinc have also been

examined. The intensity of the luminescence was enhanced after annealing and it was then possible to examine the excitation spectra at both room temperature and 85 K. A variable interference filter was used to isolate the emission and this was optimised for the luminescence band of interest. The pass band of the isolating filter was approximately 400 Å.

The excitation spectra obtained for the range of mixed crystals are shown in Figs. 6.12 and 6.13 at room temperature and 85 K respectively. At room temperature, monitoring the green emission in the sample of ZnS:I,Cu,Zn through to the red emission in ZnSe:I,Cu,Zn, the spectra consisted of a broad band of excitation shifting with composition from 4150 Å (3.00 eV) to approximately 5300 Å (2.34 eV). The excitation spectra for the crystals containing a low percentage of sulphur was clearly a super-position of three different bands. With the sample of ZnSe:I,Cu,Zn there were excitation bands at ~4700 Å (2.64 eV), ~5150 Å (2.41 eV) and ~5500 Å (2.25 eV); the short wavelength peak corresponded to an excitation close to the band-edge. When the proportion of sulphur in the crystals was increased, a single broad excitation band only was observed. Cooling the samples to 85 K caused the excitation bands to shift slightly towards shorter wavelengths and become narrower. The crystal of ZnS:I,Cu,Zn showed a single excitation peak at 4140 Å (2.99 eV) whereas the crystal of ZnSe:I,Cu,Zn had three bands at 4510 Å (2.75 eV), 5000 Å (2.48 eV) and 5250 Å (2.36 eV).

Iida (1969) has examined the excitation of the red emission from copper-doped zinc selenide at 77 K and observed a broad band of excitation consisting of peaks at 4550 Å (2.72 eV), ~4800-4900 Å (~2.55 eV) and 5200 Å (2.38 eV). Jones and Woods (1974) examined crystals of zinc selenide heated in zinc plus copper and observed a broad excitation band

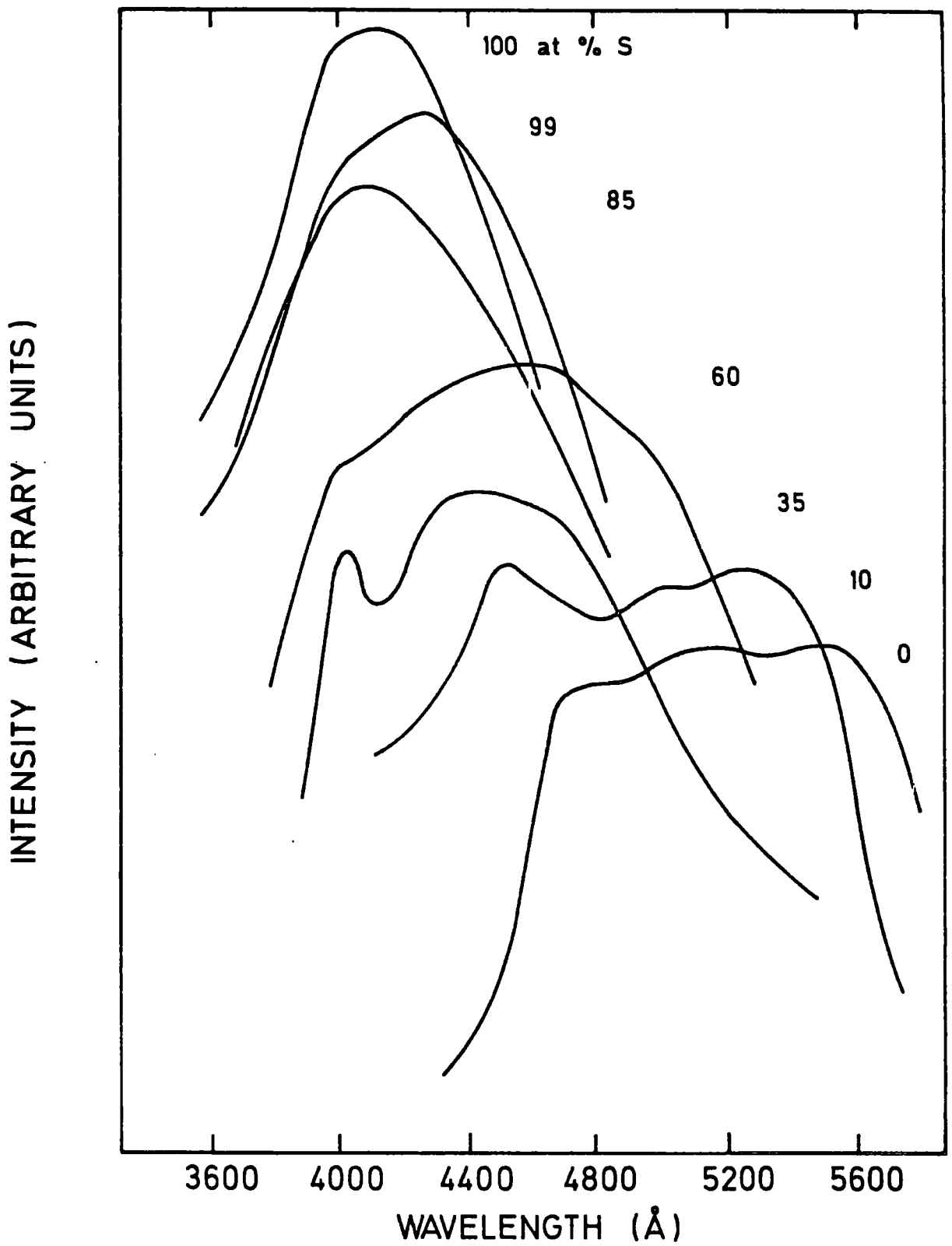


FIG. 6.12 Excitation spectra of  $\text{Zn}(\text{S}, \text{Se}) : \text{I}, \text{Cu}, \text{Zn}$  at  $300^\circ\text{K}$ .

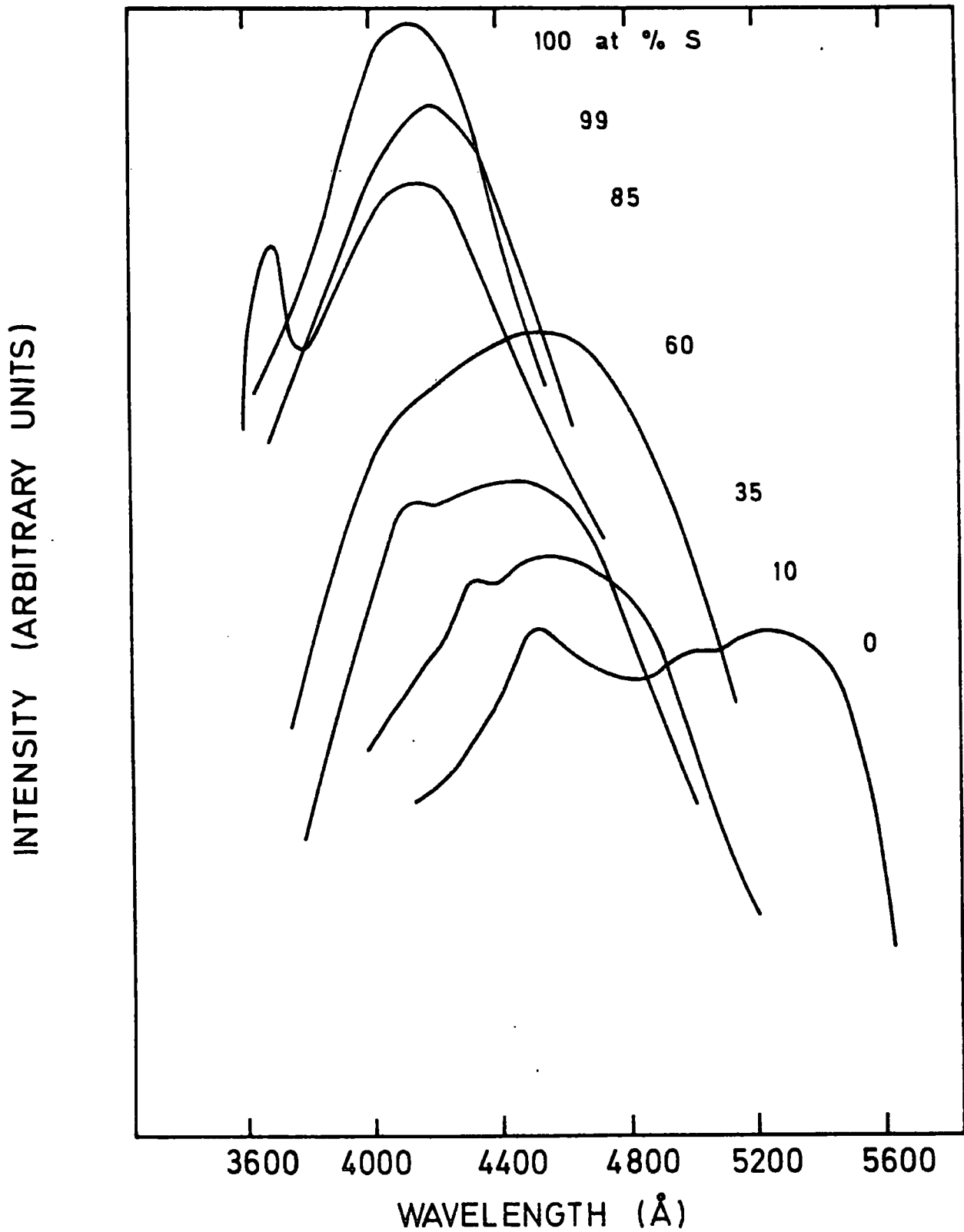


FIG. 6.13 Excitation spectra of Zn(S,Se) :I,Cu,Zn at 85°K

for the red emission with peaks at 4500 Å (2.75 eV), 4700 Å (2.64 eV) and 5100 Å (2.43 eV). A comparison with the results obtained for the undoped crystals given in the previous chapter, see Fig. 5.24, indicates that the self-activated emission in zinc selenide is excited by a band at  $\sim 4900$  Å (2.53 eV). Narita and Sugiyama (1965) examined the green emission in copper-doped zinc sulphide crystals and observed a broad excitation band extending from the band edge which peaked at 4000 Å (3.10 eV). Melamed (1958) examined crystals of zinc sulphide containing copper and chlorine and observed a peak in the excitation of the green emission at 3950 Å (3.14 eV). With zinc sulphide, the self-activated emission is excited in a band centred at 3600 Å (3.44 eV) as is shown in Fig. 5.24. The lower energy 'copper-green' emission observed in the range of mixed crystals subsequent to annealing in zinc appears to be excited by a broad band which extends to longer wavelengths than the excitation bands of the self-activated or 'copper-blue' emissions. Apart from band-to-band excitation, up to a composition of approximate 60 at.% sulphur two separate peaks are resolved in the excitation band for the 'copper-green' emission; above this composition a single band is observed. The 'copper-green' emission is most strongly excited in a band centred at 5250 Å (2.36 eV) in zinc selenide and in a band at 4140 Å (2.99 eV) in zinc sulphide.

The variation of the energies of the excitation bands with composition is shown in Fig. 6.6. The curves demonstrate that as many as three excitation peaks can be detected in the annealed, copper-doped mixed crystals; these are a high energy band close to the band-edge which shifts continuously from 2.75 eV in ZnSe to 3.35 eV in  $\text{ZnS}_{0.85}\text{Se}_{0.15}$ , this band was not observable in the sample of ZnS, and two deeper-lying bands. The deepest excitation band appears to move parallel to the band edge as the composition is varied.

### 6.3.3 Thermal Quenching

The quenching of the 'copper-green' luminescence was examined in the temperature range from 85 - 350 K. The quenching of the luminescence intensity with temperature is shown in Fig. 6.14 for a number of crystals of different composition. It is apparent that there was a much slower rate of quenching for the 'copper-green' emission than for the 'copper-blue' emission observed before treatment in zinc. With the sample of ZnSe the emission intensity had decreased by only 20% at 200 K whereas before annealing the intensity had decreased by 90%. As the proportion of sulphur in the crystal composition was increased, the quenching of the emission became less pronounced: in sample 977  $\text{ZnS}_{0.6}\text{Se}_{0.4}$  there was negligible quenching up to 350 K and for higher compositions no change at all in the emission intensity was observed.

It is assumed that the luminescence efficiency can be described by the relationship used in Section 6.2.3. The thermal quenching curves of Fig. 6.14 were replotted in the form  $\ln (1/\eta - 1)$  against  $1/T$ , and the result is shown in Fig. 6.15. The curves obtained appear to consist of segments of straight lines over most of the temperature range examined. The activation energies  $\omega$  for the thermal quenching of the luminescence were calculated from the slopes of the curves and the values obtained are listed in Table 6.4. The activation energies calculated vary from 0.033 eV to 0.046 eV; these values are of the same order as the low temperature activation energies observed for the 'copper-blue' emission in the untreated crystals. There was no high temperature quenching energy observed comparable with that seen for the 'copper-blue' emission.

Narita and Sugiyama (1965) have reported a high temperature quenching energy of 0.95 eV for the copper-green emission in crystals of ZnS:Br,Cu; no mention was made of a low temperature activation energy.

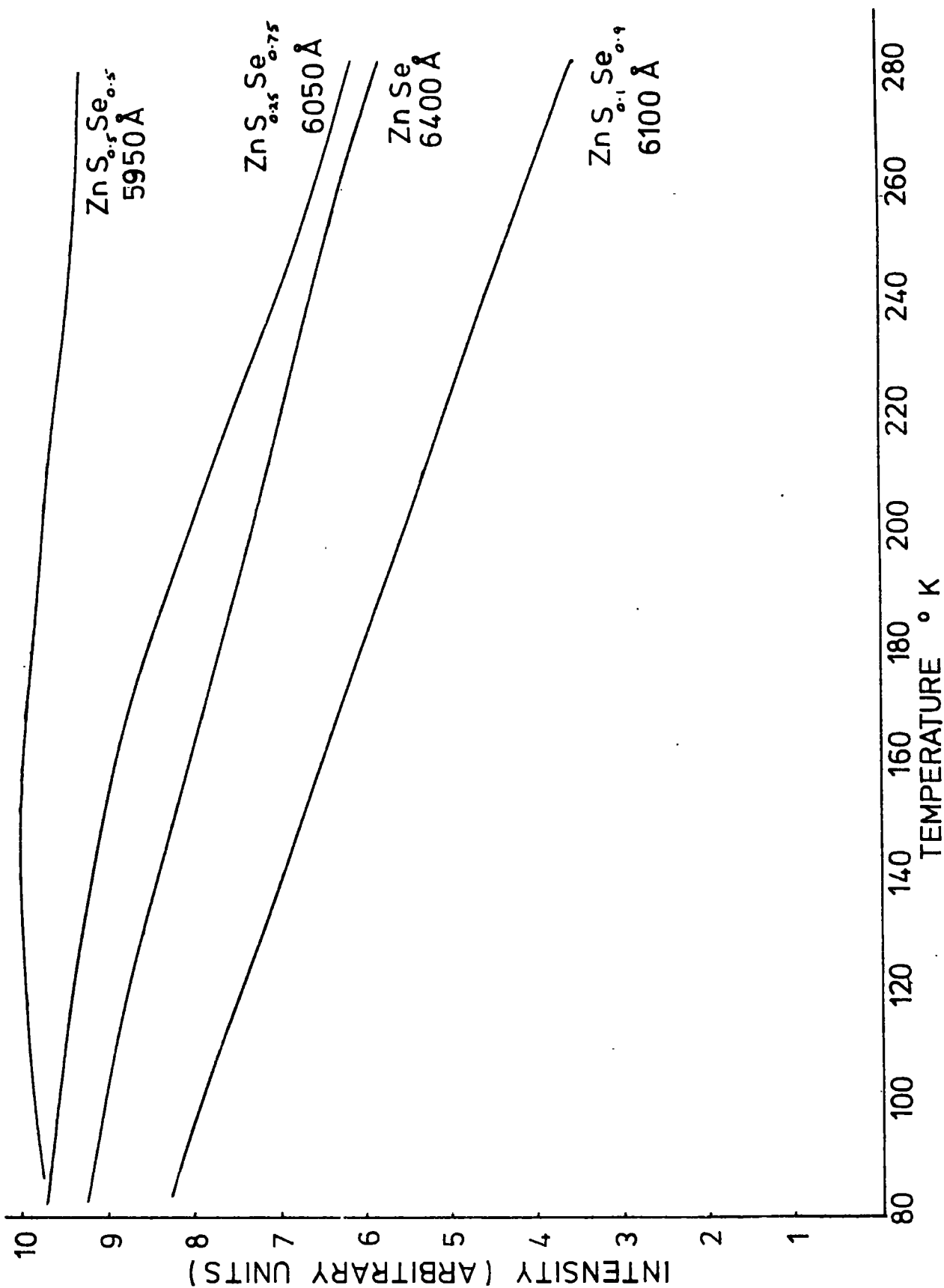


FIG 6.14 THERMAL QUENCHING OF Zn(S,Se):I,Cu,Zn

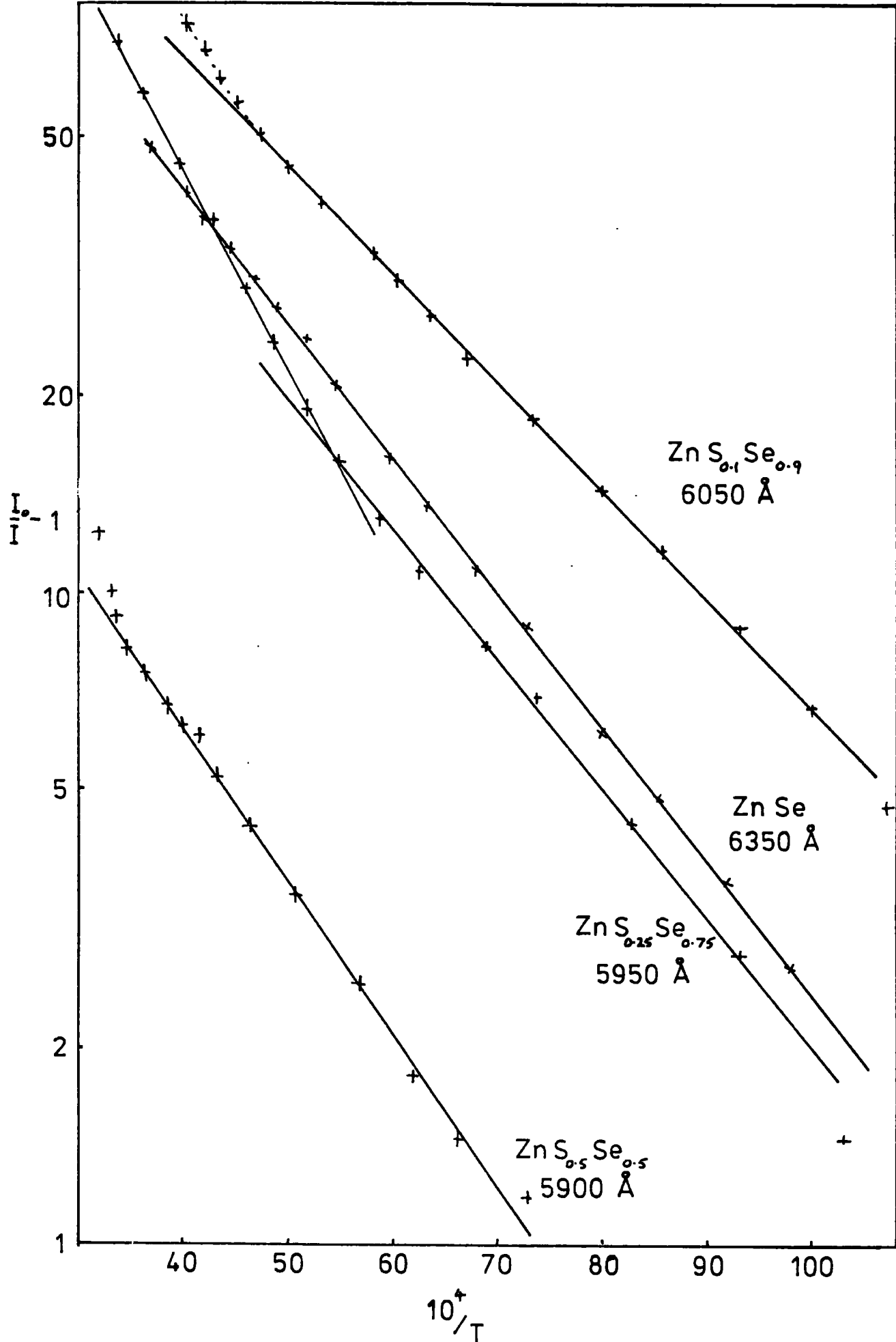


FIG 6.15 THERMAL QUENCHING CURVES FOR  
 $\text{Zn}(\text{S}, \text{Se}) : \text{I}, \text{Cu}, \text{Zn}$

Jones and Woods (1974) examined the 'copper-green' type, red luminescence in ZnSe and reported observing rapid quenching near 300 K in a copper-doped sample with an activation energy of 1.0 eV. However, these authors noted that a crystal of ZnSe which had been annealed in zinc plus copper showed no measurable quenching on heating to temperatures in excess of 400 K. It may be necessary to make measurements at temperatures greater than were possible with the present apparatus in order to study thermal quenching in the mixed alloys.

The zinc-annealed crystals exhibited limited quenching of the luminescence, and samples with sulphur compositions in excess of 60% showed negligible changes in intensity with temperature up to 400 K. Diffusing zinc into crystals of ZnS and ZnSe is believed to have an effect not only on the concentration of impurities present, but also on the number of crystal defects. Annealing in zinc may change the concentration of non-radiative and recombination centres and affect the process of thermal quenching. In order to examine this possibility it would be necessary to compare annealed and unannealed samples doped with the same level of copper impurity.

#### 6.4 Discussion

The problem of contamination is inherent in the preparation of crystals of Zn(S,Se). Copper is often present at levels of a few p.p.m. owing to the nature of the techniques of crystal growth and the difficulties of purification. Copper was deliberately incorporated into the mixed crystals, therefore, in order to study the emission bands produced and to distinguish these from the self-activated emissions which occur in the same spectral region. There have been reports of discontinuities

in the shift of the position of the emission bands with composition in the Zn(S,Se) alloy system, see Ozawa and Hersh (1973), Lehmann (1966, 1967). The emission bands in Zn(S,Se) single crystals doped with copper have been examined in order to resolve this problem.

ZnS phosphors containing copper have been widely studied, see Van Gool and Cleiren (1960), Van Gool (1961), Curie and Prener (1967), and the details of the observed luminescence processes are quite well understood. Comparatively little work has been done on the related ZnSe phosphors, but the reported positions of the emission bands associated with copper are fairly consistent, see the review by Halsted et al (1965). Lehmann (1966) and Morehead (1963) have examined the 'copper-blue' and 'copper-green' emissions in ZnS and in the alloy system formed between ZnS and ZnSe. Morehead varied the composition of the powdered phosphors of Zn(S,Se) in large steps, and noted a linear shift of the low energy 'copper-green' band from the green spectral region through to the red on reducing the sulphur content. Halsted (1965) assumed a comparable steady shift for the high energy 'copper-blue' emission throughout the range of composition. Lehmann made a detailed study of the substitution of ZnSe in Zn(S,Se) powdered phosphors and observed an anomalous rapid shift of the luminescence emission bands of ZnS on incorporating small percentages of ZnSe. He reported that the replacement of < 1% ZnS with ZnSe caused the two emission bands in ZnS to decrease in intensity and be replaced by two new bands, approximately 0.2 eV lower in energy, which then shifted slowly to longer wavelengths with further increase in the ZnSe content. From this evidence, there is the suggestion that the centres responsible for the emission in ZnS are not analogous to those in ZnSe.

The copper-doped crystals of Zn(S,Se):I examined in this work show two characteristic bands of photoluminescence at 85 K: a short wavelength 'copper-blue' emission in crystals doped with a high concentration of copper, estimated to be  $> 100$  p.p.m.; and a longer wavelength 'copper-green' emission in the annealed crystals with a reduced copper doping, containing estimated concentrations of a few p.p.m. The variation of these emission bands with composition is shown in Figure 6.16. In this diagram the conduction band is shown as remaining fixed in energy since, in the ionic picture, a variation in the composition of the host material from ZnS to ZnSe causes a variation of the valence band position which is associated with the anion. The higher energy 'copper-blue' emission shifts continuously in energy from the blue region in ZnS at  $4400 \text{ \AA}$  (2.82 eV) through to the green region in ZnSe at  $5400 \text{ \AA}$  (2.30 eV). The lower energy 'copper-green' emission also shifts continuously from the green region in ZnS at  $5340 \text{ \AA}$  (2.32 eV) through to the red region in ZnSe at  $6420 \text{ \AA}$  (1.93 eV).

For both the 'copper-green' and 'copper-blue' emissions the shift in the peak position with composition becomes more rapid when the proportion of sulphur exceeds 60 at.%. Mixed crystal samples were grown containing small percentages ( $\sim 1\%$ ) of ZnSe in ZnS. These crystals showed the same 'copper-blue' and 'copper-green' emission bands that were observed throughout the range of composition; the peak positions were only slightly displaced to longer wavelengths compared to the bands in zinc sulphide. The discontinuous behaviour of the bands with changing composition reported by Lehmann was not observed. It may be worth emphasizing that the crystals examined in

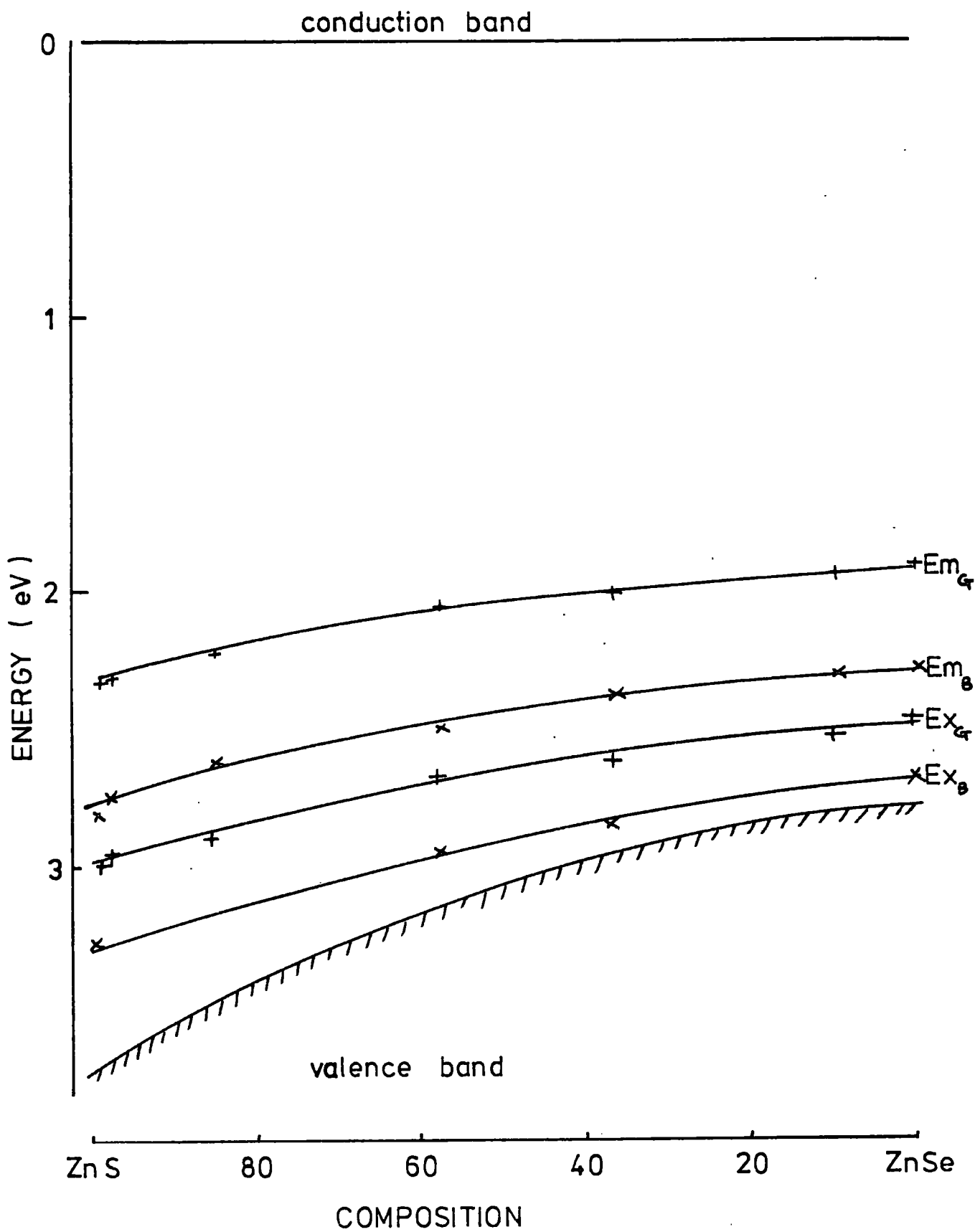


FIG 6.16 variation of excitation and emission energy with composition in Zn (S,Se) : I,Cu

this present work appeared to be cubic throughout the range of composition. This was established from X-ray powder photographs which were taken for the range of mixed crystals in order to calculate the lattice parameters. Zinc sulphide also grows in the wurtzite (hexagonal) modification and, in this crystal form, the material possesses a higher band-gap energy than in the cubic modification with values of 3.90 eV and 3.83 eV respectively. Shionoya (1966) has reported that the emission bands are shifted to shorter wavelengths in the hexagonal phase.

The room temperature luminescence in the highly-doped samples varies from 4920 Å (2.52 eV) in ZnS through to 6280 Å (1.97 eV) in ZnSe; in the lightly-doped annealed samples the luminescence varies from 5320 Å (2.33 eV) in ZnS through to 6450 Å (1.92 eV) in ZnSe. In both types of sample a single broad emission band is observed at room temperature which shifts from the red region to the green when the proportion of sulphur in the crystals is increased. By comparison, however, the emission from the highly-doped samples is slightly displaced to shorter wavelengths; this may be due to the presence of overlapping 'copper-blue' or self-activated emission. At 85 K the emission bands in the annealed samples shift to slightly higher energies, whereas the highly-doped samples show a short wavelength band in addition to the longer wavelength band observed at room temperature. It is suggested that the lightly-doped annealed crystals exhibit the low energy copper emission analogous to the copper-green emission which has been reported in ZnS. The high energy 'copper-blue' emission is observed at 85 K in the crystals containing a high concentration of copper. Also, in the sulphur-rich highly-doped crystals the room temperature emission is

shifted towards the blue; as the proportion of sulphur is reduced in these samples, the 'copper-green' emission predominates. This would agree with the results of Shionoya (1964) who observed that a 'copper-blue' band was present in ZnS:I,Cu at room temperature, and with those of Iida (1969) and Jones (1973) who noted that the 'copper-blue' emission in ZnSe:Cu appears only at temperatures below  $\sim 200$  K.

The behaviour of the copper emissions in the mixed Zn(S,Se) crystals appears to be quite different from that observed for the self-activated emission. The blue and green emissions in copper-doped ZnS are entirely analogous to the green and red emissions in ZnSe; there is a continuous shift in the energy of the emission bands with varying composition. However, in the undoped samples there are two self-activated bands in the mixed crystals and there is no continuous shift between the single self-activated band in ZnS and that in ZnSe.

An examination of the thermal quenching of the emission throughout the range of composition demonstrates that the 'copper-blue' emission is rapidly quenched at temperatures above  $\sim 200$  K; by comparison, the intensity of the 'copper-green' emission observed in the annealed samples was comparatively little dependent on temperature in the range up to  $\sim 350$  K. The activation energies which were calculated for the quenching of the emissions were small, of the order of  $\sim 0.05$  eV, which indicates the presence of a shallow trapping level. This trap may be due to the donor levels associated with the presence of iodine in the crystals.

The excitation spectra for the 'copper-blue' luminescence indicates that the emission is excited in a single narrow band very close to the band-edge; the excitation band appears at  $4600 \text{ \AA}$  (2.69 eV)

in ZnSe shifting through to 3750 Å (3.31 eV) in ZnS. In the low copper concentration annealed samples, the 'copper-green' luminescence is excited in a broad band well removed from the band-gap; the main peak is positioned 0.6 eV below the edge in ZnSe and 0.8 eV in ZnS. This broad excitation band shows structure and three separate peaks can be resolved, especially in those crystals with a low sulphur content: in ZnSe the peak positions at 85 K occur at 4510 Å (2.75 eV), 5000 Å (2.48 eV) and 5250 Å (2.38 eV); the high energy band corresponds to band-gap excitation. Jones and Woods (1974) have reported observing a broad excitation band for the 'copper-green' emission at 6400 Å in ZnSe, this was composed of at least two sub-bands with maxima at 5100 Å (2.43 eV), and 4700 Å (2.64 eV). Iida (1969) observed a main excitation peak for the emission at 5200 Å (2.38 eV) with a shoulder on the high energy side which extended to the band edge. It is suggested that the low energy copper emission in ZnSe is predominantly excited in a band at 5250 Å and in a second band at approximately 5000 Å. As the proportion of sulphur in the crystals is increased, the excitation band shifts towards higher energies and a single band is observed in ZnS at 4140 Å (2.99 eV). Narita and Sugiyama (1965) examined the excitation of the 'copper-green' emission in zinc sulphide and observed a broad band extending from the band-edge which peaked at 4200 Å (2.95 eV), but they could not resolve any structure on the high energy shoulder. The variation of the peak position of the 'copper-green' and 'copper-blue' excitation bands with composition is shown in Figure 6.16. The excitation bands show a continuous shift to higher energies with increasing sulphur content, and move parallel in energy with the position of the emission bands.

There have been many different models proposed to describe the low and high-energy copper emission bands observed in ZnS. A schematic representation of one of the possible models for the copper

emissions in the Zn(S,Se) mixed crystals is shown in Figure 6.17. This representation is based on a Schön-Klasens type transition. Broser and Schulz (1961) have attempted to assign the blue and green emissions of ZnS:Cu to the same doubly ionizable centre: the green emission is considered to be a transition to the  $\text{Cu}^+$  centre and the blue emission is a transition to the  $\text{Cu}^{2+}$  centre. Morehead (1963) concluded that the Schön-Klasens model can be applied to both the 'blue' and 'green' emissions for the whole range of Zn(S,Se):Cu phosphors. There have been alternative suggestions that the 'copper-green' emission in ZnS and ZnSe is due to a donor-acceptor pair recombination, from a donor lying close to the conduction band to a copper acceptor level. Some workers have used time-resolved spectroscopy to examine the 'copper-green' emission in ZnSe, but the results at present are inconclusive: Fujiwara and Fukai (1967) reported observing a shift in the emission peak position typical of a pair recombination, whereas Iida (1969) reported observing no shift. Recently, however, James et al (1976) have examined the 'copper-green' emission in ZnS using an optically detected magnetic resonance technique. They noted an isolated donor resonance associated with the 'copper-green' emission and concluded that this gave strong evidence for a donor-acceptor recombination model. This tends to confirm the time-resolved spectroscopy work of Bryant and Manning (1974), Era et al (1969) and Shionoya et al (1966) on the 'copper-green' emission. Monitoring the thermal quenching of the 'copper-green', 'copper-blue' and self-activated emissions in our samples has shown a low-temperature activation energy of approximately 0.05 eV; this could be caused by a shallow donor level due to crystal defects or iodine coactivator ions. This suggests that a donor-acceptor model is appropriate for the copper emission.

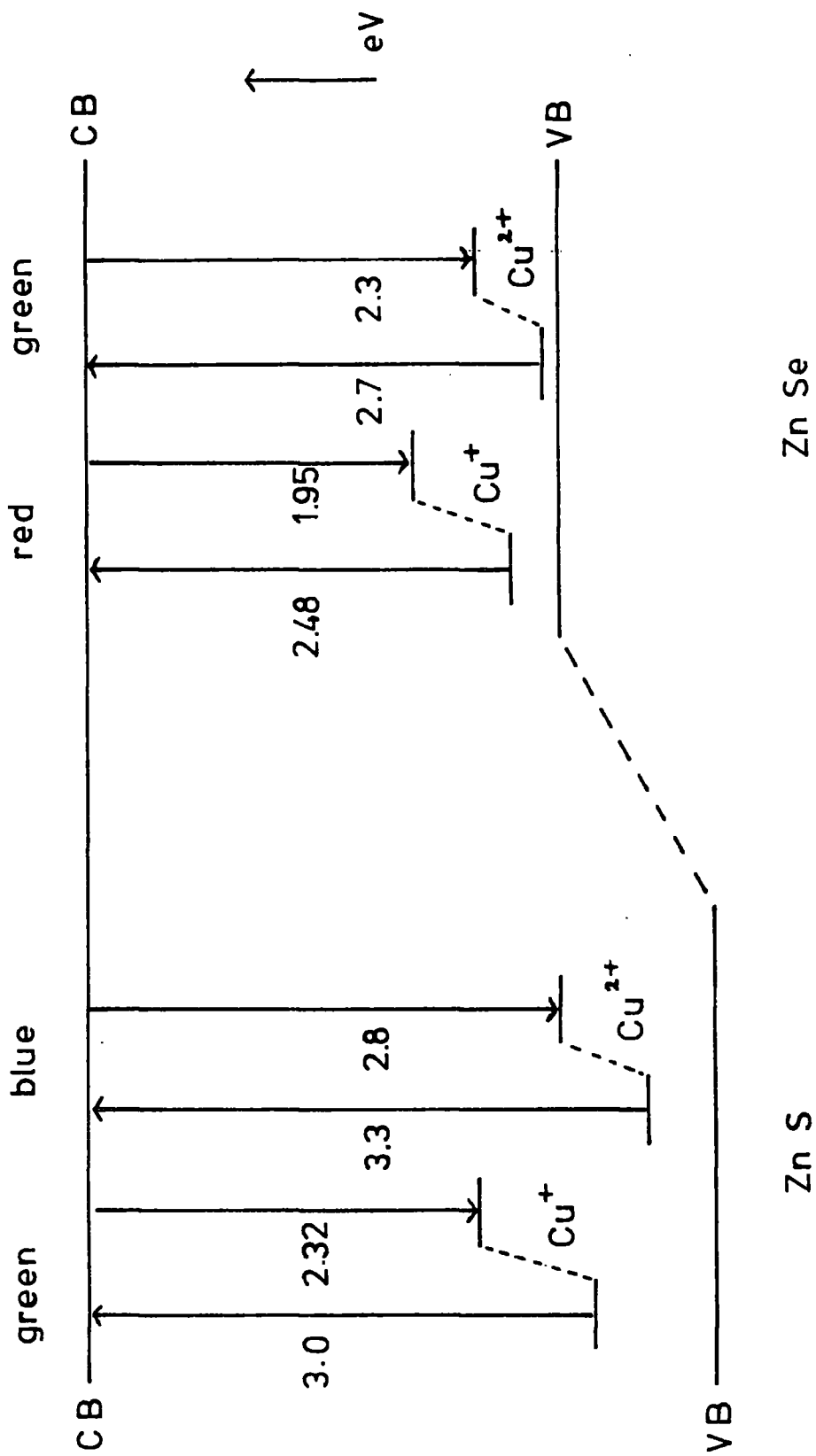


FIG 6.17 schematic representation of possible emission and excitation processes in Zn (S,Se) : Cu

An examination of the emission spectra from the sample of ZnSe:I,Cu showed a third band of luminescence which was not observed in the samples containing some sulphur. In addition to the 'copper-green' and 'copper-blue' emissions at 6300 Å (1.97 eV) and 5400 Å (2.30 eV) respectively, a band of luminescence was observed in the yellow region at 5900 Å (2.10 eV) in this highly doped sample of ZnSe. This yellow band was not observed in the sample after annealing in zinc, or in samples which did not contain copper and it is suggested that this band is due to the presence of copper. Iida (1969) has also observed a yellow band of emission at 5700 Å (2.17 eV) in zinc selenide doped with copper. Ozawa and Hersh (1973) have reported a yellow emission at 5600 Å (2.21 eV) in ZnSe:I which they attributed to the presence of excess iodine. The nature of this yellow emission is unknown but it may be due to a copper complex centre, or a copper centre in association with an impurity or defect centre.

## CHAPTER 7

### MANGANESE DOPED CRYSTALS

#### 7.1 Introduction

Divalent manganese is well known as a luminescence activator in zinc sulphide, see for example Klick and Schulman (1957), Langer and Ibuki (1965). It is generally agreed that the  $Mn^{2+}$  ion at a substitutional site in ZnS emits a bright orange luminescence with a peak at about 5850 Å (2.12 eV) and a half-width of approximately 0.23 eV (Beserman and Balkanski, 1971). By comparison little work has been carried out on ZnSe:Mn, and an examination of the manganese luminescence is complicated by the overlap of the self-activated and copper emissions. In this chapter the results of the measurement of the photoluminescence emission spectra, excitation spectra and photoconductivity of manganese-doped, mixed crystals of Zn(S,Se) are presented. Copper was incorporated in certain samples and the results were compared in order to establish the effect that the presence of copper impurity might have on the manganese luminescence. The experimental curves which have been corrected for the response of the photomultiplier and the energy distribution of the quartz-halogen excitation source have been normalised.

#### 7.2 Manganese doped Zn(S,Se)

##### 7.2.1 Photoluminescence of crystals of Zn(S,Se):I,Mn

The photoluminescence of crystals of Zn(S,Se):I,Mn grown by the iodine transport technique was examined using 3650 Å ultra-violet

excitation. The crystals all possessed a pale orange body colour and emitted intense luminescence in the orange-red region of the spectrum. The emission spectra are shown in Figures 7.1 and 7.2 at 300 K and 85 K, respectively. At room temperature the emission maxima occurred at 6550 Å (1.89 eV) with a half-width of 0.33 eV in ZnSe:I,Mn shifting to 5880 Å (2.11 eV) with a half-width of 0.20 eV in ZnS:I,Mn; at 85 K the luminescence band lay at 6250 Å (1.98 eV) with half-width 0.32 eV in ZnSe:I,Mn shifting to 5880 Å (2.11 eV) with half-width 0.16 eV in ZnS:I,Mn. The peak positions and half-widths for the whole range of manganese-doped, mixed crystals are listed in Table 7.1. There was a large shift in the peak position towards higher energy on introducing up to 40% of sulphur into the mixed crystals. With a further increase in the sulphur content the emission band initially moved slightly towards longer wavelength and subsequently moved towards shorter wavelength. The width of the emission band decreased as the sulphur content was increased, and above 60% sulphur the half-width remained constant at approximately 0.23 eV (300 K) and 0.16 eV (85 K).

It has been shown in Chapters 5 and 6 that the self-activated and low energy copper emissions in ZnSe occur in the region of 6000 Å and 6400 Å, respectively. Since these emissions are strongly excited by 3650 Å ultra-violet radiation, the luminescence of the manganese-doped samples was re-examined when excitation was made using a 5300 Å radiation in the green. This wavelength was chosen since it corresponds closely to the optical absorption band at 5350 Å in crystals of ZnS:Mn reported by Ibuki and Langer (1964), Ryskin (1964), McClure (1963) and Gumlich (1963). The resultant spectral emission distribution is shown in Figures 7.3 and 7.4 at 300 K and 85 K, respectively, and the peak positions and half-widths are listed in Table 7.2. At room temperature the emission maximum

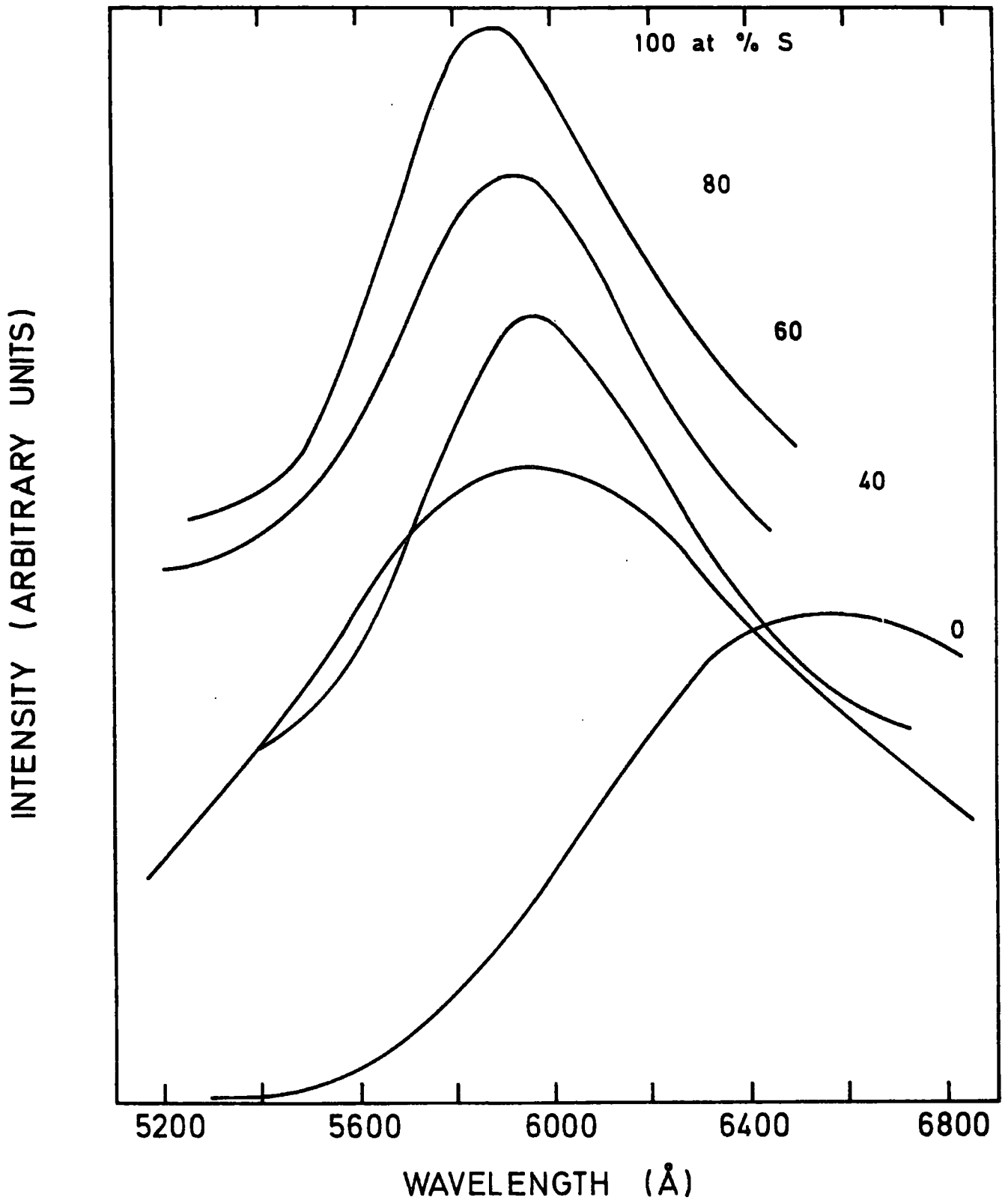


FIG. 7-1 Photoluminescence spectra of  $\text{Zn}(\text{S}, \text{Se}) : \text{I}, \text{Mn}$  excited by  $3650 \text{ \AA}$  source at  $300^\circ\text{K}$ .

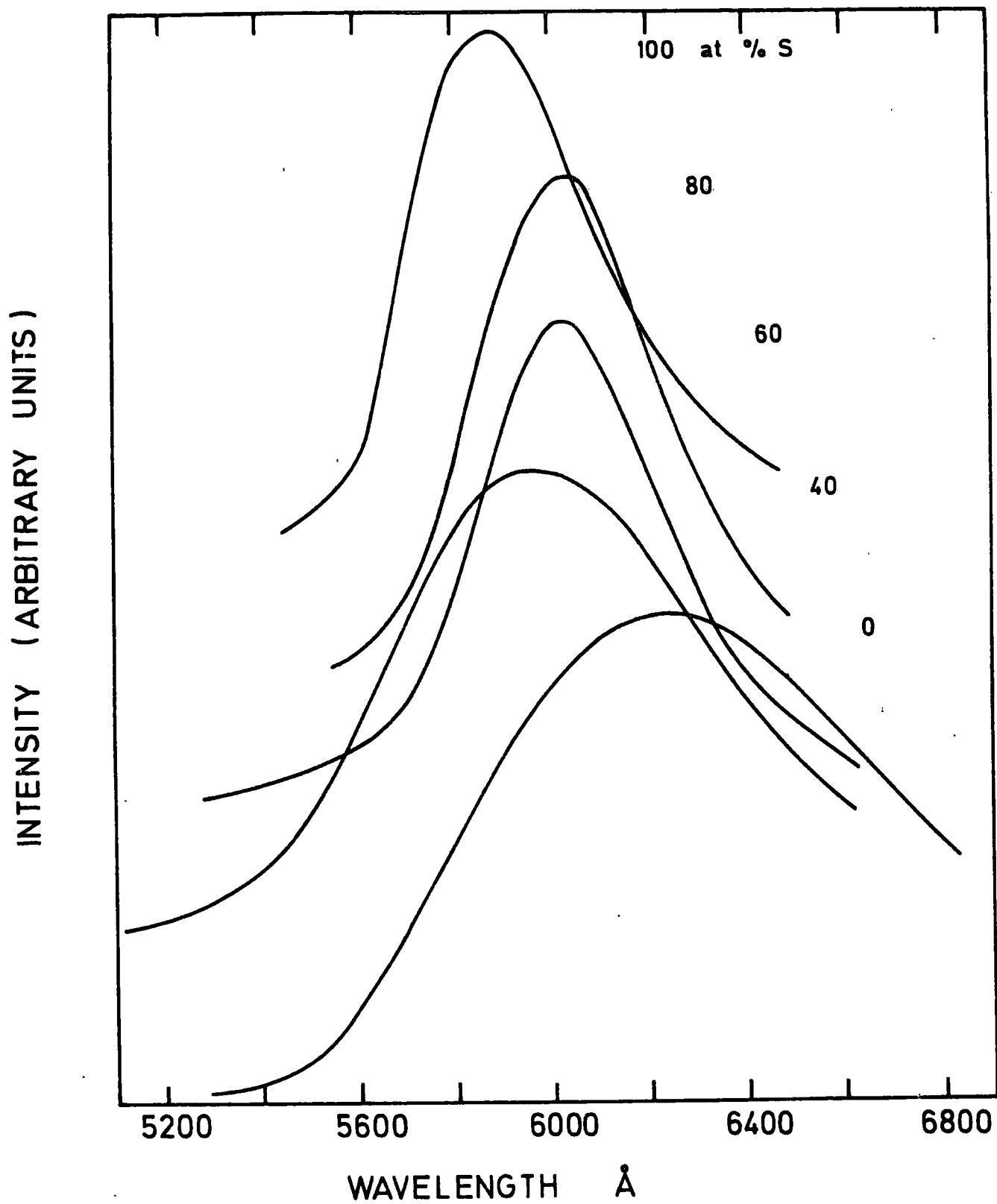


FIG. 7.2 Photoluminescence spectra of  $\text{Zn}(\text{S},\text{Se}) : \text{I}, \text{Mn}$  excited by  $3650 \text{ \AA}$  source at  $85^\circ\text{K}$ .

TABLE 7.1

EMISSION BANDS OBSERVED UNDER 3650 Å EXCITATION

Sample	300 K		85 K	
	Peak Position Å	Half-width eV	Peak Position Å	Half-width eV
969 ZnSe:I,Mn	6550	0.33	6250	0.32
975 ZnS <sub>0.4</sub> Se <sub>0.6</sub> :I,Mn	5960	0.39	5980	0.28
971 ZnS <sub>0.6</sub> Se <sub>0.4</sub> :I,Mn	5980	0.23	6010	0.16
978 ZnS <sub>0.8</sub> Se <sub>0.2</sub> :I,Mn	5930	0.23	6030	0.15
973 ZnS:I,Mn	5880	0.20	5880	0.16

TABLE 7.2

EMISSION BANDS OBSERVED UNDER 5300 Å EXCITATION

Sample	300 K		85 K	
	Peak Position Å	Half-width eV	Peak Position Å	Half-width eV
969 ZnSe:I,Mn	5880	0.20	5850	0.12
975 ZnS <sub>0.4</sub> Se <sub>0.6</sub> :I,Mn	5900	0.20	5870	0.15
971 ZnS <sub>0.6</sub> Se <sub>0.4</sub> :I,Mn	5970	0.23	6000	0.15
978 ZnS <sub>0.8</sub> Se <sub>0.2</sub> :I,Mn	5950	0.21	5960	0.15
973 ZnS:I,Mn	5880	0.19	5860	0.14

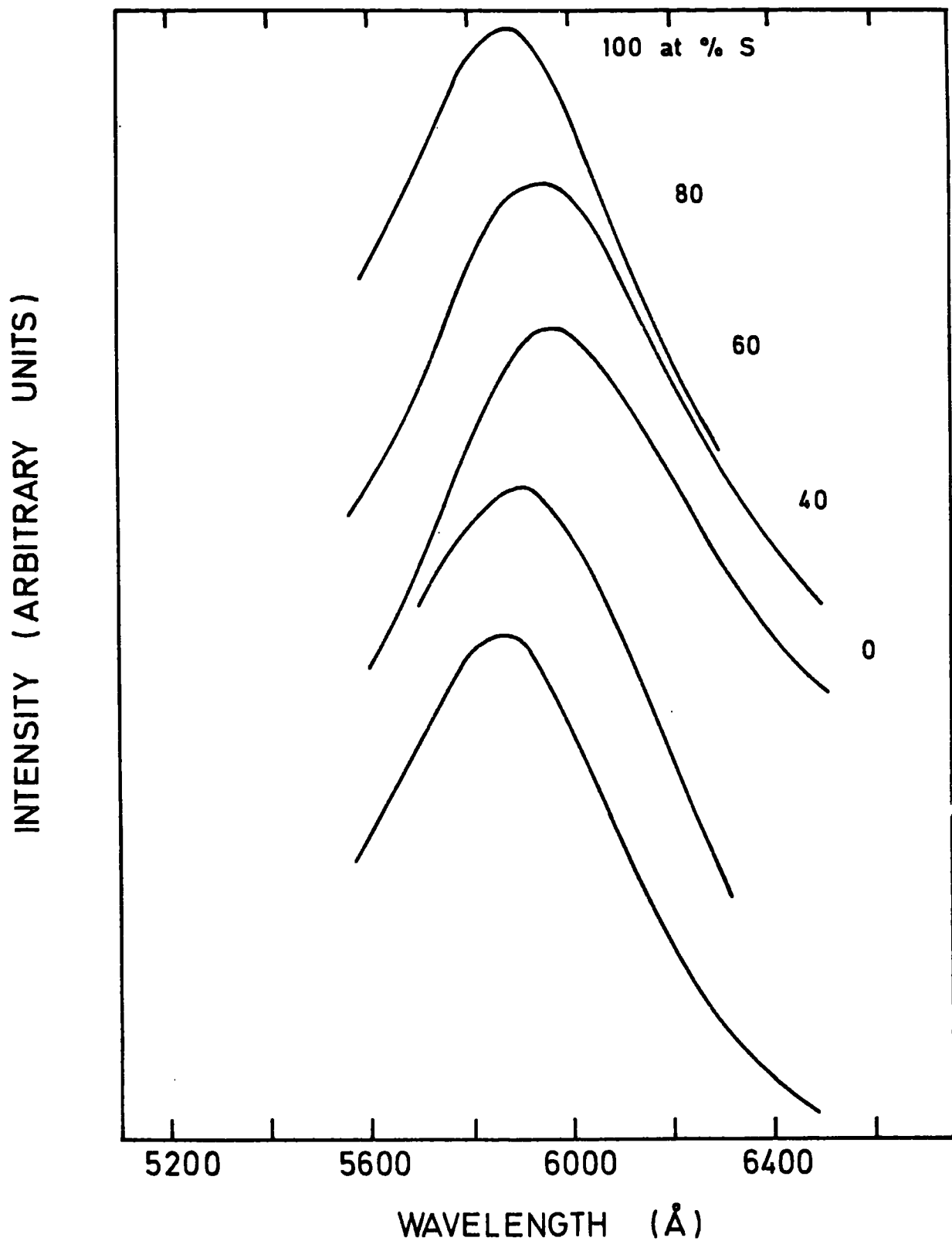


FIG. 7-3 Photoluminescence spectra of Zn(S,Se) :I,Mn excited by 5300 Å source at 300°K.

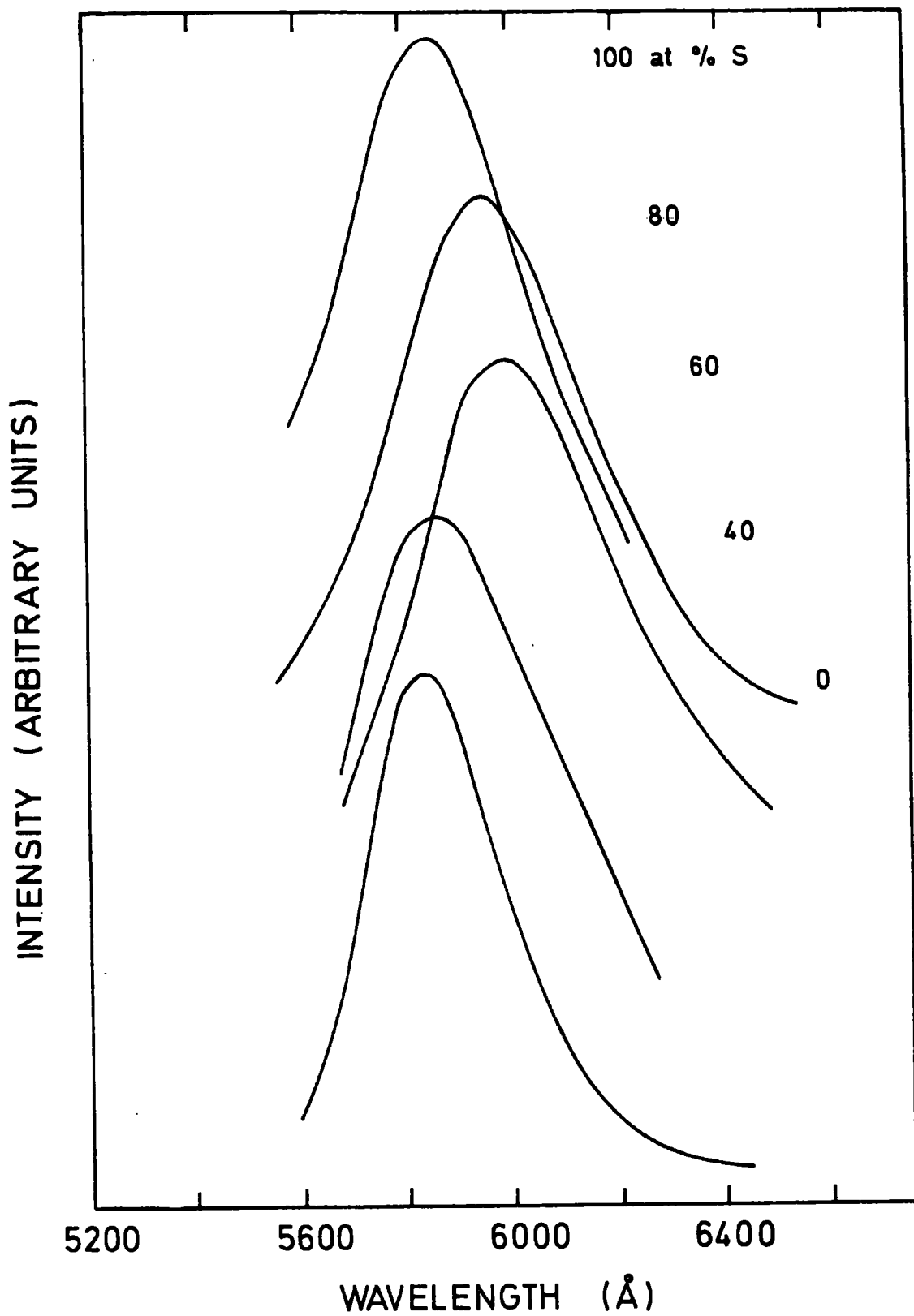


FIG. 7-4 Photoluminescence spectra of Zn(S,Se) :I,Mn excited by 5300 Å source at 85°K.

occurred at 5880 Å (2.108 eV) in ZnSe:I,Mn. This band shifted towards longer wavelength as the proportion of sulphur in the mixed crystals was increased, and then finally shifted to shorter wavelength as the sulphur content was further increased. With ZnS:I,Mn the maximum lay at 5880 Å (2.108 eV). At 85 K a similar behaviour was observed with the emission band centred at 5850 Å (2.119 eV) in ZnSe:I,Mn and at 5860 Å (2.115 eV) in ZnS:I, Mn. The half-widths for the complete range of mixed crystals were approximately the same, reducing from 0.20 eV at room temperature to 0.15 eV at 85 K. These results compare well with the value of  $\sim 0.20$  eV reported for the half-width of the manganese emission in ZnS, and are much smaller than the values observed for the self-activated and copper emissions in the mixed crystals. Illuminating the samples with 5300 Å radiation evidently excites the manganese emission selectively.

The variation of the energy of the emission peak with composition is shown in Figure 7.5 for excitation by both 3650 Å and 5300 Å radiation. The behaviour of the emission bands excited by light from both sources was consistent for crystals containing more than 40% sulphur: the emission peak reached a minimum energy at  $\sim 2.07$  eV (5990 Å) for a composition of  $\text{ZnS}_{0.75}\text{Se}_{0.25}$ ; it shifted slightly to lower energy on cooling to 85 K, although with ZnS there was no change. For crystals with less than 40% sulphur the emissions excited by 3650 Å and 5300 Å radiation showed considerable differences: the position of the U.V. excited band shifted markedly to longer wavelength with reducing sulphur content, whilst the 5300 Å excited emission band was relatively unaffected and corresponded to the position of the band observed in ZnS. In this range of composition the emission peak shifted to slightly higher energy on cooling the sample to 85 K.

Asano, Yamashita and Oishi (1968) have examined Zn(S,Se) powders

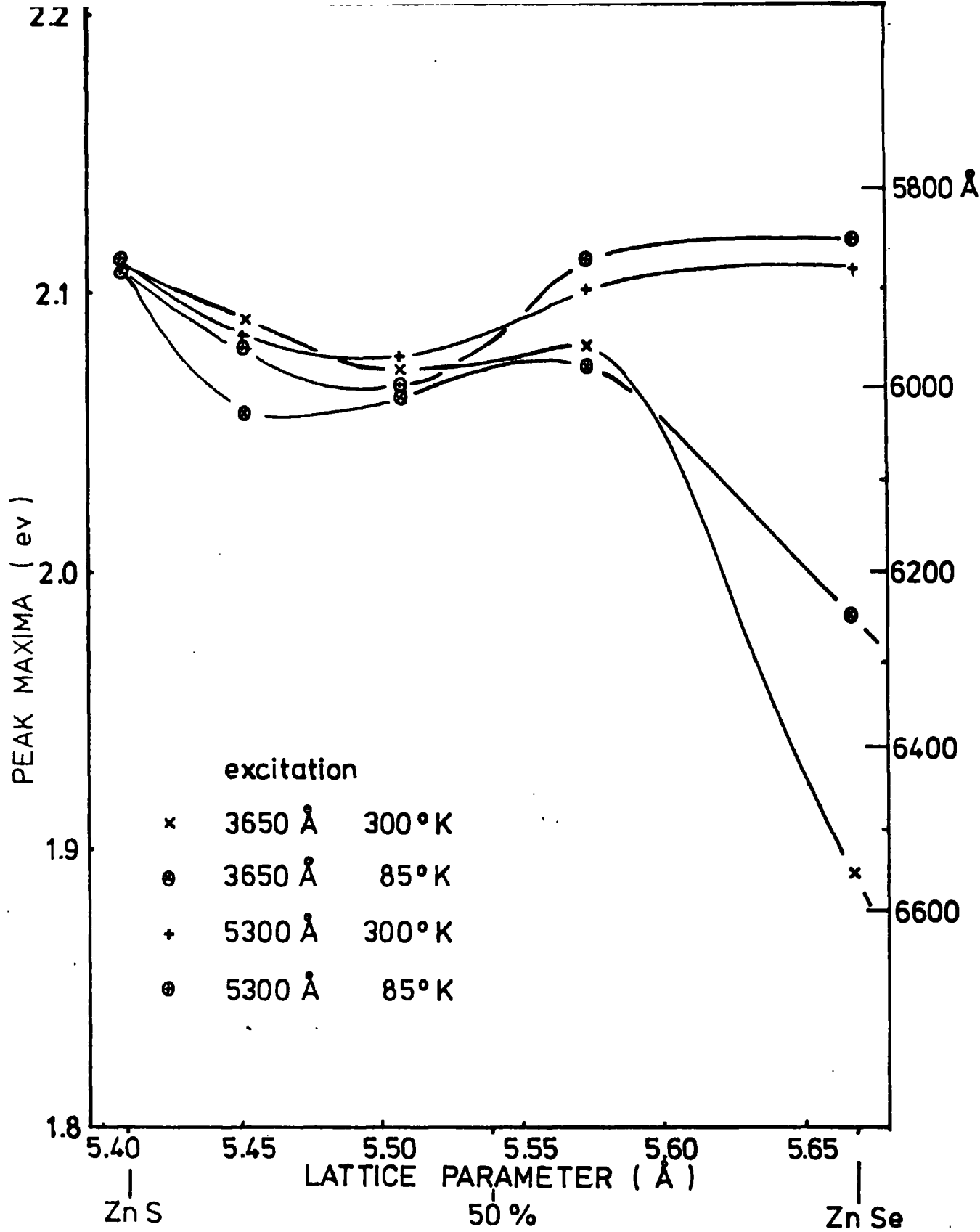


FIG 7.5 VARIATION OF PEAK MAXIMA WITH COMPOSITION  
FOR Zn(S,Se):I,Mn

doped with  $\text{MnCl}_2$ , and reported that the emission band excited by  $3650 \text{ \AA}$  radiation shifted non-linearly in position from  $6500 \text{ \AA}$  in ZnSe to  $5880 \text{ \AA}$  in ZnS; the shift of the peak position with composition and temperature was similar to that shown in Figure 7.2 under  $3650 \text{ \AA}$  excitation. However, these authors noted that the emission bands shifted towards longer wavelengths when the crystals with low sulphur content were excited with  $5300 \text{ \AA}$  radiation, and they concluded that the manganese emission in ZnSe:Mn lies at  $6400 \text{ \AA}$ . Apperson et al (1967) have also observed a band in ZnSe:Mn with a maximum at  $6350 \text{ \AA}$  and  $700 \text{ \AA}$  wide at 90 K. The results for ZnSe:Mn reported here agree well with the band reported by Jones and Woods (1973) at  $5860 \text{ \AA}$  with half-width  $300 \text{ \AA}$  at 85 K. The crystals examined in the present work had a high manganese content, up to 1% by weight. It is suggested that this high concentration, together with the use of selective excitation, make it possible to isolate the  $\text{Mn}^{2+}$  emission from the overlapping self-activated and copper emissions in the samples with low sulphur composition. As has been shown in Chapters 5 and 6, the self-activated and low energy 'copper-green' emissions shift monotonically in wavelength from well below  $5900 \text{ \AA}$  in ZnS to just above this wavelength in ZnSe. In  $\text{ZnS}_{0.5}\text{Se}_{0.5}$  the self-activated and copper emission peaks occur at  $5900 \text{ \AA}$  approximately. The shift of the emission bands on cooling, and possibly also the minimum in the variation of the energy of the emission peak with composition may be explained by the overlapping of the manganese emission with a contribution from the self-activated and copper emissions which have their own temperature dependence.

### 7.2.2 Excitation spectra for Zn(S,Se):I,Mn

The excitation spectra for the range of mixed crystals doped with manganese were measured while monitoring the orange emission band at

approximately 5900 Å. A variable interference filter was used to isolate the luminescence and this was optimised on the wavelength of interest from a sample of a particular composition. The excitation spectra obtained at room temperature and 85 K are shown in Figures 7.6 and 7.7, respectively; the curves have been corrected for the spectral distribution of the excitation source. The excitation spectra observed at room temperature were almost identical to those measured at 85 K, except that each excitation band was slightly wider at room temperature. In ZnS:Mn, six separate bands of excitation could be resolved at 5350 Å (2.317 eV), 5000 Å (2.479 eV), 4650 Å (2.666 eV), 4320 Å (2.869 eV), 3920 Å (3.162 eV) and 3550 Å (3.492 eV); in ZnSe:Mn four separate bands could be distinguished at 5340 Å (2.321 eV), 5030 Å (2.464 eV), 4650 Å (2.666 eV) and 4450 Å (2.786 eV). The band at 3550 Å in ZnS shifted to 3670 Å (3.378 eV), and the band at 4450 Å in ZnSe was not resolved when the samples were examined at 300 K; the positions of the other bands remained fixed on changing the temperature. It is suggested that the high energy band is associated with band to band excitation. The absorption edge in Zn(S,Se) mixed crystals shifts progressively to higher energies as the proportion of sulphur is increased. As this occurs, more of the higher energy manganese excitation bands, which are observed in ZnS:Mn, become apparent.

The excitation bands in ZnS:Mn at 5350 Å, 5000 Å and 4650 Å have been assigned by McClure (1963) and Langer and Ibuki (1963) to transitions from the ground  ${}^6A_1({}^6S)$  level to various excited crystal field states: these transitions are denoted  ${}^6A_1({}^6S) - {}^4T_1({}^4G)$ ,  ${}^6A_1({}^6S) - {}^4T_2({}^4G)$ ,  ${}^6A_1({}^6S) - ({}^4A_1, {}^4E)({}^4G)$  respectively. There is some disagreement over the shorter wavelength excitation bands at 4320 Å and 3920 Å which McClure, and Langer and Ibuki assign to  ${}^6A_1({}^6S) - {}^4T_1({}^4P)$  and  ${}^6A_1({}^6S) - {}^4E({}^4D)$  and  ${}^4T_2({}^4D)$ , whereas Ford et al (1963) assign the transitions to

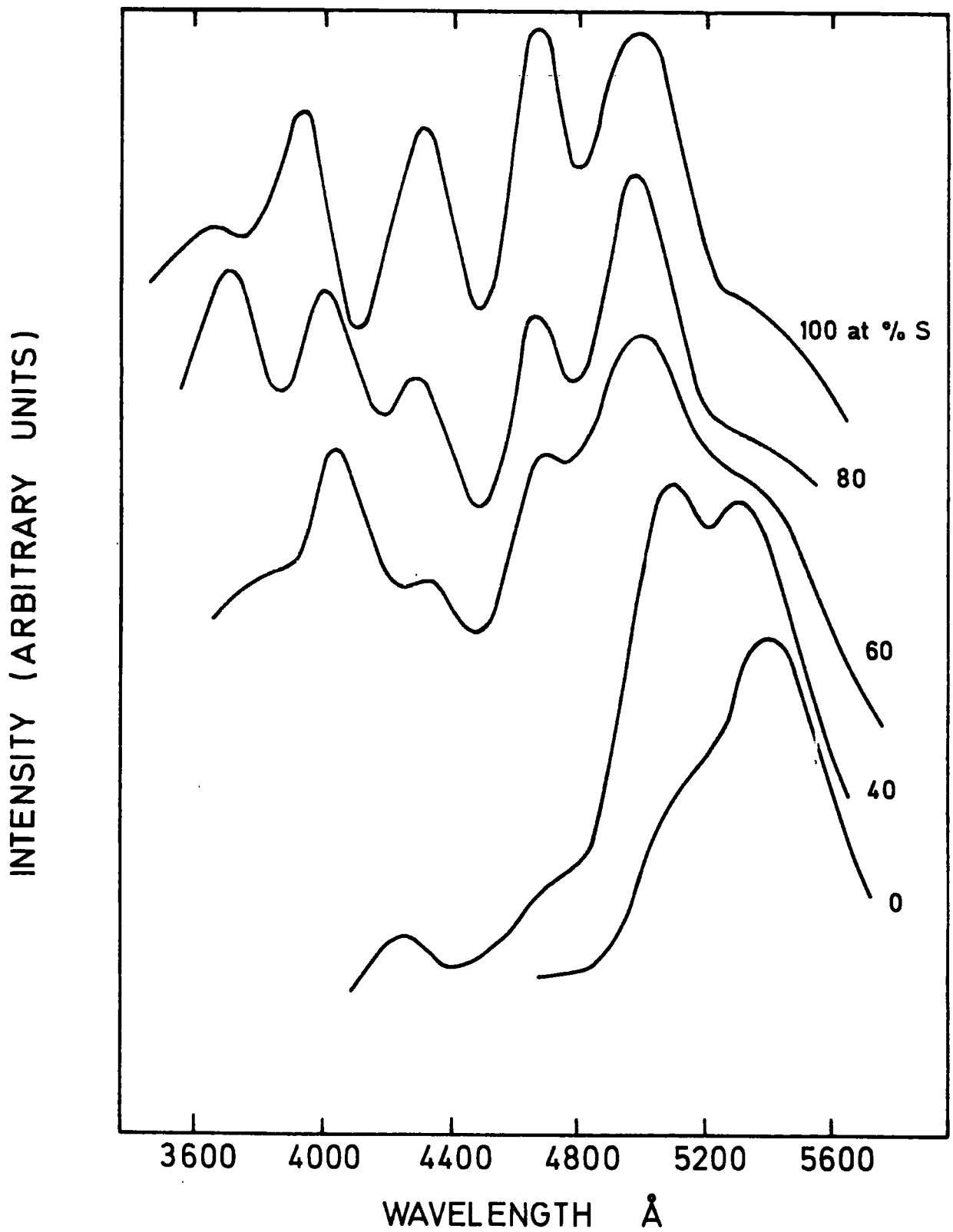


FIG. 7-6 Excitation spectra of Zn(S,Se) :I, Mn at 300°K.

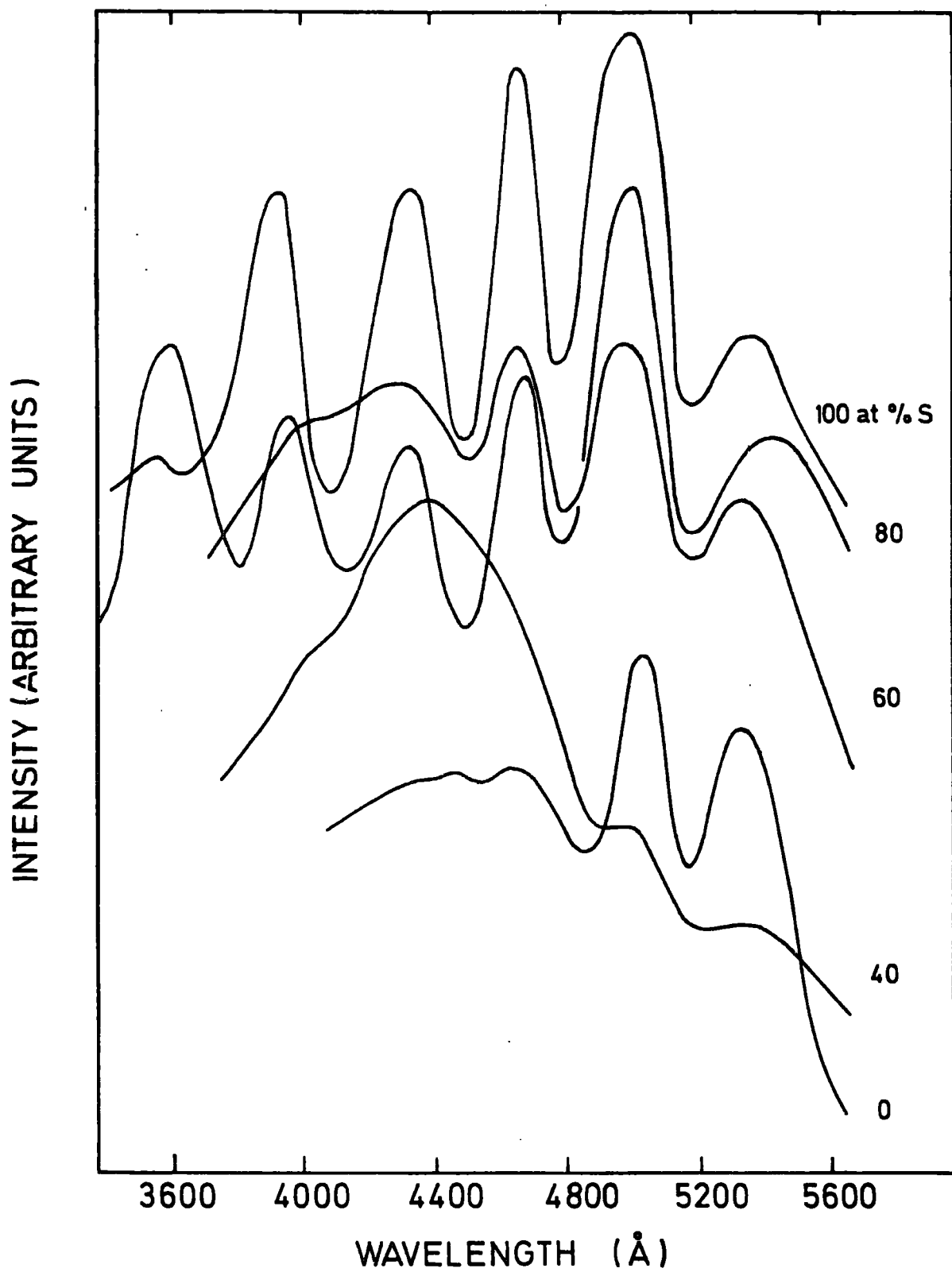


FIG.7-7 Excitation spectra of Zn(S, Se) : I, Mn at 85 °K

${}^6A_1({}^6S) - {}^4T_2({}^4D)$  and  ${}^6A_2({}^6S) - {}^4E({}^4D)$  respectively. By making a comparison with the excitation band structure observed in ZnS:Mn, the bands observed at 5340 Å, 5030 Å and 4650 Å in ZnSe:Mn can be ascribed to the transitions  ${}^6A_1({}^6S) - {}^4T_1({}^4G)$ ,  ${}^6A_1({}^6S) - {}^4T_2({}^4G)$  and  ${}^6A_1({}^6S) - ({}^4A_1, {}^4E)({}^4G)$  respectively. This is in agreement with the optical absorption work of Langer and Richter (1966) on melt-grown crystals of ZnSe:Mn.

The similarity of the excitation spectra throughout the range of Zn(S,Se):I,Mn mixed crystals implies that the  $Mn^{2+}$  ion occupies a tetrahedrally coordinated substitutional site for all compositions, and that the crystal field splitting energies of ZnS and ZnSe are approximately equal. Allen (1963) has reported the values of the crystal field parameter,  $D_q$ , for  $V^{3+}$  in ZnS and ZnSe as being  $550\text{ cm}^{-1}$  and  $515\text{ cm}^{-1}$ , respectively, which would tend to agree with this suggestion. Since the 5350 Å excitation band is observed in all the samples, this confirms that the emission stimulated by radiation of this wavelength is due to the incorporation of manganese.

### 7.2.3 Photoconductivity of Zn(S,Se):I,Mn

Measurements were also made of the spectral response of the photoconductivity for the range of manganese doped mixed crystals. Samples were cut into rectangular bars 5 mm x 2 mm x 2 mm, and prepared by etching in a solution of bromine/methanol followed by washing in carbon disulphide and cleaving of the end faces. Contacts were made to the samples by alloying pellets of indium into the cleaved surfaces in an atmosphere of argon. The curves showing the photoconductive responses in Figures 7.8 and 7.9, at room temperature and 85 K respectively, have been corrected for the spectral distribution of the excitation source and have been normalised. It was not possible to measure the photoresponse at 85 K in

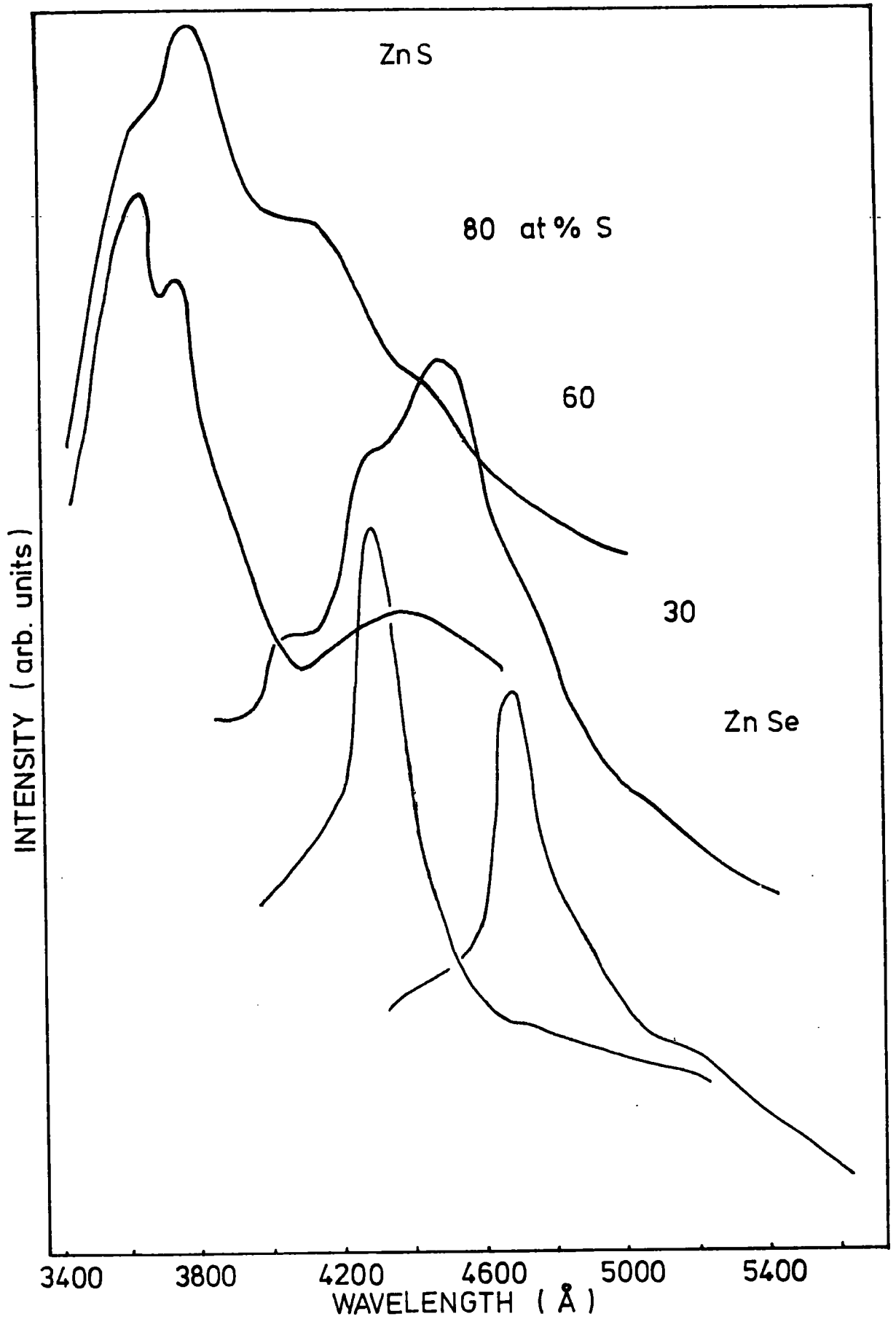


FIG 7.8 PHOTOCONDUCTIVITY OF Zn(S,Se):I,Mn AT 300 ° K

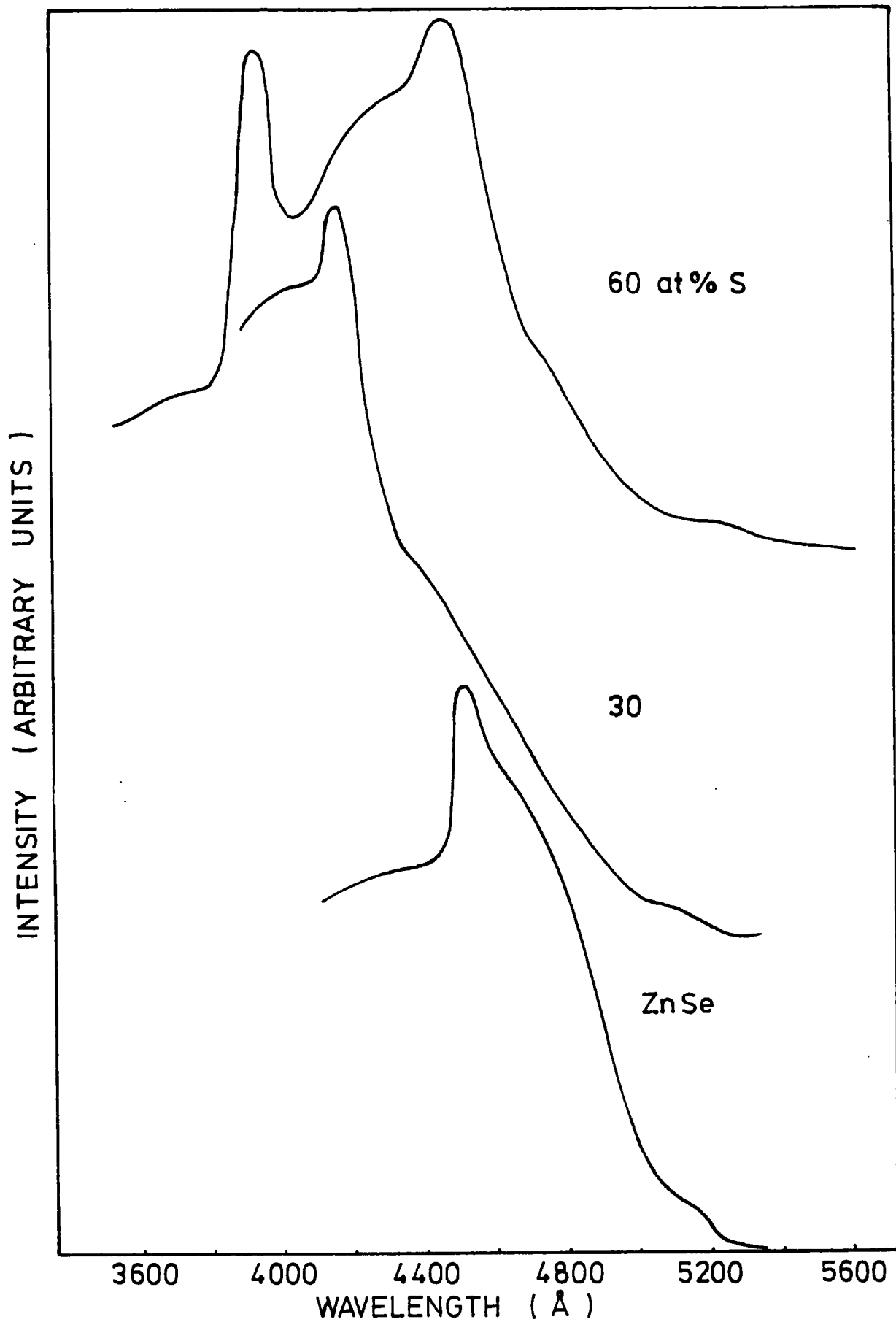


FIG 7.9 PHOTOCONDUCTIVITY OF Zn(S,Se):I,Mn  
AT 85 K

the two samples with sulphur content in excess of 60%. This was due to a combination of two effects: the high resistivity of such samples and the fact that it was not possible to produce ohmic contacts on the samples with high sulphur compositions. It is evident that there is considerable structure in the photoconductive spectral response of the manganese-doped samples: 951  $\text{ZnS}_{0.6}\text{Se}_{0.4}:\text{I,Mn}$ , and an undoped sample with the same sulphur-selenium composition, 954  $\text{ZnS}_{0.6}\text{Se}_{0.4}:\text{I}$ , are shown superimposed in Figure 7.10. The undoped sample has a sharp high-energy band peaking at  $3890 \text{ \AA}$  (3.186 eV), with a broad low energy shoulder. In comparison the sample containing manganese shows a similar sharp high-energy peak at  $3880 \text{ \AA}$  (3.195 eV) with bands on the low energy side at  $4220 \text{ \AA}$  (2.935 eV),  $4450 \text{ \AA}$  (2.785 eV),  $4740 \text{ \AA}$  (2.615 eV) and  $4910 \text{ \AA}$  (2.525 eV). The positions of the maxima and minima in the photoconductivity measured at 85 K are listed in Table 7.3 and are compared with the excitation bands observed in the same sample. The high energy peak observed at  $\sim 3890 \text{ \AA}$  in the excitation spectra also appears as a maximum in the photoconductivity for both the undoped and manganese-doped samples of the same composition. This peak can be attributed to a band-to-band transition producing free electron-hole pairs. A comparison between the excitation and photoconductivity spectra for the lower energy bands observed in the  $\text{Mn}^{2+}$  doped crystal shows a close agreement between the excitation band maxima and the photoconductivity minima. The short wavelength dip in the photocurrent at  $4050 \text{ \AA}$  (3.06 eV) is thought to correspond to the excitation band which is observed at  $3920 \text{ \AA}$  (3.16 eV) in  $\text{ZnS:Mn}$ . The apparent position of the photoconductivity minimum may be slightly displaced because of the proximity of the absorption edge at  $\sim 3880 \text{ \AA}$  in the mixed crystal. It is suggested that the photoconductivity response of manganese-doped samples is a result of the localised transitions within the  $\text{Mn}^{2+}$

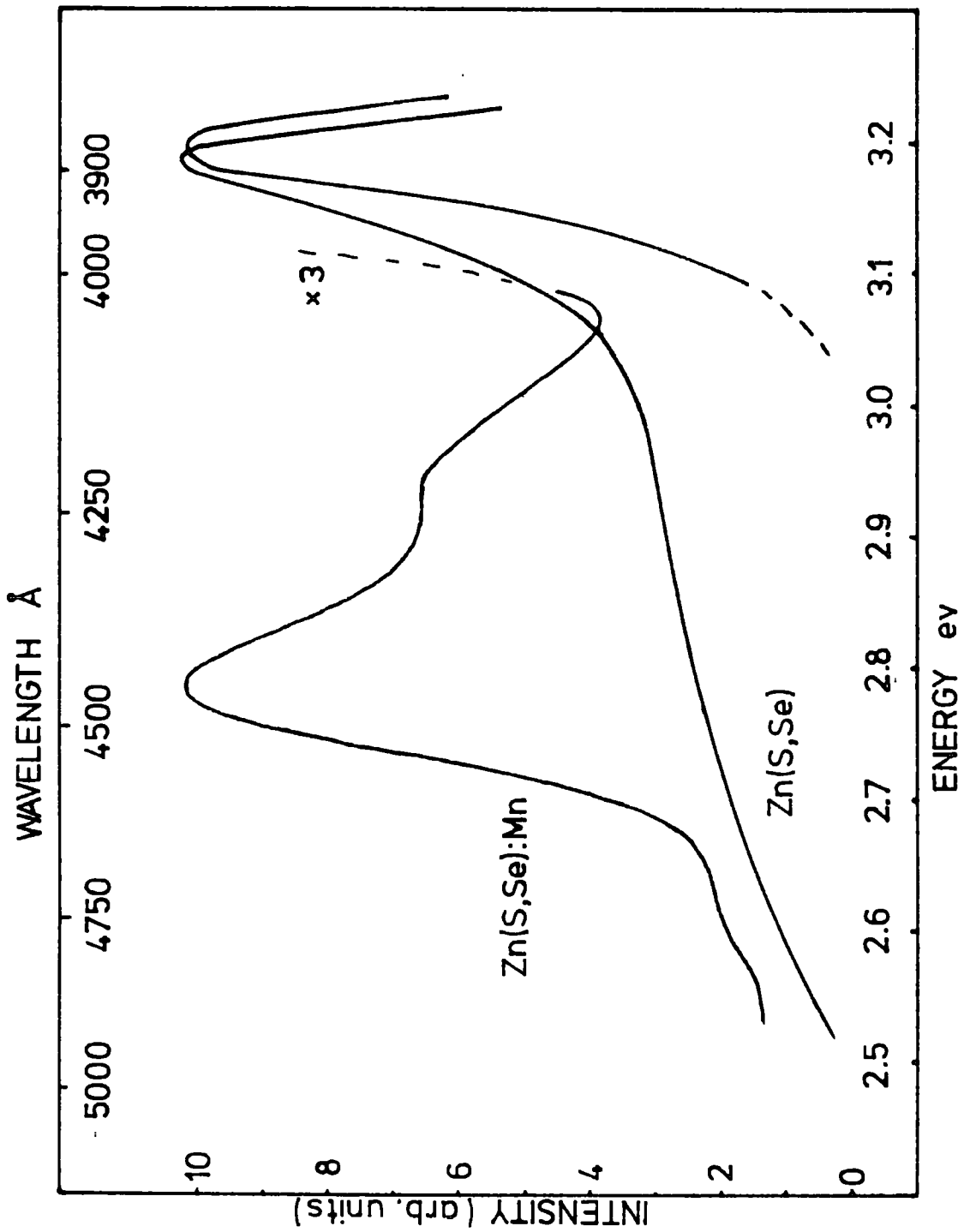


FIG 7.10 PHOTOCONDUCTIVITY OF  $ZnS_{0.6}Se_{0.4}:I, Mn$  AND  $ZnS_{0.6}Se_{0.4}:I$  AT  $85^{\circ} K$

TABLE 7.3

COMPARISON OF EXCITATION AND PHOTOCONDUCTIVITY

BANDS OBSERVED IN Zn(S,Se)

Sample:                   No. 951   ZnS<sub>0.6</sub>Se<sub>0.4</sub>:I,Mn

Temperature:           85 K

Excitation Band Peaks		Photoconductivity Maxima		Photoconductivity Minima	
Å	eV	Å	eV	Å	eV
5330	2.325	4910	2.525	5350	2.317
4960	2.500	4740	2.615	4980	2.490
4650	2.665	4450	2.785	4680	2.650
4300	2.885	4220	2.935	4280	2.900
3920	3.162	-	-	4050	3.060
3890	3.190	3880	3.195		

Sample:                   No. 954   ZnS<sub>0.6</sub>Se<sub>0.4</sub>:I

Temperature:           85 K

Excitation Band Peaks		Photoconductivity Maxima	
Å	eV	Å	eV
4220	2.935	-	-
3890	3.190	3890	3.190

ion selectively absorbing particular bands of radiation; the energy absorbed by the ion is then not available for the generation of photo-carriers and is subsequently released in a radiative transition to the ground state. There seems to be no support for the possibility that a localised electron in an excited state of the  $Mn^{2+}$  ion can become auto-ionized to the conduction band and thereby contribute to the photocurrent. This would produce coincident maxima in the excitation and photoconductivity spectra.

The photoconductivity spectra, shown in Figures 7.8 and 7.9, each contain a major short wavelength peak associated with the generation of free carriers by band-to-band transitions, with structure on the low energy side associated with absorption within the  $Mn^{2+}$  ion. The energies of the short wavelength peaks and of the minima possibly associated with  $Mn^{2+}$  ion absorption are listed in Table 7.4. The data show that the high energy peak shifts to shorter wavelength when the samples are cooled to 85 K, whilst the positions of the low energy minima are unaffected. As the proportion of sulphur in the crystals is increased, the absorption edge shifts to higher energy and more structure can be resolved at shorter wavelengths. This result parallels that observed in the excitation spectra, where the higher energy transitions become apparent as the sulphur content in the mixed crystals is increased. Crystals with different compositions showed a good correspondence between the positions of the observed minima in the photoconductivity. In the whole range of  $Zn(S,Se):I,Mn$  crystals, the measured photoconductivity is modified by the absorption and emission of radiation within the  $Mn^{2+}$  ion. Since the electronic transitions are confined to the  $Mn^{2+}$  ion and do not involve ionization to the conduction band, it was not possible to determine the positions of the energy levels of the ion with respect to the band edge.

TABLE 7.4

PHOTOCONDUCTIVITY BANDS OF Zn(S,Se):I,Mn CRYSTALS

Sample	ZnSe		ZnS <sub>0.4</sub> Se <sub>0.6</sub>		ZnS <sub>0.6</sub> Se <sub>0.4</sub>		ZnS <sub>0.8</sub> Se <sub>0.2</sub>		ZnS	
Temperature	300 K	85 K	300 K	85 K	300 K	85 K	300 K	85 K	300 K	85 K
High Energy Peak (Å)	4720	4520	4310	4150	4070	3940	3650			
Low Energy Minima (Å)					4050		4100		3990	
			4350		4320	4350			4350	
		4600	4700		4670	4670			4700	
		5050	5050	4900	5050	5100	5050			
						5350				

### 7.3 Copper doped Zn(S,Se):Mn

Copper was introduced into the manganese-doped mixed crystals in order to study its effect on the luminescence. To diffuse copper into the crystals samples grown by the iodine-transport technique were annealed for a period of 5 days at 850°C in a solution of zinc containing 10% by weight of copper. After this annealing, the body colour of the crystal of ZnSe:Mn changed from orange to bright red, but the colours of the crystals of  $\text{ZnS}_{0.6}\text{Se}_{0.4}$ :Mn and ZnS:Mn similarly treated, remained orange and pale orange respectively. The crystals which were treated in zinc/copper were cut from the same boules used in the experiments described in the previous sections so that the results obtained could be compared directly. A few crystals were grown by the vapour phase method with copper added to the charge; measurements made on these samples are also included.

#### 7.3.1 Photoluminescence of Zn(S,Se):I,Mn,Cu,Zn

The photoluminescence of crystals of Zn(S,Se):I,Mn annealed in zinc/copper is shown in Figure 7.11. The excitation was provided by a 3650 Å ultra-violet radiation source. At 85 K, the emission band maxima were observed at 5860 Å (2.115 eV), 6000 Å (2.066 eV) and 6400 Å (1.937 eV) in ZnS,  $\text{ZnS}_{0.6}\text{Se}_{0.4}$  and ZnSe respectively; in the samples containing some sulphur a shoulder was observed on the short wavelength side of the main emission band. On raising the temperature to 300 K, the emission bands broadened and shifted to 5850 Å (2.119 eV), 5910 Å (2.098 eV) and 6500 Å (1.907 eV), respectively. The wavelengths of the emission bands and their shifts with temperature are in close agreement with the results obtained with the unannealed samples. The short wavelength shoulders are attributed to the presence of copper; it was shown

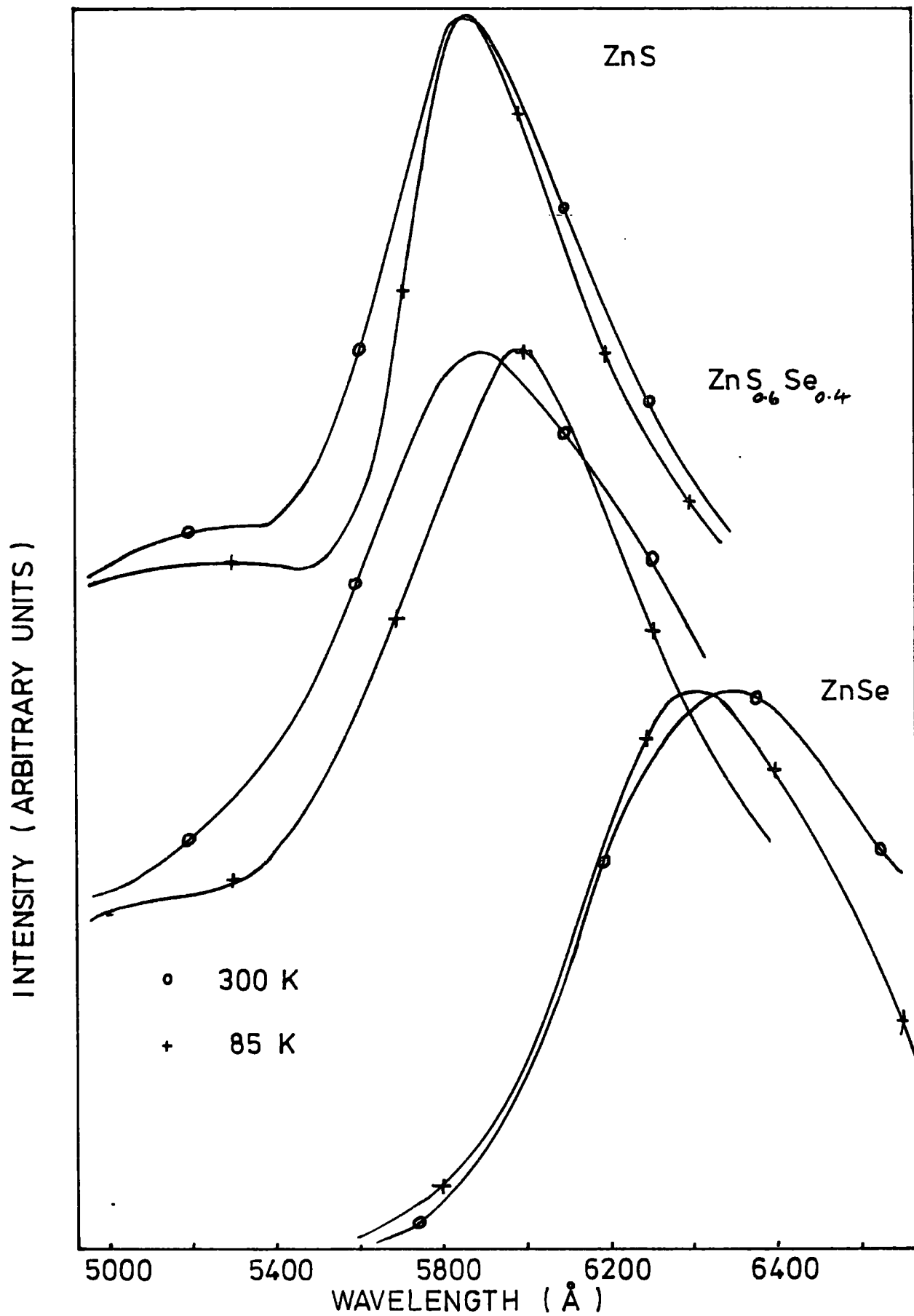


FIG 7.11 PHOTOLUMINESCENCE OF Zn(S,Se):I,Mn,Cu EXCITED BY 3650 Å SOURCE.

in Chapter 6 that copper gives emission bands at 5320 Å (2.33 eV), 5950 Å (2.09 eV) and 6400 Å (1.94 eV) in ZnS, ZnS<sub>0.6</sub>Se<sub>0.4</sub> and ZnSe.

The luminescence under excitation by 5300 Å radiation is shown in Figure 7.12. It was not possible to measure the emission from the crystal of ZnS<sub>0.6</sub>Se<sub>0.4</sub> at 300 K because of the low level of the luminescence. With the crystals of ZnS and ZnS<sub>0.6</sub>Se<sub>0.4</sub> the emission peaks occurred at 5870 Å (2.112 eV) and 6050 Å (2.049 eV) respectively and the short wavelength shoulders were no longer apparent. These results agree with the measurements made on the crystals which were not doped with copper, and indicate that manganese is still present in the samples and dominates the emission. In the crystal of ZnSe:I,Mn(Cu+Zn) the emission was located at 6500 Å (1.907 eV) at 300 K shifting to 6450 Å (1.922 eV) on cooling to 85 K. This band is not comparable with that observed at 5850 Å (2.119 eV) in the sample of ZnSe:I,Mn under 5300 Å excitation, but is similar in position to the low energy copper emission which occurs at 6400 Å (1.937 eV). Atomic absorption spectroscopy has shown that treating samples of ZnSe:Mn in zinc has no effect on the manganese content.

The results suggest that annealing the manganese-doped mixed crystals in zinc/copper has the effect of incorporating copper in the samples, causing the additional appearance of the low energy copper emission in crystals containing some sulphur. With ZnSe:I,Mn, however, the manganese emission was no longer apparent after treatment in zinc/copper and the low energy copper-emission dominated the emission even when 5300 Å radiation lying entirely within a characteristic manganese band was used as excitation. An explanation for this behaviour will be offered later, but it is worth noting that the copper emission lies at a higher energy than that of the manganese emission in both crystals containing some sulphur.

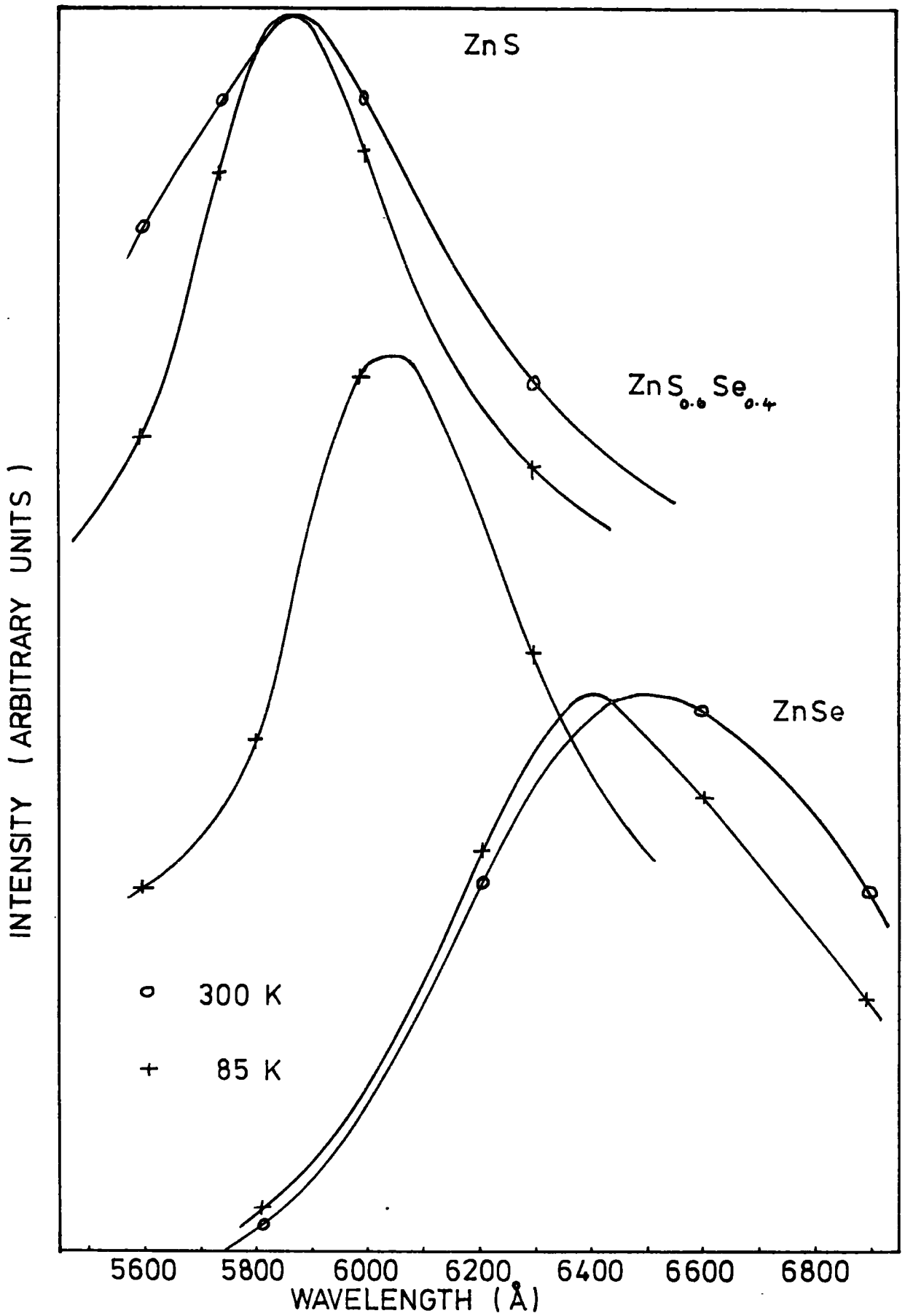


FIG 7.12 PHOTOLUMINESCENCE OF  $Zn(S,Se):I,Mn,Cu,Zn$  EXCITED BY  $5300 \text{ \AA}$  SOURCE.

### 7.3.2 Excitation Spectra

The excitation spectra of the manganese doped mixed crystals that had been annealed in zinc/copper were next examined, and the results compared with those for the untreated crystals. The excitation spectra at room temperature and 85 K are shown in Figures 7.13 and 7.14 respectively. The variable interference filter used to isolate the emission was optimised on the observed emission maximum, and for the sample of ZnSe was additionally centred on the wavelength at which the manganese emission should appear at  $\sim 5800 \text{ \AA}$ .

The crystals of ZnS and  $\text{ZnS}_{0.6}\text{Se}_{0.4}$  showed five bands of excitation when the manganese emission was monitored at  $5850 \text{ \AA}$ . The excitation bands at 85 K were at  $5370 \text{ \AA}$  (2.308 eV),  $4980 \text{ \AA}$  (2.489 eV),  $4650 \text{ \AA}$  (2.666 eV),  $4350 \text{ \AA}$  (2.850 eV) and  $3920 \text{ \AA}$  (3.162 eV). These wavelengths are very similar to those of the excitation bands of the unannealed manganese doped crystals. This confirms that manganese is still present in the samples following the treatment in zinc/copper. The excitation bands were not so well defined after the annealing treatment, and some only became apparent after the sample was cooled to 85 K. This may have been due to the fact that the efficiency of the manganese emission is reduced in the presence of copper and self-activated recombination centres. With the treated sample of ZnSe:I,Mn, the excitation spectra were measured while the emission was monitored at both  $5800 \text{ \AA}$  and  $6300 \text{ \AA}$ , Figures 7.13 and 7.14. The excitation spectra exhibited a great deal of structure when the sample was cooled to 85 K; the wavelengths and energies of the excitation peaks are given in Table 7.5 and are compared with those measured in the untreated crystal. Monitoring both the manganese emission at  $5800 \text{ \AA}$  and the low energy copper emission at  $6300 \text{ \AA}$  gives excitation bands in approximately the same positions at  $5350 \text{ \AA}$  (2.317 eV),  $5070 \text{ \AA}$  (2.445 eV)

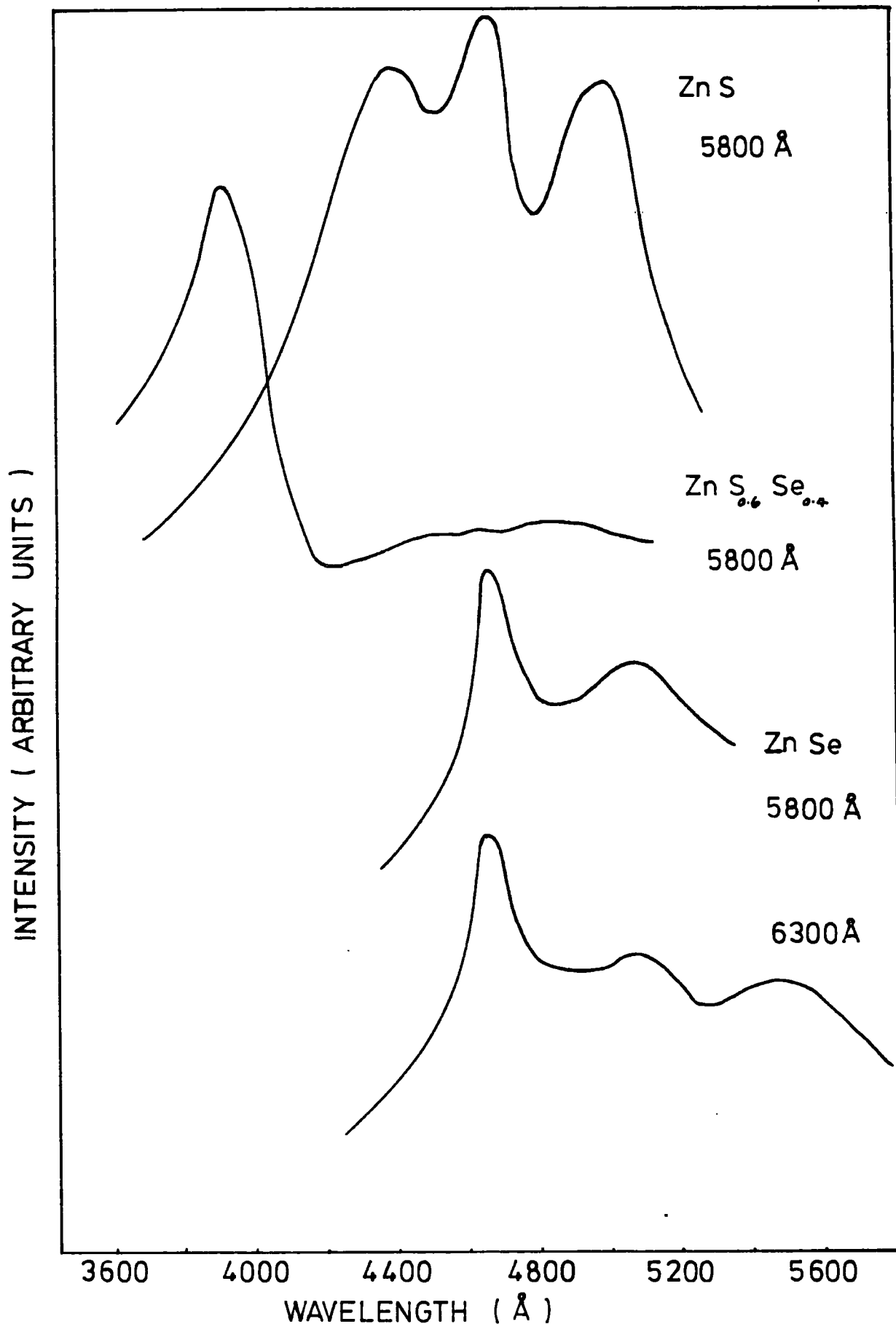


FIG 7.13 EXCITATION SPECTRA OF Zn(S,Se):I,Mn,Cu,Zn AT 300 K MONITORING 5800 Å AND 6300 Å.

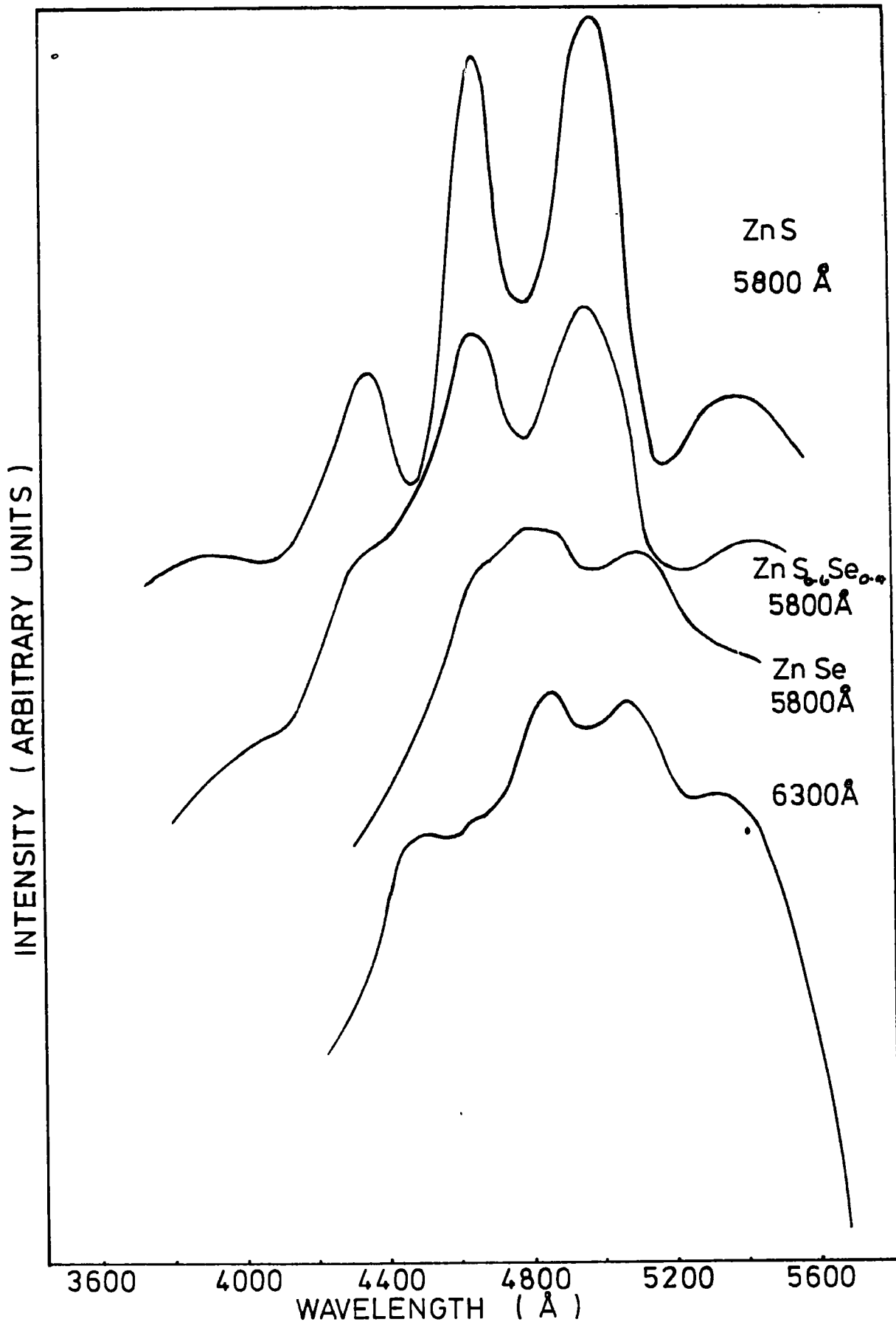


FIG 7.14 EXCITATION SPECTRA OF Zn(S,Se):I,Mn,Cu,Zn AT 85 K MONITORING 5800 Å AND 6300 Å.

TABLE 7.5

EXCITATION BANDS OBSERVED IN ZnSe:I,Mn

AND ZnSe:I,Mn,Cu,Zn AT 85 K

Sample	ZnSe:I,Mn	ZnSe : I,Mn,Cu,Zn	
Monitoring	5800 Å	5800 Å	6400 Å
Position of excitation band Å	5320		5350
	5040	5100	5070
		4850	4970
	4650	4700	4650
	4460		4510

and 4650 Å (2.666 eV). These bands lie at wavelengths close to those of the first three manganese excitation bands observed in the untreated sample of ZnSe:I,Mn. There appears to be an additional band at 4870 Å (2.545 eV), and the 6300 Å emission can also be excited in a band close to the energy gap. The emission band at 6300 Å dominates the luminescence in the ZnSe crystal treated in zinc/copper and the emission is sufficiently broad to overlap any band at 5800 Å. The excitation band at 4870 Å may be equivalent to the band observed at ~4900 Å in undoped crystals which has been reported in Chapter 5. This excitation band was associated with the self-activated luminescence from iodine-doped ZnSe and compares well with the band at 4880 Å reported by Jones and Woods (1974) in ZnSe:I treated in zinc.

From these results it would appear that the crystals of ZnS:I,Mn and ZnS<sub>0.6</sub>Se<sub>0.4</sub>:I,Mn treated in zinc/copper show the same excitation spectra as those reported in Section 7.2.2 for the unannealed samples. However, for ZnSe:I,Mn,Cu,Zn, in which both the self-activated and 'low energy copper' emissions have smaller energies than the manganese emission, the results are quite different. In these crystals the characteristic Mn<sup>2+</sup> emission is no longer apparent and is replaced by a long wavelength band at 6400 Å; monitoring this band reveals an excitation spectrum very similar to that observed for the manganese emission in the untreated crystals.

#### 7.4 Crystals without iodine

Crystals of zinc selenide grown using the vertical furnace technique were examined since they contained no iodine. Undoped and manganese-doped samples were treated in zinc plus 10% by weight of copper and the results compared. Both undoped and doped crystals showed a single band

of luminescence at  $\sim 6400 \text{ \AA}$  with half-width 0.25 eV when excited with  $3650 \text{ \AA}$  ultra-violet radiation. Samples produced by this technique were doped with manganese by introducing it as the chloride into the growth tube. The concentration of manganese which could be introduced by this method was limited to  $\sim 1000$  ppm compared with up to 1% in crystals grown by the iodine transport method. The excitation spectra of ZnSe:Cu,Zn and ZnSe:Mn,Cl,Cu,Zn are shown in Figure 7.15 measured while monitoring the copper emission at  $6400 \text{ \AA}$  and the  $\text{Mn}^{2+}$  emission at  $5800 \text{ \AA}$ . The crystal without manganese shows a broad band of excitation extending from the band-edge at  $\sim 4550 \text{ \AA}$  to  $\sim 5440 \text{ \AA}$  for the copper emission at  $6400 \text{ \AA}$ . By comparison the excitation spectra for the manganese doped crystal, monitoring  $6400 \text{ \AA}$ , show a number of bands at 85 K with peaks at  $4520 \text{ \AA}$  (2.74 eV),  $4880 \text{ \AA}$  (2.54 eV),  $5150 \text{ \AA}$  (2.41 eV) and a shoulder at  $\sim 5400 \text{ \AA}$  (2.30 eV); monitoring at  $5800 \text{ \AA}$  reveals a broad band peaking at  $\sim 4650 \text{ \AA}$  (2.66 eV) with a small shoulder at  $\sim 5120 \text{ \AA}$  (2.42 eV). These bands lie at wavelengths close to those for bands observed in ZnSe:I,Mn. The nature of the excitation bands will be discussed more fully later, however it is worth noting that the structure in the excitation spectrum was only observed in the crystal containing manganese when the emission at  $6400 \text{ \AA}$  was monitored.

#### 7.5 ZnSe:Mn annealed in zinc and selenium

The method of introducing copper into the crystals discussed in the previous sections, was to anneal the samples in a solution of zinc containing 10% by weight of copper. The effect of heating crystals of zinc selenide in liquid zinc alone is to increase the electrical conductivity by several orders of magnitude by decreasing the concentration of acceptors associated with impurities and zinc vacancies. It was felt, therefore,

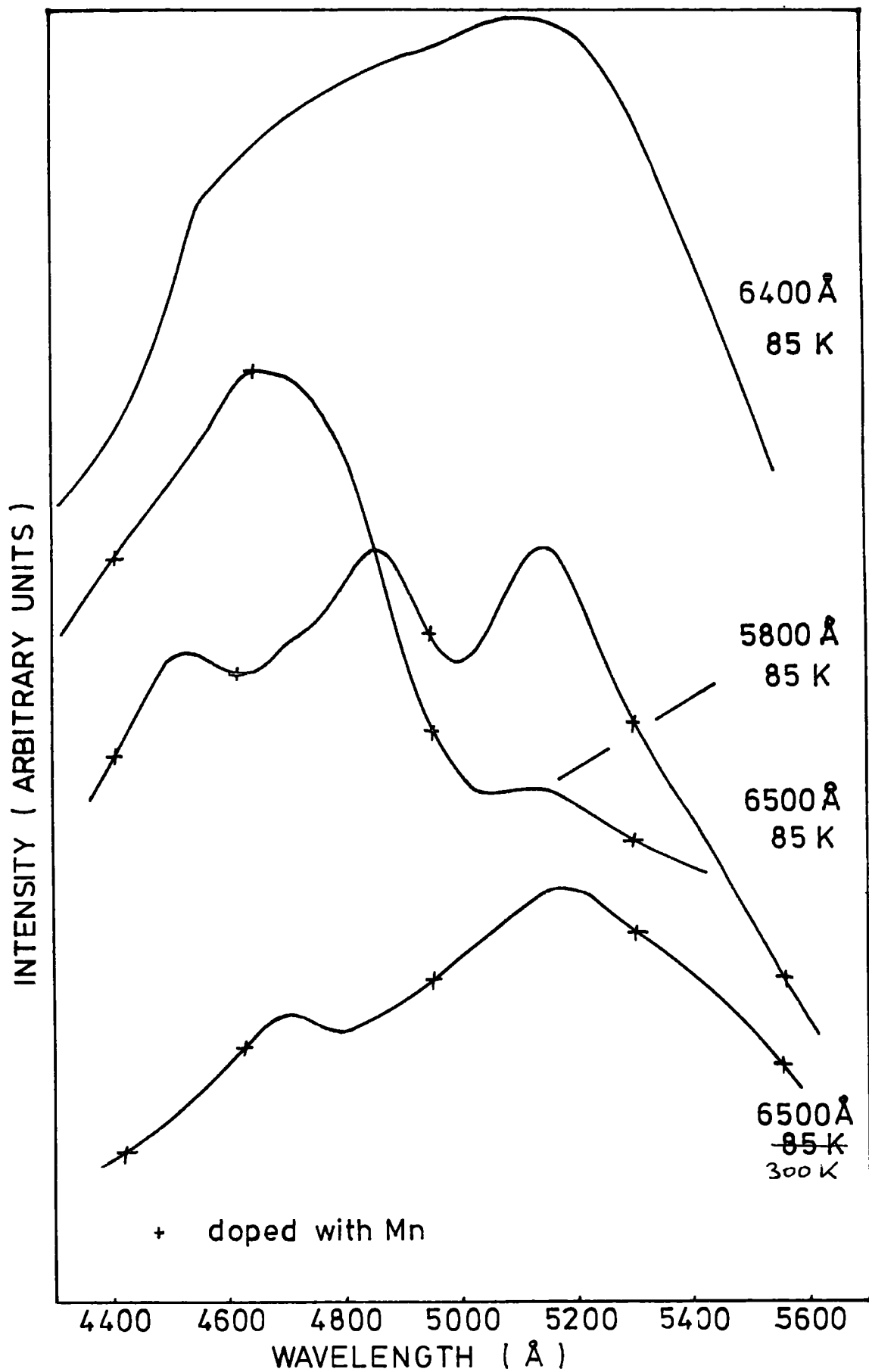


FIG 7.15 EXCITATION SPECTRA OF ZnSe:Cl,Mn,Cu,Zn AND ZnSe:Cl,Cu,Zn MONITORING 5800Å AND 6500Å.

that the method of doping might be producing effects more attributable to the heating in zinc than to the doping with copper. In order to examine this, a crystal of zinc selenide doped with manganese was annealed in zinc alone and the crystal of ZnSe:I,Mn,Cu,Zn was re-annealed in selenium since it has been shown (Aven and Woodbury 1962) that this reverses the effect of treatment in zinc.

The photoluminescence emission spectra for these crystals under 3650 Å excitation are shown in Figure 7.16. The copper doped sample had an emission band at 6500 Å (1.91 eV) and a half-width of 0.23 eV; this is very similar to the emission observed in the crystal of ZnSe:I,Mn,Cu,Zn which had not been annealed in selenium. The zinc treated, manganese-doped crystal shows a band of emission peaking at 6200 Å (2.00 eV) with a half-width of 0.28 eV which is similar to the emission observed in self-activated crystals. Because of the low intensity of the emission, it was not possible to measure the emission spectra excited by 5300 Å radiation. The excitation spectra for these crystals, measured while monitoring the observed emission maxima and the wavelength position of the Mn<sup>2+</sup> emission at 5800 Å, are shown in Figure 7.17. The crystal of ZnSe:I,Mn annealed in zinc shows a broad band of excitation at ~4700 Å (2.64 eV) with a small shoulder at 5150 Å (2.41 eV). This compares well with the excitation spectra for the 5800 Å emission band in the crystal of ZnSe:Cl,Mn,Cu,Zn. Monitoring the red emission in the crystal of ZnSe:I,Mn,Cu,Zn annealed in selenium gives an excitation band at 4500 Å (2.75 eV), close to the band edge, with bands at 4800 Å (2.58 eV), 5180 Å (2.39 eV) and a shoulder at ~5400 Å (2.30 eV) measured at 85 K. Monitoring the Mn<sup>2+</sup> emission at 5800 Å gives bands at 4680 Å (2.65 eV) and 5030 Å (2.46 eV). Comparing the measurements on this crystal before and after treatment in selenium, it would appear that the intensity of the manganese emission diminishes

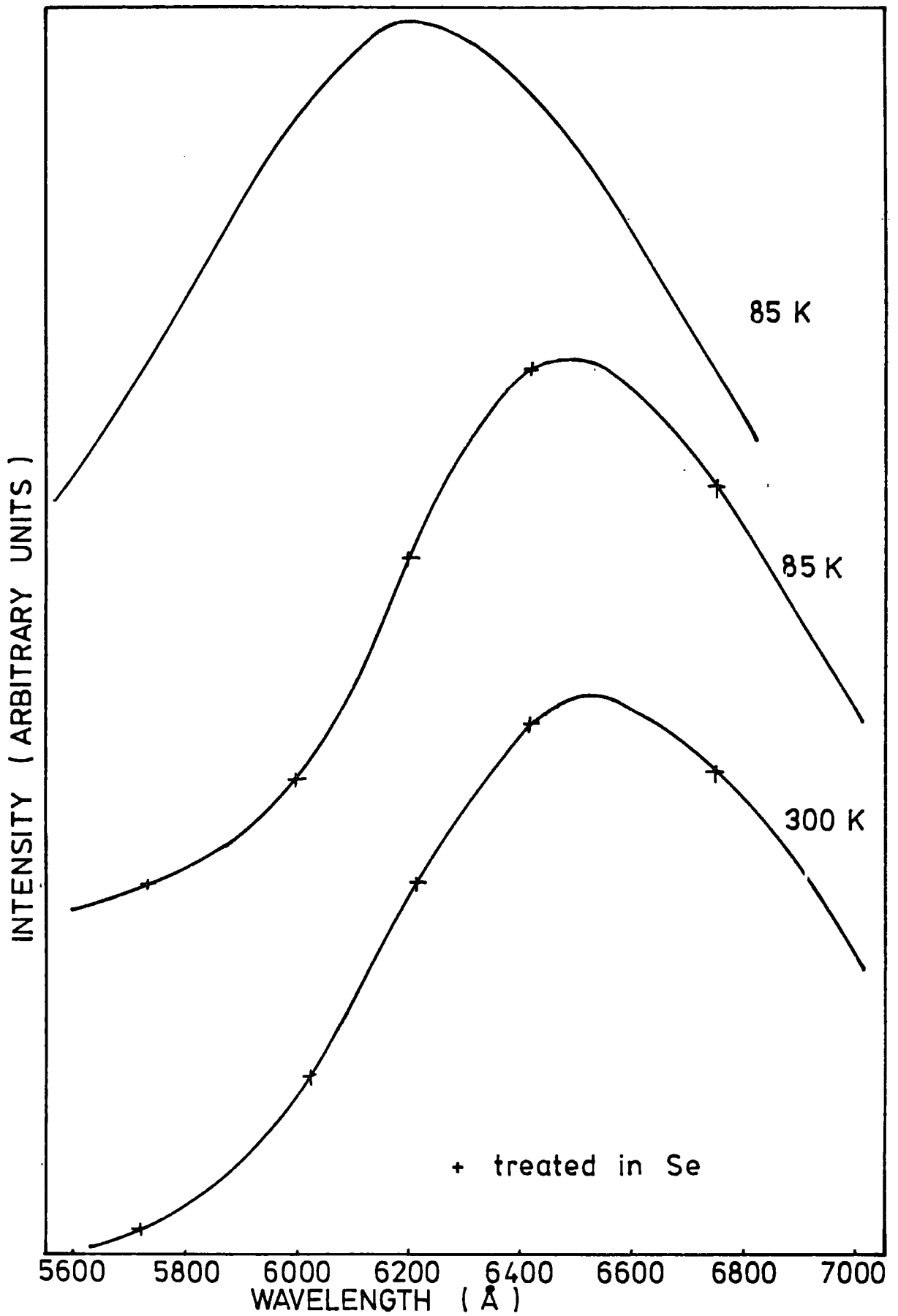


FIG 7.16 PHOTOLUMINESCE SPECTRA OF ZnSe: I, Mn, Zn  
AND ZnSe: I, Mn, Cu, Zn, Se

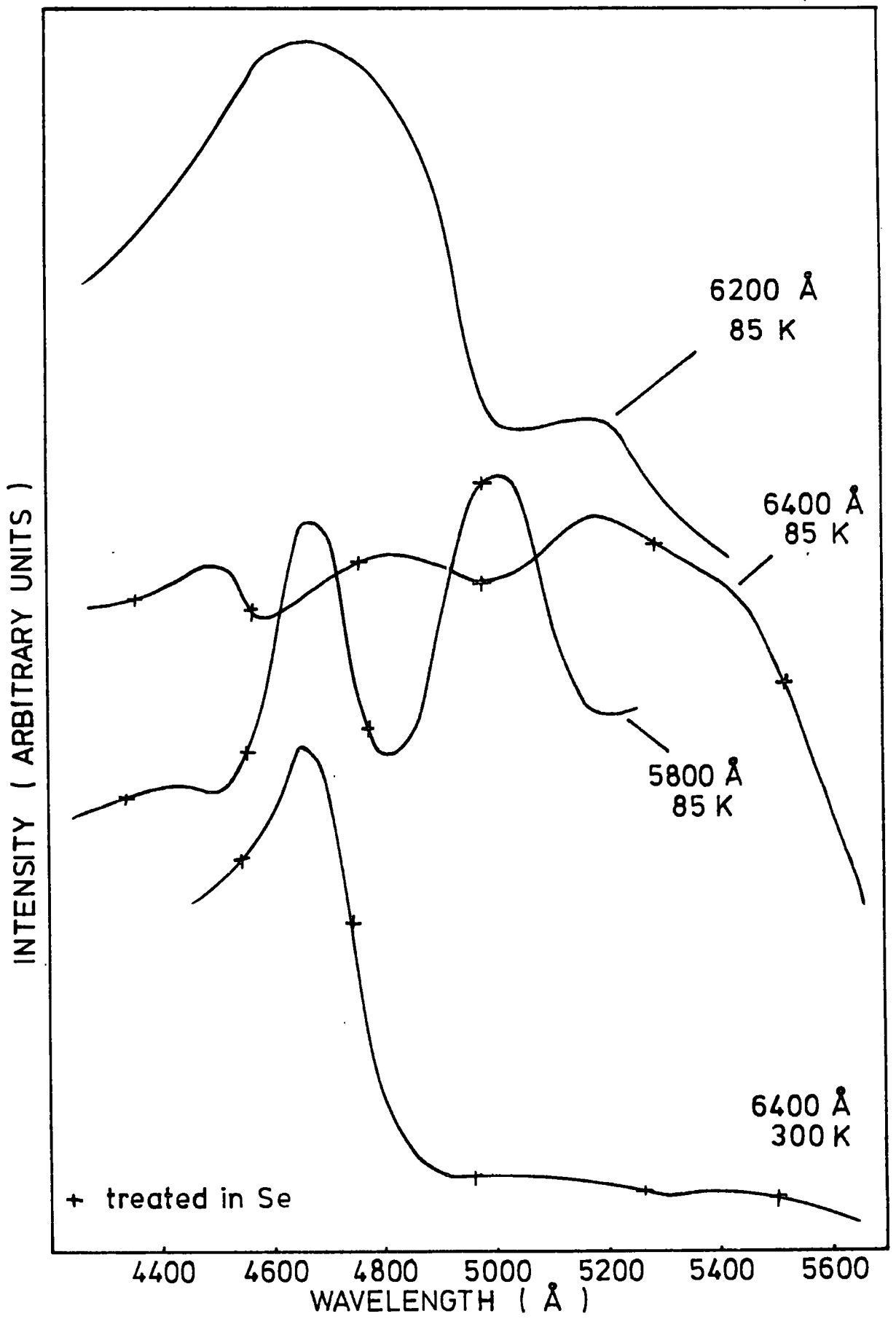


FIG 7.17 EXCITATION SPECTRA OF ZnSe:I,Mn,Cu,Zn,Se AND ZnSe:I,Mn,Zn.

on annealing in zinc and that the characteristic excitation becomes less distinct; however, annealing in selenium reverses this effect and restores the emission almost to its original level.

The effect of heating the crystals of ZnSe:Mn in (a) zinc, or (b) zinc/copper is to eliminate the manganese emission band and replace it with the self-activated emission at 6150 Å or the low energy copper emission at 6400 Å respectively. Monitoring the emission at the wavelength of the manganese band in the treated crystals reveals bands of excitation at ~4700 Å and ~5100 Å. Annealing a zinc-treated crystal of ZnSe:Mn in selenium causes the Mn<sup>2+</sup> excitation bands to become more distinct at 4680 Å and 5030 Å. When the self-activated emission band at 6150 Å in the crystal of ZnSe:I,Mn,Zn is monitored, an excitation spectrum is revealed which is similar to that observed while monitoring the manganese emission in zinc-treated crystals. The excitation spectrum for the 6400 Å copper emission from ZnSe:Mn,Cu,Zn shows four bands at approximately 4550, 4850, 5100 and 5400 Å.

## 7.6 Discussion

The purpose of the work reported in this chapter was to examine the properties of manganese-doped crystals of Zn(S,Se) throughout the whole range of composition. Exciting the manganese-doped crystals with ultra-violet radiation ( $\lambda = 3650 \text{ \AA}$ ) causes the Mn<sup>2+</sup> emission to be masked by the self-activated emission band in crystals with a low sulphur content. This could be attributed to the fact that the energy of the exciting radiation is greater than the band-gap energy up to a composition of ~60% sulphur. The band-gap for ZnS<sub>0.6</sub>Se<sub>0.4</sub> is approximately 3.35 eV compared with an energy of 3.40 eV for 3650 Å radiation. However, if the samples are excited by 5300 Å radiation in the first absorption band of the Mn<sup>2+</sup>

ion, an orange band is observed at 5850 Å in ZnSe and 5860 Å in ZnS. The half-width of this emission is 0.15 eV throughout the range of composition and is much narrower than the bands associated with self-activated or copper emissions; this luminescence can be unambiguously attributed to the characteristic  $Mn^{2+}$  emission. The wavelength of the  $Mn^{2+}$  emission band passes through a minimum energy when the composition of the crystal is varied, shifting to 5990 Å in  $ZnS_{0.7}Se_{0.3}$ . This has been explained (Asano et al 1968) on the basis that the  $Mn^{2+}$  ion is surrounded by various combinations of  $S^{2-}$  and  $Se^{2-}$  ions as the composition of the mixed crystal changes, thus altering the crystalline field which causes the splitting of the manganese levels.

There is a marked similarity between the excitation spectra of the manganese emission in all the mixed crystals; three bands are observed in ZnSe:Mn at 4650, 5030 and 5340 Å and these bands appear in the whole range of compositions. As the absorption edge shifts from 2.7 eV in ZnSe to 3.7 eV in ZnS, additional bands become apparent in the excitation spectra. In ZnS:Mn five peaks can be observed at 3920, 4320, 4650, 5000 and 5350 Å. The lowest energy excitation band does not change in position, but the higher energy bands shift slightly to shorter wavelengths when the proportion of sulphur is increased. The similarity of the excitation spectra indicates that the  $Mn^{2+}$  ion occupies a tetrahedrally coordinated substitutional site throughout the range of composition, but the crystal field splitting increases marginally in going from ZnSe to ZnS. Cooling a sample from room temperature to 85 K causes the excitation spectrum to become more sharply defined, however the positions of the peaks do not alter. This suggests that the variation of the manganese emission band energy with composition and with temperature cannot be solely explained by a change in the crystal field

surrounding the  $\text{Mn}^{2+}$  ion.

An examination of the photoconductivity spectra for the manganese doped crystals reveals a number of peaks in the response which are only observed in the samples containing manganese. The photocurrent tends to be dominated by excitation across the band-gap but there are a number of bands at longer wavelengths which remain fixed in position when the composition of the samples is varied. A comparison indicates that the positions of the minima in photocurrent agree with the maxima in the absorption by the  $\text{Mn}^{2+}$  ion. It is suggested that this absorption of radiation, which leads to photoluminescence, is superimposed on the intrinsic production of photo-carriers within the crystal giving rise to the observed spectra. Since the excitation of the manganese ion did not lead to the production of free-carriers, it was not possible to determine the position of the  $\text{Mn}^{2+}$  ground state in the range of mixed crystals.

Copper was deliberately introduced into manganese-doped crystals to examine its influence on the emission since the metal is an important contaminant in our samples. The effect of treating crystals of  $\text{ZnS}$  and  $\text{ZnS}_{0.6}\text{Se}_{0.4}$  in a solution of zinc plus copper is to superimpose the low energy copper emission on the characteristic  $\text{Mn}^{2+}$  emission; the manganese band still dominates the luminescence and the excitation spectra for this emission is unaffected. Treating  $\text{ZnSe}$  in zinc or zinc/copper causes the emission to be replaced by the self-activated and low energy copper band respectively. Subsequent annealing of a zinc treated crystal in selenium causes the manganese emission to reappear as can be demonstrated by examining the excitation spectra. The annealing treatment in zinc or zinc/copper increases the conductivity of the crystals at the same time as increasing the number of self-activated and copper centres respectively. Allen et al (1973) and Jones and Woods (1973) have suggested that the

manganese emission in ZnSe cannot be excited in the presence of a large concentration of free electrons because Auger processes quench the emission. Since the conductivity of the crystals decreases with the increase in the proportion of sulphur, this model could be used to explain the fact that the  $\text{Mn}^{2+}$  emission is not quenched in the samples of ZnS and  $\text{ZnS}_{0.6}\text{Se}_{0.4}$  on the basis that the concentration of free electrons is not high enough. An alternative suggestion is that the  $\text{Mn}^{2+}$  emission is quenched as a result of competitive radiative transitions to the self-activated and copper centres. These centres shift to higher energies when the proportion of sulphur is increased and in both ZnS and  $\text{ZnS}_{0.6}\text{Se}_{0.4}$  have energies higher than the manganese emission. An examination of the excitation spectra for ZnSe, measured while monitoring the copper emission at  $6400 \text{ \AA}$ , reveals a number of bands at 4520, 4650, 4870, 5070 and  $5350 \text{ \AA}$ ; three of these bands show a good correspondence with the excitation bands of the  $\text{Mn}^{2+}$  emission. In addition, the  $4520 \text{ \AA}$  band is attributed to excitation across the energy gap and the  $4870 \text{ \AA}$  band is associated with the excitation of the self-activated emission. It is not possible to determine conclusively whether the quenching of the manganese emission in zinc-treated ZnSe is due to de-excitation by Auger processes or by radiative processes. Indeed both processes may be operative. It might be possible to establish the effectiveness of each quenching process by making a careful study of the effect of increasing conductivity on the manganese emission.

CHAPTER 8

CONCLUSION

8.1 Summary of results

The purpose of this work was to examine the luminescence processes in the mixed alloys of zinc sulpho-selenide and to relate these transitions to those observed in ZnS and ZnSe. It has been explained that the luminescence in ZnS has received a great deal of attention and theories have been put forward to describe many of the emission centres that are observed. ZnSe has received much less attention, but many of the emission centres present have been established and described by analogy with those observed in ZnS. The whole range of Zn(S,Se) mixed alloys has received little attention in spite of the fact that these compounds cover a range of band-gaps varying in energy from the red to the blue. The interest in examining these materials stems from the possibility of using them for the production of electroluminescent devices.

The crystals examined during the course of the present work were grown in this department using the iodine transport technique; this method was used to produce cubic single crystals of Zn(S,Se) throughout the range of composition. In addition, a few samples were grown by a vapour phase technique. This high temperature method produced cubic material for composition samples up to 60 at.% sulphur, but above this the samples were usually hexagonal in structure. Doped crystals were produced by adding impurities such as manganese and copper during the growth procedure. Certain samples were also heat-treated in liquid zinc; this technique had the effect of removing impurities from the as-grown crystals and of

reducing the concentration of copper in the doped crystals.

The photoluminescence of the Zn(S,Se):I mixed crystals shows clearly the presence of two distinct deep-lying emission bands. This contrasts markedly with the observations made on both ZnS and ZnSe samples where it is only possible to detect single emission bands. It has been conclusively established that these emission bands are not associated with the presence of copper, and the bands also appear in samples which have been heat-treated in liquid zinc to remove unintentional impurities. The lower energy emission band shifts linearly from 2.08 eV (5950 Å) in ZnSe to 2.23 eV (5560 Å) in  $\text{ZnS}_{0.8}\text{Se}_{0.2}$  at 85 K. Above a composition of 60% sulphur the higher energy emission can be resolved as a separate band; this band shifts continuously from 2.38 eV (5200 Å) in  $\text{ZnS}_{0.6}\text{Se}_{0.4}$  through to 2.59 eV (4780 Å) in ZnS. The positions of the single bands observed in ZnSe and ZnS agree with the reports of other workers on the positions of the self-activated luminescence. Throughout the range of composition, the high and low energy bands shift to lower energies when the temperature of the samples is reduced to 85 K; this behaviour is consistent with a localised, self-activated transition.

It is concluded that there are two distinct self-activated luminescence processes in the zinc sulpho-selenide mixed crystals. In ZnS and ZnSe, by comparison, there are single emission bands, and hence there is no direct relationship between the self-activated band in ZnSe and that in ZnS. It has been suggested here that interstitial sulphur and selenium may contribute to these two distinct centres. In the self-activated centre, the zinc vacancy is coordinated with three native anion sites and a substitutional iodine coactivator ion. Sulphur or selenium ions in any combination fill the anion sites, depending on the composition of the alloy, and these produce the  $C_{3v}$  symmetry of the centre; the substitutional iodine ion displaces a sulphur or selenium ion and creates an interstitial atom

which remains in the close proximity and perturbs the environment of the centre thus causing the two distinct luminescence centres.

The behaviour of the copper emission in the Zn(S,Se):Cu system contrasts markedly with that observed for the self-activated emission. The two copper bands in ZnS at 4400 Å (2.82 eV) and 5320 Å (2.33 eV) show a continuous shift of position to 5350 Å (2.32 eV) and 6450 Å (1.92 eV) in ZnSe as the composition of the mixed alloys is varied. However, the shift in the energy of the peak positions becomes more rapid towards the sulphur-rich end. This continuous shift in the energy of the emission bands is consistent with a random distribution of sulphur and selenium anions around the luminescence centre, and with the depth of the centre changing as the band-gap of the alloy alters. It is concluded that the green and blue copper emission bands in ZnS are directly comparable with the red and green bands in ZnSe.

In contrast to the self-activated emission, the 'copper-green' and 'copper-blue' emission bands shift to higher energy when the samples are cooled to 85 K. The 'copper-blue' emission is apparent in all the highly copper-doped samples at 85 K and in the sulphur-rich samples at 300 K.

The manganese emission band in the Zn(S,Se):Mn mixed alloys is complicated by the overlap of other impurity bands. However, the Mn<sup>2+</sup> emission has been unambiguously identified as being centred at 5880 Å (2.11 eV) in both ZnS and ZnSe at 300 K, and in the vicinity of 5900 Å (2.10 eV) throughout the range of composition. On cooling to 85 K the emission band shifts to 5850 Å (2.12 eV) in ZnSe and to 5860 Å (2.12 eV) in ZnS; in the mixed alloys the behaviour is not so consistent, however the emission band remains close to 5900 Å (2.10 eV). The half-widths of the emission bands reduce from 0.20 eV at 300 K to 0.15 eV at 85 K in all the samples. These half-widths are much narrower than are observed

for copper or self-activated bands. The excitation spectra for the manganese emission have a marked similarity for all compositions. Three bands are observed in ZnSe:Mn at 4650 Å, 5030 Å and 5340 Å; as the absorption edge shifts from 2.7 eV in ZnSe to 3.7 eV in ZnS, additional bands become apparent until five bands are observed in ZnS:Mn at 3920 Å, 4320 Å, 4650 Å, 5000 Å and 5350 Å. The excitation processes occur within the manganese ion itself with transitions between the  $6A_1$  ground state and the higher energy levels of the ion. It is concluded from the excitation spectra that the  $Mn^{2+}$  ion occupies a tetrahedrally coordinated substitutional site throughout the range of composition.

The photoconductivity of manganese-doped mixed crystals shows considerable structure, however this appears to be consistent with a selective absorption within the  $Mn^{2+}$  ion producing a luminescence transition which is superimposed on the intrinsic photoconductivity of the crystal. There is no evidence to suggest that the  $Mn^{2+}$  ion can be excited to produce free carriers.

Manganese-doped samples of Zn(S,Se) have been heat-treated in molten copper/zinc. The effect of this treatment on samples of both ZnS and  $ZnS_{0.6}Se_{0.4}$  is to superimpose the 'copper-green' emission on the characteristic  $Mn^{2+}$  emission, however this latter emission still dominates the luminescence. By contrast, in the treated sample of ZnSe the self-activated and red copper-emission dominate the luminescence; both these emissions lie lower in energy than the  $Mn^{2+}$  emission. The excitation spectra for the copper emission in this sample indicate that the copper band can be excited by radiation in the characteristic  $Mn^{2+}$  excitation bands. Heat-treating crystals of Zn(S,Se) in zinc has the effect of increasing the conductivity of the samples; Allen et al (1973) and Jones and Woods (1973) have suggested that the  $Mn^{2+}$  emission in ZnSe may be quenched in the presence of a large concentration of free electrons

by an Auger process. An alternative suggestion in the copper/zinc treated ZnSe:Mn is that the  $Mn^{2+}$  emission is quenched by a radiative de-excitation process to the lower-lying 'copper-green' centre.

## 8.2 Suggestions for further work

Two distinct self-activated (S.A.) emissions have been observed in the mixed Zn(S,Se):I crystals, whereas there is only a single band in ZnS and ZnSe. An electron spin resonance technique has been used to give information about the geometry of the S.A. centre in ZnS. This technique could provide useful information about the environment of the two S.A. centres in the mixed crystals.

The majority of crystals examined in this work were grown by a chemical transport method and contain iodine as a coactivator. The group VII ion which substitutes for an anion may influence the two S.A. centres which are present in the mixed crystals. An examination of samples doped with group III elements Ga or Al, which substitute for the Zn ion, may give more evidence about the nature of these S.A. centres.

Several additional techniques would be useful in order to understand the mechanisms involved in the luminescence processes. Time resolved spectroscopy would be useful in identifying pair recombination processes and might clarify the position with the 'copper-green' emission. Infra-red quenching of the various emission processes would enable the optical depths of the luminescence centres to be obtained; this would be especially useful in the sulphur-rich mixed crystals where the centres are believed to be deep and hence the energies are difficult to obtain from thermal quenching measurements.

Braun et al (1972) have used a phot capacitance technique in order to establish the ground state position of the  $Mn^{2+}$  ion in ZnSe. The application of a similar technique to the range of manganese-doped

Zn(S,Se) mixed crystals might provide information about the position of the ground state as the composition of the alloy is varied. The characteristic manganese emission has been shown to be quenched in ZnSe by heat-treating samples in zinc/copper solution. Treatment in zinc affects the conductivity of the crystals, and the concentration of copper affects the interatomic separation of the copper and manganese atoms. An examination of the quenching as a function of both the conductivity and concentration of copper might provide useful information about the quenching mechanism.

REFERENCES

- ALLEN J W (1964) Proc. 7th International Conference on the Physics of Semiconductors Paris p.781
- ALLEN J W (1963) Physica 29 764
- ALLEN J W, RYALL M D and WRAY E M (1973) Phys. Stat. Sol. (A) 17 K101
- APPERSON J, VOROBIOV Y and GARLICK G F J (1967) Br. J. Appl. Phys. 18 389
- ASANO S, YAMASHITA N and OISHI M (1968) J. Phys. Soc. Japan 24 6 1302
- AVEN M (1967) Int. Conference on II-VI Semiconducting Compounds
- AVEN M, MARPLE D T F and SEGALL B (1961) J. App. Phys. 32 10 2261
- AVEN M and POTTER R (1958) J. Electrochem. Soc. 105 134
- AVEN M and SEGALL B (1963) Phys. Rev. 130 1 81
- AVEN M and WOODBURY H (1962) App. Phys. Lett. 1 3 53
- BANCIE-GRILLOT M (1954) Compt. Rend. 238 1216
- BERGSTRESSER T K and COHEN M L (1967) Phys. Rev. 164 1069
- BESERMAN R and BALKANSKI (1971) Phys. Stat. Sol. 44 535
- BIRCHAK I, SERDYUK V and CHEMERESYUK G (1976) Phys. Stat. Sol. A 33 K145
- BIRMAN J L (1959) Phys. Rev. Lett. 2 157
- BIRMAN J L (1960) J. Electrochem. Soc. 107 409
- BLOUNT G H, FISHER M W, MORRISON R G and BUBE R H (1966) J. Electrochem. Soc. 113 690
- BOWERS R and MELAMED N T (1955) Phys. Rev. 99 1781
- BRAUN S, GRIMMEIS H G and ALLEN J W (1972) Phys. Stat. Sol. A 14 527
- BROSER I and SCHULZ H (1961) J. Electrochem. Soc. 108 545
- BRYANT F J and MANNING P S (1974) J. Phys. Chem. Sol. 35 97

- BUBE R H (1960) Sol. St. Phys. 11 223
- BUBE R H and LIND E L (1958) Phys. Rev. 110 1040
- BUNDEL A, GURETSKAYA Z and NOSKOVA M (1961) J. Electrochem Soc.  
11 352
- BURR K F and WOODS J (1971) J. Cryst. Growth 9 183
- CARDONA M (1961) J. Appl. Phys. Suppl. 32 2151
- CLARK L and WOODS J (1968) J. Cryst. Growth 3 127
- COHEN M L and BERKSTRESSER T K (1966) Phys. Rev. 141 789
- CURIE D (1964) Acta. Phys. Polon. 26 613
- CURIE D (1964) Compt. Rend. 258 3269
- CURIE G and CURIE D (1960) J. Phys. Rad. 21 127
- CURIE D and PRENER J S (1967) Physics and Chemistry of II-VI  
Compounds (North Holland)
- CUTTER J R and WOODS J (1975) J. Phys. D. 8 314
- CUTTER J R, RUSSELL G J and WOODS J (1976) J. Cryst. Growth 32 179
- DESTRIAU G (1936) J. Chem. Phys. 33 587
- DIELEMANN J, DE BRUIN S H, VAN DOORN C and HAANSTRA J (1964)  
Philips Res. Rept. 19 311
- DISCHLER B, RAUBER A and SCHNEIDER J (1964) Phys. Stat. Sol. 6 507
- EWLES J (1938) Proc. Roy. Soc. A 167 34
- ERA K, SHIONOYA S and WASHIZAWA Y (1969) J. Phys. Chem. Sol. 29 1827
- FISCHER A G (1959) J. Electrochem. Soc. 106 9 838
- FISCHER A G (1964) Phys. Rev. Lett. 12 313
- FONGER W H (1965) Phys. Rev. 137 A 1038
- FORD R, KAUER E, RABENAU A and BROWN D (1963) Ber. Bunsenges Physik.  
Chem. 67 460
- FUJIWARA S and FUKAI M (1966) J. Phys. Soc. Japan 21 1463
- FUJIWARA S and FUKAI M (1967) J. Phys. Soc. Japan 23 657
- FUJIWARA S and FUKAI M (1967) J. Phys. Soc. Japan 23 669

- FUKUDA Y and FUKAI M (1967) J. Phys. Soc. Japan 23 902
- GEZCI S (1973) Ph.D. Thesis University of Durham
- GEZCI S (1975) J. Luminescence 10 267
- GHOSH A and ADDISS R (1973) J. Appl. Phys. 44 10
- GUMLICH H E (1963) Bull. Am. Phys. Soc. 118 303
- HALSTED R E and AVEN M (1965) Phys. Rev. Lett. 14 64
- HALSTED R E, AVEN M and COGHILL H G (1965) J. Electrochem. Soc.  
112 177
- HERMANN F and SKILLMAN S (1961) Proc. Int. Conf. Semiconductor Physics  
Prague
- HOLTON W C, DE WIT M and ESTLE T L (1964) Bull. Am. Phys. Soc. 9 249
- HOLTON W C, DE WIT M and ESTLE T L (1965) Int. Symp. Luminescence  
Munich
- HOPFIELD J J, THOMAS D G and GERSHENZON M (1963) Phys. Rev. Lett.  
10 162
- IBUKI S and LANGER D W (1964) J. Phys. Soc. Japan 19 422
- IIDA S (1968) J. Phys. Soc. Japan 25 1 177
- IIDA S (1969) J. Phys. Soc. Japan 26 5 1140
- JAMES J, NICHOLLS J, CAVENETT B, DAVIES J and DUNSTAN D (1975)  
Sol. State Comm. 17 969
- JAMES J, CAVENETT B, NICHOLLS J, DAVIES J and DUNSTAN D (1976)  
J. Lumin. 12/13 447
- JENNY D and BUBE R H (1954) Phys. Rev. 96 1190
- JONES G (1973) Ph.D. Thesis University of Durham
- JONES G and WOODS J (1973) J. Phys. D. Appl. Phys. 6 1640
- JONES G and WOODS J (1974) J. Lumin. 9 389
- KASAI P and OTOMO Y (1961) Phys. Rev. Lett. 7 17

- KASAI P and OTOMO Y (1962) J. Chem. Phys. 37 1263
- KAUFMANN R G and DOWBER P (1974) J. Appl. Phys. 45 10 4487
- KLASENS H A (1946) Nature 158 306
- KLASENS H A (1953) J. Electrochem. Soc. 100 72
- KLICK C C (1953) Phys. Rev. 89 274
- KLICK C C and SHULMAN J H (1957) Sol. St. Phys. 5 97
- KODA T and SHIONOYA S (1963) Phys. Rev. Lett. 11 77
- KODA T and SHIONOYA S (1964) Phys. Rev. Lett. 136 A541
- KRÖGER F A (1940) Physica 7 1
- KRÖGER F A and HELLINGMAN J E (1949) J. Electrochem Soc. 95 68
- KRÖGER F A and VINK H J (1954) J. Chem. Phys. 22 250
- LAMBE J J and KLICK C C (1955) Phys. Rev. 98 5 909
- LANGER D and IBUKI S (1965) Phys. Rev. 128 A809
- LANGER D and RICHTER H J (1966) Phys. Rev. 146 554
- LARACH S (1953) J. Chem. Phys. 21 756
- LARACH S, SHRADER R and STOCKER C (1957) Phys. Rev. 108 587
- LEHMANN W (1966) J. Electrochem. Soc. 113 449
- LEHMANN W (1967) J. Electrochem. Soc. 114 85
- LEHOVEC K, ACCANDO C and JAMGOCHIAN E (1951) Phys. Rev. 83 603
- LEHOVEC K, ACCANDO C and JAMGOCHIAN E (1953) Phys. Rev. 89 20
- LEMPICKI A (1959) Phys. Rev. Lett. 2 155
- LEMPICKI A (1960) J. Electrochem. Soc. 107 409
- LEMPICKI A (1961) Proc. Int. Conf. Semiconductor Physics Prague
- LEVERENZ H W (1950) An Introduction to Luminescence of Solids (Wiley)
- McCLURE D S (1963) J. Chem. Phys. 39 2850
- MELAMED N (1958) J. Phys. Chem. Sol. 7 146
- MOREHEAD F F (1963) J. Phys. Chem. Sol. 24 37
- NARITA S (1960) J. Phys. Soc. Japan 15 128

- NARITA S and SUGIYAMA N (1965) J. Phys. Soc. Japan 20
- NITSCHKE R (1960) J. Phys. Chem. Sol. 17 163
- de NOBEL D (1959) Philips Res. Rept. 14 361
- ORGEL L E (1955) J. Chem. Phys. 23 6 1004
- OZAWA L and HERSH H (1973) J. Electrochem Soc. 120 938
- ÖZSAN M E (1976) Ph.D. Thesis University of Durham
- ÖZSAN M E and WOODS J (1974) J. Appl. Phys. Lett. 25 489
- ÖZSAN M E and WOODS J (1975) Sol. Stat. Electron. 18 519
- PARMENTER R H (1955) Phys. Rev. 100 573
- PEDROTTI L S and REYNOLDS D C (1960) Phys. Rev. 120 5 1664
- PIPER W W and WILLIAMS F E (1952) Phys. Rev. 87 151
- PIPER W W and POLICH S J (1961) J. Appl. Phys. 32 1273
- PRENER J S and WILLIAMS F E (1956) J. Chem. Phys. 25 361
- PRENER J S and WILLIAMS F E (1958) J. Electrochem. Soc. 103 342
- ROUND H J (1907) Electrical World 19 309
- RYSKIN A I (1964) Opt. Spect. 16 149
- SAGAR A, LEHMANN W and FAUST J (1968) J. App. Phys. 39 11 5336
- SCHNEIDER J, RÄUBER A, DISCHLER N, ESTLE T and HOLTON W (1965)  
J. Chem. Phys. 42 1839
- SCHÖN M (1942) Z. Physik. 119 463
- SCHÖN M (1948) Ann. Physik. 3 333
- SEITZ F (1939) Trans. Faraday Soc. 35 74
- SHIONOYA S (1966) Luminescence of Solids (Goldberg)
- SHIONOYA S, ERA K and KATAYAMA H (1965) J. Phys. Chem. Sol. 26 697
- SEIONOYA S, KODA T, ERA K and FUJIWARA H (1963) J. Phys. Soc. Japan  
18 II 299
- SHIONOYA S, KODA T, ERA K and FUJIWARA H (1964) J. Phys. Soc. Japan  
19 1157
- SHIONOYA S, ERA L and WASHIZAWA Y (1966) J. Phys. Soc. Jap. 21 1624

- SHIONOYA S (1965) J. Phys. Soc. Japan 20 2046
- SHRADER R and LARACH S (1956) Phys. Rev. 103 1899
- STRINGFELLOW G B and BUBE R H (1967) Int. Conf. II-VI Semiconducting  
Compounds
- STRINGFELLOW G B and BUBE R H (1968) Phys. Rev. 171 3 903
- TERADA K (1976) J. Phys. Soc. Japan 40 4
- THOMAS D G and HOPFIELD J J (1962) Phys. Rev. 128 2135
- THOMAS D G, GERSHENZON M and TRUMBORE F (1964) Phys. Rev. 133 A269
- TSUJIMOTO Y, ONODERA Y and FUKAI M (1966) Jap. J. Appl. Phys. 5 636
- UCHIDA I (1964) J. Phys. Soc. Japan 19 670
- VAN GOOL W (1961) Philips Res. Rept. Suppl. 3
- VAN GOOL W and CLEIREN A (1960) Philips Res. Rept. 15 238
- VECHT A, WERRING N J, ELLIS R and SMITH P J (1970) J. Phys. D.  
3 L65
- WILLIAMS F E (1953) J. Phys. Chem. 57 776
- WOODBURY H H (1967) Physics and Chemistry of II-VI Compounds  
(North Holland)
- WOODBURY H H and AVEN M (1964) Int. Conf. Phys. Semiconductors  
(Paris)

